UNIVERSITÀ
DEGLI STUDI
DI PADOVA

Sede Amministrativa: Università degli Studi di Padova

Dipartimento di Scienze chimiche

CORSO DI DOTTORATO DI RICERCA IN: SCIENZE MOLECOLARI
CURRICOLO: CHIMICA
CICLO: XXXIV

THEORETICAL METHODS IN THE STUDY OF QUANTUM TUNNELING

Tesi redatta con il contributo finanziario della fondazione CARIPARO

Coordinatore: Ch.mo Prof. Leonard J. Prins
Supervisore: Ch.mo Prof. Giorgio Moro

Dottorando: Pierpaolo Pravatto

Contents

Abstract

The tunneling splitting represents an important nuclear quantum effect that can be detected in a large number of molecular systems spectra. The work presented in this thesis aims to propose a novel approach to the computation of these quantities by harnessing, thanks to the isomorphic relation existing between the Born-Oppenheimer nuclear Hamiltonian and the symmetrized Fokker-Planck-Smoluchowski operator, the localization function approach, usually employed in the computation of kinetic constants of activated processes, in the field of tunneling splitting estimation. Following this strategy, an analytic approximation, characterized by exponentially better convergence in the limit of high barriers, has been obtained for the case of one-dimensional systems opening, as such, a new paradigm in the problem of tunneling splitting computation. Starting from this asymptotic approach, a broad range of theoretical tools has been developed allowing us to tackle, either with an approximated approach or a numerical solution, the ground and excited-state tunneling splitting estimation in one and many-dimensional model systems with a variable degree of accuracy.

Chapter 1

Introduction

The quantum nature of physical systems opens the way to a broad set of effects that cannot be described by a classical theory and, as such, appears strange to a classical observer. Among these, quantum tunneling is surely one of the most striking manifestations, allowing a particle to enter and cross classically forbidden regions in which the repulsive potential energy is greater than the kinetic energy possessed by the particle itself [1]. In these regions, the momentum of the particle assumes an imaginary value and its probability amplitude usually experience an exponential damping. The degree of penetration into the classically forbidden region depends upon the geometrical features of the system and the mass of the incident particle. In general terms, a smaller probability of tunneling is associated with massive particles with a vanishing probability encountered in the classical limit of large masses. For this reason, significant tunneling contributions are usually observed in systems characterized by a relatively small mass such as electrons or light atoms.

In chemistry, quantum tunneling plays a significant role in a multitude of situations and a wide range of experimental pieces of evidence have been collected throughout the years. In chemical kinetics, the tunneling effect represents an alternative way to cross the activation barrier resulting, as such, in a temperature-independent contribution to the kinetic constant that, in the low-temperature regime, plays the role of dominant factor. In the field of spectroscopy, the tunneling effect contributes to a multitude of phenomena such as the rotational pre-dissociation of small molecules, the spectroscopic response of systems characterized by hindered rotations and the determination of the dynamics of labile systems that, in turn, has profound implications onto the nuclear magnetic resonance response of many species [2]. Among these effects, one should not forget the phenomenon of tunneling splitting that, due to its phenomenological relevance, probably represents one of the more discussed nuclear quantum effects on spectroscopy. In general terms, whenever two symmetry-related molecular configurations are kept apart by a potential energy barrier, a tunneling-mediated interaction exists between the states of each molecule located under the barrier. Under these circumstances, the symmetry-degenerate molecular states, computed under the hypotheses of dealing with isolated molecular conformers, are not the proper set of states to describe the system. The proper set of eigenstates, computed by solving the corresponding Hamiltonian eigenvalue problem, can be recovered by considering the proper symmetric and anti-symmetric combinations of site-states. This new set of states is no more degenerate and a progression of doublet of levels, separated by a small energy quantity known as tunneling splitting, can be observed. The study of tunneling splitting represents the core of this thesis and a general outline of our work will be presented in what follows.

The starting point of our analysis is represented by the isomorphic relation existing between the Born-Oppenheimer nuclear Hamiltonian, for a molecular system, and the symmetrized Fokker-Planck-Smoluchowski operator usually adopted in the field of describing the diffusive evolution of a stochastic system in the configuration space. This similarity relation can easily be obtained if one considers that the potential energy surface appearing in the Born-Oppenheimer Hamiltonian can be recovered by starting from a model of the ground-state defined in the form of either the ground-state wave-function or the associated probability distribution. Under these hypotheses, a quantum potential model, hereafter addressed as shifted quantum potential, can be defined with the only unknown quantity being an energy bias equal to the zero-point energy. Under these circumstances, a direct relation can be found between the stochastic equilibrium distribution and the square of the ground state wave-function that, together with a direct relation connecting the diffusion tensor to the mass tensor appearing in the quantum Hamil-

tonian, allow us to recover a direct proportionality relation between the two operators. This equivalence represents a powerful connection that allows us to transfer theoretical tools, regularly adopted in the field of stochastic analysis, to the quantum framework. Please notice how such a relation is purely mathematical and it concerns the structure of the corresponding operators; as such, it does not represent a connection between time evolutions in the two contexts that, in fact, show radically different behaviors. Under this new theoretical framework, an interesting parallelism can be found between the problem of computing ground-state tunneling splitting estimates and the problem of computing kinetic constants of activated processes starting from the description given by the Fokker-Planck-Smoluchowski equation. In essence, the separation between the ground state doublet of quantum levels and the progression of the other quantum states finds a direct correspondence in the eigenvalue gap observed between kinetic and librational modes of the Fokker-Planck-Smolucowski operator creating a direct connection between quantum tunneling splittings and the so-called Kramers problem [3]. Under these circumstances the localization function approach, commonly adopted in the stochastic framework, can be transferred to the quantum problem, allowing for the definition of a new paradigm for the analysis of the tunneling splitting problem. This new protocol presents numerous interesting features among which a generally better accuracy in the limit of high potential energy barriers. This allowed us to tackle the asymptotic description of the tunneling splitting in the limit of high barriers allowing us to directly examine, in the quantum mechanical context, the concept of the Kramers limit.

With this spirit in mind, this thesis has been structured so to guide the reader through the main highlight of this new approach by giving, along the way, all the necessary information about the theoretical context and the obtained results. Our discussion is opened by chapter 2 where a general introduction on the tunneling problem is presented. Particular attention has been reserved to the phenomenon of tunneling splitting and to the theoretical tools used in the literature for its estimation. In the same chapter, a short presentation of the main experimental observation of the phenomenon has been included. An overall pedagogical structure has been imparted to this chapter in order to facilitate the readers approaching the problem for the first time. The readers already familiar with the basic quantum mechanical concepts at the foundation of the tunneling splitting problem can directly skip the introductory part and move to the discussion of the theoretical foundations at the basis of this thesis. These are presented in chapter 3 where, starting from the molecular Hamiltonian in Cartesian coordinates, the isomorphic relation between the Born-Oppenheimer quantum Hamiltonian and the symmetrized Fokker-Planck-Smoluchowski operator is discussed. In chapter 4, starting from the results presented in chapter 3, a general analysis of the tunneling splitting problem is presented for the simple case of one-dimensional systems and the quantum localization function, defined as the ratio between the first-excited state wave-function and the ground-state one, is introduced as the function capable of recovering the proper set of site-states from the ground-state definition. By invoking the asymptotic limit of high potential energy barriers a simple analytical expression for the tunneling splitting, solvable by simple one-dimensional integration, is recovered and tested with simple two-Gaussian model systems, returning an exponential accuracy when a linear increase in the barrier height is considered. In the same chapter, the problem of describing the tunneling splitting behavior in the asymptotic limit of high barriers has been discussed and the proper treatment for the two-Gaussian distribution model has been obtained and characterized. Under these circumstances we verified how our result, contrary to what obtained by applying the usual Kramers-like procedure based upon the Laplace approximation of the involved integrals, is capable of capturing the correct asymptotic behavior. Chapter 4 is closed by sec. 4.3 where a general analysis of the vibrational excited-state tunneling problem is presented adopting the point of view of our asymptotic theory. This represents an interesting problem that has no classical counterpart in the stochastic description where, usually, the focus is set onto the kinetic modes and little attention is given to the fast relaxing librational ones. In order to address the problem, the concept of fixed reference localization function is introduced as the ratio between a generic state of the eigenvalue spectrum and the ground state. Starting from the two-Gaussian model structure an approximated definition of the second-excited state wave-function is recovered and the excited state tunneling splitting is expressed in terms of localization function theory. An asymptotical convergence is obtained also in the case of excited state tunneling splitting even if, due to the larger degree of approximation, a somewhat reduced accuracy is observed. In chapter 5 a formulation of a multidimensional asymptotic theory is presented for the case of a multidimensional two-Gaussian model with a constant mass-tensor. The accuracy of the multidimensional theory has been tested in the case of two-dimensional model systems by recovering estimates of moderate accuracy characterized by an overall improvement in the limit of high barriers. In chapter 6, starting from the results obtained in chapter 4 for the one-dimensional localization functions, an asymptotically inspired

basis set has been defined for one and many-dimensional systems and a procedure, involving only the computation of one-dimensional integrals, has been defined for the solution of a generic multidimensional two-Gaussian problem with a constant mass tensor and a single anti-symmetric coordinate. This newly introduced basis set demonstrated good accuracy in both one and multi-dimensional calculations proving an excellent candidate for real-world applications. The thesis is closed by chapter 7 where some final remarks and perspectives are discussed.

Chapter 2

Recalls on quantum tunneling

The aim of this chapter is that of introducing the reader to the concept of quantum tunneling splitting whose evaluation represents the central focus of this thesis work. The chapter is opened by section 2.1 where some general quantum mechanical recalls are presented with the purpose of both introducing the reader to the concept of quantum tunneling and to outline the formal structure used, throughout the chapter, to discuss standard calculation procedures commonly applied in the literature. In sec. 2.2 the focus of the discussion will be moved onto the evaluation of the tunneling properties of potential barriers that will represent a powerful conceptual tool to understand the general phenomenology related to the tunneling effect. In sec. 2.3 the concept of tunneling splitting will be presented in general terms and the concept of tunneling frequency will be introduced. A general overview of the theoretical methods adopted in the literature to estimate tunneling splitting in molecular systems will be discussed in sec. 2.4 while, a short review of some significant experimental manifestations of tunneling splitting will be presented in sec. 2.5.

2.1 Quantum mechanical methods

According to the rules of quantum mechanics, the behavior of a quantum particle, considered as an isolated (closed) quantum system, can be spatially described in terms of the time-evolution of the associated wave-function $\psi(\mathbf{x}, t)$, where $\mathbf{x}$ denotes the Cartesian position in space [1, 4]. The physical meaning of the wave-function is not directly specified by the common interpretation of quantum mechanics and its ontological nature still represents an open question. As a matter of fact, the wave-function is usually regarded as a purely abstract mathematical function that, despite not being directly observable, has profound and tangible physical outcomes. The properties of the wave-function are well described by quantum mechanics and its physical implications are defined by the Born rule which, as a particular case, fixes the correspondence between the value assumed by the squared modulus of the wave-function $|\psi(\mathbf{x}, t)|^2$ in a given point $\mathbf{x}$ in space and the correspondent probability density $\rho(\mathbf{x}, t)$ of finding the particle in a neighborhood of such a point.[1] Given this probability-amplitude-interpretation of $\psi(\mathbf{x}, t)$ it is easy to understand how such a function must be square-integrable in order to ensure normalization. The time-evolution of the wave-function $\psi(\mathbf{x}, t)$ is dictated by the time-dependent Schrödinger equation that, in general terms, can be written according to [1, 4]:

$$i\hbar\frac{\partial}{\partial t}\psi(\mathbf{x}, t) = \hat{H}\psi(\mathbf{x}, t) \tag{2.1}$$

where $\hbar = h/2\pi$ is the reduced Planck constant[2] while $\hat{H}$ represents the Hamiltonian operator encoding the energy state of the particle. For a single particle of mass m, experiencing an external potential $V(\mathbf{x})$, the Hamiltonian operator assumes the form:

$$\hat{H} = -\frac{\hbar^2}{2m}\nabla^2 + V(\mathbf{x}) \tag{2.2}$$

[1] Please notice how the therm "in a neighborhood of such a point" is here adopted in a colloquial sense. A more formal definition of the meaning associate with the probability density can be given considering the expression $\rho(\mathbf{x}, t)d\mathbf{x}$ that represents the probability of finding the particle in an infinitesimal volume $d\mathbf{x}$ centered around the point $\mathbf{x}$.

[2] The Planck constant assumes the value $h = 6.62607015 \cdot 10^{-34} J \cdot s$.

where the first term on the right hand side of the equation represents the kinetic energy component $\hat{K}$ quadratically depending upon the linear momentum operator $\hat{p}$:

$$\hat{K} = \frac{\hat{p}^2}{2m} = -\frac{\hbar^2}{2m}\nabla^2 \qquad \text{with} \qquad \hat{p} = -i\hbar\nabla \tag{2.3}$$

The structure of the Hamiltonian operator determines the energy states E_n accessible to the system. These, together with their correspondent wave-functions $\psi_n(\mathbf{x})$, can be determined by solving the eigenvalue problem associated to the Hamiltonian operator itself according to the so called time-independent Schrödinger equation:

$$\hat{H}\psi_n(\mathbf{x}) = E_n\psi_n(\mathbf{x}) \tag{2.4}$$

Let us observe that the Hamiltonian operator is self-adjoint and, as such, must be characterized by real eigenvalues and by a set of orthogonal eigenfunctions.[3] The Hamiltonian eigenfunctions are a fundamental ingredient of the quantum mechanical treatment and represent a convenient complete basis set to expand a generic system wave-function. Adopting the Hilbert space notation, formally introduced in appendix A, the following expression can be adopted to represent a generic wave function $\psi(\mathbf{x}, t)$:

$$\psi(\mathbf{x}, t) = \sum_n c_n(t)\psi_n(\mathbf{x}) \qquad \text{with} \qquad c_n(t) = \langle\psi_n|\psi(t)\rangle \tag{2.5}$$

where the summation over the index n must be converted into the proper integral form if the considered Hamiltonian is characterized by a continuous eigenvalue spectrum. Please notice how, according to eq. 2.1, the following expression can be recovered for the time evolution of the wave-function introduced in eq. 2.5:

$$\psi(\mathbf{x}, t) = e^{-\frac{i}{\hbar}\hat{H}(t-t_0)}\psi(\mathbf{x}, t_0) = \sum_n c_n(t_0)e^{-\frac{i}{\hbar}E_n(t-t_0)}\psi_n(\mathbf{x}) \tag{2.6}$$

where $c_n(t_0) = \langle\psi_n|\psi(t_0)\rangle$ represents the set of expansion coefficients defining the wave-function at the initial time $t = t_0$. Please notice how each eigenstate $\psi_n(\mathbf{x})$ must evolve in time according to the phase factor $U_n(t - t_0) = \exp[-iE_n(t - t_0)/\hbar]$ and, as such, needs to be associated with a time-independent probability distribution $|U_n(t - t_0)\psi_n(\mathbf{x})|^2 = |\psi_n(\mathbf{x})|^2$. As it will be demonstrated shortly, the Hamiltonian eigenstates must be characterized by time-independent observable and, for this reason, they are usually referred to as stationary-states.

Now that a general overview of the formal apparatus adopted in the quantum mechanical treatment has been presented, one may wonder how a given observable value can be predicted and, more generally, what does the word "measurement" means in the quantum mechanical context. Giving a complete answer to such a question is far beyond the purposes of this introduction but a general overview of the formal situation can be given starting from what already presented in this chapter. In general terms, whenever a quantum mechanical observable needs to be measured, some sort of measuring device must be connected to the quantum system under exam in order to obtain the required information about its properties. This, however, is somewhat oxymoronic if examined from the point of view of what previously stated, due to the fact that the same concept of system wave-function is well defined under the hypotheses of an isolated system in a pure quantum state and, as such, non interacting with other entities. In more formal terms, the measuring apparatus and the system under observation cannot be described separately and an overall wave-function needs to be considered for the overall isolated system formed by the two parts. Only under these conditions the measurement process can be formally described in terms of a wave-function and the properties of each sub-units can be investigated by invoking the density-matrix formalism. Keep in mind, however, that this observation is strongly correlated to the concept of decoherence and only interprets part of the problem since it does not justify the transition experienced by the system moving from a pure state of coherent superposition to a mixed state of classical alternatives [5]. The act of observing the system causing some degree of wave-function collapse, i.e. the random choice of one and only one of the possible classical alternatives, still represents an open question without a definitive explanation and, in the common interpretation of quantum mechanics, it is usually considered as a postulate of the measurement theory. At this point, one can easily see how the perturbation induced on the system by the measuring apparatus is intrinsic of the quantum description and, as such, the state of a given quantum system is irreversibly altered by the measurement process. In general terms different

[3] To be more precise all the eigenfunctions corresponding to different eigenvalues are orthogonal. In the case in which two or more states share the same eigenvalue an orthogonal basis set can be defined in order to represent the degenerate sub-space

types of measurements can be performed on a quantum system each of which characterized by different degrees of extracted information and different types of perturbations induced on the system under study.

The simplest measurement process possible is usually referred to as projective measurement and, as the name suggests, it is essentially equivalent to measure the projection of a given wave-function $|\psi(t)\rangle$ on the set of possible measurement outcomes described by the states $|m\rangle$. In order to better understand what does this imply and what kind of information can be obtained with this procedure, let us consider that each quantum mechanical observable must be associated to a given self-adjoint operator $\hat{M}$ and, as such, all the possible outcomes are defined by its real eigenvalues λ_m. These can be computed solving the eigenvalue problem associated to the operator $\hat{M}$:

$$\hat{M}|m\rangle = \lambda_m|m\rangle \tag{2.7}$$

Each possible outcome λ_m is in turn associated to an eigenstate $|m\rangle$ whose ensemble represents a complete orthonormal basis-set for the Hilbert space. The completeness of the basis-set is a fundamental element of the quantum analysis that can be represented in compact form by specifying the identity operator $\hat{I}$ as the following combination of projection operators:

$$\hat{I} = \sum_m |m\rangle\langle m| \tag{2.8}$$

This relation allows us to easily rewrite the normalized wave-function $|\psi(t)\rangle$ as the linear combination of eigenvectors $\{|m\rangle\}$ of the $\hat{M}$ operator:

$$|\psi(t)\rangle = \sum_m c_m(t)|m\rangle \qquad \text{with} \qquad c_m(t) := \langle m|\psi(t)\rangle \tag{2.9}$$

where the $c_m(t)$ coefficients implicitly define the population $|c_m(t)|^2$ of each normalized state $|m\rangle$ that, in turn, is associated with the probability of obtaining the outcome λ_m in the measurement. In practical terms, during a projective measurement process the wave-function, initially free to represent any generic superposition of states defined by the coefficient set $c_m(t)$, randomly collapses to a single state $|m\rangle$ resulting in a defined outcome λ_m. If a set of identical wave-functions $|\psi(t)\rangle$ is prepared and measured a statistical distribution of values, distributed according to the population coefficients $|c_m(t)|^2$, will be obtained and the average observable value $\langle\hat{M}\rangle$ will be represented by the quantity:

$$\langle\hat{M}\rangle = \sum_m \lambda_m|c_m(t)|^2 = \sum_m \lambda_m\langle\psi(t)|m\rangle\langle m|\psi(t)\rangle = \langle\psi(t)|\hat{M}|\psi(t)\rangle \tag{2.10}$$

from which, the expectation value definition can be introduced in order to express the average value $\langle\hat{M}\rangle$ of an observable associated to a given operator $\hat{M}$:

$$\langle\hat{M}\rangle = \langle\psi(t)|\hat{M}|\psi(t)\rangle \tag{2.11}$$

This result represents a crucial result of this section and will be used extensively throughout this thesis to compute observable average values. Please notice how, as anticipated, if the considered wave-function represents a stationary state, the correspondent expectation value, associated to a generic time-independent operator $\hat{M}$, will be constant in time.

2.1.1 Heisenberg's uncertainty principle and quantum tunneling

In the previous paragraph, a general reminder about the fundamental rules of quantum mechanics has been presented and the concept of measurement has briefly been reviewed. In the present paragraph, we will examine how the quantum mechanical nature of a system impacts the simultaneous measurement of pairs of physical quantities imposing, in the case of canonically conjugate variables, a limit to the accuracy of their estimation. This result will prove to be a powerful illustrative tool that will allow us to show to the reader how the quantum tunneling phenomenon can, in fact, be ultimately traced back to the fundamental uncertainty relation existing between the position and linear momentum variables describing the motion of a quantum particle.

To this purpose, let us indicate with $\hat{A}$ and $\hat{B}$ the operators associated with the two canonically conjugated quantities that we want to measure and let us indicate their non-vanishing commutator

according to $[\hat{A}, \hat{B}] = iK$, with $K \in \mathbb{R}$. Starting from these assumptions, a new set of operators $\Delta\hat{A}$ and $\Delta\hat{B}$, representing the displacement of an observable from its mean value, can be conveniently introduced according to:

$$\Delta\hat{A} := \hat{A} - \langle\hat{A}\rangle \qquad \text{and} \qquad \Delta\hat{B} := \hat{B} - \langle\hat{B}\rangle \tag{2.12}$$

from which, the uncertainty associated to the observable measurements can be expressed in terms of the root-mean-squared displacements σ_A and σ_B:

$$\sigma_A := \sqrt{\langle\Delta\hat{A}^2\rangle} \qquad \text{and} \qquad \sigma_B := \sqrt{\langle\Delta\hat{B}^2\rangle} \tag{2.13}$$

At this point, a generic normalized wave-function $|\psi(t)\rangle$ can be adopted as a template and, starting from its definition, the following transformed function $|\phi_\xi(t)\rangle$, parametrically dependent upon a real-valued control parameter ξ, can be introduced:

$$|\phi_\xi(t)\rangle := (\Delta\hat{A} + i\xi\Delta\hat{B})|\psi(t)\rangle \tag{2.14}$$

This newly introduced wave-function is not normalized and its normalization integral, once again parametrically dependent upon the control parameter ξ, can be introduced as the non-negative function $f(\xi)$ that, due to its definition, needs to respond to the following relations:

$$\begin{aligned} f(\xi) &:= \langle\phi_\xi(t)|\phi_\xi(t)\rangle = \langle(\Delta\hat{A} + i\xi\Delta\hat{B})\psi(t)|(\Delta\hat{A} + i\xi\Delta\hat{B})\psi(t)\rangle = \\ &= \langle\psi(t)|\Delta\hat{A}^2|\psi(t)\rangle + \xi^2\langle\psi(t)|\Delta\hat{B}^2|\psi(t)\rangle + i\xi\langle\psi(t)|[\Delta\hat{A}, \Delta\hat{B}]|\psi(t)\rangle = \\ &= \xi^2\sigma_B^2 - \xi K + \sigma_A^2 \geq 0 \end{aligned} \tag{2.15}$$

What just obtained clearly demonstrates how the $f(\xi)$ function is represented by a non-negative parabolic function characterized by a minimum located at $\xi_0 = K/2\sigma_B$. Considering the expression of the function $f(\xi)$ in such a point, the following condition can be obtained:

$$\sigma_A^2 - \frac{K^2}{4\sigma_B^2} \geq 0 \tag{2.16}$$

from which the following relation, representing the generalized form of the Heisenberg's uncertainty principle, can be obtained for the root-mean-squared displacements associated with the best estimate accuracy:

$$\sigma_A\sigma_B \geq \frac{|K|}{2} \tag{2.17}$$

This condition fixes, as anticipated, a limit accuracy to the simultaneous estimation of the observable associated to the operators $\hat{A}$ and $\hat{B}$ that show how an intrinsic uncertainty exists in the properties associated with a given quantum system. A couple of conjugate variables responding to such an uncertainty relation are represented by the position x and its associated linear momentum p_x that, as can be easily verified starting from the definition $\hat{p}_x = -i\hbar\partial_x$, must be related by the commutation relation $[\hat{x}, \hat{p}_x] = i\hbar$ and, as such, must respond to the uncertainty relation $\sigma_x\sigma_{p_x} \geq \hbar/2$. This apparently simple relation captures the essence of many aspects of quantum mechanics conceptually opening the way to exquisitely quantum phenomena such as quantum tunneling and the existence of the zero-point energy in some bounded systems.

A clear example of the meaning associated with the position-momentum uncertainty relation can be examined by simply studying the problem associated with the free motion of a particle in a one-dimensional space characterized by a constant potential $V(x) = V_0$. In order to study such a problem let us set, due to the arbitrariness of the energy scale, the value V_0 as the zero of our energy scale such that the Hamiltonian for the system can be written only in terms of the Kinetic energy component:

$$\hat{H} = -\frac{\hbar^2}{2m}\frac{\partial^2}{\partial x^2} \tag{2.18}$$

The solution of the eigenvalue problem associated to such an Hamiltonian is trivial and a continuous set of eigenfunctions $\psi_k(x)$ and eigenvalues E_k, ordered by the real wave-number k, can be easily obtained according to:

$$\psi_k(x) = e^{ikx} \qquad \text{with} \qquad E_k = \frac{\hbar^2 k^2}{2m} \tag{2.19}$$

At this point one can easily see how the Hamiltonian in eq. 2.18 commutes, due to the constant nature of the potential, with the linear momentum operator $\hat{p}$ and, as such, it must share with it a common basis-set of orthogonal eigenstates. As a matter of fact, by applying such an operator to the eigenfunctions from eq. 2.19, one can easily see how these are eigenfunction also of the momentum operator $\hat{p}$ corresponding with the eigenvalues p_k defined by the relation:

$$p_k = \hbar k \tag{2.20}$$

with the sign of k indicating the direction of motion. This result is particularly interesting if observed from the Heisenberg's uncertainty principle standpoint since it represents the limit condition in which one of the two canonically conjugate variables is perfectly known while the other cannot be inferred with a finite uncertainty. As a matter of fact, if a particle free of moving in space is prepared in an eigenstate of the Hamiltonian, a well defined linear momentum value can be associated to its motion, at the same time, however, this choice results in a completely undefined position due to the fact that the probability density of finding the particle around a given position in space is constant over all the domain of the configurational variable x. The only way to achieve a more particle-like behavior, having as such a more precise indication about the spatial position of the particle, would be to invoke a wave-packet model in which a distribution of probability characterized by a finite mean-squared-displacement can be composed by considering a superposition of system eigenstates. This would result in an overall reduced uncertainty in the position estimation that, however, directly translates to a greater uncertainty in the momentum state due to the fact that a superposition of momentum eigenfunctions has been considered. This shows how the Heisenberg's uncertainty principle naturally describes the essence of a quantum system in which the classical concept of determined position and momentum simply cannot be represented.

This principle is universal and clearly holds also for more complex systems. If, for example, a quantum particle is sent toward a potential energy barrier the idea of classical turning-point, in which the particle reaches zero linear momentum exactly at the point in which the barrier height equals its kinetic energy, cannot be satisfied in the quantum world where an intrinsic uncertainty characterizes the position-momentum variables. As such the classical boundaries determining the so-called classically forbidden regions can be crossed by a quantum particle giving rise to the phenomenon of quantum tunneling.

In section 2.2 a more quantitative discussion of the tunneling-mediated crossing of a potential energy barrier will be presented in terms of an ideal scattering experiment. In such a mental setup an ideal flux of quantum particles of variable energy is sent toward a potential energy barrier experimenting, as such, either reflection of transmission. As it will be discussed, striking differences are observed between the behavior of a classical particle and its quantum counterpart, with the latter experiencing both quantum tunneling and non-classical reflection. Before doing so, however, the concept of probability current needs to be introduced. This quantity, formally defined in sec. 2.1.3, will allow for an easy handling of the non-normalized wave-function terms, adopted for describing unbounded particles, giving an easy way to formalize the concept of reflected and transmitted amplitudes.

2.1.2 The semi-classical hypothesis and the WKB approach

In the previous section, the case of the free-particle has been investigated and we have shown how the proper eigenfunction to describe its motion, defined by eq. 2.19, also represents the eigenfunction of the linear momentum operator correspondent to a momentum eigenvalue defined by the relation in eq. 2.20. As such, one can clearly appreciate how the linear momentum p of a free particle is associated to the correspondent wave-number k by the relation $k = 2\pi p/h$ or, in equivalent terms, how the solution in eq. 2.19 must be characterized by a wavelength λ defined by the equation:

$$\lambda = \frac{h}{p} \tag{2.21}$$

This quantity represents the De Broglie wavelength and relates the quantum mechanical undulatory behavior of a system to a corpuscular-like parameter such as the linear momentum. As a matter of fact, the De Broglie wavelength λ represents a meter of the quantum mechanical nature of a system with a classical system being identified by the limit of vanishing λ values. In the present section, the limit case of a semi-classical quantum system characterized, as such, by a small enough De Broglie wavelength will be presented. The results obtained from this assumption, representing the so-called Wentzel, Kramers and Brillouin approximation (or shortly WKB approximation), will prove to be valuable tools in the study of

tunneling problems and will be used throughout this introductory chapter.

In order to analyze how a semi-classical formal apparatus can be adopted to describe a generic quantum system, let us start by expressing the complex-valued eigenfunction of the latter in terms of the complex exponential form:

$$\psi(x) = e^{\frac{i}{\hbar}\sigma(x)} \tag{2.22}$$

where, in order for the wave-function $\psi(x)$ to be a solution of the time-independent Schrödinger equation, the newly introduced $\sigma(x)$ function needs to comply with the condition expressed by the following relation:

$$\frac{i\hbar}{2m}\frac{\partial^2\sigma(x)}{\partial x^2} - \frac{1}{2m}\left(\frac{\partial\sigma(x)}{\partial x}\right)^2 = V(x) - E \tag{2.23}$$

Starting from this result, the idea of a semi-classical system can easily be expressed by expanding the exponential function $\sigma(x)$ around a vanishing Planck constant value ($\hbar/i = 0$) obtaining, as such, the following expression:

$$\sigma = \sigma_0 + \frac{\hbar}{i}\sigma_1 + \left(\frac{\hbar}{i}\right)^2\sigma_2 + ... \tag{2.24}$$

This, as colloquially anticipated before using the De Broglie wavelength as a meter of the quantum nature of the system, directly translates to assuming the classical limit as the zero-order factor that, by considering terms dependent upon higher Planck constant powers, is subsequently corrected to account for the quantum mechanical behavior of the system.

At this point the $\sigma_n(x)$ terms, appearing in equation 2.24, need to be computed. In order to do so, subsequent approximations of $\sigma(x)$, generated by considering expansions of progressively higher order in $\hbar/i$, must be substituted into equation 2.23 in order to identify the proper structure of each $\sigma_n(x)$ term. As an example of this, let us consider the evaluation of σ_0 that, as anticipated, can be easily obtained substituting $\sigma = \sigma_0$ into eq. 2.23. By omitting the term in $\hbar$, the following condition can be easily obtained:

$$-\frac{1}{2m}\left[\frac{\partial\sigma_0}{\partial x}\right]^2 = V(x) - E \tag{2.25}$$

from which, the functional form of σ_0 can be computed by simple integration according to:

$$\sigma_0 = \pm\int dx\sqrt{2m\left[E - V(x)\right]} = \pm\int p\,dx \tag{2.26}$$

where the linear momentum has been introduced according to $p = \sqrt{2m\left[E - V(x)\right]}$ where $E - V(x) > 0$ represents the kinetic energy of the system. Please notice how in doing so, we have implicitly assumed that the particle is moving across classically allowed regions. The proper treatment of classically forbidden regions will be discussed further on in this section.

Now that the results for σ_0 has been obtained, we should stop for a moment to discuss the meaning of the assumption implicitly made in neglecting from eq. 2.23 the term in $\hbar$. This, in fact, directly implies the following condition:

$$\hbar\frac{\partial^2\sigma(x)}{\partial x^2} \ll \left(\frac{\partial\sigma(x)}{\partial x}\right)^2 \tag{2.27}$$

that, in simple terms, can be rewritten according to:

$$\left|\hbar\frac{\partial}{\partial x}\left(\frac{\partial\sigma(x)}{\partial x}\right)^{-1}\right| \ll 1 \tag{2.28}$$

This expression, as suggested by Landau and Lifšits [1], implicitly represents a measure of the semi-classical nature of the system. In fact, if the σ_0 definition from eq. 2.26 is applied to the condition in eq. 2.28 the following can be easily obtained:

$$\left|\frac{\partial}{\partial x}\frac{\hbar}{p}\right| = \left|\frac{1}{2\pi}\frac{\partial\lambda}{\partial x}\right| \ll 1 \tag{2.29}$$

where λ, once again, represents the De Broglie wavelength presented in eq. 2.21. This result clearly represents the meaning associated with the semi-classical limit where the variation of the system wavelength

needs to be small if compared with the characteristic size of the system itself. A clear example of a situation under which the semi-classical approximation cannot be applied is represented by the classical turning points around which the linear-momentum tends to vanish invalidating, as such, the condition from eq. 2.29. This represents a critical point during the application of the semi-classical theory to tunneling problems and, as will be discussed in sec. 2.2.3 and 2.4.2, a substantial effort needs to be paid in order to connect local solutions belonging to regions kept apart by the classical turning points. Before moving on, we should stress how the condition from eq. 2.29, derived by explicitly neglecting the second-order derivative from eq. 2.23, only gives a general indication of the semi-classical nature of the system that, as discussed by Landau and Lifšits [1], needs to be judged taking into account also higher orders of the equation expansion.

Now that the aspects related to the semi-classical approximation validity have been discussed, we can now move our attention to the evaluation of the functional form associated to the $\sigma_1(x)$ term. In order to do so, the condition:

$$\sigma = \sigma_0 + \frac{\hbar}{i}\sigma_1 \tag{2.30}$$

needs to be substituted into eq. 2.23 in order to obtain the following equation:

$$\frac{i\hbar}{2m}\frac{\partial^2}{\partial x^2}\left(\sigma_0 + \frac{\hbar}{i}\sigma_1\right) - \frac{1}{2m}\left[\frac{\partial}{\partial x}\left(\sigma_0 + \frac{\hbar}{i}\sigma_1\right)\right]^2 = V(x) - E \tag{2.31}$$

If, at this point, the term in $\hbar^2$ is neglected, the following can be obtained:

$$\frac{\partial \sigma_1}{\partial x} = -\frac{1}{2}\left(\frac{\partial \sigma_0}{\partial x}\right)^{-1}\frac{\partial^2 \sigma_0}{\partial x^2} \tag{2.32}$$

that, by simple integration, allows us to recover the following expression:

$$\sigma_1 = -\frac{1}{2}\int\left(\frac{\partial \sigma_0}{\partial x}\right)^{-1}\frac{\partial^2 \sigma_0}{\partial x^2}dx = -\frac{1}{2}ln\left|\frac{\partial \sigma_0}{\partial x}\right| + c = -\frac{1}{2}ln\left(p\right) + c \tag{2.33}$$

Now that both the expressions of σ_0 and σ_1 are available a first-order semi-classical formulation can be obtained by explicitly adopting the approximation from eq. 2.30 into the wave-function definition from eq. 2.22. In doing so, the following result can be obtained:

$$\psi = \frac{c_1}{\sqrt{p}}e^{\frac{i}{\hbar}\int p dx} + \frac{c_2}{\sqrt{p}}e^{-\frac{i}{\hbar}\int p dx} \tag{2.34}$$

where c_1 and c_2 represents two arbitrary complex coefficients defining the relative weight associated to each wave-function component.

At this point one can observe how, whenever a particle is moving in classically forbidden regions its momentum assumes imaginary nature due to the $E - V(x)$ term assuming negative values. Under these circumstances, the relation previously presented in this section can be rewritten in terms of the linear-momentum modulus $|p| = \sqrt{2m\left|E - V\right|}$ and, as such, the proper wave-function formulation assumes the form:

$$\psi = \frac{c_1}{\sqrt{|p|}}e^{-\frac{1}{\hbar}\int |p| dx} + \frac{c_2}{\sqrt{|p|}}e^{\frac{1}{\hbar}\int |p| dx} \tag{2.35}$$

Please notice how, as highlighted by Landau and Lifšits [1], the precision associated to the semi-classical approximation is insufficient to justify the conservation of exponentially small terms. As such, one of the two terms of eq. 2.35 is often neglected in favor of the other.

2.1.3 Probability current

As discussed at the beginning of this chapter, the probability density $\rho(\mathbf{x}, t)$ of finding a particle around a given point $\mathbf{x}$ in space is equal, thanks to the relation fixed by the Born rule, to the square modulus of the wave-function $\psi(\mathbf{x}, t)$ evaluated in the same point:

$$\rho(\mathbf{x}, t) = \left|\psi(\mathbf{x}, t)\right|^2 \tag{2.36}$$

If the time derivative of such a function is computed, the following result can easily be obtained:

$$\frac{\partial \rho(\mathbf{x},t)}{\partial t} = \psi(\mathbf{x},t)\frac{\partial \psi^*(\mathbf{x},t)}{\partial t} + \psi^*(\mathbf{x},t)\frac{\partial \psi(\mathbf{x},t)}{\partial t} \tag{2.37}$$

Recalling the time-dependent Schrödinger equation introduced in eq. 2.1 and the definition of the real-valued Hamiltonian operator given in eq. 2.2, the following can be obtained:[4]

$$\begin{aligned}\frac{\partial \rho(\mathbf{x},t)}{\partial t} &= \frac{i}{\hbar}\left[\psi(\mathbf{x},t)\hat{H}^*\psi^*(\mathbf{x},t) - \psi^*(\mathbf{x},t)\hat{H}\psi(\mathbf{x},t)\right] = \\ &= -\frac{i\hbar}{2m}\left[\psi(\mathbf{x},t)\nabla^2\psi^*(\mathbf{x},t) - \psi^*(\mathbf{x},t)\nabla^2\psi(\mathbf{x},t)\right] = \\ &= -\frac{i\hbar}{2m}\boldsymbol{\nabla}\cdot\left[\psi(\mathbf{x},t)\boldsymbol{\nabla}\psi^*(\mathbf{x},t) - \psi^*(\mathbf{x},t)\boldsymbol{\nabla}\psi(\mathbf{x},t)\right]\end{aligned} \tag{2.38}$$

At this point the continuity equation, can be invoked and, starting from the result presented in eq. 2.38, the following expression for the probability current $\mathbf{j}(\mathbf{x},t)$ can be easily introduced:

$$\frac{\partial \rho(\mathbf{x},t)}{\partial t} + \boldsymbol{\nabla}\cdot\mathbf{j}(\mathbf{x},t) = 0 \qquad \text{with} \qquad \mathbf{j}(\mathbf{x},t) = \frac{i\hbar}{2m}\left[\psi(\mathbf{x},t)\boldsymbol{\nabla}\psi^*(\mathbf{x},t) - \psi^*(\mathbf{x},t)\boldsymbol{\nabla}\psi(\mathbf{x},t)\right] \tag{2.39}$$

This newly introduced quantity plays a fundamental role in the study of quantum mechanical systems allowing for the description of the probability transfer between different regions of space. In order to better clarify the role played by the probability current $\mathbf{j}$, let us observe how the integral of the probability distribution $\rho(\mathbf{x},t)$ computed, at the time t, over the domain $\mathcal{D}$ must represent the probability $P_{\mathcal{D}}(t)$ of finding the system in the correspondent volume of configuration space:

$$P_{\mathcal{D}}(t) = \int_{\mathcal{D}} \rho(\mathbf{x},t)d\mathbf{x} \tag{2.40}$$

Once this has been obtained, the continuity condition from eq. 2.39 can be invoked and the following integral form can be obtained:

$$\frac{\partial P_{\mathcal{D}}(t)}{\partial t} = \int_{\mathcal{D}} \frac{\partial \rho(\mathbf{x},t)}{\partial t}d\mathbf{x} = -\int_{\mathcal{D}} \boldsymbol{\nabla}\cdot\mathbf{j}(\mathbf{x},t)d\mathbf{x} \tag{2.41}$$

At this point, observing that, thanks to the divergence theorem, the integral of the divergence of a vector field over a closed volume $\mathcal{D}$ can be rewritten as the integral of the vector field flux computed on the surface Σ enclosing $\mathcal{D}$, the following can be written:

$$\frac{\partial P_{\mathcal{D}}(t)}{\partial t} = -\oint_{\Sigma} \mathbf{j}(\mathbf{x},t)\cdot d\boldsymbol{\sigma} \tag{2.42}$$

with $d\boldsymbol{\sigma}$ representing the infinitesimal vector $d\boldsymbol{\sigma} = \mathbf{n}d\sigma$ oriented along the direction $\mathbf{n}$ orthogonal to the infinitesimal surface element $d\sigma$. As anticipated, the vector field $\mathbf{j}(\mathbf{x},t)$ plays a primary role in describing the probability flow between different regions of space indicating the probability entering and exiting every infinitesimal volume in space. As such, this quantity represents a natural candidate in examining those situations in which the behavior of a non-bounded particle, described by a non-normalizable wave-function, must be analyzed in probabilistic terms and, for this reason, will be the central ingredient of the scattering-like treatment presented in sec. 2.2.

2.2 Quantum tunneling as a scattering process

As anticipated in section 2.1.1, a quantum particle can have a non-vanishing probability of exploring classically forbidden regions in which the repulsive potential is greater than the energy possessed by the particle itself. This not only allows for the exploration of classically inaccessible portion of the configuration space but can also lead, as a direct consequence, to the crossing of classically impenetrable potential energy barriers. In this section, this problem will be analyzed from the point of view of a scattering

[4] Please notice how the second derivative terms can be readily rewritten in vectorial form thanks to the following relation:

$$\boldsymbol{\nabla}\cdot[f(\mathbf{x},t)\boldsymbol{\nabla}g(\mathbf{x},t)] = [\boldsymbol{\nabla}f(\mathbf{x},t)]\cdot[\boldsymbol{\nabla}g(\mathbf{x},t)] + f(\mathbf{x},t)\nabla^2 g(\mathbf{x},t)$$

experiment where a constant flow of probability, associated with particles of variable energy, is directed toward the barrier with the purpose of evaluating its transmission coefficient, i.e. the probability that a particle incident on the barrier passes through it instead of being reflected back.

In order to study such a problem, let us consider the simple case of a one-dimensional unbounded potential system in which two semi-infinite regions of essentially constant potential $V(x) = 0$ are smoothly connected to a central finite region containing some form of potential energy barrier. Obtaining a direct solution of the problem by exactly estimating its transmission coefficient is often not possible or, at least, very impractical; nevertheless, a general asymptotic procedure capable of giving a clear picture of the problem can easily be formulated on the base of the wave-function behavior far away from the barrier region. The core hypothesis at the base of this procedure is represented by the idea that for $x \to \pm\infty$ the effect of the barrier is negligible and, with good approximation, the wave-function of a moving particle can be expressed in terms of the solutions obtained for the free-particle Hamiltonian. In order to give a clear picture of what does this mean, let us observe how the probability current associated with such a plane-wave solution can be easily computed according to eq. 2.39 leading to the following time-independent expression:[5]

$$j_k(x,t) = j_k(x) = \frac{\hbar k}{m} \tag{2.43}$$

In simple terms, a generic plane wave solution represents a constant flow of probability moving in the direction fixed by the sign of the wave-number k and moving with a "speed" determined by its magnitude. If such a stream of probability is sent toward a potential energy barrier a quantum scattering experiment can be performed in which the incident probability flux is elastically diverted either into a transmitted probability current or into a reflected one. Under these hypotheses the following asymptotic condition can be imposed on the wave function:

$$\psi_k(x) := \begin{cases} Ie^{ikx} + Re^{-ikx} & x \to -\infty \\ Te^{ikx} & x \to +\infty \end{cases} \qquad \text{with} \qquad k > 0 \tag{2.44}$$

where the coefficients I, R and T represent the weight factor setting, respectively, the amplitude of the incident, reflected and transmitted wave-function components. Please notice how, for the convenience of dealing with wave-number magnitudes, the sign of the wave-number has been set according to $k > 0$. This translates into an incident probability flux moving toward the barrier from the left side. This, however, is purely arbitrary and, clearly, the same formalism can be recovered also in the case of an incident probability flux moving from the right to the left. At this point, one can easily appreciate how, given the elastic nature of the process, all the exponent are functions of the same k value and, as such, by invoking the probability current definition from eq. 2.39, the following probability current definition can be obtained:

$$j_k(x) := \frac{\hbar k}{m} \begin{cases} |I|^2 - |R|^2 & x \to -\infty \\ |T|^2 & x \to +\infty \end{cases} \qquad \text{with} \qquad k > 0 \tag{2.45}$$

Recalling the continuity relation from eq. 2.39 and operating under the condition of dealing with a stationary solution, one can easily conclude that the flux entering the barrier region must be equal to the one exiting it. As such, the following condition can be easily recovered:

$$|I|^2 = |R|^2 + |T|^2 \tag{2.46}$$

Please notice how this relation represents a simple yet interesting result establishing, through the introduction of the probability current concept, a continuity relation between wave-function components that, due to their unbounded nature, cannot be normalized directly. At this point, the relation existing between the reflected and transmitted terms can be established on the basis of the specific barrier definition and the transmission coefficient P_T of the barrier can be computed according to the ratio between the transmitted probability flux and the incident one:

$$P_T := \frac{|T|^2}{|I|^2} \tag{2.47}$$

[5] Please notice how, thanks to the fact that the plane-wave solution is an eigenfunction of the free-particle Hamiltonian, its time evolution must be described by a single multiplicative complex exponential factor. As such, the spatial derivative in eq. 2.39 does not act on the time-dependent term that, consequently, directly simplifies with its complex conjugate counterpart. This imparts to the probability current a constant profile. Please notice how this consideration is true in general and applies to all the stationary states.

Please notice how, even if not explicitly indicated, the transmission coefficient depends upon the energy associated with the incident probability flux and, as such, it is a function of the selected k parameter. In the following section, some practical examples will be made on how the continuity solution, relating the transmitted and reflected components to the incident one, can be established. In section 2.2.1 the pedagogic case of the rectangular barrier will be considered while the more realistic case of the parabolic barrier will be discussed in sec. 2.2.2.

2.2.1 The rectangular barrier

The case of a rectangular-shaped barrier represents one of the simplest examples of tunneling problems for which an analytic expression for the transmission coefficient can be recovered. The formal definition of such a system can be given according to:

$$V(x) := \begin{cases} 0 & x < 0 \\ V_b & 0 \leq x \leq l \\ 0 & x > l \end{cases} \tag{2.48}$$

where V_b represents the barrier height while l represents its width. In order to compute the proper continuity conditions, smoothly connecting transmitted, reflected and incident probability currents, a proper wave-function expression needs to be recovered for each potential region. This is trivially done in the regions characterized by the null potential $V(x) = 0$ where the plane-wave solutions defined in eq. 2.44 can be directly adopted due to the problem being locally described by a free-particle Hamiltonian. In the case of the barrier region the problem is more complex due to the fact that, depending upon the energy of the incident particle, different wave-function definitions need to be considered. In order to clarify this point, let us consider that, by simply rearranging the Hamiltonian eigenvalue problem from eq. 2.4 and taking into account the Hamiltonian definition given in eq. 2.2, the following expression can be obtained:

$$\frac{\partial^2 \psi_k(x)}{\partial x^2} = \frac{2m}{\hbar^2} \left[V_b - E_k \right] \psi_k(x) \tag{2.49}$$

where the $V(x)$ term has been substituted by the proper potential value V_b characterizing the barrier region. Just by examining such a relation, one can easily see how the wave-function behavior strongly depends upon the sign of the $V_b - E_k$ term. If the energy of the particle E_k is greater than the barrier V_b, a positive value is found for the $V_b - E_k > 0$ term and, consequently, the proper wave-function describing the barrier region can be defined in terms of the following plane-wave solution:

$$\psi(x) = a e^{ik'x} + b e^{-ik'x} \qquad \text{with} \qquad k' = \sqrt{\frac{2m}{\hbar^2}(E_k - V_b)} \tag{2.50}$$

If, instead, the energy of the incident particle is lower than the barrier top, a negative $V_b - E_k < 0$ term is encountered and the following real exponential form must be considered as the opportune solution:

$$\psi(x) = A e^{i\kappa x} + B e^{-i\kappa x} \qquad \text{with} \qquad \kappa = \sqrt{\frac{2m}{\hbar^2}(V_b - E_k)} \tag{2.51}$$

where the a, b and A, B coefficients appearing in eqs. 2.50 and 2.51 must be matched, through the proper continuity conditions, to the coefficients belonging to the wave-functions in the other regions.

At this point, let us consider, as an example, the resolution of the continuity problem associated with the second case in which the energy of the particle is lower than the one associated with the barrier and, as such, the associated transmitted probability flux can directly be ascribed to the tunneling process. Starting from what previously presented, the wave-function for the system can be defined according to the following piece-wise definition:

$$\psi(x) = \begin{cases} e^{ikx} + R e^{-ikx} & x < 0 \\ A e^{\kappa x} + B e^{-\kappa x} & 0 \leq x \leq l \\ T e^{ikx} \end{cases} \tag{2.52}$$

in which the incident plane-wave amplitude I has been set to unitary value. By invoking the continuity of the wave-function and that of its first derivative at the boundaries, the following system of equations

can easily be obtained:[6]

$$\begin{cases} 1 + R = A + B \\ ik(1 - R) = \kappa(A - B) \\ Ae^{\kappa l} + Be^{-\kappa l} = Te^{ikl} \\ \kappa Ae^{\kappa l} - \kappa Be^{-\kappa l} = ikTe^{ikl} \end{cases} \tag{2.53}$$

With little elaboration, the just obtained system of equations can be solved and the following set of coefficients can be obtained:

$$A = \frac{2k(k - i\kappa)}{e^{2\kappa l}(k + i\kappa)^2 - (k - i\kappa)^2} \tag{2.54}$$

$$B = \frac{2k(k + i\kappa)e^{2\kappa l}}{e^{2\kappa l}(k + i\kappa)^2 - (k - i\kappa)^2} \tag{2.55}$$

$$R = \frac{(k^2 - \kappa^2)\sinh(\kappa l)}{2ik\kappa\cosh(\kappa l) + (k^2 - \kappa^2)\sinh(\kappa l)} \tag{2.56}$$

$$T = \frac{2ik\kappa e^{-2ikl}}{2ik\kappa\cosh(\kappa l) + (k^2 - \kappa^2)\sinh(\kappa l)} \tag{2.57}$$

Starting from these results and recalling the definition from eq. 2.47, the following expression can be recovered for the transmission coefficient $P_T^{E_k<V_b}$:

$$P_T^{E_k<V_b} = \frac{4k^2\kappa^2}{(k^2 + \kappa^2)^2\sinh^2(\kappa l) + 4k^2\kappa^2} \tag{2.58}$$

where the apex label $E_k < V_b$ has been used as a reminder that the approximation hold its validity only for energies lower than the barrier top. Following a similar process the transmission coefficient $P_T^{E_k>V_b}$, valid in the case of incident particles having an energy greater than the barrier, can be recovered according to the expression:

$$P_T^{E_k>V_b} = \frac{4k^2k'^2}{(k^2 - k'^2)^2\sin^2(k'l) + 4k^2k'^2} \tag{2.59}$$

The relations obtained in eqs. 2.58 and 2.59 represent a remarkably interesting result clearly showing the profound difference existing between the behavior of classical and quantum particles when interacting with a simple rectangular potential energy barrier. In order to better visualize the typical transmission profile produced by such equations, let us look at figure 2.1 where, as an illustrative example, we have reported the transmission probability observed when an electron of mass $m_e = 9.1093837015(28) \cdot 10^{-31}kg$, characterized by a variable energy, interacts with a rectangular barrier of adjustable height and width.

Just by rapidly examining such a figure one can clearly see how two striking effects characterize the system: Firstly, as expected from the existence of quantum tunneling, a non-zero transmission probability is encountered for particles characterized by a kinetic energy lower than the barrier top. Secondly, a non-unitary transmission probability can be observed, due to the existence of interference phenomena resulting in non-classical reflections, for the case of particles having an energy greater than the barrier height. Furthermore, besides these early observations, one can easily appreciate how the efficiency of the tunneling-mediated transfer of probability is strongly influenced by the characteristic parameter of the systems; with the transmission coefficient being significantly depressed by either wider or higher potential energy barriers. Evaluating how these factors impact the tunneling efficiency is an interesting question that, however, given the complexity of the relation from eq. 2.58, is far from trivial. In order to discuss such a problem in simpler terms, let us introduce the concept of penetration length l_p as the function of the particle energy E_k defined according to:

$$l_p(E_k) := \frac{1}{\kappa} = \sqrt{\frac{\hbar^2}{2m(V_b - E_k)}} = \frac{l_p^0}{\sqrt{1 - \frac{E_k}{V_b}}} \qquad \text{with} \qquad l_p^0 := l_p(0) = \sqrt{\frac{\hbar^2}{2mV_b}} \tag{2.60}$$

[6] Please notice how the continuity of both the wave-function and its derivative is required in order to describe a physically meaningful quantum system characterized by both an unique wave-function value for every point in space and a continuous expression for the probability flux.

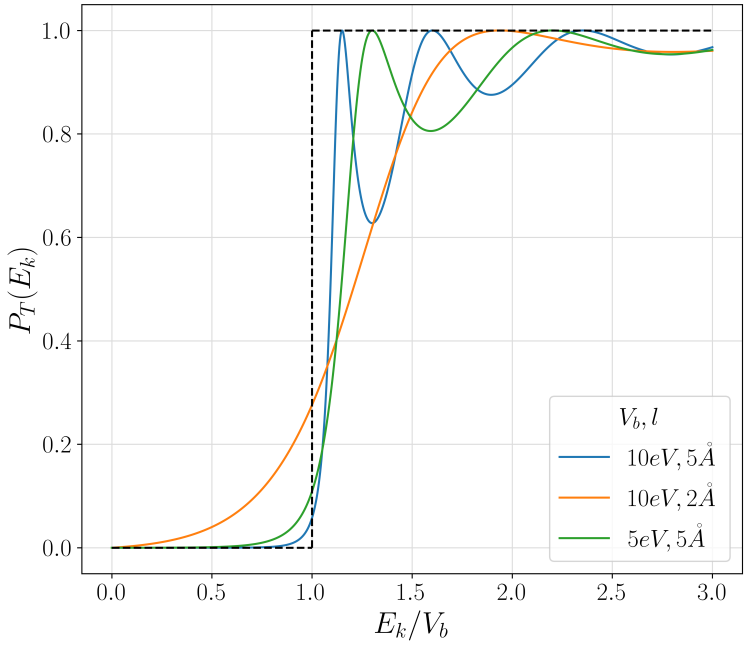

Figure 2.1: Transmission coefficient P_T computed for an electron of mass m_e and variable energy E_k, passing through a rectangular barrier of height V_b and width l. The barrier characteristics are indicated in the legend. The dashed line represents the transmission coefficient expected for a classical particle.

Adopting such a definition in eq. 2.58 and recalling the definitions of k and κ as a function of E_k and V_b, indirectly presented in eqs. 2.19 and 2.51, the following result can easily be obtained:[7]

$$P_T^{E_k<V_b} = \frac{4\frac{E_k}{V_b}\left(1-\frac{E_k}{V_b}\right)}{\sinh^2\left(\frac{l}{l_p^0}\sqrt{1-\frac{E_k}{V_b}}\right)+\frac{E_k}{V_b}\left(1-\frac{E_k}{V_b}\right)} \tag{2.61}$$

At this point, invoking the asymptotic limits of low particle energy $E_k/V_b << 1$ and high width barriers $l/l_p^0 >> 1$, the following relation can be recovered:[8]

$$P_T^{E_k<V_b} \simeq 16\frac{E_k}{V_b}e^{-\frac{2l}{l_p^0}} \tag{2.62}$$

This asymptotic result points to the barrier width, appearing as the exponential argument, as the dominant factor determining the transmission coefficient while a weaker dependence is associated with the other factors with the tunneling efficiency being directly proportional to the particle energy and inversely proportional to the barrier height. All the considerations discussed up until now, referred mainly to the influence on the tunneling efficiency induced by the structure of the system itself, however, one should also highlight how the l_p^0 term depends upon the inverse of the square root of the mass. As such an exponentially smaller transmission coefficient is expected when an increased particle mass is considered.

[7] Please notice how:

$$k^2 = \frac{2mE_k}{\hbar^2} \qquad \text{while} \qquad \kappa^2 = \frac{2m}{\hbar^2}(V_b - E_k)$$

Starting from these definition the following conditions can easily be obtained:

$$k^2+\kappa^2 = \frac{2mV_b}{\hbar^2} \qquad \text{while} \qquad k^2\kappa^2 = \left(\frac{2m}{\hbar^2}\right)^2 E_k(V_b-E_k)$$

[8] Where the following condition has been invoked to simplify the equation:

$$\lim_{x\to+\infty}[\sinh(x)] = \lim_{x\to+\infty}\left[\frac{e^x-e^{-x}}{2}\right] = \frac{1}{2}e^x$$

2.2.2 The parabolic barrier

The rectangular barrier model, which has been presented in the previous section, surely represents a very pedagogic example capable of highlighting the main features characterizing the tunneling phenomenon. Its simple piece-wise definition, however, comes with the disadvantage of a quite unrealistic potential profile that, in many situations, is not suited to represent real tunneling problems. This calls for a more realistic definition of the potential model capable, at least, of giving a continuous parametrization of the system. The parabolic barrier represents a first attempt in this direction and, as such, it represents a classic textbook example that has been widely applied in the literature to evaluate tunneling correction in the context of computing kinetic constants of chemical reactions.

The simplest possible definition of a parabolic model is represented by an infinite inverted parabolic profile characterized by a variable amplitude. Indicating with $A > 0$ the parameter setting the barrier curvature, the following formulation can be adopted:

$$V(x) = -\frac{1}{2}Ax^2 \tag{2.63}$$

Starting from this definition, the time-independent Schrödinger equation associated with the problem can easily be written according to the expression:

$$\frac{\partial^2\psi_p(x)}{\partial x^2} = -\frac{2m}{\hbar^2}\left(E_p + \frac{1}{2}Ax^2\right)\psi_p(x) \tag{2.64}$$

Finding a solution to such an equation, in the form of the proper set of eigenfunctions $\psi_p(x)$ and eigenvalues E_p, is not a trivial task but, fortunately, procedures for its solution have already been presented in the literature. In order to show how the problem can be tackled, let us rewrite the equation in a more convenient form and, in order to do so, let us introduce the following definitions:

$$\xi := x\sqrt[4]{\frac{mA}{\hbar^2}} \qquad \text{and} \qquad \lambda := 2\frac{E_p}{\hbar}\sqrt{\frac{m}{A}} \tag{2.65}$$

By adopting these newly introduced variables in eq. 2.64 the following differential equation can be obtained:

$$\frac{\partial^2\psi_p(\xi)}{\partial\xi^2} + \left(\lambda + \xi^2\right)\psi_p(\xi) = 0 \tag{2.66}$$

whose analytic solutions are known and can be expressed in terms of Weber's functions. Such a direct approach to the problem is, however, far from being easy and, often, a simpler asymptotic approach is preferred. In what follows, the latter solution method will be presented by exactly following the treatment proposed by Bell [2].

The first step in finding a simple solution to the problem is to observe how, in the asymptotic limit of large coordinates values $|\xi| \to \pm\infty$, the relation from eq. 2.66 can be rewritten according to the condition:

$$\frac{\partial^2\psi_p(\xi)}{\partial\xi^2} + \xi^2\psi_p(\xi) = 0 \tag{2.67}$$

that, as it will be shortly demonstrated, can be asymptotically solved by the expression:

$$\psi_p^{\pm}(\xi) \propto e^{\pm\frac{i}{2}\xi^2} \tag{2.68}$$

This fact can be easily verified if, once again, the asymptotic limit of large $|\xi|$ values is considered. Under those circumstances, the imaginary part, that would be extracted from the $\psi_p^{\pm}$ solution by the second derivative operation in eq. 2.67, can be neglected:

$$\frac{\partial^2\psi_p^{\pm}(\xi)}{\partial\xi^2} = \frac{\partial}{\partial\xi}\left[\pm i\xi e^{\pm\frac{i}{2}\xi^2}\right] = \left(\pm i - \xi^2\right)e^{\pm\frac{i}{2}\xi^2} \simeq -\xi^2 e^{\pm\frac{i}{2}\xi^2}$$

and, as such, the relation from eq. 2.68 can be adopted as the asymptotic solution of eq. 2.67. This result is very important since, taking inspiration from it, the solution of the expression from eq. 2.66 can be searched according to the form:

$$\psi_p^{\pm}(\xi) \propto e^{\pm\frac{i}{2}\xi^2} f_{\pm}(\xi) \tag{2.69}$$

where $f_{\pm}(\xi)$ represents the correction function needed to adjust the functional behavior in order to satisfy the newly considered equation. The proper definition of this correction factor can be searched by simply plugging the definition from eq. 2.69 into eq. 2.66, obtaining, as a result, the following expression:

$$\frac{\partial^2 f_{\pm}(\xi)}{\partial \xi^2} \pm 2i\xi \frac{\partial f_{\pm}(\xi)}{\partial \xi} + (\lambda \pm i)\, f_{\pm}(\xi) = 0 \tag{2.70}$$

At this point, invoking, once again, the limit of $|\xi| \to \pm\infty$ the second derivative component in the previous equation can be neglected leaving us with the following first order differential equation as the definition for the $f_{\pm}(\xi)$ correction function:

$$\frac{\partial f_{\pm}(\xi)}{\partial \xi} = \frac{(\pm i\lambda - 1)}{2\xi} f_{\pm}(\xi) \tag{2.71}$$

The obtained relation can, at this point, be solved by simple integration allowing us to obtain the following expression:

$$ln\,|f_{\pm}(\xi)| = \frac{1}{2}\,(\pm i\lambda - 1)\,ln\,|\xi| \qquad \text{or} \qquad f_{\pm}(\xi) = |\xi|^{\frac{1}{2}(\pm i\lambda - 1)} \tag{2.72}$$

Adopting this result in eq. 2.69, the following form can, finally, be obtained for the asymptotic solution of the problem:

$$\psi_p^{\pm}(\xi) \propto e^{\pm\frac{i}{2}\xi^2}\,|\xi|^{\frac{1}{2}(\pm i\lambda - 1)} \tag{2.73}$$

This solution clearly represents the correct asymptotic form to describe the motion of a particle far away from the barrier with an associated probability flux, dependent upon the wave-function first derivative, clearly oriented by the sign adopted into the coordinate exponential. As such, similarly to what already presented in eq. 2.44 for the case of plane wave-solutions, the following asymptotic set of conditions can be defined in order to represent the scattering experiment:

$$\psi(\xi) = \begin{cases} e^{-\frac{i}{2}\xi^2}\,|\xi|^{\frac{1}{2}(-i\lambda-1)} + Re^{\frac{i}{2}\xi^2}\,|\xi|^{\frac{1}{2}(i\lambda-1)} & \xi \to -\infty \\ Te^{\frac{i}{2}\xi^2}\xi^{\frac{1}{2}(i\lambda-1)} & \xi \to +\infty \end{cases} \tag{2.74}$$

where, once again, the coefficients T and R represent the amplitude of the transmitted and reflected wave-function components. At this point, in order to find the expression for the transmission coefficient P_T, the proper continuity condition must be invoked in order to relate the transmitted and reflected probability currents to the incident one. This task, however, is not trivial given the fact that the only known wave-function solutions, previously presented in eq. 2.73, are valid only in the asymptotic limit and, as such, cannot be matched through some sort of relation valid within the barrier region.

In order to solve the continuity problem one can invoke a simple mathematical trick: if the coordinate ξ is fictitiously assumed to have complex nature, a semi-circular trajectory of constant radius $|\xi|$, passing through the positive complex semi-plane, can be constructed in order to connect two given points $\pm\rho$ belonging to the real coordinate axis. If, by construction, these two $\pm\rho$ points are selected to be sufficiently far away from the barrier region, such that the validity of the asymptotic condition is ensured, then the structure of the asymptotic solution from eq. 2.73 would be conserved along the whole trajectory. Under these circumstances, the overall process can simply be expressed by a rotation of π in the complex coordinate plane that, as such, can be encoded by the application of a $e^{i\pi}$ factor to the coordinate ξ of the point ρ. At this point, observing the asymptotic form presented in eq. 2.74 one can easily see how the first term of the first equality shows a negative square dependence upon the coordinate ξ. From this observation, one can easily conclude how, for large values of $|\xi|$, such a term can be neglected leaving the second one as the dominant factor along the whole complex trajectory. Taking into account these considerations, the following condition can be easily recovered:

$$R = Te^{i\frac{\pi}{2}(i\lambda - i)} = Te^{-\frac{\pi}{2}(\lambda + i)} = -iTe^{-\frac{\lambda\pi}{2}} \tag{2.75}$$

that, after imposing the probability current conservation, expressed by the relation $|T|^2 + |R|^2 = 1$, leads to the equality:

$$|T|^2 \left(1 + e^{-\lambda\pi}\right) = 1 \tag{2.76}$$

Recalling the definition of the transmission coefficient introduced in eq. 2.47 the following expression can be recovered:

$$P_T = \frac{1}{1 + e^{-\lambda\pi}} = \frac{1}{1 + e^{-\frac{2\pi E_p}{\hbar}\sqrt{\frac{m}{A}}}} \tag{2.77}$$

where the definition of λ from eq. 2.65 has been employed in order to rewrite the expression in terms of the characteristic parameters of the system. An example of transmission profile, generated adopting eq. 2.77, is reported in figure 2.2 for the case of an electron of variable energy interacting with a parabolic barrier of fixed width. Once again the computed transmission coefficient shows a strong deviations from the classical counterpart showing both the effect of tunneling and non-classical reflections.

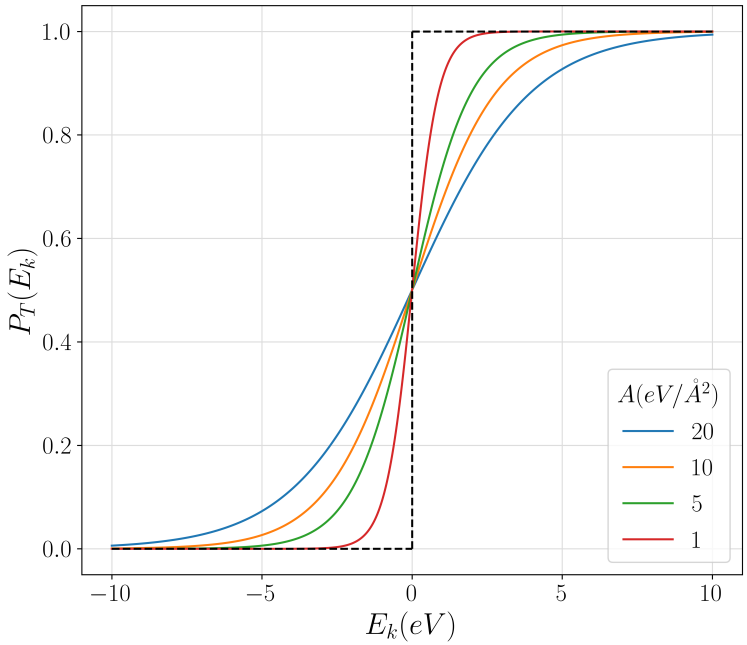

Figure 2.2: Transmission coefficient P_T computed for an electron of mass m_e and variable energy E_k, passing through a parabolic barrier characterized by a variable A parameter (listed in the legend). The dashed line represents the transmission coefficient expected for a classical particle.

2.2.3 WKB transmission coefficient

In the previous sections, some notable examples of barrier models have been presented and ad-hoc analytic procedures have been defined in order to obtain an analytic expression for their transmission coefficients. The adoption of such an analytic approach in the case of a generic barrier model is, however, often not possible and approximated procedures need to be invoked for their study. In the present section the semi-classical WKB theory, introduced in sec. 2.1.2, will be adopted in order to define an approximated formulation of the transmission coefficient associated with a generic barrier.

In order to describe in semi-classical terms the crossing of a potential energy barrier, the proper semi-classical forms for the classically accessible and forbidden regions, obtained respectively in eqs. 2.34 and 2.35, need to be matched in order to find the proper continuity relation between reflected, transmitted and incident probability currents. This operation is however not trivial given that, as discussed in sec. 2.1.2, the semi-classical hypothesis does not hold around the so-called classical turning points. For this reason, special care should be taken in defining the proper matching conditions that, as discussed in what follows, must depend upon the local structure of the potential. In order to show how these conditions can be recovered, our discussion will start from the pedagogical case of a bi-partied system in which a semi-infinite classically accessible region, on the left, is connected with a classically forbidden one, on the right. As it will be presented, under those circumstances, a linear potential approximation can be invoked around the classical turning point and Airy-functions-based matching conditions can be naturally formulated. Making use of the obtained results, the case of a generic tunneling problem will then be discussed and a general expression for the semi-classical transmission coefficient will be formulated.

Linear potential approximation and Airy functions

In order to show how the proper set of matching conditions can be obtained, let us start by considering a classical turning point located at $x = a$ dividing a classically accessible region, on the left, from a classically forbidden region, on the right. According to what presented before the following definition can be given for the semi-classical wave-function of the system:

$$\psi(x) = \begin{cases} \frac{c_1}{\sqrt{p}} e^{\frac{i}{\hbar}\int_a^x p dx} + \frac{c_2}{\sqrt{p}} e^{-\frac{i}{\hbar}\int_a^x p dx} & x < a \\ \frac{C}{2\sqrt{|p|}} e^{-\frac{1}{\hbar}\left|\int_a^x p\, dx\right|} & x > a \end{cases} \tag{2.78}$$

where the negative exponential term has been selected in order to represent the proper wave-function damping in the classically forbidden region and the proper matching condition between the C, c_1 and c_2 coefficients needs to be found. This operation can be carried out considering the local behavior of the potential around the classical turning point a that, for this purpose, can be linearly approximated according to the expression:

$$V(x) \simeq V(a) + V'(a)(x - a) \tag{2.79}$$

Recalling that for $x = a$ the potential value matches the energy of the incoming particle $V(a) = E$, the following relation can be established:

$$V(x) = E + |F_0|\,(x - a) \qquad \text{where} \qquad V'(a) = \left.\frac{\partial V(x)}{\partial x}\right|_{x=a} = -F_0 = |F_0| \tag{2.80}$$

where $F_0 < 0$ represents the force, pointing toward the left side, acting on the particle on the classical turning point. Substituting this result into the time-independent Schrödinger equation, the following expression can be easily obtained:

$$\frac{\partial^2 \psi(x)}{\partial x^2} - \frac{2m}{\hbar^2}\,|F_0|\,(x - a)\psi(x) = 0 \tag{2.81}$$

where the energy term E does not appear explicitly due to the fact that it has been implicitly selected as the potential energy reference value according to the condition: $V(x) - E = |F_0|\,(x - a)$. The previous expression can now be rewritten in a simpler form by considering the variable substitution $x \to \xi$, where the latter can be defined as:

$$\xi = \left(\frac{2m\,|F_0|}{\hbar^2}\right)^{\frac{1}{3}} (x - a) \tag{2.82}$$

In doing so, the following relation, known as Airy equation, can be obtained:

$$\frac{\partial^2 \psi(\xi)}{\partial \xi^2} - \xi\psi(\xi) = 0 \tag{2.83}$$

The solutions of this equation, here not explicitly derived for sake of brevity, are known in the literature and can be expressed according to:[9]

$$\psi(\xi) = \alpha \mathrm{Ai}(\xi) + \beta \mathrm{Bi}(\xi) \tag{2.84}$$

where $\mathrm{Ai}(\xi)$ and $\mathrm{Bi}(\xi)$ represents the Airy functions [6] defined according to:

$$\mathrm{Ai}(\xi) = \frac{1}{\pi}\int_0^\infty \cos\left(\frac{y^3}{3} + \xi y\right) dy \tag{2.85}$$

$$\mathrm{Bi}(\xi) = \frac{1}{\pi}\int_0^\infty \left[e^{-\frac{y^3}{3} + \xi y} + \sin\left(\frac{y^3}{3} + \xi y\right)\right] dy \tag{2.86}$$

Please notice how, in the asymptotic limit of $\xi \to \pm\infty$ the previous functions can be approximated by the following asymptotic forms:

$$\mathrm{Ai}(\xi) \simeq \begin{cases} \frac{1}{2\sqrt{\pi}\xi^{\frac{1}{4}}} e^{-\frac{2}{3}\xi^{\frac{3}{2}}} & \xi \to +\infty \\ \frac{1}{\sqrt{\pi}(-\xi)^{\frac{1}{4}}} \sin\left[\frac{2}{3}(-\xi)^{\frac{3}{2}} + \frac{\pi}{4}\right] & \xi \to -\infty \end{cases} \tag{2.87}$$

[9] We refer the interested reader to the demonstration given by Landau and Lifšits [1].

$$\mathrm{Bi}(\xi) \simeq \begin{cases} \frac{1}{\sqrt{\pi}\xi^{\frac{1}{4}}} e^{\frac{2}{3}\xi^{\frac{3}{2}}} & \xi \to +\infty \\ \frac{1}{\sqrt{\pi}(-\xi)^{\frac{1}{4}}} \cos\left[\frac{2}{3}(-\xi)^{\frac{3}{2}} + \frac{\pi}{4}\right] & \xi \to -\infty \end{cases} \tag{2.88}$$

In figure 2.3 the Airy functions from eqs. 2.85 and 2.86 are compared with their asymptotic counterparts from eqs. 2.87 and 2.88.

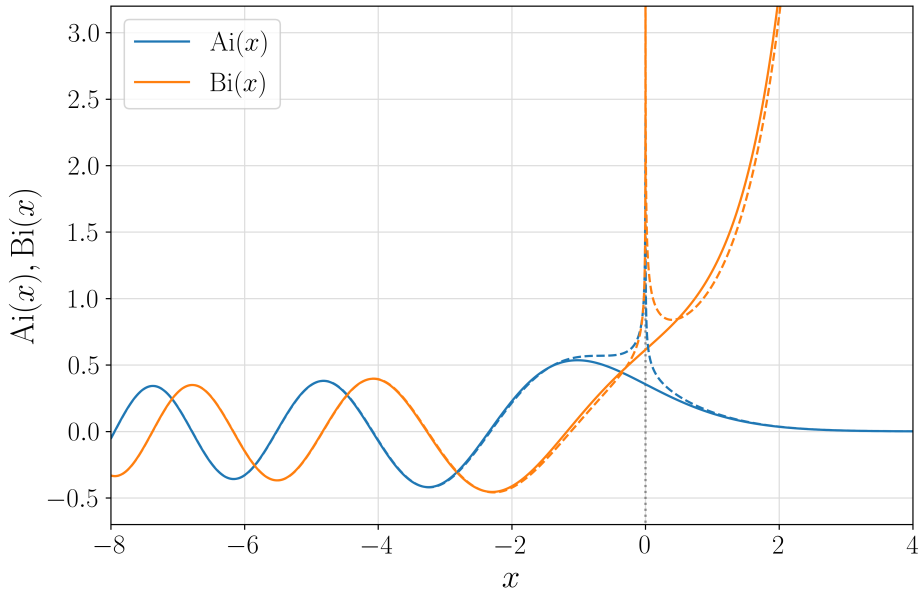

Figure 2.3: Comparison between the Airy functions from eqs. 2.85 and 2.86 (solid lines) and their asymptotic approximations from eqs. 2.87 and 2.88 (dashed lines).

Now that the proper wave-function, locally describing the system around the classical turning point a, has been obtained the matching between the semi-classical solutions from eq. 2.78 can be found by assuming that both of them hold their validity in the region in which the linearized solution from eq. 2.84 is justified. Under this hypothesis, in the linearized potential region the linear-momentum definition can easily be rewritten according to $p(x) \simeq \sqrt{-2m\,|F_0|\,(x-a)}$; from which the following expression can be obtained for the semi-classical solution in the forbidden region:[10]

$$\psi^{(x>a)}_{\mathrm{WKB}}(x) = \frac{C}{2\sqrt[4]{2m\,|F_0|\,(x-a)}} e^{-\frac{2}{3\hbar}\sqrt{2m|F_0|}(x-a)^{\frac{3}{2}}} \tag{2.89}$$

If such an expression is compared, for $x > a$ and $\xi \gg 1$, with the asymptotic form of the solution from eq. 2.84, that in explicit form, can be written according to:

$$\psi^{(x>a)}_{\mathrm{Airy}}(\xi) = \frac{\alpha}{2\sqrt{\pi}\xi^{\frac{1}{4}}} e^{-\frac{2}{3}\xi^{\frac{3}{2}}} + \frac{\beta}{\sqrt{\pi}\xi^{\frac{1}{4}}} e^{\frac{2}{3}\xi^{\frac{3}{2}}} \tag{2.90}$$

one can immediately verify how, due to the linear relation fixed by eq. 2.82 between the ξ and x variables, the β coefficient must assume vanishing value $\beta = 0$ and, as such, the proper linearized solution to consider must be defined according to:

$$\psi^{(x>a)}_{\mathrm{Airy}}(x) = \frac{\alpha}{2\sqrt{\pi}\,(x-a)^{\frac{1}{4}}\left(\frac{2m|F_0|}{\hbar^2}\right)^{\frac{1}{12}}} e^{-\frac{2}{3\hbar}\sqrt{2m|F_0|}(x-a)^{\frac{3}{2}}} \tag{2.91}$$

[10] Where, thanks to the linear dependence of the integral argument, the following relation can easily be obtained:

$$\left|\int_a^x p\,dx'\right| \simeq \frac{2}{3}\sqrt{2m\,|F_0|}(x-a)^{\frac{3}{2}}$$

By directly comparing eqs. 2.89 and 2.91, the following relation between coefficients can easily be obtained:

$$\alpha = \pi^{\frac{1}{2}} \left(2m\hbar \left|F_0\right|\right)^{-\frac{1}{6}} C \tag{2.92}$$

A completely equivalent procedure can now be applied to the classically permitted region where the semi-classical solution must be represented by the relation:[11]

$$\psi_{\mathrm{WKB}}^{(x<a)}(x) = \left(2m\left|F_0\right|\right)^{-\frac{1}{4}} (a-x)^{-\frac{1}{4}} \left[c_1 e^{-\frac{2i}{3\hbar}\sqrt{2m|F_0|}(a-x)^{\frac{3}{2}}} + c_2 e^{\frac{2i}{3\hbar}\sqrt{2m|F_0|}(a-x)^{\frac{3}{2}}}\right] \tag{2.93}$$

Observing that, according to what discussed previously in the case of the classically forbidden region, the β coefficient must assume a vanishing value $\beta = 0$; the following asymptotic expression, obtained in the case of $x < a$ and $|\xi| \gg 1$, can be adopted for the linearized solution:

$$\psi_{\mathrm{Airy}}^{(x<a)}(\xi) = \frac{\alpha}{\sqrt{\pi}(-\xi)^{\frac{1}{4}}} \sin\left[\frac{2}{3}(-\xi)^{\frac{3}{2}} + \frac{\pi}{4}\right] \tag{2.94}$$

Recalling, at this point, the ξ variable definition presented in eq. 2.82, the following expression can be obtained:

$$\psi_{\mathrm{Airy}}^{(x<a)}(x) = \frac{\alpha}{\pi^{\frac{1}{2}}(a-x)^{\frac{1}{4}}\left(\frac{2m|F_0|}{\hbar^2}\right)^{\frac{1}{12}}} \sin\left[\frac{2}{3\hbar}\sqrt{2m\left|F_0\right|}(a-x)^{\frac{3}{2}} + \frac{\pi}{4}\right] \tag{2.95}$$

that, by rewriting the sine function in exponential form, can be rewritten according to:

$$\psi_{\mathrm{Airy}}^{(x<a)}(x) = \frac{\alpha}{2i}\pi^{-\frac{1}{2}}(a-x)^{-\frac{1}{4}}\left(\frac{2m\left|F_0\right|}{\hbar^2}\right)^{-\frac{1}{12}} \left[e^{i\frac{\pi}{4}} e^{i\frac{2}{3\hbar}\sqrt{2m|F_0|}(a-x)^{\frac{3}{2}}} - e^{-i\frac{\pi}{4}} e^{-i\frac{2}{3\hbar}\sqrt{2m|F_0|}(a-x)^{\frac{3}{2}}}\right] \tag{2.96}$$

By directly comparing the relation from eqs. 2.93 and 2.96, the following relations between coefficients can be obtained:

$$c_1 = i\frac{\alpha}{2} e^{-i\frac{\pi}{4}} \pi^{-\frac{1}{2}} \left(2m\hbar\left|F_0\right|\right)^{\frac{1}{6}} \tag{2.97}$$

$$c_2 = -i\frac{\alpha}{2}\pi^{-\frac{1}{2}} e^{i\frac{\pi}{4}} \left(2m\hbar\left|F_0\right|\right)^{\frac{1}{6}} \tag{2.98}$$

At this point, by considering the condition fixed by the eqs. 2.92, 2.97 and 2.98 the searched continuity condition between the semi-classical coefficients c_1, c_2 and C, can be established according to the relations:

$$c_1 = \frac{i}{2} C e^{-i\frac{\pi}{4}} = \frac{1}{2} C e^{i\frac{\pi}{4}} \tag{2.99}$$

$$c_2 = -\frac{i}{2} C e^{i\frac{\pi}{4}} = \frac{1}{2} C e^{-i\frac{\pi}{4}} \tag{2.100}$$

that coincides with the results obtained by Landau and Lifšits [1] and by Griffiths [6].

The tunneling problem

Starting from the results presented in the previous paragraph, one can now easily discuss the problem of computing the semi-classical transmission coefficient associated with a generic potential energy barrier. In order to do so, let us indicate with a and b the two classical turning points marking the boundaries existing between a central classically forbidden region and the two neighboring semi-infinite classically accessible ones. Under these assumptions, the following piece-wise definition can be given for the semi-classical wave-function:

$$\psi(x) = \begin{cases} \frac{I}{\sqrt{p}} e^{\frac{i}{\hbar}\int_x^a p(x')dx'} + \frac{R}{\sqrt{p}} e^{-\frac{i}{\hbar}\int_x^a p(x')dx'} & x < a \\ \frac{A}{\sqrt{|p|}} e^{\frac{1}{\hbar}\int_a^x |p(x')|dx'} + \frac{B}{\sqrt{|p|}} e^{-\frac{1}{\hbar}\int_a^x |p(x')|dx'} & a < x < b \\ \frac{T}{\sqrt{p}} e^{\frac{i}{\hbar}\int_b^x p(x')dx'} & x > b \end{cases} \tag{2.101}$$

[11] Where, considering that:

$$\int_a^x \sqrt{-\epsilon(x'-a)}\, dx' = \epsilon^{\frac{1}{2}} \int_a^x (a-x')^{\frac{1}{2}} dx' = -\epsilon^{\frac{1}{2}} \int_0^{a-x} z^{\frac{1}{2}} dz = -\frac{2}{3}\epsilon^{\frac{1}{2}}(a-x)^{\frac{3}{2}}$$

the following expression for the linear-momentum integral can easily be obtained:

$$\int_a^x p dx \simeq -\frac{2}{3}\sqrt{2m\left|F_0\right|}(a-x)^{\frac{3}{2}}$$

where, as discussed before, the relations existing between the I, R, T, A and B coefficients must be properly computed through the adoption of a appropriate set of matching conditions.

In order to do so, let us firstly consider the inversion point located at $x = a$ for which, similarly to what presented in eq. 2.89, one can rewrite the classically forbidden wave-function component according to:

$$\psi_{\text{WKB}}^{(a<x<b)} = \left[2m\left|F_0\right|(x-a)\right]^{-\frac{1}{4}}\left[Ae^{\frac{2}{3\hbar}\sqrt{2m|F_0|}(x-a)^{\frac{3}{2}}} + Be^{-\frac{2}{3\hbar}\sqrt{2m|F_0|}(x-a)^{\frac{3}{2}}}\right] \tag{2.102}$$

Considering that, according to eq. 2.90, the following Airy solution can be formulated for the classically forbidden region:

$$\psi_{\text{Airy}}^{(a<x<b)}(x) = \frac{1}{2}\pi^{-\frac{1}{2}}(x-a)^{-\frac{1}{4}}\left(\frac{2m\left|F_0\right|}{\hbar^2}\right)^{-\frac{1}{12}}\left[\alpha e^{-\frac{2}{3\hbar}\sqrt{2m|F_0|}(x-a)^{\frac{3}{2}}} + 2\beta e^{-\frac{2}{3\hbar}\sqrt{2m|F_0|}(x-a)^{\frac{3}{2}}}\right] \tag{2.103}$$

one can easily observe how, by directly comparing eqs. 2.102 and 2.103, the following set of relations can be established:

$$\alpha = 2\pi^{\frac{1}{2}}\left(2m\hbar\left|F_0\right|\right)^{-\frac{1}{6}}B \tag{2.104}$$

$$\beta = \pi^{\frac{1}{2}}\left(2m\hbar\left|F_0\right|\right)^{-\frac{1}{6}}A \tag{2.105}$$

Please notice how this time, due to the non-vanishing nature of the A coefficient, the β value is non-zero and as such the asymptotic contribution of the Bi function must be considered in the study of the classically accessible region. In such a region the WKB wave-function assumes the form:

$$\psi_{\text{WKB}}^{(x<a)}(x) = \left(2m\left|F_0\right|\right)^{-\frac{1}{4}}(a-x)^{-\frac{1}{4}}\left[Ie^{\frac{2i}{3\hbar}\sqrt{2m|F_0|}(a-x)^{\frac{3}{2}}} + Re^{-\frac{2i}{3\hbar}\sqrt{2m|F_0|}(a-x)^{\frac{3}{2}}}\right] \tag{2.106}$$

while, due to what just mentioned, the proper Airy-function-based solution can be written according to:

$$\begin{aligned}\psi_{Airy}^{(x<a)}(x) = \pi^{-\frac{1}{2}}(a-x)^{-\frac{1}{4}}\left(\frac{2m\left|F_0\right|}{\hbar^2}\right)^{-\frac{1}{12}}\Bigg\{&\alpha\sin\left[\frac{2}{3\hbar}\sqrt{2m\left|F_0\right|}(a-x)^{\frac{3}{2}} + \frac{\pi}{4}\right] + \\ &+\beta\cos\left[\frac{2}{3\hbar}\sqrt{2m\left|F_0\right|}(a-x)^{\frac{3}{2}} + \frac{\pi}{4}\right]\Bigg\}\end{aligned} \tag{2.107}$$

By rewriting the last expression in exponential form, the following can easily be obtained:

$$\begin{aligned}\psi_{Airy}^{(x<a)}(x) = \frac{1}{2}\pi^{-\frac{1}{2}}(a-x)^{-\frac{1}{4}}\left(\frac{2mF_0}{\hbar^2}\right)^{-\frac{1}{12}}\Big[&(\beta - i\alpha)\,e^{i\frac{\pi}{4}}e^{\frac{2i}{3\hbar}\sqrt{2mF_0}(a-x)^{\frac{3}{2}}} + \\ &+(\beta + i\alpha)\,e^{-i\frac{\pi}{4}}e^{-\frac{2i}{3\hbar}\sqrt{2mF_0}(a-x)^{\frac{3}{2}}}\Big]\end{aligned} \tag{2.108}$$

At this point one can easily compare the just obtained relation with the one presented in eq. 2.106 obtaining the following set of conditions:

$$I = \frac{1}{2}\pi^{-\frac{1}{2}}\left(2m\hbar\left|F_0\right|\right)^{\frac{1}{6}}(\beta - i\alpha)\,e^{i\frac{\pi}{4}} \tag{2.109}$$

$$R = \frac{1}{2}\pi^{-\frac{1}{2}}\left(2m\hbar\left|F_0\right|\right)^{\frac{1}{6}}(\beta + i\alpha)\,e^{-i\frac{\pi}{4}} \tag{2.110}$$

Considering this results together with the ones obtained in eqs. 2.104 and 2.105. The following relation can be obtained between semi-classical coefficients at the a turning point:

$$I = \left(\frac{A}{2} - iB\right)e^{i\frac{\pi}{4}} \tag{2.111}$$

$$R = \left(\frac{A}{2} + iB\right)e^{-i\frac{\pi}{4}} \tag{2.112}$$

Now that the matching problem has been solved for the $x = a$ turning point, we can move our attention to the study of the inversion point located at $x = b$. The procedure required to solve this second problem

is essentially equivalent to the one just presented, with the only difference being that when considering the linear expansion of the potential around the turning point $x = b$ the force $\mathcal{F}_0 > 0$ must point toward the classically allowed region on the right side and, as such, the potential must be defined according to $V(x) = E - \mathcal{F}_0(x - b)$. If, at this point, the semi-classical wave-function expression from eq. 2.101 for the classically forbidden region is considered, the following alternative form can easily be obtained:

$$\psi_{\text{WKB}}^{(a<x<b)} = \frac{A}{\sqrt{|p|}} e^{\frac{1}{\hbar}\int_a^b |p(x')|dx' + \frac{1}{\hbar}\int_b^x |p(x')|dx'} + \frac{B}{\sqrt{|p|}} e^{-\frac{1}{\hbar}\int_a^b |p(x')|dx' - \frac{1}{\hbar}\int_b^x |p(x')|dx'} \tag{2.113}$$

that, by simple substitution, can be rewritten in compact form:

$$\psi_{\text{WKB}}^{(a<x<b)} = \frac{Ae^{\gamma}}{\sqrt{|p|}} e^{\frac{1}{\hbar}\int_b^x |p(x')|dx'} + \frac{Be^{-\gamma}}{\sqrt{|p|}} e^{-\frac{1}{\hbar}\int_b^x |p(x')|dx'} \qquad \text{where} \qquad \gamma = \frac{1}{\hbar}\int_a^b |p(x')|\, dx' \tag{2.114}$$

By invoking, once again, the linear approximation of the potential around the classical turning point $x = b$, the previous equation can easily be rewritten in terms of the force $\mathcal{F}_0$ acting on the particle:[12]

$$\psi_{\text{WKB}}^{(a<x<b)} = \frac{1}{(2m\mathcal{F}_0)^{\frac{1}{4}}(b-x)^{\frac{1}{4}}} \left[Ae^{\gamma} e^{-\frac{2}{3\hbar}(2m\mathcal{F}_0)^{\frac{1}{2}}(b-x)^{\frac{3}{2}}} + Be^{-\gamma} e^{\frac{2}{3\hbar}(2m\mathcal{F}_0)^{\frac{1}{2}}(b-x)^{\frac{3}{2}}} \right] \tag{2.115}$$

and the proper Airy-based asymptotic expression can be written according to:

$$\psi_{\text{Airy}}^{(a<x<b)}(x) = \frac{1}{2}\pi^{-\frac{1}{2}}(b-x)^{-\frac{1}{4}} \left(\frac{2m\mathcal{F}_0}{\hbar^2}\right)^{-\frac{1}{12}} \left[\alpha e^{-\frac{2}{3\hbar}\sqrt{2m\mathcal{F}_0}(b-x)^{\frac{3}{2}}} + 2\beta e^{-\frac{2}{3\hbar}\sqrt{2m\mathcal{F}_0}(b-x)^{\frac{3}{2}}} \right] \tag{2.116}$$

By comparing eqs. 2.115 and 2.116 one can easily verify how the following relations must be verified:

$$\alpha = 2Ae^{\gamma}\pi^{\frac{1}{2}}(2m\hbar\mathcal{F}_0)^{-\frac{1}{6}} \tag{2.117}$$

$$\beta = Be^{-\gamma}\pi^{\frac{1}{2}}(2m\hbar\mathcal{F}_0)^{-\frac{1}{6}} \tag{2.118}$$

At this point, one can consider the matching between the Airy asymptotic solution for the classically accessible region and the correspondent semi-classical expression for the transmitted portion of the wave-function. The former, similarly to what already presented in eq. 2.107, can be easily written according to:

$$\begin{aligned} \psi_{\text{Airy}}^{(x>b)}(x) = \pi^{-\frac{1}{2}}(x-b)^{-\frac{1}{4}} \left(\frac{2m\mathcal{F}_0}{\hbar^2}\right)^{-\frac{1}{12}} \Bigg\{ & \alpha \sin\left[\frac{2}{3\hbar}\sqrt{2m\mathcal{F}_0}(x-b)^{\frac{3}{2}} + \frac{\pi}{4}\right] + \\ & + \beta \cos\left[\frac{2}{3\hbar}\sqrt{2m\mathcal{F}_0}(x-b)^{\frac{3}{2}} + \frac{\pi}{4}\right] \Bigg\} \end{aligned} \tag{2.119}$$

The previous relation can be also rewritten in exponential form according to:

$$\begin{aligned} \psi_{Airy}^{(x>b)}(x) = \frac{1}{2}\pi^{-\frac{1}{2}}(x-b)^{-\frac{1}{4}} \left(\frac{2m\mathcal{F}_0}{\hbar^2}\right)^{-\frac{1}{12}} \Big[& (\beta - i\alpha)\, e^{i\frac{\pi}{4}} e^{\frac{2i}{3\hbar}\sqrt{2m\mathcal{F}_0}(x-b)^{\frac{3}{2}}} + \\ & + (\beta + i\alpha)\, e^{-i\frac{\pi}{4}} e^{-\frac{2i}{3\hbar}\sqrt{2m\mathcal{F}_0}(x-b)^{\frac{3}{2}}} \Big] \end{aligned} \tag{2.120}$$

Comparing such a relation with the correspondent semi-classical wave function component:

$$\psi_{WKB}^{(x>b)} = \frac{T}{(2m\mathcal{F}_0)^{\frac{1}{4}}(x-b)^{\frac{1}{4}}} e^{\frac{2i}{3\hbar}(2m\mathcal{F}_0)^{\frac{1}{2}}(x-b)^{\frac{3}{2}}} \tag{2.121}$$

[12] Please notice how, according to what discussed before, the linear momentum at the turning point b must be defined according to $p(x) = \sqrt{2m\mathcal{F}_0(x-b)}$ and as such, in the classically forbidden region ($x < b$) the following can be written: $|p(x)| = \sqrt{2m\mathcal{F}_0(b-x)}$. Taking into account this consideration, one can easily see how the following integral expression must be verified:

$$\int_b^x |p(x')|\, dx' = (2m\mathcal{F}_0)^{\frac{1}{2}} \int_b^x (b-x')^{\frac{1}{2}}\, dx' = -(2m\mathcal{F}_0)^{\frac{1}{2}} \int_0^{b-x} z^{\frac{1}{2}}\, dz = -\frac{2}{3}(2m\mathcal{F}_0)^{\frac{1}{2}}(b-x)^{\frac{3}{2}}$$

allows us to obtain the following relation between coefficients:

$$\beta + i\alpha = 0 \tag{2.122}$$

$$T = \frac{1}{2}\pi^{-\frac{1}{2}} \left(2m\hbar\mathcal{F}_0\right)^{\frac{1}{6}} (\beta - i\alpha)\, e^{i\frac{\pi}{4}} \tag{2.123}$$

Adopting the condition from eq. 2.122 into eq. 2.123 allows us to obtain:

$$T = \beta\pi^{-\frac{1}{2}} \left(2m\hbar\mathcal{F}_0\right)^{\frac{1}{6}} e^{i\frac{\pi}{4}} = -i\alpha\pi^{-\frac{1}{2}} \left(2m\hbar\mathcal{F}_0\right)^{\frac{1}{6}} e^{i\frac{\pi}{4}} \tag{2.124}$$

By simply comparing this result with the one presented in eqs. 2.117 and 2.118 one can easily observe how the following relation between coefficients must hold:

$$A = \frac{i}{2} T e^{-\gamma} e^{-i\frac{\pi}{4}} \tag{2.125}$$

$$B = T e^{\gamma} e^{-i\frac{\pi}{4}} \tag{2.126}$$

that, according to eq. 2.111, translates to the condition:

$$I = iT\left(\frac{1}{4}e^{-\gamma} - e^{\gamma}\right) \tag{2.127}$$

Starting from this result and recalling the definition of transmission coefficient from eq. 2.47 the following result can easily be obtained:

$$P_T = \frac{1}{\left(\frac{1}{4}e^{-\gamma} - e^{\gamma}\right)^2} = \frac{e^{-2\gamma}}{\left[1 - \left(\frac{e^{-\gamma}}{2}\right)^2\right]^2} \qquad \text{with} \qquad \gamma = \frac{1}{\hbar}\int_a^b |p(x')|\, dx' \tag{2.128}$$

That represents the desired WKB estimate for the transmission coefficient.

2.3 The origin of tunneling splitting

In the previous sections, the concept of quantum tunneling has been introduced as a direct consequence of the quantum nature of physical systems and the tunneling properties displayed by an unbounded quantum particle interacting with a potential energy barrier have been characterized in terms of an ideal scattering experiment. These examples, despite being of fundamental importance in understanding the nature of the tunneling process, only cover a small fraction of the phenomenology connected to the quantum tunneling effect that, in fact, plays a fundamental role in many other physical situations. In this section, the case of a bounded symmetrical bi-stable system will be considered as a pedagogical example and the origin of the so-called tunneling splitting will be discussed. The study and determination of this quantity represent the core of this thesis work and, as will be presented in section 2.5, it represents an interesting spectroscopic observable that influence the behavior of a multitude of molecular systems.

In order to understand what does the term tunneling splitting means, let us consider a simple bi-stable potential profile characterized by two equivalent, symmetry-related, potential energy sites hereafter indicated with the labels A and B. Let us suppose that each one of these sites can be described by a set of "site-states" $|\phi_{i,n}\rangle$, with $i \in [A, B]$ and $n = 0, 1, 2...$, capturing the behavior that would be expected from the potential site itself under the hypothetical absence of interaction with the other one. At this point, let us focus our attention on the couple of symmetry-degenerate energy ground-states, $|\phi_A\rangle = |\phi_{A,0}\rangle$ and $|\phi_B\rangle = |\phi_{B,0}\rangle$, associated to each site that, by hypothesis, are assumed to be located at an energy ε lower than the top of the barrier dividing the two sites. Let us, for sake of simplicity, operate under the assumption of dealing with a barrier large enough to both justify the hypothesis of considering the two site-states as orthogonal $\langle\phi_A|\phi_B\rangle = 0$ and to ensure a large separation in energy between states belonging to the same site. Under these hypotheses, the couple of low lying states $|\phi_A\rangle$ and $|\phi_B\rangle$ can be used as a basis-set to expand the Hamiltonian of the system from which the first two system eigenvalues can be computed. Under these circumstances, the tunneling effect plays a fundamental role in mediating the interaction between states that, due to their lower energy in respect to the barrier top, would be classically isolated. This interaction results in a non-diagonal Hamiltonian matrix $\mathbf{H}$ that can be represented according to:

$$\mathbf{H} = \begin{pmatrix} \varepsilon & V \\ V & \varepsilon \end{pmatrix} \tag{2.129}$$

where $\varepsilon = \langle\phi_A|\hat{H}|\phi_A\rangle = \langle\phi_B|\hat{H}|\phi_B\rangle$ represents the energy of the site states while $V = \langle\phi_A|\hat{H}|\phi_B\rangle = \langle\phi_B|\hat{H}|\phi_A\rangle < 0$ represents the tunneling mediated interaction term. Starting from such a definition the eigenvalues and eigenstates of the system can be computed by simple diagonalization allowing us to obtain the following:

$$|\psi_0\rangle = \frac{1}{\sqrt{2}}|\phi_A\rangle + \frac{1}{\sqrt{2}}|\phi_B\rangle \qquad \text{with} \qquad \lambda_0 = \varepsilon + V \tag{2.130}$$

$$|\psi_1\rangle = \frac{1}{\sqrt{2}}|\phi_A\rangle - \frac{1}{\sqrt{2}}|\phi_B\rangle \qquad \text{with} \qquad \lambda_1 = \varepsilon - V \tag{2.131}$$

As can be seen from such results, the proper set of eigenstates to describe the tunneling system is defined as the symmetric and anti-symmetric combination of site-states that, in turn, corresponds to a non-degenerate energy spectrum in which a doublet of level is observed. The tiny energy separation δE between the two states of the doublet is usually referred to as tunneling splitting and it is directly dictated by the magnitude of the coupling term V:

$$\Delta E = E_1 - E_0 = 2|V| \tag{2.132}$$

The symmetry of the system plays a fundamental role in the definition of the problem structure both by ensuring the degeneracy of the set of site-states, fundamental in practical terms for the observation of the small tunneling-induced splitting, and by imposing a precise symmetry relation for the structure of the system eigenstates. As a matter of fact, the symmetry operator $\hat{R}$ commutes with the Hamiltonian $\hat{H}$ and, as such, share with it a common set of eigenstates. This observation, together with the fact that the symmetry operator and the identity one $\hat{I}$ form a group, justifies the need for the eigenstates to either have symmetrical or anti-symmetrical character.

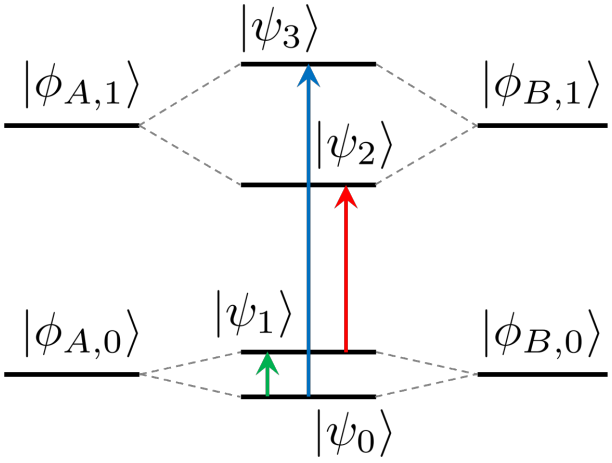

Figure 2.4: Schematic representation of the electric-dipole-mediated transition allowed by the selection rules for the case of the first two doublet of levels $|\psi_n\rangle$, with $n = 0, 1, 2, 3$, originated from the mixing of the site-states $|\phi_{s,i}\rangle$, with $s = A, B$ and $i = 0, 1$.

Excited-state tunneling splitting

In the previous paragraph, the concept of tunneling splitting has been introduced in the context of the tunneling-induced mixing of ground site-states located at an energy lower than the one characterizing the top of the barrier. This phenomenon is, however, not a particular attribute of the sole ground-state, but, quite on the contrary, is a rather general property of all the site-states located under the barrier top. In general terms, all the couples of site-state can mix giving rise to an energy spectrum characterized by a progression of doublets of energy levels, each one of which is spaced by tunneling splitting of variable entity with a higher splitting encountered for energy levels close to the barrier top.

Also in this case the symmetry of the system plays a crucial role in the definition of the nature of the involved states with the lower one of each doublet being symmetric and the upper one being anti-symmetric. This, clearly, has strong implications on the spectroscopic properties of the system: if for example an electric-dipole-mediated transition is induced between states belonging to different doublets,

the selection rules will allow only the transition from the lower state of the lower doublet to the upper state of the upper one and the transition from the upper state of the lower doublet and the lower state of the upper one. A schematic representation of the allowed transitions is visible in figure 2.4. This will be fundamental in understanding the spectroscopic observation presented in section 2.5 in which couples of spectroscopic transition, separated by an energy equivalent to the sum of the ground-state and first-excited state tunneling splitting, will be observed.

2.3.1 The tunneling frequency

In the previous paragraph, the origin of the ground-state tunneling splitting has been introduced in simple terms as the difference in energy originated from the mixing of site-states localized in the minima. In this paragraph, the effects induced by this energy separation on the time-evolution of the system will be presented and the concept of tunneling frequency will be introduced.

In order to discuss the dynamics of the system, let us consider a generic wave-function $\psi(x,t)$ originated from the superposition of the two eigenstates $\psi_0(x)$ and $\psi_1(x)$ belonging to the ground state doublet. The time evolution of this quantity can be expressed according to:

$$\psi(x,t) = c_0(t)\psi_0(x) + c_1(t)\psi_1(x) \tag{2.133}$$

where the time dependence of the coefficients c_j, with $j = 0, 1$, is dictated, according to eq. 2.6, by the relation:

$$c_j(t) = c_j(0)e^{-\frac{iE_j t}{\hbar}} \tag{2.134}$$

The probability distribution $\rho(x,t) = |\psi(x,t)|^2$ correspondent to the wave-function from eq. 2.133 can easily be written according to:

$$\rho(x,t) = |c_0(t)|^2 |\psi_0(x)|^2 + |c_1(t)|^2 |\psi_1(x)|^2 + c_0^*(t)c_1(t)\psi_0^*(x)\psi_1(x) + c_0(t)c_1^*(t)\psi_0(x)\psi_1^*(x) \tag{2.135}$$

that, by recalling the relation from eq. 2.134, can be easily rearranged in order to obtain the following form:

$$\begin{aligned}\rho(x,t) &= P_0 |\psi_0(x)|^2 + P_1 |\psi_1(x)|^2 + 2\mathrm{Re}\left[c_0^*(0)c_1(0)e^{\frac{-i\Delta E t}{\hbar}}\psi_0^*(x)\psi_1(x)\right] = \\ &= P_0 |\psi_0(x)|^2 + P_1 |\psi_1(x)|^2 + 2\sqrt{P_0 P_1}\psi_0(x)\psi_1(x)\cos\left(\frac{\Delta E t}{\hbar}\right)\end{aligned} \tag{2.136}$$

where $\Delta E = E_1 - E_0$ represents the tunneling splitting introduced in eq. 2.132 while $P_j = |c_j(t)|^2 = |c_j(0)|^2$, with $j = 0, 1$, represents the stationary population associated to the j-th eigenstate. What we have obtained in the previous equation, represents the relation describing the time-evolution of the overall probability distribution. This formulation, however, does not give a clear picture of the probability dynamics within each site and, for this reason, we should rewrite it explicitly referring to the site-states, $\phi_A(x)$ and $\phi_B(x)$, introduced in the previous paragraph. If this is done one can verify how, with little elaboration, the following relation can be obtained:

$$\begin{aligned}\rho(x,t) = \phi_A(x)\phi_B(x)\left[P_0 - P_1\right] &+ \frac{1}{2}\left[P_0 + P_1 + 2\sqrt{P_0 P_1}\cos\left(\frac{\Delta E t}{\hbar}\right)\right]\phi_A(x)^2 + \\ &+ \frac{1}{2}\left[P_0 + P_1 - 2\sqrt{P_0 P_1}\cos\left(\frac{\Delta E t}{\hbar}\right)\right]\phi_B(x)^2\end{aligned} \tag{2.137}$$

At this point one can clearly see how if an equal value is set in eq. 2.133 for both c_0 and c_1, or, in equivalent terms, if at the time $t = 0$ the probability is completely localized onto the site A, the following relation can easily be obtained:

$$\rho(x,t) = \frac{1}{2}\phi_A(x)^2\left[1 + \cos\left(\frac{\Delta E t}{\hbar}\right)\right] + \frac{1}{2}\phi_B(x)^2\left[1 - \cos\left(\frac{\Delta E t}{\hbar}\right)\right] \tag{2.138}$$

from which the following can be written:[13]

$$\rho(x,t) = \phi_A(x)^2\cos^2\left(\frac{\Delta E t}{2\hbar}\right) + \phi_B(x)^2\sin^2\left(\frac{\Delta E t}{2\hbar}\right) \tag{2.139}$$

[13] Please notice how the following elementary relation has been employed:

$$\cos(x) = \cos^2\left(\frac{x}{2}\right) - \sin^2\left(\frac{x}{2}\right) = 2\cos^2\left(\frac{x}{2}\right) - 1$$

As can be easily seen the just obtained equation predict an oscillatory behavior in which the probability of finding the particle is continuously transferred, thanks to tunneling, between the two potential sites with an overall oscillation frequency ν_{osc} defined by:

$$\nu_{\text{osc}} = \frac{\Delta E}{2\pi\hbar} = \frac{\Delta E}{h} \tag{2.140}$$

Please notice how during each oscillation the barrier is crossed two times and, as such, the overall oscillation frequency represents half the value of the frequency associated to the tunneling event $\nu_{\text{t}} = 2\nu_{\text{osc}}$.

2.3.2 The Herring formula

In the present section, an important relation known as the Herring formula will be derived following the procedure illustrated by Garg [7]. This approximated relation, fundamental for the derivation of the WKB tunneling splitting estimate presented in sec. 2.4.2, will allow us to relate the ground state tunneling splitting for a bi-stable potential system to the value of both the ground-state site-function and its first derivative computed at the barrier top.

In order to show how this relation can be obtained let us start by recalling the result obtained in eq. 2.139 for a bi-stable system characterized by a probability distribution localized, for $t = 0$, in the site A. Let us assume the barrier maximum to be located at the origin ($x = 0$) and let us indicate with A the rightmost site. Under these hypotheses, the population $P_A(t)$ of the site A, that can be computed by simple integration of the positive semi-axis, can be expressed according to:

$$P_A(t) = \int_0^{+\infty} p(x,t)dx = \cos^2\left(\frac{\Delta E}{2\hbar}t\right) \tag{2.141}$$

By computing the time derivative of both terms, the following equation can easily be obtained:

$$\int_0^{+\infty} \frac{\partial p(x,t)}{\partial t}dx = -\frac{\Delta E}{2\hbar}\sin\left(\frac{\Delta E}{\hbar}t\right) \tag{2.142}$$

Recalling the continuity relation from eq. 2.39, the following can be written:

$$\begin{aligned}\frac{\partial p(x,t)}{\partial t} &= -\frac{i\hbar}{2m}\frac{\partial}{\partial x}\left[\psi(x,t)\frac{\partial}{\partial x}\psi^*(x,t) - \psi^*(x,t)\frac{\partial}{\partial x}\psi(x,t)\right] = \\ &= -\frac{\hbar}{m}\frac{\partial}{\partial x}\text{Im}\left[\psi^*(x,t)\frac{\partial}{\partial x}\psi(x,t)\right]\end{aligned} \tag{2.143}$$

Substituting this result into eq. 2.142 allow us to simplify the integral form obtaining the following relation:

$$-\frac{\hbar}{m}\text{Im}\Big[\psi^*(0,t)\psi'(0,t)\Big] = -\frac{\Delta E}{2\hbar}\sin\left(\frac{\Delta E}{\hbar}t\right) \tag{2.144}$$

where, a part from a global phase factor, the wave-function for the system can be written, in a manner compatible with the eq. 2.139, according to the form:

$$\psi(x,t) = \phi_A(x)\cos\left(\frac{\Delta E}{2\hbar}t\right) + i\phi_B(x)\sin\left(\frac{\Delta E}{2\hbar}t\right) \tag{2.145}$$

Recalling that the symmetry of the system imposes that $\phi_A(x) = \phi_B(-x)$, one can easily see how the relations $\phi_A(0) = \phi_B(0)$ and $\phi'_A(0) = -\phi'_B(0)$ must be satisfied. Taking into account these consideration and starting from the definition in eq. 2.145, the following expression can be obtained for the left hand side of eq. 2.144:

$$\text{Im}\left[\psi^*(0,t)\frac{\partial}{\partial x}\psi(0,t)\right] = 2\phi_a^*(0)\phi'_a(0)\sin\left(\frac{\Delta E}{2\hbar}t\right)\cos\left(\frac{\Delta E}{2\hbar}t\right) = \phi_a^*(0)\phi'_a(0)\sin\left(\frac{\Delta E}{\hbar}t\right) \tag{2.146}$$

By comparing the results from eqs. 2.144 and 2.146 the following relation can easily be obtained:

$$\Delta E = \frac{2\hbar^2}{m}\phi_a^*(0)\phi'_a(0) \tag{2.147}$$

that represents the Herring formula obtained by Garg [7].

2.4 Theoretical methods for computing tunneling splitting

The theoretical estimation of tunneling splittings represents a challenging problem whose complexity rapidly increases with the dimensionality of the system. Many theoretical tools have been adopted in the literature throughout the years to tackle the problem each of which is characterized by a different level of accuracy and connected complexity. These ranges from numerical treatment like path-integral molecular dynamics method [8–10], diffusion Monte Carlo [11, 12], quantum mechanical [13–16], spectral and pseudo-spectral methods [17, 18]; to approximated treatment like the semi-classical WKB approach [19] and the instanton theory [20, 21]. Giving a formal and complete description of all the before mentioned approaches and, as such, comparing their performances and accuracy is very difficult and somewhat out of the scope of this thesis. Nevertheless, we think that giving a general description of the concept at the foundation of some of these methods can be useful to give to the reader an insight into the theoretical framework in which the work presented in this thesis must be considered. With this spirit in mind, we will start, in sec. 2.4.1, by discussing the solution of the Hamiltonian eigenvalue problem by expansion over a set of basis-functions. This discussion will be complemented by the more in-depth analysis presented in chapter 6 where our approach to the definition of an asymptotically inspired basis-set will be presented. In sec. 2.4.2, the WKB approach, already introduced in sec. 2.1.2, will be adapted to compute tunneling splitting estimates while, in sec. 2.4.3, a gentle introduction to the path-integral formulation and the related instanton methods will be discussed.

2.4.1 Basis-set expansion

The solution of the Hamiltonian eigenvalue problem by expansion over a properly constructed set of basis functions probably represents the most straightforward way to approach the problem of tunneling splitting computation and a wide range of basis-sets, either orthogonal or non-orthogonal, has been applied throughout the years in the study of the vibrational and vibro-rotational energy spectrum of molecules [22, 23]. In practical terms, once the proper definition of a generic complete basis-set has been chosen, some form of eigenvalue problem, explicitly derived in generalized form in appendix B, can be obtained. Such a matrix problem can be solved by invoking the proper diagonalization procedure capable of returning the eigenvalues and the eigenvectors of the system. The conceptual simplicity associated to these approaches, however, should not overshadow the intrinsic difficulties encountered in their application both in terms of the rapidly increasing number of basis functions, required in order to treat multidimensional many-body nuclear systems, and the complexity associated with the evaluation, through multidimensional integration, of the required matrix elements. Many techniques to mitigate these problems have been invoked in the literature with variable degrees of success [24].

2.4.2 The WKB tunneling splitting estimate

The semi-classical approximation presented in sec. 2.1.2 and already applied, in sec. 2.2.3, to the problem of computing the transmission coefficient of a generic barrier, can also be adapted to obtain tunneling splitting estimates in one and many dimensions. The core of the process is represented by the Herring formula already derived, in the context of quantum tunneling, in sec. 2.3.2. As a matter of fact, once the proper semi-classical site wave function has been constructed, such a relation can be directly applied to the problem in order to obtain the correspondent tunneling splitting approximation.

In one dimension the process of finding the proper semi-classical solution is simple and can be achieved starting from the concept already presented in this introductory chapter. The simplicity of the notation however should not overshadow the intrinsic sensitivity of the final result to the set of matching conditions employed to connect semi-classical solutions belonging to classically allowed and forbidden regions. An example of this can be easily appreciated by analyzing the tunneling splitting estimate obtained by Landau and Lifšits [1] that, according to the results obtained by Garg [7], appears to recover the wrong pre-exponential factor for the ground-state splitting. Both of the treatments just mentioned will be discussed in detail in the final part of this section.

The study of multidimensional problems can also be tackled by the WKB approach. The evaluation of the connection formulas between classically accessible and forbidden regions together with the wave-function propagation through classically inaccessible regions is however far more complex and beyond the scope of this introductory section. We point the interested reader to the original procedure proposed by Takada and Nakamura [19].

The Landau's pre-exponential factor

In order to understand the procedure proposed by Landau and Lifšits [1] to find the tunneling splitting estimate in the case of a double minimum potential, let us start by considering a single potential well in which the classically accessible region is contained between two classical turning point located at $x = a$ and $x = b$ such that $0 < b < x < a$. Under those circumstances, the problem of finding the proper form of the semi-classical wave-function in the classically accessible region can be broken down into a double matching problem in which the WKB solution for the classically accessible region is connected to the proper exponential damping in the classically forbidden ones. As the reader may recall this is exactly the same problem discussed in the first paragraph of sec. 2.2.3 where the semi-classical wave-function for a classically accessible region on the left has been matched with the proper solution for the classically forbidden region on the right. This represents exactly the situation encountered at the turning point located at $x = a$ and, as such, the proper semi-classical solution for the classically accessible region can be found substituting the results form eqs. 2.99 and 2.100 into the first relation in eq. 2.78. In doing so, the following equation can easily be obtained:

$$\psi(x) = \frac{C}{\sqrt{p}} \cos\left(\frac{1}{\hbar}\int_b^x p\,dx - \frac{\pi}{4}\right) \tag{2.148}$$

where C represents the amplitude of the exponential damping characterizing the forbidden region for $x > a$. Following a similar procedure the proper matching can be found also for the $x = b$ turning point. In doing so, the following result can be obtained:

$$\psi(x) = \frac{C'}{\sqrt{p}} \cos\left(\frac{1}{\hbar}\int_x^a p\,dx - \frac{\pi}{4}\right) \tag{2.149}$$

where C' represent the amplitude of the exponential damping characterizing the forbidden region for $x < b$. The solutions from eqs. 2.148 and 2.149, obtained considering the separate matching at the two turning points, must represent the same semi-classical wave-function for the classically accessible region and, as such, the sum of their cosine phases must, as discussed by Landau and Lifšits [1], be a multiple of π:[14]

$$\frac{1}{\hbar}\int_b^a p\,dx - \frac{\pi}{2} = n\pi \tag{2.150}$$

where n represents the number of zeros of the wave-function and, as such, the order of the stationary state. Please notice how this condition directly translates to the relation $C = (-1)^n C'$ for the amplitude coefficients in the classically forbidden regions.

Now that the relation between the obtained solutions has been established one can normalize the wave-function from eq. 2.148 by simple integration over the classically accessible region. Please observe how, given the exponential damping observed in the classically forbidden regions, a negligible error is expected. For large values of n, where the smallness of the De Broglie wave function ensures the validity of the semi-classical hypothesis, the integral argument is represented by the square of a rapidly oscillating cosine that, as such, can be approximated by its average value of $1/2$. In doing so the following can be obtained:

$$\int_b^a |\psi(x)|^2\,dx \simeq \frac{C^2}{2}\int_b^a \frac{1}{p(x')} = \frac{\pi C^2}{2m\omega} = 1 \qquad \Longrightarrow \qquad C = \sqrt{\frac{2m\omega}{\pi}} \tag{2.151}$$

where $\omega = 2\pi/T$ represents the frequency of the periodic classical motion of the particle. Applying the obtained normalization condition to eq. 2.148 allow us to obtain the following expression:

$$\psi(x) = \sqrt{\frac{2\omega}{\pi v}} \cos\left(\frac{1}{\hbar}\int_b^x p\,dx - \frac{\pi}{4}\right) \tag{2.152}$$

where v represents the velocity of the particle. Please notice how the ω term explicitly depends upon the energy of the state.

[14] Please notice how integrating over an entire period of the classical motion the following expression can easily be obtained:

$$\frac{1}{2\pi\hbar}\oint p\,dx = n + \frac{1}{2} \qquad \text{where} \qquad \oint p\,dx = \int_b^a p\,dx$$

that represent the Bohr-Sommerfeld quantization rule of the old quantum theory.

Now that this solution has been recovered one can go back to the problem of computing the proper tunneling splitting estimate. This can easily be achieved by invoking the Herring formula from eq. 2.147 in which the proper wave-function value for the right site can easily be constructed starting from the results already presented. As a matter of fact, in the classically forbidden region near the barrier (for $0 \leq x < b$), the following WKB wave-function expression can be invoked:

$$\psi(x) = \frac{C}{2\sqrt{|p|}} e^{\frac{1}{\hbar}\int_b^x |p|\, dx} \tag{2.153}$$

By recalling the proper definition of the coefficient C, obtained in eq. 2.151, the previous relation can easily be rewritten according to the form:

$$\psi(x) = \sqrt{\frac{m\omega}{2\pi\,|p|}} e^{\frac{1}{\hbar}\int_b^x |p|\, dx} \tag{2.154}$$

Starting from this result one can easily appreciate how for $x = 0$ the following definitions must be obtained:

$$\psi(0) = \sqrt{\frac{\omega}{2\pi v_0}} e^{-\frac{1}{\hbar}\int_0^b |p|\, dx} \qquad \text{and} \qquad \psi'(0) = \frac{m v_0}{\hbar}\psi(0) \tag{2.155}$$

where $v_0 = |p(0)|\,/m = \sqrt{2(V_0 - E)/m}$. By directly substituting these results into the Herring formula from eq. 2.147, the following can easily be obtained:

$$\Delta E = \frac{\omega\hbar}{\pi} e^{-\frac{1}{\hbar}\int_{-b}^b |p|\, dx} \tag{2.156}$$

This result represents the tunneling splitting estimate proposed by Landau and Lifšits [1].

The Garg's pre-exponential factor

The approach followed by Garg [7] to obtain a semi-classical estimate of the tunneling splitting is quite different from the one proposed by Landau and Lifšits [1] and it is based upon the direct matching between the WKB solution for the classically forbidden region, strictly valid under the barrier, and the harmonic approximation of the wave-function near the minima at $x = \pm a$. Please notice how, in order to justify the matching procedure, the harmonic solution should hold its validity for a reasonable portion of the classically forbidden region in order to ensure some form of overlap with the semi-classical solution.

If the rightmost minimum is considered the proper semi-classical solution for the classically forbidden region should be represented by the form:

$$\psi^{\mathrm{WKB}}(x) = \frac{C}{\sqrt{|v(x)|}} e^{\frac{1}{\hbar}\int_0^x |p(x')| dx'} \tag{2.157}$$

where $v(x)$ represents the velocity of the particle while C represents the arbitrary coefficient to be computed through the application of the matching conditions. At the same time the harmonic oscillator ground state for the right minimum, centered at $x = a$, can be written according to the form:

$$\psi^{\mathrm{HO}}(x) = \sqrt[4]{\frac{m\omega}{\pi\hbar}} e^{-\frac{m\omega}{2\hbar}(x-a)^2} \tag{2.158}$$

where the ω parameter sets the width of the parabolic approximation near the minimum. In order to show how the matching condition can be obtained let us recover an expression for the semi-classical particle momentum $p(x)$ in terms of the harmonic oscillator parameters. This can be done by considering the action of the $\hat{p}^2$ operator on the harmonic solution $\psi^{\mathrm{HO}}(x)$ that leads to: $\hat{p}^2\psi^{\mathrm{HO}}(x) = p(x)^2\psi^{\mathrm{HO}}(x)$. Doing so, allow us to obtain the following relation:

$$p(x)^2 = \hbar m\omega \left[1 - \frac{m\omega}{\hbar}(x-a)^2\right] \tag{2.159}$$

Considering that $p(x)$ must vanish at the classical turning point, the following equality must be satisfied:

$$\frac{m\omega}{\hbar}(a'-a)^2 = 1 \tag{2.160}$$

or, in equivalent terms, the expression from eq. 2.159 can be rewritten according to:

$$p(x)^2 = m^2\omega^2\left[(a'-a)^2 - (x-a)^2\right] \tag{2.161}$$

In the classically forbidden region the linear momentum $p(x)$ assumes pure imaginary value and its modulus can be expressed by the relation:

$$|p(x)| = m\omega\sqrt{(a-x)^2 - (a-a')^2} \tag{2.162}$$

If this expression is adopted in eq. 2.157 and, as suggested by Garg [7], the $(a-a')^2$ term is omitted from the pre-exponential factor, the following relation can be recovered:

$$\psi^{\text{WKB}}(x) = \frac{C}{\sqrt{\omega(a-x)}} e^{\frac{1}{\hbar}\int_0^{a'}|p(x')|dx' - \frac{m\omega}{\hbar}\int_x^{a'}\sqrt{(a-x)^2-(a-a')^2}dx} \tag{2.163}$$

As suggested by Garg [7], the integral term can be rewritten in approximated form according to:

$$-\frac{m\omega}{\hbar}\int_x^{a'}\sqrt{(a-x)^2-(a-a')^2}dx \simeq -\frac{m\omega}{2\hbar}(a-x)^2 + \ln\left[\frac{2(a-x)}{a-a'}\right]^{\frac{1}{2}} + \frac{1}{4} + \mathcal{O}\left(\frac{a-a'}{a-x}\right)^2 \tag{2.164}$$

Substituting the just obtained approximated form into eq. 2.163, the following expression can be obtained for the semi-classical solution in the forbidden region:

$$\psi^{\text{WKB}}(x) = \sqrt{2}C\frac{e^{\frac{1}{4}}}{\sqrt{\omega(a-a')}} e^{\frac{1}{\hbar}\int_0^{a'}|p(x')|dx'} e^{-\frac{m\omega}{2\hbar}(a-x)^2} \tag{2.165}$$

At this point, the relation from eq. 2.165 can be compared with the one from eq. 2.158 allowing us to obtain, recalling the definition of classical turning point from eq. 2.160, the following expression for the C coefficient:

$$C = \sqrt[4]{\frac{\omega^2}{4\pi e}} e^{-\frac{1}{\hbar}\int_0^{a'}|p(x')|dx'} \tag{2.166}$$

Now that the expression for the coefficient C has been obtained the Herring formula from eq. 2.147 can be invoked to compute the tunneling splitting. In order to do so, one can easily see how, starting from eq. 2.157, the following relation can be obtained:

$$\psi'(0) = \frac{m|v(x)|}{\hbar}\psi(0) \tag{2.167}$$

from which the tunneling splitting can be computed according to:

$$\Delta E = 2\hbar C^2 = \frac{\hbar\omega}{\sqrt{e\pi}} e^{-\frac{1}{\hbar}\int_{-a'}^{a'}|p(x')|dx'} \tag{2.168}$$

This expression represents the proper form for estimating the tunneling splitting according to the WKB approximation; its calculation, however, must be carried on with care due to the fact that the integration limit coincides with the classical turning point that, as such, must be carefully computed. In order to avoid this issue one can extend the integration limit to the potential minima at $x = \pm a$ obtaining the following result [7]:

$$\Delta E = 2\hbar\omega\sqrt{\frac{m\omega a^2}{\pi\hbar}} e^A e^{-\frac{S_0}{\hbar}} \tag{2.169}$$

where S_0 and A are defined according to:

$$S_0 = \int_{-a}^{a}\sqrt{2mV(x)}dx \tag{2.170}$$

$$A = \int_0^a\left[\frac{m\omega}{\sqrt{2mV(x)}} - \frac{1}{a-x}\right]dx \tag{2.171}$$

Please notice how the form from eq. 2.169 has also the side effect of showing the true dependence of the pre-exponential factor upon the $\hbar^{1/2}$ factor [7].

2.4.3 Path integral formulation

Up until now, the description of a quantum mechanical process has been carried out in terms of time-evolution of the correspondent wave-function and concepts like the possible path followed by the system have never been invoked. In this section, this idea will be explored and the path integral formulation of quantum mechanics will be briefly presented.

In order to give to the reader an intuitive idea of the meaning of path integral let us start by re-examining the classical textbook example of the double-slit experiment in which a series of quantum particles is directed toward a screen in which two apertures are present. On the other side of the screen a mobile detector, moving parallel to the screen, is installed with the purpose of estimating, when a large number of single-particle experiments are performed, the probability of detecting a particle as a function of the position in space. It is a well-known fact that whenever one of the two apertures is closed a smooth probability distribution, characterized by a single maximum, is observed behind the open aperture while, when both apertures are open, a diffraction pattern is observed across the whole screen. This clearly shows how the arrival probability distribution on the screen $p(x)$ is not equal to the sum of the individual probability distributions, $p_1(x)$ and $p_2(x)$, associated to the particle passing through one of the slits and that some sort of complex amplitude $\phi(x)$, defined by the sum of the oscillating amplitudes $\phi(x) = \phi_1(x) + \phi_2(x)$ associated to the passage through each slit, must be invoked in order to explain the observed pattern $p(x) = |\phi(x)|^2$. This idea of interfering alternatives represents a powerful illustrative tool in which the probability of transferring the particle from the point source to a given point on the detector plane can be expressed by the combination of two alternative possible paths across the screen. This idea can be easily used to formalize the concept of path $x(t)$ in space: let us suppose that an infinite series of screens is installed between the source and the detector and that a progressively bigger amount of holes is created on each screen. In doing so one can imagine that each path between different aperture on the screens, connecting the source to the detector plane, represents a possible alternative and, as such, that the amplitude associated with each path $\phi[x(t)]$ must contribute to the final amplitude. If an infinite number of holes is drilled on each screen, removing it completely from the path of the particle, an infinite set of adjacent paths must be considered in order to describe the behavior of the particle.

In general terms, if a function $K(b, a)$, also referred to as kernel, is defined as the amplitude associated with the transfer of a particle from the point a to the point b, such that the probability of the process is given by $p(b, a) = |K(b, a)|^2$, the sum of all the amplitudes $\phi[x(t)]$ associated to all paths $x(t)$, starting from a at the time t_a and ending in b at the time t_b, must be considered:

$$K(b, a) = \sum_{x(t)} \phi[x(t)] \qquad \forall x(t) : x(t_a) = a \wedge x(t_b) = b \tag{2.172}$$

As can be seen from the just obtained relation all the path contributes equally to the overall final amplitude with the only difference being represented by their phases. As discussed by Feynman [25], one can assume the phase of each amplitude term to be proportional to the action integral A across the path such that:

$$\phi[x(t)] \propto e^{\frac{i}{\hbar} A[x(t)]} \tag{2.173}$$

where the proportionality constant must be properly selected in order to normalize the kernel function K [25]. At this point, one can easily verify how this assumption ensures the correct behavior at the classical limit. The trajectory $\tilde{x}(t)$ followed by a classical particle can easily be computed enforcing the minimum action principle that identifies the classical path as the one correspondent to an extremum of the action A. In the classical limit, in which A is substantially bigger than the $\hbar$ value, a small variation of a generic path $x(t)$ from the classical one $\tilde{x}(t)$ induces a small variation, in the classical energy scale, of the correspondent action that, however, given the smallness of $\hbar$, results in a very abrupt change in the phase leading to a rapid oscillatory behavior [25]. This directly translates to the fact that infinitesimally close paths assume opposite phases and, as such, cancel each other out from the summation in eq. 2.172. The only path surviving this effect is represented by the least action one that being located in a minimum of the action is, in an infinitesimal sense, surrounded by a region of nearly in-phase paths.

In what follows, starting from these early considerations, the path integral formalism will be derived and a general discussion about how it can be used to estimate tunneling splitting in bi-stable systems will be presented.

The canonical density matrix and the evolution operator

In order to discuss how the path integral formalism can be derived let us start by considering the simple case of a single particle moving in a one dimensional space under the influence of a potential $V(x)$. The Hamiltonian operator describing such a system assumes the form:

$$\hat{H} = \frac{\hat{p}^2}{2m} + V(\mathbf{x}) = \hat{K} + \hat{V} \tag{2.174}$$

such that the time-evolution of a given quantum state can be computed by applying the evolution operator $\hat{U}(t)$ defined according to:

$$\hat{U}(t) = e^{-\frac{i}{\hbar}\hat{H}t} \tag{2.175}$$

Under these hypotheses, the amplitude $U(x, x', t)$ associated with the process in which a particle moves in a time t from a position x to a position x', can be defined according to:

$$U(x, x', t) = \langle x'|\hat{U}(t)|x\rangle = \langle x'|e^{-\frac{i}{\hbar}\hat{H}t}|x\rangle \tag{2.176}$$

where, as discussed in appendix A, the states $|x\rangle$ and $|x'\rangle$ represents the eigenstates of the position operator $\hat{x}$ associated to the starting and end point respectively. Please notice how this quantity represents the proper kernel function mapping the quantum behavior of the particle in space and, as such, is directly connected to the time-evolution of its wave-function according to:

$$\psi(x', t) = \langle x'|\psi(t)\rangle = \langle x'|e^{-\frac{i}{\hbar}\hat{H}t}|\psi(0)\rangle = \int dx\, \langle x'|e^{-\frac{i}{\hbar}\hat{H}t}|x\rangle\langle x|\psi(0)\rangle = \int dx\, U(x, x', t)\psi(x, 0) \tag{2.177}$$

At this point one may notice how the time evolution operator from eq. 2.175 share an interesting relation with the canonical density matrix $\hat{\rho}$ defined according to:

$$\hat{\rho}(\beta) = e^{-\beta\hat{H}} \qquad \text{with} \qquad \beta = \frac{1}{k_B T} \tag{2.178}$$

As a matter of fact if the time propagator for eq. 2.175 is evolved in imaginary time $t = -i\beta\hbar$ it becomes equivalent to the density matrix and, equivalently, if the canonical density matrix from eq. 2.178 is evaluated in imaginary inverse temperature $\beta = it/\hbar$ it becomes equivalent to a real-time propagator. In simple terms, one can imagine the time and temperature as being part of a complex time parameter θ defined as $\theta = t + i\beta\hbar$ and the previously mentioned transformations to be represented by 90 degrees rotation, known in the literature as Wick rotations, in the θ-plane. The transformation from the real-time evolution operator to the density matrix form, also known as imaginary-time evolution operator, has the great advantage of removing the imaginary unit from the exponential terms leaving us to deal with easier to handle exponential damping. For this reason the coordinate-space matrix-element of the imaginary-time propagator $\hat{\rho}(\beta)$ can be introduced according to:

$$\rho(x, x', \beta) = \langle x'|\hat{\rho}(\beta)|x\rangle = \langle x'|e^{-\beta\hat{H}}|x\rangle \tag{2.179}$$

and the correspondent real-time evolution operator can be recovered at any time by applying the proper Wick rotation. The expression just obtained can now be easily elaborated and in order to do so it is convenient to divide the contribution originated from the kinetic term $\hat{K}$, explicitly dependent upon the linear momentum operator $\hat{p}$, and the potential term $\hat{V}$, dependent only upon the coordinate operator $\hat{x}$. This operation is complex given that the two operator components do not commute. For this reason, the Trotter theorem needs to be invoked and the following result can easily be obtained:

$$e^{-\beta\hat{H}} = e^{-\beta(\hat{K}+\hat{V})} = \lim_{P\to\infty}\left[e^{-\frac{\beta\hat{V}}{2P}}e^{-\frac{\beta\hat{K}}{P}}e^{-\frac{\beta\hat{V}}{2P}}\right]^P = \lim_{P\to\infty}\hat{\Omega}^P \qquad \text{with} \qquad \hat{\Omega} = e^{-\frac{\beta\hat{V}}{2P}}e^{-\frac{\beta\hat{K}}{P}}e^{-\frac{\beta\hat{V}}{2P}} \tag{2.180}$$

Starting from this result the imaginary-time propagator matrix element can be readily rewritten according to:

$$\rho(x, x', \beta) = \lim_{P\to\infty}\langle x'|\hat{\Omega}^P|x\rangle \tag{2.181}$$

Rewriting the previous equation making use of the identity operator for the configuration space, introduced in appendix A, the following expression can easily be obtained:

$$\rho(x, x', \beta) = \lim_{P\to\infty}\int dx_2, ..., dx_P\, \langle x'|\hat{\Omega}|x_P\rangle\langle x_P|\hat{\Omega}|x_{P-1}\rangle\langle x_{P-1}|...|x_2\rangle\langle x_2|\hat{\Omega}|x\rangle \tag{2.182}$$

At this point the evaluation of each involved integral can be done in general terms according to:

$$\langle x_{k+1}|\hat{\Omega}|x_k\rangle = \langle x_{k+1}|e^{-\frac{\beta\hat{V}}{2P}}e^{-\frac{\beta\hat{K}}{P}}e^{-\frac{\beta\hat{V}}{2P}}|x_k\rangle = e^{-\frac{\beta}{2P}V(x_{k+1})}\langle x_{k+1}|e^{-\frac{\beta\hat{K}}{P}}|x_k\rangle e^{-\frac{\beta}{2P}V(x_k)} \tag{2.183}$$

where the fact that the coordinate eigenstates $|x_k\rangle$ and $|x_{k+1}\rangle$ are eigenstates of the potential operator $\hat{V}$ as well has been invoked. The evaluation of the remaining integral, explicitly dependent upon the kinetic term and, as such, upon the momentum operator $\hat{p}$, can now be tackled considering the following equality:

$$\langle x_{k+1}|e^{-\frac{\beta\hat{K}}{P}}|x_k\rangle = \int dp\,\langle x_{k+1}|e^{-\frac{\beta\hat{K}}{P}}|p\rangle\langle p|x_k\rangle = \int dp\,\langle x_{k+1}|p\rangle\langle p|x_k\rangle e^{-\frac{\beta p^2}{2mP}} \tag{2.184}$$

where, the identity operator for the momentum space, introduced in appendix A, has been invoked. Recalling the expression obtained in appendix A for the $\langle x|p\rangle$ product, the following result can easily be obtained:

$$\langle x_{k+1}|e^{-\frac{\beta\hat{K}}{P}}|x_k\rangle = \frac{1}{2\pi\hbar}\int dp\,e^{-\frac{\beta p^2}{2mP}}e^{\frac{i}{\hbar}p(x_{k+1}-x_k)} \tag{2.185}$$

The integral form just obtained represents a regular Gaussian integral that, as suggested by Tuckerman [26], can be computed by simply completing the square term according to:

$$\frac{\beta p^2}{2mP} - \frac{ip(x_{k+1}-x_k)}{\hbar} = \frac{\beta}{2mP}\left[p - \frac{imP(x_{k+1}-x_k)}{\beta\hbar}\right]^2 + \frac{mP}{2\beta\hbar^2}(x_{k+1}-x_k)^2 \tag{2.186}$$

By considering the variable substitution $\tilde{p} = p - imP(x_{k+1}-x_k)/\beta\hbar$ the following result can easily be obtained:

$$\langle x_{k+1}|e^{-\frac{\beta\hat{K}}{P}}|x_k\rangle = \frac{1}{2\pi\hbar}e^{-\frac{mP}{2\beta\hbar^2}(x_{k+1}-x_k)^2}\int_{-\infty}^{+\infty}d\tilde{p}\,e^{-\frac{\beta\tilde{p}^2}{2mP}} = \sqrt{\frac{mP}{2\pi\beta\hbar^2}}e^{-\frac{mP}{2\beta\hbar^2}(x_{k+1}-x_k)^2} \tag{2.187}$$

Substituting this result into eq. 2.183 finally allow us to obtain the following expression for the $\hat{\Omega}$ integral:

$$\langle x_{k+1}|\hat{\Omega}|x_k\rangle = \sqrt{\frac{mP}{2\pi\beta\hbar^2}}e^{-\frac{\beta}{2P}[V(x_{k+1})+V(x_k)]}e^{-\frac{mP}{2\beta\hbar^2}(x_{k+1}-x_k)^2} \tag{2.188}$$

Once this result has been obtained the following expression can be obtained for the imaginary-time propagator matrix element from eq. 2.182:

$$\begin{aligned}\rho(x,x',\beta) = \lim_{P\to\infty}\left(\frac{mP}{2\pi\beta\hbar^2}\right)^{\frac{P}{2}}\int dx_2,...,dx_P \\ \exp\left\{-\frac{1}{\hbar}\sum_{k=1}^{P}\left[\frac{mP}{2\beta\hbar}(x_{k+1}-x_k)^2 + \frac{\beta\hbar}{2P}\left(V(x_{k+1})+V(x_k)\right)\right]\right\}\Bigg|_{x_1=x}^{x_{P+1}=x'}\end{aligned} \tag{2.189}$$

This result represents a discretized path integral representation of the density matrix in which all the possible paths between the x and x' endpoints are taken into account. Please notice how the kinetic energy term has been represented by an harmonic term between subsequent points of a given path. At this point, making use of the proper Wick rotation, the real-time propagator can be obtained according to:

$$\begin{aligned}U(x,x',t) = \lim_{P\to\infty}\left(\frac{mP}{2i\pi\hbar t}\right)^{\frac{P}{2}}\int dx_2,...,dx_P \\ \exp\left\{\frac{i}{\hbar}\sum_{k=1}^{P}\left[\frac{mP}{2t}(x_{k+1}-x_k)^2 - \frac{t}{2P}\left(V(x_{k+1})+V(x_k)\right)\right]\right\}\Bigg|_{x_1=x}^{x_{P+1}=x'}\end{aligned} \tag{2.190}$$

in which a change in sign can be observed between the kinetic and potential terms.

Now that an explicit expression for the imaginary-time propagator matrix element has been obtained, one can compute the canonical partition function $Q(L,T)$ for a generic system confined within the range $x \in [0,L]$ by considering the trace of the propagator over the coordinate basis:

$$Q(L,T) = \mathrm{Tr}\left[e^{-\beta\hat{H}}\right] = \int_0^L dx\,\langle x|e^{-\beta\hat{H}}|x\rangle = \int_0^L dx\,\rho(x,x,\beta) \tag{2.191}$$

that, recalling the relation from eq. 2.189, can be written in explicit form according to:

$$Q(L,T) = \lim_{P\to\infty}\left(\frac{mP}{2\pi\beta\hbar^2}\right)^{\frac{P}{2}}\int dx_1 dx_2,...,dx_P \exp\left\{-\frac{1}{\hbar}\sum_{k=1}^{P}\left[\frac{mP}{2\beta\hbar}(x_{k+1}-x_k)^2+\frac{\beta\hbar}{2P}\left(V(x_{k+1})+V(x_k)\right)\right]\right\}\Bigg|_{x_{P+1}=x_1} \tag{2.192}$$

where the integration is now performed on all the cyclic path starting and ending at the point x. Observing how for a cyclic path the following relation must be verified:

$$\frac{1}{2}\sum_{k=1}^{P}\left[V(x_{k+1})+V(x_k)\right] = \sum_{k=1}^{P}V(x_k) \tag{2.193}$$

the following result can easily be obtained:

$$Q(L,T) = \lim_{P\to\infty}\left(\frac{mP}{2\pi\beta\hbar^2}\right)^{\frac{P}{2}}\int dx_1 dx_2,...,dx_P \exp\left\{-\frac{1}{\hbar}\sum_{k=1}^{P}\left[\frac{mP}{2\beta\hbar}(x_{k+1}-x_k)^2+\frac{\beta\hbar}{P}V(x_k)\right]\right\}\Bigg|_{x_{P+1}=x_1} \tag{2.194}$$

in which the integration domain has been omitted for sake of a lighter notation. Please notice how, as highlighted by Tuckerman [26], in the limit of high temperatures $T\to\infty$ the β term vanishes and the spring constant connecting different point of the cyclic path becomes infinite. Under these circumstances all the cyclic path tend to collapse on a single point correspondent to the case of a classical particle.

Now that an explicit expression for the partition function has been obtained, the evaluation of the thermodynamic average of an observable associated to an Hermitian operator $\hat{A}$ can be performed according to the relation:

$$\langle\hat{A}\rangle = \frac{1}{Q(L,T)}\,\mathrm{Tr}\left[\hat{A}e^{-\beta\hat{H}}\right] = \frac{1}{Q(L,T)}\int dx\,\langle x|\hat{A}e^{-\beta\hat{H}}|x\rangle \tag{2.195}$$

The evaluation of the obtained integral form strongly depends upon the structure of the involved $\hat{A}$ operator. A general discussion of the topic is presented by Tuckerman [26]. The study of quantum dynamical quantities will not be presented here since beyond the purposes of this introductory section. We point the interested reader to the book by Tuckerman [26] or to other excellent papers [27, 28] on the topic.

In the next paragraph, the numerical evaluation of the partition function through the use of the Path Integral Molecular Dynamics scheme (PIMD) will be briefly presented giving a practical approach to the calculation of thermodynamic averages and to the estimation of tunneling splittings. The latter problem will be discussed in general terms further on in this section.

Path integral molecular dynamics

In this paragraph, the path integral molecular dynamic procedure will be discussed in the simple case of a single quantum particle. The theory here presented can easily be generalized to the case of many-particle systems in which the coupling between paths associated with different particles must be taken into account.

In order to practically evaluate the expression for the partition function from eq. 2.194 a finite value of P must be selected and, as such, the following expression must be evaluated:

$$Q_P(L,T) = \left(\frac{mP}{2\pi\beta\hbar^2}\right)^{\frac{P}{2}}\int dx_1,...,dx_P \exp\left\{-\frac{1}{\hbar}\sum_{k=1}^{P}\left[\frac{mP}{2\beta\hbar}(x_{k+1}-x_k)^2+\frac{\beta\hbar}{P}V(x_k)\right]\right\}\Bigg|_{x_{P+1}=x_1} \tag{2.196}$$

Such an equation can be rewritten in an alternative form in which it resembles the partition function of a ring polymer of beads, connected by harmonic springs, moving under the influence of a classical potential $V(x)/P$. This, as suggested by Tuckerman [26], can be done recasting the integral pre-factor in a set of Gaussian integrals dependent upon a set of variables $p_1, ..., p_P$ resembling the linear momenta conjugated with coordinate variables $x_1, ..., x_P$. In doing so, the following expression can be obtained:

$$Q_P(L,T) = \left(\frac{mP}{2\pi\beta\hbar^2}\right)^{\frac{P}{2}} \int dp_1, ..., dp_P \int dx_1, ..., dx_P \exp\left\{-\beta \sum_{k=1}^{P} \left[\frac{p_k^2}{2m'} + \frac{1}{2}m\omega_P^2(x_{k+1} - x_k)^2 + \frac{1}{P}V(x_k)\right]\right\}\Bigg|_{x_{P+1}=x_1} \tag{2.197}$$

where $m' = mP/(2\pi\hbar)^2$ represents the fictitious mass of a bead of the ring polymer[15] while $\omega_P = \sqrt{P}/\beta\hbar$ represents the chain frequency associated to the nearest-neighbor coupling between beads. The isomorphism existing between the partition function from eq. 2.197 and that of a cyclic polymer suggest that the former can be computed by sampling the configuration space adopting a classical molecular dynamic protocol in which the classical Hamiltonian:

$$H_{\mathrm{cl}}(x,p) = \sum_{k=1}^{P} \left[\frac{p_k^2}{2m'} + \frac{1}{2}m\omega_P^2(x_{k+1} - x_k)^2 + \frac{1}{P}V(x_k)\right]\Bigg|_{x_{P+1}=x_1} \tag{2.198}$$

giving rise to the following set of equations of motion:

$$\frac{\partial x_k}{\partial t} = \frac{p_k}{m'} \qquad \text{and} \qquad \frac{\partial p_k}{\partial t} = -m\omega_P^2(2x_k - x_{k+1} - x_{k-1}) - \frac{1}{P}\frac{\partial V(x)}{\partial x_k} \tag{2.199}$$

can be canonically sampled by coupling with a properly defined thermostat. The direct application of the method just described represents one of the first attempt in the field of path integral molecular dynamics simulation from Parrinello and Rahman [29] that, however, is afflicted by the problem of dealing with a, difficult to sample, broad range of involved time-scales. In this brief introduction the practical implementation of an efficient path integral molecular dynamics protocol will not be discussed. We point the interested reader to the text from Tuckerman [26] and to some reference papers [30, 31].

Computing tunneling splitting estimates

Now that the theoretical framework of the path integral molecular dynamics scheme has been introduced one may wonder how the tunneling splitting can be estimated. In order to answer such a question let us start by considering a one-dimensional bi-stable system in which two minima are symmetrically arranged around the origin. This simple system represents a simple prototype of the problem already discussed, in general terms, in sec. 2.3. The symmetry of the system is captured by the operator $\hat{R}$ whose action has the effect of inverting the sign of the coordinate $x' = \hat{R}x = -x$. As already discussed the ground-state doublet of levels is characterized by eigenfunctions of opposite symmetry with the node-less ground state having even parity $\psi_0(x) = \psi_0(-x)$ and the first excited state being characterized by odd symmetry $\psi_1(x) = -\psi_1(-x)$. If, under these circumstances, the expression for the canonical density matrix element is considered:

$$\rho(x,x',\beta) = \langle x'|\hat{\rho}(\beta)|x\rangle = \sum_n \langle x'|\psi_n\rangle\langle\psi_n|x\rangle e^{-\beta E_n} = \sum_n \psi_n^*(x)\psi_n(x')e^{-\beta E_n} \tag{2.200}$$

the following results can easily be verified:

$$\rho(x,x,\beta) = |\psi_0(x)|^2 e^{-\beta E_0} + |\psi_1(x)|^2 e^{-\beta E_1} + ... \tag{2.201}$$

$$\rho(x,\hat{R}x,\beta) = |\psi_0(x)|^2 e^{-\beta E_0} - |\psi_1(x)|^2 e^{-\beta E_1} + ... \tag{2.202}$$

If the low-temperature limit, correspondent to the case of large β values, is considered the high energy states ($n \geq 2$) can be neglected from the previous expressions and the following relation can be obtained:

$$\frac{\rho(x,\hat{R}x,\beta)}{\rho(x,x,\beta)} = \frac{|\psi_0(x)|^2 e^{-\beta E_0} - |\psi_1(x)|^2 e^{-\beta E_1}}{|\psi_0(x)|^2 e^{-\beta E_0} + |\psi_1(x)|^2 e^{-\beta E_1}} \tag{2.203}$$

[15] Please notice how, as discussed by Tuckerman [26], given that the pre-factor has no effect on the evaluation of equilibrium observable averages, we are free to chose m' as we like.

Introducing the quantities $\alpha(x)$ and $\tilde{\beta}(x)$ according to the definitions:

$$\tilde{\beta}(x) = \frac{2}{\Delta E} \ln |\alpha(x)| \qquad \text{with} \qquad \alpha(x) = \frac{\psi_1(x)}{\psi_0(x)} \tag{2.204}$$

where $\Delta E = E_1 - E_0$ represents the previously defined tunneling splitting, the following expression can easily be obtained:

$$\frac{\rho(x, \hat{R}x, \beta)}{\rho(x, x, \beta)} = \tanh\left[\frac{1}{2}\Delta E\left(\beta - \tilde{\beta}(x)\right)\right] \tag{2.205}$$

As discussed by Mátyus *et al.* [8], the considered value of x is in principle arbitrary and can be selected as the point in which the two eigenfunctions have a sufficient amplitude to capture the phase change induced by the symmetry operator $\hat{R}$. In practical terms the point x can usually be identified by a configuration near to the minimum. Please notice how, in the special case in which the approximation $\tanh[\Delta E(\beta - \tilde{\beta}(x))/2] \simeq \Delta E(\beta - \tilde{\beta}(x))/2$ can be made, the tunneling splitting ΔE can be estimated directly from the ratio $\rho(x, \hat{R}x, \beta)/\rho(x, x, \beta)$ computed considering two different values of β [8].

The definition of a general procedure to evaluate the $\rho(x, \hat{R}x, \beta)/\rho(x, x, \beta)$ will, for sake of brevity, not be presented in the present thesis. We suggest to the interested reader the excellent paper by Mátyus *et al.* [8] in which the discretized path integral approach to the problem, involving the phase space integration of a linear polymer, is presented in detail for the general case of a multidimensional system.

Functional integrals

Before moving on with our discussion, let us consider how the path integral formalism, previously derived in terms of a path constructed from a series of P intermediate steps, can be rewritten in the continuous limit of $P \to \infty$. In order to do so, let us consider the real-time propagator matrix element definition introduced in eq. 2.190 that, by introducing the scaled time parameter $\epsilon = t/P$, can be rewritten according to the form:

$$\begin{aligned} U(x, x', t) = \lim_{P\to\infty} \left(\frac{m}{2i\pi\hbar\epsilon}\right)^{\frac{P}{2}} \int dx_2, ..., dx_P \\ \exp\left\{\frac{i\epsilon}{\hbar}\sum_{k=1}^{P}\left[\frac{m}{2}\left(\frac{x_{k+1} - x_k}{\epsilon}\right)^2 - \frac{1}{2}\left(V(x_{k+1}) + V(x_k)\right)\right]\right\}\Bigg|_{x_1=x}^{x_{P+1}=x'} \end{aligned} \tag{2.206}$$

In the limit of $P \to \infty$ the succession of point x_k describes a continuous path in space $x(s)$ in which the time step s sets the position of the system along the path:

$$x_k = x(s) = x((k-1)\epsilon) \qquad \text{with} \qquad x(0) = x \qquad \text{and} \qquad x(t) = x' \tag{2.207}$$

Under these circumstances, an infinitesimal distance exists between the position of the point x_k from the subsequent one in the path x_{k+1}. As such the infinitesimal difference $x_{k+1} - x_k$, divided by the infinitesimal time difference ϵ, represents the velocity of the particle along the path. At the same time, the average of the potential value measured in the two infinitesimally close points can be rewritten as the continuous potential function $V(x(s))$ encountered along the trajectory. Taking into account these considerations and observing how the summation can, in the limit of $\epsilon \to 0$, be rewritten in integral form, the following can easily be obtained:

$$\lim_{\epsilon\to 0} \epsilon \sum_{k=1}^{P}\left[\frac{m}{2}\left(\frac{x_{k+1} - x_k}{\epsilon}\right)^2 - \frac{1}{2}\left(V(x_{k+1}) + V(x_k)\right)\right] = \int_0^t ds\, \left[\frac{1}{2}m\dot{x}^2(s) - V(x(s))\right] \tag{2.208}$$

where the integrand of the right-hand-side of the equation represents the Lagrangian $\mathcal{L}(x(s), \dot{x}(s))$ of the system along the path $x(s)$ and, as such, the overall term represents the action $A[x(s)]$ computed along the selected trajectory. At this point one can easily observe how the integral operation in eq. 2.206 can be expressed in term of functional integral in which the notation $\mathcal{D}x(s)$, introduced according to:

$$\lim_{P\to\infty} \left(\frac{m}{2i\pi\hbar\epsilon}\right)^{\frac{P}{2}} dx_2, ..., dx_P = \mathcal{D}x(s) \tag{2.209}$$

can be used to denote the integration over all the possible paths $x(s)$. Under these assumptions the real-time propagator can be represented by the following continuous form:

$$U(x, x', t) = \int_{x(0)=x}^{x(t)=x'} \mathcal{D}x(s)\, e^{\frac{i}{\hbar}A[x(s)]} \tag{2.210}$$

Please notice how this equation exactly corresponds to the formalization of the original idea, discussed at the beginning of this section in the form of eq. 2.172, of expressing a the kernel function describing the motion of a particle from one point to another in a time t by summing an infinite number of alternative paths characterized by a phase dictated by the action along each path.

Now that a general real-time propagator form has been obtained one can perform the proper Wick rotation ($t = -i\beta\hbar$) in order to obtain the correspondent expression for the imaginary-time propagator. In order to do so, an imaginary time variable $\tau = is$ can be introduced and the following expression can be easily verified:

$$\int_0^t ds \left[\frac{1}{2}m\left(\frac{\partial x}{\partial s}\right)^2 - V(x(s))\right] = i\int_0^{\beta\hbar} d\tau \left[\frac{1}{2}m\left(\frac{\partial x}{\partial \tau}\right)^2 + V(x(\tau))\right] \tag{2.211}$$

where we made use of the property that $\tau = \beta\hbar$ for $s = t = -i\beta\hbar$. The argument of the right hand side integral represents the imaginary-time Lagrangian $\Lambda(x, \dot{x})$ whose imaginary-time integral represents the imaginary action $S[x(\tau)]$ computed along the path. Starting from these results the proper continuous expression for the imaginary-time propagator can be written according to the following form:

$$\rho(x, x', \beta) = \int_{x(0)=x}^{x(\beta\hbar)=x'} \mathcal{D}x(\tau)\, e^{-\frac{1}{\hbar}S[x(\tau)]} \tag{2.212}$$

At this point, as discussed by Tuckerman [26], given the positive-definite nature of the exponential term, the most important path contributing to the functional integral can be computed by minimizing the imaginary action as a functional of the path $x(\tau)$. This can be easily done by fixing the endpoints of the path and imposing to the action variation $\delta S = S[x+\delta x] - S[x]$ to vanish, at the first order, as a function of the infinitesimal path variation δx. This procedure, similar to the one followed in identifying the classical path from the imposition of the minimum action principle, lead to the following Euler-Lagrange equation for the imaginary Lagrangian Λ:

$$\frac{d}{d\tau}\left(\frac{\partial \Lambda}{\partial \dot{x}(\tau)}\right) - \frac{\partial \Lambda}{\partial x(\tau)} = 0 \tag{2.213}$$

Please notice how applying this relation to the imaginary time Lagrangian, the following equation can be obtained:

$$m\frac{\partial^2 x}{\partial \tau^2} = \frac{\partial V}{\partial x} \tag{2.214}$$

This relation is similar to the Newton's second equation of motion in which, however, the force appears with an opposite sign. In equivalent terms, the imaginary-time motion of the system can be imagined as a Newtonian evolution over an inverted potential profile $-V(x)$. At this point, the functional integral expression for the imaginary-time partition function can be computed according to:

$$Q(\beta) = \int dx\, \rho(x, x, \beta) = \int dx \int_{x(0)=x}^{x(\beta\hbar)=x} \mathcal{D}x(\tau)\, e^{-\frac{1}{\hbar}S[x(\tau)]} = \oint \mathcal{D}x(\tau)\, e^{-\frac{1}{\hbar}S[x(\tau)]} \tag{2.215}$$

where the last integral form represents the functional integral taken over all the closed path, of period $\beta\hbar$, satisfying the condition $x(0) = x(\beta\hbar)$. As recalled by Tuckerman [26] the dominant contribution to the partition function will be found around the solution of eq. 2.214 that satisfies the before mentioned periodicity constraint.

Instanton based methods

Starting from the path integral formulation presented in this section, one can now discuss another approach to the problem of computing tunneling splitting estimates, based on the concept of instanton. In order to give to the reader a general overview of how an instantonic theory of tunneling splitting can

be formulated, let us start by recalling the discussion presented at the beginning of sec. 2.3, where the tunneling splitting concept has been introduced as the energy separation observed between two states, characterized by an energy equal to $\varepsilon \pm \Delta E/2$, when two symmetrically degenerate site-states, of energy ε, are subject to a coupling term $\Delta E/2$.[16] Under these circumstances and in the low-temperature limit ($\beta \to \infty$) the following relation can be easily obtained:

$$\lim_{\beta\to\infty} \frac{Q(\beta)}{Q_0(\beta)} = \frac{e^{-\beta(\varepsilon-\Delta/2)} + e^{-\beta(\varepsilon+\Delta/2)}}{2e^{-\beta\varepsilon}} = \cosh\left(\frac{\beta\Delta}{2}\right) \tag{2.216}$$

where $Q(\beta)$ represent the partition function associated with the double minimum system in presence of tunneling while $Q_0(\beta)$ represents the same quantity computed with no-tunneling. In order to understand how these quantities can be computed let us adopt the theoretical treatment proposed by Richardson *et al.* [21] in which, according to what already discussed before in eq. 2.194, the following expression can be obtained for the partition function:

$$Q(\beta) = \lim_{P\to\infty} \left(\frac{1}{2\pi\beta_P\hbar^2}\right)^{\frac{P}{2}} \int d\mathbf{x} e^{-\beta_P \mathcal{U}_P(\beta,\mathbf{x})} \tag{2.217}$$

where $\beta_P = \beta/P$, $\mathbf{x} = (x_1, ..., x_P)$ represents the set of mass-weighted coordinates describing the position of the ring polymer beads[17], while $\mathcal{U}_P(\beta, \mathbf{x})$ can be conveniently defined according to:

$$\mathcal{U}_P(\beta,\mathbf{x}) = \sum_{i=1}^{P} \left[V(x_i) + \frac{(x_{i+1}-x_i)^2}{2(\beta_P\hbar)^2}\right] \tag{2.218}$$

At this point the so called steepest-descent approximation can be invoked by applying a Laplace approximation, whose derivation is discussed in appendix C, to the integral around the minimum $\tilde{\mathbf{x}}$ defined by the condition:

$$\frac{\partial \mathcal{U}(\beta,\mathbf{x})}{\partial x_i} = 0 \qquad \forall i \in [1, P] \tag{2.219}$$

that, in turn, translates to the condition:

$$V'(\tilde{x}_i) = \frac{\tilde{x}_{i+1} - 2\tilde{x}_i + \tilde{x}_{i-1}}{(\beta_P\hbar)^2} \qquad \forall i \in [1, P] \tag{2.220}$$

In doing so, the following expression can be obtained for the $\mathcal{U}_P(\beta, \mathbf{x})$ function:

$$\mathcal{U}_P(\beta,\mathbf{x}) = \mathcal{U}_P(\beta,\tilde{\mathbf{x}}) + \frac{1}{2}\sum_{i=1}^{P}\sum_{j=1}^{P}(x_i - \tilde{x}_i)G_{ij}(x_j - \tilde{x}_j) \tag{2.221}$$

where the G_{ij} term represents the Hessian matrix element computed on the $\tilde{\mathbf{x}}$ minimum:

$$G_{ij} = \frac{2\delta_{i,j} - \delta_{i,j-1} - \delta_{i,j+1}}{(\beta_P\hbar)^2} + V''(\tilde{x}_i)\delta_{i,j} \tag{2.222}$$

Please observe how, due to the ring nature of the system, cyclic boundary conditions must be imposed on the Kronecker delta functions $\delta_{i,j-1}$ and $\delta_{i,j+1}$. At this point the Hessian matrix $\mathbf{G}$ can be diagonalized and the following expression can be obtained for the exponential argument:

$$\mathcal{U}_P(\beta,\mathbf{s}) = \mathcal{U}_P(\beta,\tilde{\mathbf{x}}) + \frac{1}{2}\sum_{i=1}^{P}\eta_i^2 s_i^2 \tag{2.223}$$

where s_i represents the normal-mode coordinate associated with the correspondent η_i frequency. At this point, the finite approximation $\tilde{Q}(\beta)$ of the partition function for the system can be explicitly computed, for a fixed number of beads P, as the sum of the partition functions computed for each minimum. This can easily be done by recalling that the Hessian matrix $\mathbf{G}$ is symmetric and, as such, can be diagonalized

[16] Please notice how, in order to avoid confusion with the potential the coupling between site-states, indicated by $|V|$ in sec. 2.3, is now indicated as half the value of the tunneling splitting ΔE

[17] With the term mass-weighted coordinates we refer to the set of coordinates obtained multiplying the position by the square root of the mass

by a unitary determinant orthogonal matrix. Considering these observations and completing the Gaussian integral terms, the following result can easily be obtained:

$$\tilde{Q}(\beta) = \left(\frac{1}{\beta_P \hbar}\right)^P \sum_{\text{minima}} \frac{1}{\sqrt{\det(\mathbf{G})}} e^{-\beta_P \mathcal{U}_P(\beta, \tilde{\mathbf{x}})} \tag{2.224}$$

where the product of Hessian matrix eigenvalues has been rewritten in terms of the determinant of the Hessian matrix itself. Starting from this definition the partition functions for the system with and without tunneling can now be computed and a general idea about the relevant minima to be considered, can be obtained by observing how each minimum $\tilde{\mathbf{x}}$ must represent a finite-difference approximation of a periodic orbit, of period $\beta\hbar$, describing the imaginary-time evolution of the system on the inverted potential surface $-V(x)$ [21]. This, for example, allows us to clearly see how, in the case of the system without tunneling, the inverted potential must be represented by two upside-down potential wells that, as such, are compatible with a couple of collapsed periodic paths located on the potential minima (at $\pm x_0$) for the whole $\beta\hbar$ duration. Adopting the potential of the minimum as the zero of the energy scale $V(\pm x_0) = 0$ allow us to obtain the following result:

$$\tilde{Q}_0(\beta) = \left(\frac{1}{\beta_P \hbar}\right)^P \frac{2}{\sqrt{\det(\mathbf{G}_0)}} \qquad \text{with} \qquad (\mathbf{G}_0)_{ij} = \frac{2\delta_{i,j} - \delta_{i,j-1} - \delta_{i,j+1}}{(\beta_P \hbar)^2} + \omega_0^2 \delta_{i,j} \tag{2.225}$$

where ω_0 represents the harmonic frequency of each well. Now that the result in the no-tunneling hypotheses has been obtained we can now move our attention to the full problem in which not only one has to take into account the previously presented periodic orbits collapsed at $\pm x_0$ but also has to take into account all the cyclic path going back and forth between the minima describing, as such, trajectories characterized by an even number of passages across the barrier region. Each one of these passages, referred in the literature with the term "kink", increases the value of the $\beta_P \mathcal{U}_P(\beta, \tilde{\mathbf{x}})$ exponent and, hence, the path integral of the system will be dominated by minima with a low number n of kinks. Each one of these kinks will appear as a rapid change in position followed by a large portion of trajectory located on either one of the minima at $\pm x_0$. Starting from these considerations one can easily see how the overall partition function $\tilde{Q}(\beta)$ can be factored in the sum of partition functions $\tilde{Q}_n(N1, N2, ..., N_n; \beta)$ referred to orbits characterized by a different number n of kinks:

$$\tilde{Q}(\beta) = \tilde{Q}_0(\beta) + \sum_{N_1, N_2} \tilde{Q}_2(N1, N2; \beta) + \sum_{N_1, N_2, N_3, N_4} \tilde{Q}_4(N1, N2, N_3, N_4; \beta) + ... \tag{2.226}$$

with $N_1, N_2, ..., N_n$ representing the index of the bead at the center of the kink. As discussed by Richardson *et al.* [21], all the terms of the previous expression can be conveniently expressed as a power series of terms obtained by considering the contribution made by a single linear polymer of M beads connected with harmonic springs to the points $\pm x_0$ and experiencing a single kink.

Before doing so, however, one should solve another problem that is represented by the fact that each n-kink minimum is associated with a set of n low-frequency modes that, in the limit of $\beta_P \hbar \to 0$, assume zero-frequency [21]. These modes are not compatible with the steepest-descent approach discussed before and must, for this reason, be integrated out with an ad hoc procedure. These modes can be identified considering the condition:

$$\lim_{\beta_P \hbar \to 0} \mathbf{G}\mathbf{s} = \mathcal{G} s(\tau) \qquad \text{with} \qquad \mathcal{G} = -\frac{d^2}{d\tau^2} + V''[\tilde{x}(\tau)] \tag{2.227}$$

Observing how $\dot{x}(\tau)$ assumes null value anywhere except that in the kinks region and considering that, thanks to eq. 2.214, the following condition must be verified:

$$\mathcal{G}\dot{x}(\tau) = -\frac{d^2 \dot{x}(\tau)}{d\tau^2} + V''[\tilde{x}(\tau)]\dot{x}(\tau) = \frac{d}{d\tau}\Big\{V'[\tilde{x}(\tau)] - \ddot{x}(\tau)\Big\} = 0 \tag{2.228}$$

it is easy to understand how $\mathcal{G}$ need to accept n-zero $\dot{x}(\tau)$ eigenfunctions assuming non zero value in correspondence of each kink. As discussed by Richardson *et al.* [21], this results shows how the $\mathbf{G}$ matrix is characterized by n zero-frequency modes s_j corresponding to the discrete approximation of $\dot{x}(\tau)$ for each j-th kink:

$$s_j = \frac{1}{\sqrt{\beta_P \hbar S_{\text{kink}}}} \sum_{i \in j\text{-th kink}} (\tilde{x}_{i+1} - \tilde{x}_i) x_i \qquad \text{with} \qquad S_{\text{kink}} = \sum_{i \in \text{kink}} \frac{(\tilde{x}_{i+1} - \tilde{x}_i)^2}{\beta_P \hbar} \tag{2.229}$$

where S_{kink} represents the finite-difference approximation of the classical action correspondent to a single kink.[18] Starting from these results Richardson *et al.* [21] demonstrated how the following substitution needs to be applied in order to take into account the contribution of the zero-frequency modes:

$$\frac{1}{\sqrt{\det(\mathbf{G})}} \rightarrow \left(\frac{S_{\text{kink}}}{2\pi\hbar}\right)^{\frac{n}{2}} \frac{(\beta_P\hbar)^n}{\sqrt{\det(\mathbf{G}')}} \tag{2.230}$$

where the primed $\mathbf{G}'$ matrix symbol, adopted inside the determinant, indicates that the before mentioned η_i zero-frequencies components have to be neglected from the computation.

Now that the low-frequency component issue has been solved one can focus on the problem of factoring the partition function expression into kink contributions. This can be done by considering that the assumption of $V(\pm x_0) = 0$ imposes that the only non-zero contributions to the $\mathcal{U}_P(\beta, \tilde{\mathbf{x}})$ should comes from the beads of the kink and as such, recalling the definition of S_{kink} given in eq. 2.229, the following relation can easily be written:

$$\mathcal{U}_P(\beta, \tilde{\mathbf{x}}) = \frac{nS_{\text{kink}}}{\beta_P\hbar} \tag{2.231}$$

At this point, a single kink linear polymer of M beads and length $\beta\hbar$, connected from both ends to the minima $\pm x_0$ with harmonic springs, can be introduced under the explicit assumption $\beta\hbar/M = \beta_P\hbar$ of matching the beads separation encountered in the previously considered ring polymers. The correspondent linear-polymer potential surface can be defined according to:

$$\mathcal{U}_M(\beta, \mathbf{x}) = \sum_{i=1}^{M} V(x_i) + \frac{1}{2(\beta_P\hbar)^2}\left[(x_1 - x_0)^2 + \sum_{i=1}^{M-1}(x_{i+1} - x_i)^2 + (x_0 - x_M)^2\right] \tag{2.232}$$

such that the kink action S_{kink} from eq. 2.229 can be computed according to:

$$S_{\text{kink}} = \beta_P\hbar\mathcal{U}_M(\beta, \tilde{\mathbf{x}}) \tag{2.233}$$

Starting from this result for the single kink action and invoking the expression from eq. 2.231, all the partition function contributions in eq. 2.226 can now be explicitly computed finding a single kink-minimum of the just described linear polymer of M beads. Taking into account the relations from eqs. 2.224, 2.230 and 2.231, the following result can be easily obtained for the n kink partition function term:

$$\lim_{\beta\to\infty} \frac{\tilde{Q}_n(N1, N2, ..., N_n; \beta)}{\tilde{Q}_0(\beta)} = \lim_{\beta\to\infty} \frac{(\beta_P\hbar)^n}{2}\left(\frac{S_{\text{kink}}}{2\pi\hbar}\right)^{\frac{n}{2}} \sqrt{\frac{\det(\mathbf{G}_0)}{\det(\mathbf{G}'_n)}} e^{-\frac{nS_{\text{kink}}}{\hbar}} \tag{2.234}$$

in which the label marking the bead at the center of the kink does not appear explicitly in the expression. The previous result can be expressed in simpler form according to:

$$\lim_{\beta\to\infty} \frac{\tilde{Q}_n(N1, N2, ..., N_n; \beta)}{\tilde{Q}_0(\beta)} = \frac{1}{2}\theta(\beta)^n \qquad \text{with} \qquad \theta(\beta) := \frac{\beta_P\hbar}{\Phi}\sqrt{\frac{S_{\text{kink}}}{2\pi\hbar}} e^{-\frac{S_{\text{kink}}}{\hbar}} \tag{2.235}$$

where the Φ term can be indirectly introduced according to:

$$\lim_{\beta\to\infty} \frac{\det(\mathbf{G}'_n)}{\det(\mathbf{G}_0)} = \Phi^{2n} \tag{2.236}$$

As demonstrated by Richardson *et al.* [21], thanks to the Hükel-like properties of the $\mathbf{G}$ matrix, the Φ term can be conveniently defined according to the expression:

$$\Phi = \sqrt{\frac{\det(\mathbf{J}')}{\det(\mathbf{J}_0)}} \tag{2.237}$$

where $\mathbf{J}$ represents the Hessian matrix defined for the single-kink linear polymer previously introduced and, as such, must be characterized by a single zero-frequency mode, while $\mathbf{J}_0$ represents the Hessian associated to the same linear polymer collapsed in one of the minima at $\pm x_0$. Please notice how the

[18] Please notice how this can be easily verified considering that, given the selection of $V(\pm x_0) = 0$, the condition $E = 0$ is verified along the kink and as such the Lagrangian corresponds to the double of the kinetic energy.

definition of **J** strongly resembles the one of the **G** matrix, with the only difference being the absence of periodic boundary conditions at the linear polymer ends:

$$J_{ij} = \frac{K_{ij}}{(\beta_P \hbar^2)} + V''(\tilde{x}_i)\delta_{i,j} \qquad \text{with} \qquad K_{ij} = \begin{cases} 2\delta_{i,j} - \delta_{i,j-1} & i = 1 \\ 2\delta_{i,j} - \delta_{i,j+1} & i = M \\ 2\delta_{i,j} - \delta_{i,j-1} - \delta_{i,j+1} & \text{otherwise} \end{cases} \tag{2.238}$$

At this point, the partition function for the system in presence of tunneling can be easily computed considering that for each n-kinks group of partition function contributions a total of $2P^n/n!$ terms can be obtained. Starting from this consideration the following expression can easily be obtained:

$$\lim_{\beta\to\infty} \frac{\tilde{Q}(\beta)}{\tilde{Q}_0(\beta)} = \lim_{\beta\to\infty} \sum_{n=0}^{\infty} \frac{P^{2n}}{(2n)!}\theta(\beta)^{2n} = \cosh\left[P\theta(\beta)\right] \tag{2.239}$$

Comparing this equation with the assumption from eq. 2.216 the following tunneling splitting expression can easily be obtained:

$$\Delta E = \lim_{\beta\to\infty} \frac{2}{\beta_P}\theta(\beta) \tag{2.240}$$

This result represents the tunneling splitting instanton estimate for the simple case of a one-dimensional system; nevertheless, the concept presented in this paragraph can also be generalized for a multidimensional tunneling problem. We direct the interested reader to the excellent paper from Richardson and Althorpe [21], used throughout this section as a reference, in which the problem is discussed in detail.

2.5 Experimental observations of the tunneling splitting

Now that the concept of tunneling splitting has been introduced and some examples of theoretical approaches to its estimation have been examined, let us focus our attention on some interesting experimental evidence of tunneling splitting that will allow us to have a better insight into the structure and properties of the involved molecular systems. In this section, we will see how a multitude of systems, characterized by two or more symmetry-related conformers, show the phenomenon of tunneling splitting with a magnitude related to the characteristic structure of the system itself.

Let us start our discussion by examining the case of the ammonia molecule that represents the most known and historically relevant example in the field of tunneling splitting. The ammonia molecule has a pyramidal gas-phase equilibrium structure with the nitrogen atom occupying one vertex of the pyramid and the three hydrogen atoms, located at a distance of 1.012Å [32] from the nitrogen one and spaced 106.7° degrees apart [32], occupying the other vertices. Starting from this geometrical configuration, two equivalent molecular conformers can be obtained inverting, in a process known as umbrella inversion, the pyramidal structure of the molecule. This opens the way to a tunneling coupling between equivalent equilibrium structures that has profound implications on the structure of the energy levels of the system. The rotational spectrum of the molecule has been discussed by many authors including Wright and Randall [33] that reported for the rotational bands in the far-infrared region between 60 and 125μm a separation of approximately 1.33cm^{-1}. These transitions, associated with a unitary variation of the J quantum number, related to the rotation around the axis perpendicular to the symmetry one [2], are subject to the selection rules presented in sec. 2.3 and, as such, must connect the lower state of a doublet with the upper state of the other and vice-versa. Considering that, as discussed by Bell [2], the tunneling splitting is expected to show a small dependence upon the rotational quantum number characterizing two adjacent rotational levels, a tunneling splitting of 0.67cm^{-1} can be estimated. The splitting between levels of the vibrational ground-state has, in fact, be probed experimentally by means of microwave spectroscopy and a tunneling splitting of 0.8cm^{-1} has been reported by Cleeton and Williams [34]. In the vibrational spectrum, a strong tunneling splitting effect is observed in those bands, namely the symmetric bending and stretching, associated with the modes characterized by a strong variation of the distance of the nitrogen from the plane formed by the three hydrogen atoms. In more geometrical terms, a stronger tunneling effect is expected for coordinate closely related to the ones describing the inversion process and, as such, a stronger splitting is expected, due to the rather flat nature of the pyramidal structure of the ammonia molecule, for the symmetric bending motion [2]. The experimental data collected both by Barker [35] and by Dennison and Hardy [36], confirm this trend with an average separation of 33cm^{-1} observed for the symmetrical bending bands located at 10.5μm ($\sim$ 950cm^{-1}) and a 1.6cm^{-1} separation

for the symmetric stretching bands at 3μm ($\sim 3330\text{cm}^{-1}$). Furthermore, it is interesting to notice how the efficiency of the tunneling coupling strongly depends upon the mass of the involved particles. If the completely deuterated analog of the ammonia molecule is considered a strongly reduced tunneling splitting of 0.05cm^{-1} is observed for the ground-state while a splitting of 3.4cm^{-1} is encountered for the first-excited one [2]. The case of partially deuterated ammonia analogs is more complex due to their different symmetry and will not be discussed in this introductory section.

Similarly to ammonia also the phosphine molecule is expected to experiment the phenomenon of tunneling splitting that, however, due to the potential structure of the system and the substantially higher mass of the phosphorus atom in respect to the nitrogen, is expected to assume a very small value that, as far as we know, no-one has ever managed to detect experimentally [37, 38].

The phenomenon of tunneling splitting is not limited to small molecules such as ammonia and phosphine but, as a matter of fact, it embraces a wide range of chemical systems in which, due to its light mass, one or more hydrogen atoms transfer, between equivalent sites, are usually involved. A problem commonly discussed in the literature is represented by the malonaldehyde molecule in which the hydrogen atom connected to one of the carbonylic oxygen of the enolic-form of the molecule is transferred, through the formation of a six-members-ring transition state, between the two carbonylic oxygen sites. The vibro-rotational ground-state tunneling splitting of the molecule has been estimated with high precision and assumes the value of $21.5831383(6)\text{cm}^{-1}$ [39, 40]. The problem of computing the malonaldehyde ground-state tunneling splitting represents a very common problem that has been tackled with a plethora of theoretical methods. We point the interested reader to the papers from Mizukami *et al.* [41] where the problem has been tackled using a Monte Carlo approach, to the paper by Mátyus *et al.* [8] and Vaillant *et al.* [9] where the problem has been discussed in terms of path-integral molecular dynamics and to the paper from Richardson *et al.* [21] in which the problem is discussed using the instanton approach.

Many other molecular systems show a relevant spectroscopic contribution from the tunneling effect; among these, we would like to recall the tropolone molecule, for which the tunneling splitting has been experimentally investigated both in the ground-state [42] and in its first electronically excited one [43], the case of carboxylic acid dimers, in which a double proton transfer between pairs of acid molecules is observed [44], the case of the S_4 molecule isomerization [45] and the case of water clusters that have been investigated experimentally [46] and received broad interest from the theoretical community [10, 47].

Before concluding this introductory section let us highlight the fact that tunneling-splitting-like phenomena are not relegated to double minimum systems but can also play a relevant role in multiple-minimum systems in which more complex splitting patterns will be observed. An example of this is represented by the phenomenon of hindered rotation in which a molecule or a functional group is subject, during its rotation motion, to a multiple minimum potential profile [2]. The tunneling in this context represents an alternative way in which the system can overcome the rotational barrier [2, 48].

Chapter 3

Tunneling splitting and activated processes

The central pillar of this thesis work is represented by the isomorphic relation existing between the Born Oppenheimer nuclear Hamiltonian and the symmetrized form of the Fokker-Planck-Smoluchowski operator. The aim of this chapter is to give to the reader an introduction to the fundamental theoretical tools required to obtain this similarity relation and to discuss the interesting parallelism that this observation creates between otherwise unrelated phenomena. The chapter is opened by section 3.1 in which the proper Hamiltonian for discussing the internal motion of a molecule is obtained. In section 3.2 the reader will be presented with a short introduction to the origin of the Fokker-Planck-Smoluchoski equation and its implication in the field of studying activated processes. The chapter is closed by section 3.3 where the actual isomorphic relation will be obtained and a generic approach to its application to tunneling problems will be outlined.

3.1 The molecular Hamiltonian

The concept of the molecule is well engraved in the chemical culture as a structure composed of a defined set of atoms interacting with each other to give rise to a stable geometrical configuration. This elementary concept is directly connected to the quantum description of the matter that not only determines which molecular configuration represents a stable molecule but also which reactive process a molecule can undergo.

Whenever a brute formula for a molecule is defined, a specific Hamiltonian, accounting for all the electronic and nuclear configurations, can be immediately obtained simply by taking into account all the electrostatic interaction between the particles in the system. If a set of N atomic nuclei and N_e electrons is considered, the following quantum Hamiltonian can be written for the system:

$$\begin{aligned}\hat{H} = &-\frac{\hbar^2}{2m_e}\sum_{i=1}^{N_e}\nabla_i^2 - \frac{\hbar^2}{2}\sum_{\lambda=1}^{N}\frac{\nabla_\lambda^2}{m_\lambda} + \\ &+\frac{1}{4\pi\varepsilon_o}\left[\sum_{\lambda=1}^{N}\sum_{\mu>\lambda}^{N}\frac{Z_\lambda Z_\mu e^2}{|\mathbf{R}_\lambda - \mathbf{R}_\mu|} + \sum_{i=1}^{N_e}\sum_{j>i}^{N_e}\frac{e^2}{|\mathbf{r}_i - \mathbf{r}_j|} - \sum_{i=1}^{N_e}\sum_{\lambda=1}^{N}\frac{Z_\lambda e^2}{|\mathbf{r}_i - \mathbf{R}_\lambda|}\right]\end{aligned} \tag{3.1}$$

where we have adopted greek letters to identify quantities referred to the nuclei such as the position $\mathbf{R}_\lambda$, the nuclear mass m_λ and the atomic number Z_λ; while regular letters have been used to represent quantities referred to the electrons such as their position $\mathbf{r}_i$. Furthermore the symbol e represents the electron charge, m_e the electron mass while ε_0 indicates the vacuum permittivity.

Solving the Hamiltonian in eq. 3.1 is extremely complex due to the great number of particles resulting in an even bigger set of coupled coordinates. In most simple cases however the complete solution of such a problem is not required to get useful insight into the structure of a molecular system. Considering that the rest mass of a proton is 1836.15 times that of the electron, it is easy to understand how the nuclear part of a molecule has a dynamic far slower than the one experienced by the electrons. This energy and

time scale separation implies that the electrons see the nuclei as substantially still in space during their evolution while the nuclei experience their interaction with the electron as a mean-field potential. These qualitative considerations allow us to divide, in a process known as Born Oppenheimer approximation, the molecular Hamiltonian $\hat{H}$ as a sum of a nuclear and an electronic part coupled by a mean-field dependence. The electronic part depends parametrically upon the nuclear configuration $\mathbf{R}$ and can be written according to:

$$\hat{H}^{\mathrm{el}}(\mathbf{R}) = -\frac{\hbar^2}{2}\sum_{i=1}^{N_e}\frac{\nabla_i^2}{m_e} + \frac{1}{4\pi\varepsilon_o}\left[\sum_{i=1}^{N_e}\sum_{j>i}^{N_e}\frac{e^2}{|\mathbf{r}_i-\mathbf{r}_j|} - \sum_{i=1}^{N_e}\sum_{\lambda=1}^{N}\frac{Z_\lambda e^2}{|\mathbf{r}_i-\mathbf{R}_\lambda|}\right] \tag{3.2}$$

By solving the electronic Hamiltonian one can recover the electronic energy spectrum $\{E_k^{\mathrm{el}}(\mathbf{R})\}$ for a given nuclear configuration. Adopting the k-th state as the electronic contribution experienced by the nuclear system the following mean-field Hamiltonian can be obtained:

$$\hat{H}_k^{\mathrm{nuc}} = -\frac{\hbar^2}{2}\sum_{\lambda=1}^{N}\frac{\nabla_\lambda^2}{m_\lambda} + \frac{1}{4\pi\varepsilon_o}\sum_{\lambda=1}^{N}\sum_{\mu>\lambda}^{N}\frac{Z_\lambda Z_\mu e^2}{|\mathbf{R}_\lambda-\mathbf{R}_\mu|} + E_k^{\mathrm{el}}(\mathbf{R}) = -\frac{\hbar^2}{2}\sum_{\lambda=1}^{N}\frac{\nabla_\lambda^2}{m_\lambda} + V_k(\mathbf{R}) \tag{3.3}$$

where $V_k(\mathbf{R})$ represents the overall mean-field potential, correspondent to the k-th electronic state, experienced by the nuclear system. The adoption of this adiabatic scheme in the case of the sole ground-state PES is usually sufficient to describe most isomerization reactions of simple molecular systems and, for this reason, will be adopted as the starting point of this thesis work. Under this assumption, all the relevant isomers correspondent to a given brute formula can be represented as local minima in a single potential energy surface (PES) and their inter-conversion will be dictated by the PES landscape. In this context, the energy spectrum of a molecular system can be influenced by neighboring isomers on the PES resulting in observable deviations from the energy spectrum that would be expected for the single isolated molecular structure. These nuclear quantum effects often result in a precise pattern of tunneling-induced splitting of the energy spectrum that, as discussed in the introductory section, can often be observed experimentally. As expected from the chemical intuition, only nearby minima, connected by reasonable reaction paths, will have strong enough coupling to induce noticeable effects.

Now that the theoretical context has been clarified let us take an additional step by rewriting the nuclear Hamiltonian from eq. 3.3 in a more compact form. Firstly let us adopt a lighter notation by both dropping the label specifying that we are referring to the nuclear part and omitting the electronic state index that, from now on, will be referred to the ground-state one. Secondly, let us consider the whole $\mathbb{R}^{3N}$ space of nuclear coordinates and let us indicate with $x^{i'}$ the i-th Cartesian component of the position vector $\mathbf{r}$. Please notice how, in this notation, the i-th Cartesian component in the configuration space will correspond to the k-th Cartesian component, with $k = i \mod 3$, of the position vector associated with the λ-th atom, with $\lambda = (i-k)/3$. Finally, introducing the mass-dependent tensor $\mu^{i'j'} = \delta^{i'j'}m_{i'}^{-1}$ and adopting the Einstein summation notation[1], it is easy to rewrite the operator from eq. 3.3 in the form:

$$\hat{H} = -\frac{\hbar^2}{2}\partial_{i'}\mu^{i'j'}\partial_{j'} + V(\mathbf{x}') \tag{3.4}$$

where we employed the short notation for the derivative $\partial_{i'} \equiv \partial/\partial x^{i'}$. The operator obtained in eq. 3.4 gives access, within the framework created by the adiabatic approximation, to a complete description of the dynamics of the nuclear skeleton of a molecule. This however not only takes into account the internal isomerization motion of the molecular structure but also its translational and rotational degrees of freedom. This poses a significant challenge in the theoretical treatment and requires a more in-depth analysis capable of either discerning how the interplay between these degrees of freedom determines the eigenvalues spectrum of the nuclear Hamiltonian; or, at least, indicating the proper theoretical framework in which an approximated degrees of freedom decoupling can be applied in order to recover a picture of the internal motion of the system. The problem will be discussed in detail in sec. 3.1.2. Such an analysis calls for the definition of a new set of generalized coordinates capable of capturing the characteristic modes associated with different types of degrees of freedom. This coordinate change, in turn, induces a new metric in the coordinate space that, as will be discussed in sec. 3.1.1, translates to a new generalized form for the nuclear Hamiltonian.

[1] In the Einstein notation the summation is implied whenever the same index is repeated twice in different positions.

3.1.1 Hamiltonian in generalized coordinates

In the previous section we introduced a $3N$ dimensional configuration space and, making use of a Cartesian basis set of orthonormal vectors $\{e_{i'}\}$, we mapped an arbitrary configuration vector $\mathbf{r} = x^{i'}\mathbf{e}_{i'}$ using a set of Cartesian components $\{x^{i'}\}$. Under these assumptions, the form reported in eq. 3.4 has been obtained for the Born Oppenheimer nuclear Hamiltonian.

The aim of this section is to evaluate how the Hamiltonian operator changes when a new metric is imposed on the system or, in other terms, when a new set of generalized, linearly independent, non-orthogonal basis vectors $\{\mathbf{e}_i\}$ is adopted to map the configuration space. Under this assumption an arbitrary configuration vector $\mathbf{r} = x^i\mathbf{e}_i$ will be represented by a set of generalized coordinates $\{x^i\}$ connected to the Cartesian ones by the coordinates transformation $\{x^{i'}\} \rightarrow \{x^i\}$. In what follows we will adopt the following notation to indicate the Jacobian matrix elements associated with the transformation:

$$\frac{\partial x^{i'}}{\partial x^j} = \mathcal{J}_j^{i'} \quad \text{and} \quad \frac{\partial x^j}{\partial x^{i'}} = \mathcal{J}_{i'}^{j} \tag{3.5}$$

The change in metric of the space requires the selection of a new definition for the scalar product in the new coordinate space. Since the normalization of a wave-function represents an invariant of the transformation the following equality between scalars must hold:

$$\int_{\mathcal{D}'} |\psi(\mathbf{x}')|^2 d\mathbf{x}' = \int_{\mathcal{D}} \sqrt{G}|\psi(\mathbf{x}')|^2_{\mathbf{x}'=\mathbf{x}'(\mathbf{x})} d\mathbf{x} \tag{3.6}$$

where the integration domains $\mathcal{D}'$ and $\mathcal{D}$ represent the whole configuration space, while $\sqrt{G}$ represents the absolute value of the Jacobian matrix determinant[2]. The integration factor, whose appearance is dictated by the change in metrics, must be taken into account in the definition of a transformation rule for the wave-function. In what follows we will operate in the assumption, commonly adopted in the framework of quantum mechanics, of dealing with an invariant wave-function defined, in the new coordinate space, by simple variable substitution $\psi(\mathbf{x}) = \psi(\mathbf{x}')|_{\mathbf{x}'=\mathbf{x}'(\mathbf{x})}$. Under this assumption the scalar product in the new space will respond to the relation:

$$\langle f|g\rangle = \int_{\mathcal{D}} \sqrt{G} f^*(\mathbf{x}) g(\mathbf{x}) d\mathbf{x} \tag{3.7}$$

In order to evaluate how the operator in eq. 3.4 changes under the coordinate transformation let us first make use of the fact that, in Cartesian coordinates, the adjoint of the derivative corresponds to the derivative operator itself changed in sign. This allows us to rewrite eq. 3.4 according to:

$$\hat{H} = \frac{\hbar^2}{2}\partial_{i'}^{\dagger}\mu^{i'j'}\partial_{j'} + V(\mathbf{x}') \tag{3.8}$$

Taking into account that the Hamiltonian expectation value must be invariant during the transformation and observing that $\partial_{i'} = \mathcal{J}_{i'}^{j}\partial_j$, it is possible to obtain the following chain of equalities:

$$\begin{aligned}
\langle\phi|\hat{H}|\psi\rangle &= \frac{\hbar^2}{2}\langle\phi|\partial_{i'}^{\dagger}\mu^{i'j'}\partial_{j'}|\psi\rangle + \langle\phi|V|\psi\rangle = \frac{\hbar^2}{2}\langle\partial_{i'}\phi|\mu^{i'j'}|\partial_{j'}\psi\rangle + \langle\phi|V|\psi\rangle = \\
&= \frac{\hbar^2}{2}\int_{\mathcal{D}'} \left[\partial_{i'}\phi^*(\mathbf{x}')\right]\mu^{i'j'}\partial_{j'}\psi(\mathbf{x}')d\mathbf{x}' + \int_{\mathcal{D}'}\phi^*(\mathbf{x}')V(\mathbf{x}')\psi(\mathbf{x}')d\mathbf{x}' = \\
&= \frac{\hbar^2}{2}\int_{\mathcal{D}} \sqrt{G}\mathcal{J}_{i'}^{a}\left[\partial_a\phi^*(\mathbf{x})\right]\mu^{i'j'}\mathcal{J}_{j'}^{b}\partial_b\psi(\mathbf{x})d\mathbf{x} + \int_{\mathcal{D}}\sqrt{G}\phi^*(\mathbf{x})V(\mathbf{x})\psi(\mathbf{x})d\mathbf{x} = \\
&= \frac{\hbar^2}{2}\int_{\mathcal{D}} \sqrt{G}\left[\partial_a\phi^*(\mathbf{x})\right]\mu^{ab}\partial_b\psi(\mathbf{x})d\mathbf{x} + \int_{\mathcal{D}}\sqrt{G}\phi^*(\mathbf{x})V(\mathbf{x})\psi(\mathbf{x})d\mathbf{x}
\end{aligned} \tag{3.9}$$

[2]The metric of the system is set by the scalar product of the $\mathbf{e}_i$ basis vectors according to $g_{ab} = \mathbf{e}_a \cdot \mathbf{e}_b$. Considering that in the transformation from Cartesian coordinates $\mathbf{e}_a = \mathcal{J}_a^{b'}\mathbf{e}_{b'}$, it is easy to obtain:

$$g_{ab} = \mathcal{J}_a^{i'}\mathcal{J}_b^{j'}\mathbf{e}_{i'}\cdot\mathbf{e}_{j'} = \mathcal{J}_a^{i'}\mathcal{J}_b^{j'}\delta_{i'j'} = \sum_i \mathcal{J}_a^{i'}\mathcal{J}_b^{i'}$$

Translating the equality in matrix form and taking the determinant of both side it is simple to verify how $G \equiv \det([g_{ab}]) = 1/\det([g^{ab}])$ corresponds to the square of the Jacobian determinant.

where $\mu^{ab} = \mathcal{J}^a_{i'} \mu^{i'j'} \mathcal{J}^b_{j'}$ represent the transformed mass tensor in the new coordinate system. Recalling the definition of adjoint operator and that of scalar product, defined by eq. 3.7, it is easy to obtain the following form for the Hamiltonian operator in generalized coordinates:

$$\hat{H} = \frac{\hbar^2}{2} \partial_a^\dagger \mu^{ab} \partial_b + V(\mathbf{x}) \tag{3.10}$$

The adjoint derivative can now be removed from the operator by expressing its definition in terms of the regular derivative operator. This can be easily done considering:

$$\langle f | \partial_i^\dagger | g \rangle = \langle \partial_i f | g \rangle = \int_D \sqrt{G} \left[\partial_i f^*(\mathbf{x}) \right] g(\mathbf{x}) d\mathbf{x} = - \int_{\mathcal{D}} f^*(\mathbf{x}) \partial_i \left[\sqrt{G} g(\mathbf{x}) \right] d\mathbf{x} \tag{3.11}$$

from which it is simple to obtain:

$$\partial_i^\dagger = -\frac{1}{\sqrt{G}} \partial_i \sqrt{G} \tag{3.12}$$

Applying this result in eq. 3.10 it is possible to obtain:

$$\hat{H} = -\frac{\hbar^2}{2\sqrt{G}} \partial_a \sqrt{G} \mu^{ab} \partial_b + V(\mathbf{x}) \tag{3.13}$$

which represents the desired form for the Born-Oppenheimer nuclear Hamiltonian in generalized coordinates.

3.1.2 Degrees of freedom separation

From the mechanical point of view, a molecule is a flexible body that can be deformed, rotated and translated. The description of the molecular dynamics requires the selection of a proper set of coordinates capable of representing the complete set of possible molecular configurations with a physically meaningful picture. In order to do so let us start by defining two reference systems in the three-dimensional space. The first one, hereafter addressed as laboratory frame (LF), is fixed in an arbitrary position in space and is oriented by the triplet of basis vectors $\{\mathbf{u}_x, \mathbf{u}_y, \mathbf{u}_z\}$. The second one, hereafter addressed as body frame (BF), is centered on the molecular center of mass $\mathbf{r}_{\mathrm{CM}}$ and is attached to the molecular skeleton by means of the definition of a set $\{\mathbf{v}_x, \mathbf{v}_y, \mathbf{v}_z\}$ of basis vectors. Under these assumptions, the translatory motion of a molecule can be described, by an observer sitting in the LF, in terms of the position of the center of mass $\mathbf{r}_{\mathrm{CM}}$ whose Cartesian components r^i_{CM} can be obtained according to:

$$r^i_{\mathrm{CM}} = M^{-1} \sum_\lambda m_\lambda R^{\lambda i'} \quad \text{with} \quad M = \sum_\lambda m_\lambda \tag{3.14}$$

where m_λ represents the mass of the λ-th atom while $R^{\lambda i'}$ represents its i-th Cartesian component in respect to the LF [3]. Under this split framework description of the system, the velocity $\mathbf{v}$ of the λ-th atom in the LF can be expressed according to:

$$\mathbf{v} = \dot{\mathbf{r}}_{\mathrm{CM}} + \omega \times \mathbf{r}_\lambda + \mathbf{v}_\lambda \tag{3.15}$$

where ω has been introduced to indicate the angular velocity of the BF while $\mathbf{v}_\lambda$ represents the velocity of the λ-th particle in such a rotating frame. Under these conditions the classical kinetic energy T would assume the form[4]:

$$2T = M \dot{r}^2_{\mathrm{CM}} + \sum_\lambda m_\lambda \left(\omega \times \mathbf{r}_\lambda \right) \cdot \left(\omega \times \mathbf{r}_\lambda \right) + \sum_\lambda m_\lambda v^2_\lambda + 2\omega \sum_\lambda m_\lambda \mathbf{r}_\lambda \times \mathbf{v}_\lambda \tag{3.16}$$

The first term of the equation represents the kinetic energy referred to the collective molecular motion described by the center of mass translation. This term is the only one making explicit reference to the

[3] Please notice how the correspondence $R^{\lambda i'} = x^{k'}$ with $k' = 3\lambda + i$ exists between the set of atomic coordinates and the configuration space ones.

[4] The following conditions, deriving from the center of mass definition, have been applied to obtain the kinetic energy expression:

$$\sum_\lambda m_\lambda \mathbf{r}_\lambda = 0 \quad \text{and} \quad \sum_\lambda m_\lambda \mathbf{v}_\lambda = 0$$

center of mass position showing how the molecular translations have no coupling terms with rotation and internal motion. The second term represents the rotational energy of the system that, being a flexible body, has an implicit dependence, in terms of its moment of inertia, from the molecular configuration. The third term represents the kinetic energy of the particles moving in the molecular frame while the fourth one represents the coupling, usually referred to as Coriolis coupling, between rotations and internal motion.

The just obtained picture is very suggestive of the nature of the system and indicates how the real obstacle in a description of the internal motion is represented by its coupling with the rotational degrees of freedom. In order to better analyze such a problem let us start by introducing a set of generalized variables describing the orientational and configurational state of the molecule. The orientation of the molecule can be expressed as a function of three Euler angles $\mathbf{\Omega}$. These angular variables completely specify the relative orientation of the two frames and allow for the definition of the cosine matrices describing the conversion of a generic vector from the LF to the BF and vice-versa. The latter, hereafter denoted as $\mathbf{C}$, can be immediately defined by computing the scalar product between the $\{\mathbf{u}_i\}$ and $\{\mathbf{v}_i\}$ vectors according to $C_{ij} = \mathbf{u}_i \cdot \mathbf{v}_j$. Under these assumptions the Cartesian position $\mathbf{R}_\lambda = \mathbf{r}_{\mathrm{CM}} + \mathbf{r}_\lambda$ of a particle in the LF can be expressed as the combination of the position of the center of mass $\mathbf{r}_{\mathrm{CM}}$ and the position $\mathbf{r}_\lambda$ of the same particle in respect to the BF. Recalling the just introduced definition for the cosine matrix the following relation can be defined between vector components in different frames:

$$R_{\lambda i} = r_{\mathrm{CM}} + \sum_j C_{ij} r_{\lambda,j} \tag{3.17}$$

Finally, once the translational and orientational variables have been specified, a set of $3N-6$ internal coordinates $\mathbf{q}$ can be adopted as a base to describe all the possible molecular configurations generated by the internal motion.

Now that the tripartite set $\mathbf{x} = (\mathbf{r}_{\mathrm{CM}}, \mathbf{\Omega}, \mathbf{q})$ of $3N$ molecular coordinates has been introduced let us focus our discussion how the kinetic energy expression from eq. 3.16 can be rewritten in terms of these three type of generalized coordinates and relative conjugate momenta. In order to do so let us start by considering the Cartesian form of the classical kinetic energy:

$$T = \frac{1}{2} \sum_{ij} M_{ij} \dot{x}_{i'} \dot{x}_{j'} = \frac{1}{2} (\dot{\mathbf{x}}')^T \mathbf{M} \dot{\mathbf{x}}' \tag{3.18}$$

where $\mathbf{M}$ represent the Cartesian mass tensor $M_{ij} = \delta_{ij} m_i$ and $\dot{x}_{i'} = \partial x_{i'}/\partial t$ represents the i-th Cartesian velocity component. If the generalized set of coordinates $\mathbf{x}$ is introduced, the relation $\dot{\mathbf{x}}' = \boldsymbol{\mathcal{J}}(\mathbf{x})\dot{\mathbf{x}}$, where $\mathcal{J}_{ij}(\mathbf{x}) = \partial x_{i'}/\partial x_j$ represents the Jacobian matrix associated with the transformation, can be used to connect derivatives in different coordinate sets. Under these conditions the kinetic energy can be rewritten according to:

$$T = \frac{1}{2} \sum_{nm} \tilde{M}_{nm}(\mathbf{x}) \dot{x}_i \dot{x}_j = \frac{1}{2} \dot{\mathbf{x}}^T \tilde{\mathbf{M}}(\mathbf{x}) \dot{\mathbf{x}} \quad \text{with} \quad \tilde{\mathbf{M}}(\mathbf{x}) = \boldsymbol{\mathcal{J}}(\mathbf{x})^T \mathbf{M} \boldsymbol{\mathcal{J}}(\mathbf{x}) \tag{3.19}$$

The set of linear momenta $\mathbf{p} = (\mathbf{p}_{\mathrm{CM}}, \mathbf{p}_\Omega, \mathbf{p}_q)$, conjugated to the generalized variables $\mathbf{x} = (\mathbf{r}_{\mathrm{CM}}, \mathbf{\Omega}, \mathbf{q})$, can now be computed considering the derivative of the system Lagrangian $\mathcal{L}(\mathbf{x}, \dot{\mathbf{x}}, t)$ in respect to each velocity component. Considering that for an isolated conservative system $\mathcal{L} = T(\dot{\mathbf{x}}) - V(\mathbf{x})$, the following expression can be obtained for i-th component of the linear momentum:

$$p_i = \frac{\partial \mathcal{L}}{\partial \dot{x}_i} = \frac{\partial T}{\partial \dot{x}_i} = \frac{1}{2} \frac{\partial}{\partial \dot{x}_i} \sum_{nm} \tilde{M}_{nm}(\mathbf{x}) \dot{x}_n \dot{x}_m = \sum_n \tilde{M}_{in}(\mathbf{x}) \dot{x}_n \tag{3.20}$$

Considering the vector form $\mathbf{p} = \tilde{\mathbf{M}}(\mathbf{x})\dot{\mathbf{x}}$ of the previous result, one can express the vector of velocity components $\dot{\mathbf{x}} = \tilde{\mathbf{M}}(\mathbf{x})^{-1}\mathbf{p}$ in terms of the correspondent linear momenta. Adopting such a definition in the kinetic energy expression one can easily conclude how:

$$T = \frac{1}{2} \mathbf{p}^T \boldsymbol{\mu} \mathbf{p} \tag{3.21}$$

where $\boldsymbol{\mu} \equiv \tilde{\mathbf{M}}(\mathbf{x})^{-1}$ corresponds to the matrix representation of the same mass-dependent tensor μ^{ab} appearing in eq. 3.13. The absence of coupling between translations and the other degrees of freedom

impart to the $\boldsymbol{\mu}$ matrix a diagonal block structure in which the momenta components $\mathbf{p}_{\mathrm{CM}}$ are not mixed with the momenta associated with the other types of motion.

In order to outline a general procedure to restrain our analysis to the internal motion problem, let us change our description of the rotational degrees of freedom moving from an expression based on the linear momenta conjugated with the Euler angles, to a description based on the total angular momentum of the system. In order to do so let us consider the angular momentum definition in Cartesian coordinates:

$$\mathbf{J} = \sum_{\lambda} m_{\lambda} \mathbf{R}_{\lambda} \times \dot{\mathbf{R}}_{\lambda} \tag{3.22}$$

Each component of such a vector can be expressed, invoking the Levi Civita symbol, according to:

$$J_k = \sum_{\lambda} m_{\lambda} \sum_{ij} \varepsilon_{ijk} R_{\lambda i} \dot{R}_{\lambda j} = \sum_{\lambda j} \dot{R}_{\lambda j} m_{\lambda} \sum_{i} \varepsilon_{ijk} R_{\lambda i} = \sum_{\lambda j} C_{kj\lambda} \dot{R}_{\lambda j} \tag{3.23}$$

where:

$$C_{kj\lambda} = m_{\lambda} \sum_{i} \varepsilon_{ijk} R_{\lambda i} \tag{3.24}$$

Recalling the relation existing between the configuration vector $x_{n'}$ and the j-th Cartesian component of the λ-th atom, one can apply a simple index reshaping to obtain the formulation:

$$J_k = \sum_{\lambda n} C_{kn}(\mathbf{x}') \dot{x}_{n'} \tag{3.25}$$

where C_{kn} can be obtained from eq. 3.24 setting $j = n \mod 3$ and $\lambda = (n - j)/3$. By adopting this expression for each component of the total angular momentum the following relation chain can be easily obtained:

$$\mathbf{J} = \mathbf{C}(\mathbf{x}')\dot{\mathbf{x}}' = \mathbf{C}(\mathbf{x})\boldsymbol{\mathcal{J}}(\mathbf{x})\dot{\mathbf{x}} = \mathbf{C}(\mathbf{x})\boldsymbol{\mathcal{J}}(\mathbf{x})\tilde{\mathbf{M}}(\mathbf{x})^{-1}\mathbf{p} \equiv \mathbf{A}(\mathbf{x})\mathbf{p} \tag{3.26}$$

where $\mathbf{A}(\mathbf{x}) = \mathbf{C}(\mathbf{x})\boldsymbol{\mathcal{J}}(\mathbf{x})\tilde{\mathbf{M}}(\mathbf{x})^{-1}$ represents the $3 \times 3N$ matrix dictating the form of the angular momentum vector in terms of the linear momentum components associated with the set of generalized coordinates. Expanding the product between the $\mathbf{A}(\mathbf{x})$ matrix and each component of the linear momentum $\mathbf{p} = (\mathbf{p}_{\mathrm{CM}}, \mathbf{p}_{\Omega}, \mathbf{p}_q)$, one can easily obtain the following expression:

$$\mathbf{J} = \mathbf{A}_{\mathrm{CM}}(\mathbf{x})\mathbf{p}_{\mathrm{CM}} + \mathbf{A}_{\Omega}(\mathbf{x})\mathbf{p}_{\Omega} + \mathbf{A}_q(\mathbf{x})\mathbf{p}_q \tag{3.27}$$

Making use of this relation, the orientational linear momentum $\mathbf{p}_{\Omega}$ can be expressed as a function of the total angular momentum $\mathbf{J}$ according to:

$$\mathbf{p}_{\Omega} = \mathbf{A}_{\Omega}(\mathbf{x})^{-1} \left[\mathbf{J} - \mathbf{A}_{\mathrm{CM}}(\mathbf{x})\mathbf{p}_{\mathrm{CM}} - \mathbf{A}_q(\mathbf{x})\mathbf{p}_q\right] \tag{3.28}$$

Looking at the angular momentum decomposition from eq. 3.27 one can easily appreciate how the first term, dependent upon the center of mass position, accounts for the collective motion of the BF in respect to the LF origin while the two remaining ones describe the angular momentum in terms of the BF orientational and internal motions. In order to obtain a clear picture of the internal motion of the molecule let us invoke the condition of a vanishing BF angular momentum that, on the base of what just discussed, is equivalent to set the condition:

$$\mathbf{J} - \mathbf{A}_{\mathrm{CM}}(\mathbf{x})\mathbf{p}_{\mathrm{CM}} = 0 \tag{3.29}$$

from this assumption the following relation, expressing the orientational momenta as a function of the internal motion variables, can be obtained:

$$\mathbf{p}_{\Omega} = -\mathbf{A}_{\Omega}(\mathbf{x})^{-1}\mathbf{A}_q(\mathbf{x})\mathbf{p}_q \equiv \mathbf{B}(\mathbf{x})\mathbf{p}_q \tag{3.30}$$

Substituting this result in the expression from eq. 3.21 and adopting the notation $\boldsymbol{\mu}_{(A,B)}$ to indicate the block of the $\boldsymbol{\mu}$ matrix connecting momenta associated with coordinates of type A and B, where $A, B \in \{\mathrm{CM}, \Omega, q\}$, one can easily obtain the following expression for the kinetic energy:

$$\begin{aligned} T = \frac{1}{2}\mathbf{p}_{\mathrm{CM}}^T\boldsymbol{\mu}_{(\mathrm{CM},\ \mathrm{CM})}\mathbf{p}_{\mathrm{CM}} + \frac{1}{2}\mathbf{p}_q^T\boldsymbol{\mu}_{(q,q)}\mathbf{p}_q + \frac{1}{2}\mathbf{p}_q^T\mathbf{B}^T\boldsymbol{\mu}_{(\Omega,\Omega)}\mathbf{B}\mathbf{p}_q + \\ + \frac{1}{2}\mathbf{p}_q^T\mathbf{B}^T\boldsymbol{\mu}_{(\Omega,q)}\mathbf{p}_q + \frac{1}{2}\mathbf{p}_q^T\boldsymbol{\mu}_{(q,\Omega)}\mathbf{B}\mathbf{p}_q \end{aligned} \tag{3.31}$$

As can be grasped looking at such a result, the kinetic energy is now expressed in terms of both internal and translational motions with the latter not affecting the former. Under this assumption a description concerning only the internal motion can be achieved by neglecting the component describing the center of mass motion. This is equivalent to evaluate the kinetic term under the explicit condition of non-translatory motion and zero total angular momentum. Under these assumptions the following form of the internal kinetic energy T_q can be recovered:

$$T_q = \frac{1}{2}\mathbf{p}_q^T \mathbf{Q}(\mathbf{x})\mathbf{p}_q \tag{3.32}$$

where the matrix $\mathbf{Q}(\mathbf{x})$ has been defined according to:

$$\mathbf{Q}(\mathbf{x}) = \boldsymbol{\mu}_{(q,q)} + \mathbf{B}^T\boldsymbol{\mu}_{(\Omega,\Omega)}\mathbf{B} + \mathbf{B}^T\boldsymbol{\mu}_{(\Omega,q)} + \boldsymbol{\mu}_{(q,\Omega)}\mathbf{B} \tag{3.33}$$

By properly quantizing such an expression it is possible to show how the structure of the Hamiltonian operator in eq. 3.13 is conserved, with the only difference being the substitution of the $\boldsymbol{\mu}(\mathbf{x})$ matrix with the $\mathbf{Q}(\mathbf{x})$ one, also in the case of an internal coordinate-based approximation.

We will not go into more detail about the presented description since the explicit derivation of each term of the expression would represent a lengthy process, requiring the precise formalization of the BF orientation, that is beyond the scope of this general introduction. For a more complete discussion of the subject, we shall point the interested reader to the paper by Islampour [49] in which the problem, in the generalized context of an Hamiltonian taking into account also the electronic degrees of freedom, has been discussed in great detail. The result presented in this section will be fundamental in section 3.3 in which the same operator structure obtained in eq. 3.13 will be recovered for the Fokker-Planck-Smoluchowski operator giving to the presented theory a general validity in the study of tunneling processes in realistic molecular systems.

3.2 The Fokker-Planck-Smoluchowski equation

With the term stochastic process, we usually indicate a process in which a set of relevant variables $\mathbf{X}(t)$ evolves in time without a deterministic rule. This kind of process is omnipresent in real systems and is often induced by random interactions with the environment or simply generated by the ignorance of the observer about the existence of some hidden degree of freedom.

The random behavior of these systems calls for a probabilistic description that, in the case of a continuous set of stochastic variables $\mathbf{x}$, is usually expressed in terms of joint probability densities $\rho^{(n)}(\mathbf{x}_1, t_1; \mathbf{x}_2, t_2; ...\mathbf{x}_n, t_n)$. In order to clarify the meaning of a joint probability density it is convenient to consider its multiplication by the proper string of infinitesimal volumes $d\mathbf{x}_1 d\mathbf{x}_2 ... d\mathbf{x}_n$; the result of the operation represents the n-times probability of finding the stochastic variable $\mathbf{x}(t)$ in the range $d\mathbf{x}_i$ centered in $\mathbf{x}_i$ for each time t_i. Given a n-times probability density a $(n-1)$-times probability density can be obtained by integration over one time step.

Another fundamental object of the stochastic description is represented by the conditional probability density $\rho^{(m|n)}(\mathbf{x}_{n+1}, t_{n+1}; ...; \mathbf{x}_{n+m}, t_{n+m}|\mathbf{x}_1, t_1; ...; \mathbf{x}_n, t_n)$ that, when multiplied by the proper n-times probability density, extends the original probability density by m time-steps:

$$\begin{aligned}\rho^{(m+n)}(\mathbf{x}_1, t_1; ...; \mathbf{x}_{n+m}, t_{n+m}) = \\ = \rho^{(m|n)}(\mathbf{x}_{n+1}, t_{n+1}; ...; \mathbf{x}_{n+m}, t_{n+m}|\mathbf{x}_1, t_1; ...; \mathbf{x}_n, t_n)\rho^{(n)}(\mathbf{x}_1, t_1; ...; \mathbf{x}_n, t_n)\end{aligned} \tag{3.34}$$

The use of a joint-probability description is fundamental in the stochastic analysis since it allows us to keep track of the previous history of the system under study allowing the formulation of statistical predictions about its future evolution; a longer intrinsic memory of the system will correspond to a greater number of time steps required to its study. A particular case of stochastic evolution is represented by the Markov process in which the knowledge of the state of the system at a single previous time is sufficient to predict its probabilistic evolution in time. The description of these memory-less processes can, therefore, be achieved by adopting one-time probability densities $\rho^{(1)}(\mathbf{x}_1, t_1)$ and two-times conditional probability densities $\rho^{(1|1)}(\mathbf{x}_2, t_2|\mathbf{x}_1, t_1)$. We will adopt the term "homogeneous" to indicate a Markov process whose two-times conditional probability density $\rho^{(1|1)}(\mathbf{x}_2, t_2|\mathbf{x}_1, t_1) = \rho^{(1|1)}(\mathbf{x}_2, t_2 + \tau|\mathbf{x}_1, t_1 + \tau)$ is invariant under an arbitrary time shift τ while we will use the term "stationary" to indicate a homogeneous Markov

process characterized by a one-time probability $\rho^{(1)}(\mathbf{x}_1, t_1) = \rho^{(1)}(\mathbf{x}_1, t_1 + \tau)$ invariant under an arbitrary time shift τ.

Now that the basic terminology has been introduced let us consider, for the case of a Markov process, a fundamental relation, known in the literature as the Chapman-Kolmogorov equation, existing between one-times probability densities evaluated at different time-steps. Let us start by considering the following relation between joint-probabilities:

$$\rho^{(3)}(\mathbf{x}_1, t_1; \mathbf{x}_2, t_2; \mathbf{x}_3, t_3) = \rho^{(1|1)}(\mathbf{x}_3, t_3|\mathbf{x}_2, t_2)\rho^{(2)}(\mathbf{x}_1, t_1; \mathbf{x}_2, t_2) \tag{3.35}$$

By simple integration over $\mathbf{x}_2$ one can easily obtain the relation connecting two times probability densities in the form:

$$\rho^{(2)}(\mathbf{x}_1, t_1; \mathbf{x}_3, t_3) = \int d\mathbf{x}_2 \; \rho^{(1|1)}(\mathbf{x}_3, t_3|\mathbf{x}_2, t_2)\rho^{(2)}(\mathbf{x}_1, t_1; \mathbf{x}_2, t_2) \tag{3.36}$$

Recalling that a single piece of information in time suffice for the description of a Markov process we can drop the $(\mathbf{x}_1, t_1)$ time-step from the two-times probability notation obtaining:

$$p(\mathbf{x}, t) = \int d\mathbf{x}' \; \rho(\mathbf{x}, t|\mathbf{x}', t_0)p(\mathbf{x}', t_0) \tag{3.37}$$

where, for sake of simplicity, we dropped the label specifying that we are referring to one-time probability densities in favor of the symbol $p(\mathbf{x}, t)$ more evocative of the fact that the distribution is normalized by simple integration over the domain of the variable $\mathbf{x}$. Furthermore the substitutions, $(\mathbf{x}, t) = (\mathbf{x}_3, t_3)$ and $(\mathbf{x}', t_0) = (\mathbf{x}_2, t_2)$, have been applied to simplify the notation even more.

Equation 3.37 represents the formal expression describing the exact evolution of the one-time probability density associated with a Markov process. The direct solution of such an equation is often too complex or impractical. A simpler approximated partial differential equation, known as the Fokker-Planck equation, is usually employed to describe the dynamics of a Markovian system. This equation, the derivation of which is presented in appendix D, assumes the following form:

$$\frac{\partial p(\mathbf{x}, t)}{\partial t} = -\sum_i \frac{\partial A_i(\mathbf{x}, t)p(\mathbf{x}, t)}{\partial x_i} + \frac{1}{2}\sum_{i,j} \frac{\partial^2 B_{i,j}(\mathbf{x}, t)p(\mathbf{x}, t)}{\partial x_i \partial x_j} \tag{3.38}$$

where $A_i(\mathbf{x}, t)$ represents the i-th component of the drift vector $\mathbf{A}(\mathbf{x}, t)$ while $B_{i,j}(\mathbf{x}, t)$ is the matrix element of the generalized diffusion matrix $\mathbf{B}(\mathbf{x}, t)$. These are defined according to:

$$A_i(\mathbf{x}, t) := \lim_{\Delta t \to 0} \frac{1}{\Delta t} \int d\mathbf{x}'(x_i' - x_i)\rho(\mathbf{x}', t + \Delta t|\mathbf{x}, t) \tag{3.39}$$

$$B_{i,j}(\mathbf{x}, t) := \lim_{\Delta t \to 0} \frac{1}{\Delta t} \int d\mathbf{x}'(x_i' - x_i)(x_j' - x_j)\rho(\mathbf{x}', t + \Delta t|\mathbf{x}, t) \tag{3.40}$$

Please notice how the r.h.s. of eq. 3.38 represents, according to the continuity equation, the divergence of the probability current $\mathbf{J}(\mathbf{x}, t)$ changed in sign. From this observation the following relation for the i-th probability current component can be obtained:

$$J_i(\mathbf{x}, t) = A_i(\mathbf{x}, t)p(\mathbf{x}, t) - \frac{1}{2}\sum_j \frac{\partial B_{i,j}(\mathbf{x}, t)p(\mathbf{x}, t)}{\partial x_j} \tag{3.41}$$

In the particular case of a homogeneous Markov process the two-times conditional probability density $\rho(\mathbf{x}', t + \Delta t|\mathbf{x}, t)$ is time-independent and, as a direct consequence, so are the $A_i(\mathbf{x})$ and $B_{i,j}(\mathbf{x})$ terms. If the stationary limit is invoked, the one-time probability density becomes the time-independent distribution $p_{\text{stat}}(\mathbf{x})$. As a consequence the probability current becomes constant and a link between the $A_i(\mathbf{x})$ and $B_{i,j}(\mathbf{x})$ terms can be obtained according to:

$$\sum_i \frac{\partial A_i(\mathbf{x}, t)\rho(\mathbf{x}, t)}{\partial x_i} = \frac{1}{2}\sum_{i,j} \frac{\partial^2 B_{i,j}(\mathbf{x}, t)\rho(\mathbf{x}, t)}{\partial x_i \partial x_j} \tag{3.42}$$

Now that the formal structure has been outlined let us look back to the concept of stochastic variables $\mathbf{x}$ and let us specify what these variables represent in the field of studying molecular motion. The study of

the classical dynamics of molecules requires, in general terms, the adoption of a phase space description in which the position and momentum of each particle are considered. These variables can fluctuate in time under both the randomizing effect of the environment and the dissipative effect induced by various forms of friction. The interplay between these factors is quite delicate and different regimes of motion can be identified. In what follows we will consider the limit case of high friction in which the self-correlation time of the particle velocities is small enough to neglect inertial effects in the motion. In this regime, often referred to as diffusive or over-damped, the momenta observe a fast relaxation to their equilibrium states leaving the configurational variables $\mathbf{q}$ as the proper set of variables to describe the system dynamics. Under these circumstances the system diffuses, under the effect of an external potential profile $U(\mathbf{q})$, toward its equilibrium probability density $p_{\text{eq}}(\mathbf{q})$ correspondent to the Boltzmann distribution:

$$p_{\text{eq}}(\mathbf{q}) = e^{-\beta U(\mathbf{q})} \quad \text{with} \quad \beta = \frac{1}{k_B T} \tag{3.43}$$

Whenever a system reaches, as its stationary state, the equilibrium distribution, the probability flux in eq. 3.41 vanishes and the following relation between the drift and generalized diffusion terms emerges:

$$A_i(\mathbf{q}) = \frac{1}{2} p_{\text{eq}}^{-1}(\mathbf{q}) \sum_j \frac{\partial B_{i,j}(\mathbf{x}) p_{\text{eq}}(\mathbf{x})}{\partial x_j} \tag{3.44}$$

By substituting this result in eq. 3.38 it is possible, with little elaboration, to obtain the equation, known in literature with the name Fokker-Planck-Smoluchowski (FPS) equation, describing the diffusive behavior of a homogeneous Markov process in the configuration space:

$$\frac{\partial p(\mathbf{q}, t)}{\partial t} = -\hat{\Gamma} p(\mathbf{q}, t) \tag{3.45}$$

where the Fokker-Planck-Smoluchowski operator $\hat{\Gamma}$ has been defined according to:

$$\hat{\Gamma} = -\frac{\partial}{\partial \mathbf{q}}^T \mathbf{D}(\mathbf{q}) p_{\text{eq}}(\mathbf{q}) \frac{\partial}{\partial \mathbf{q}} p_{\text{eq}}(\mathbf{q})^{-1} \tag{3.46}$$

Please notice how the generalized diffusion matrix $\mathbf{B}(\mathbf{q})$ has been replaced by the diffusion matrix $\mathbf{D}(\mathbf{q})$ defined according to:

$$\mathbf{D}(\mathbf{q}) = \frac{1}{2} \mathbf{B}(\mathbf{q}) \tag{3.47}$$

The Fokker-Planck-Smoluchowski operator is a real and positive semi-definite operator having the equilibrium probability distribution $p_{\text{eq}}(\mathbf{q})$ as its eigenfunction corresponding to a null eigenvalue. This has significant effects on the diffusive dynamics of a system that, over time, will relax toward the equilibrium state. This can be easily verified considering that eq. 3.45 accepts the following formal solution:

$$p(\mathbf{x}, t) = e^{-\hat{\Gamma}(t - t_0)} p(\mathbf{x}, t_0) \tag{3.48}$$

If $p(\mathbf{x}, t_0)$ is now expressed as a linear combination of the non-orthogonal eigenfunctions $\psi_n(\mathbf{x})$, defined according to $\hat{\Gamma}\psi_n(\mathbf{x}) = \lambda_n \psi_n(\mathbf{x})$, the following result can be obtained:

$$e^{-\hat{\Gamma}(t-t_0)} p(\mathbf{x}, t_0) = e^{-\hat{\Gamma}(t-t_0)} \sum_n c_n(t_0) \psi_n(\mathbf{x}) = \sum_n c_n(t_0) e^{-\lambda_n (t-t_0)} \psi_n(\mathbf{x}) \tag{3.49}$$

As can be seen from such an equation each eigenfunction of the FPS operator represents a relaxation mode whose exponential decay rate is set by the correspondent eigenvalue. In the limit of $t \to +\infty$ all the states associated with a positive eigenvalue will decay leaving, as anticipated, the equilibrium distribution $p_{\text{eq}}(\mathbf{x}) = \psi_0(\mathbf{x})$, associated with the null eigenvalue, as the sole contribution to the probability.

The obtained formal apparatus is fundamental in describing the diffusive behavior of configuration variables at different scales and plays, in the chemical context, a fundamental role in the description of the diffusion of chemical species in solution. In section 3.2.1 the problem of the description of activated processes will be presented and the role of the eigenvalue spectrum of the FPS operator in the context of transition rates estimation will be outlined.

Before discussing such a problem, however, let us make a general observation: the FPS operator from eq. 3.46 represents a non-Hermitian operator while the quantum Hamiltonian is self-adjoint. If a

relationship exists between the operators one should find a way to express the description encoded in the FPS equation in some form of description based upon a self-adjoint operator. This, fortunately, is a standard method of stochastic treatment that goes under the name of symmetrization. The process is quite simple and starts with the introduction of the symmetrized-distribution $\tilde{p}(\mathbf{q},t)$ associated with a generic probability distribution $p(\mathbf{q},t)$, according to:

$$\tilde{p}(\mathbf{q},t) = p(\mathbf{q},t)p_{\mathrm{eq}}(\mathbf{q})^{-1/2} \tag{3.50}$$

Please notice how this new distribution is not normalized by simple integration over the stochastic variables domain. Adopting such a distribution in eq. 3.45 the following relation can be obtained:

$$\frac{\partial \tilde{p}(\mathbf{q},t)}{\partial t} = -\hat{\tilde{\Gamma}}\tilde{p}(\mathbf{q},t) \tag{3.51}$$

from which the symmetrized Fokker-Planck-Smoluchowski operator $\hat{\tilde{\Gamma}}$ can be defined according to:

$$\hat{\tilde{\Gamma}} = -p_{\mathrm{eq}}(\mathbf{q})^{-\frac{1}{2}}\frac{\partial}{\partial \mathbf{q}}^{T}\mathbf{D}(\mathbf{q})p_{\mathrm{eq}}(\mathbf{q})\frac{\partial}{\partial \mathbf{q}}p_{\mathrm{eq}}(\mathbf{q})^{-\frac{1}{2}} \tag{3.52}$$

The newly obtained self-adjoint operator share the same eigenvalue spectrum with the original FPS operator while its eigenfunctions $\tilde{\psi}_n(\mathbf{q})$ are connected to the eignefunctions $\psi_n(\mathbf{q})$ of the original operator by the relation:

$$\tilde{\psi}_n(\mathbf{q}) = \psi_n(\mathbf{q})p_{\mathrm{eq}}(\mathbf{q})^{-\frac{1}{2}} \tag{3.53}$$

3.2.1 The description of activated processes

With the term "activated process" we usually refer to a transition process in which a system can move from a stable state to another by overcoming a potential energy barrier. The act of overcoming such an energy obstacle requires some sort of activation energy that, for usual chemical processes, is provided by the fluctuating thermal energy of the system. The typical dynamic of a reactive system is hence characterized by long idling periods, in which the system fluctuates around a stable state without having sufficient energy to undergo a reactive process, followed by a rapid transition bringing the system in another stable state. This rare-event nature of the fluctuating dynamic has profound effects on the theoretical apparatus required to their description excluding, in the limit of high potential energy barriers, the possibility of adopting standard trajectory-based simulations that will spend the majority of their time exploring the equilibrium structure region. This calls for a probabilistic description of the system based on some sort of Fokker-Planck equation. In what follows the case of a diffusive stochastic system will be considered and, for this reason, the Fokker-Planck-Smoluchowski equation will be invoked for the discussion of the problem.

In order to start our discussion let us consider the classical picture, usually adopted by chemical kinetic, of a simple network of uni-molecular reactive processes in which two or more stable species can inter-convert. Let P_i represent some index of the population associated with the i-th species and let us indicate with $k_{i\to j}$ the rate constant dictating the transition rate for the conversion of the i-th species into the j-th one. According to this formalism, the following set of differential equations can be used to describe the time evolution of the reactive system:

$$\frac{dP_i(t)}{dt} = \sum_{j\neq i}\left[P_j(t)k_{j\to i} - P_i(t)k_{i\to j}\right] \tag{3.54}$$

The description just presented is surely very simplified but often it represents the only viable option to study the chemical kinetics. In many situations the initial probability distribution profile is unknown and hence evaluating its time evolution, using the FPS equation, is unfeasible. Under this circumstance, one may wonder if a correspondence exists between the two descriptions and whether one can predict the kinetic constants starting from a FPS type model.

As the first step in this direction, one has to define a correspondence between the continuous probability density $p(\mathbf{q},t)$ and the discrete population $P_i(t)$ associated with each species. This requires the introduction of a "domain of attraction" that, in simple terms, translates to the definition of a hypersurface marking the boundary within which a given point in the configuration space belongs to the domain

associated with a given stable state. Different ways have been proposed in the literature on how to define such a domain and how to enforce the separation through its boundary. In what follows we will adopt a general notation in which the separation is defined according to a localization function $g(\mathbf{q})$ whose action is defined as:

$$c_i(t) = \int d\mathbf{q}\, g_i(\mathbf{q}) p(\mathbf{q}, t) \tag{3.55}$$

Please notice how, in order to have a well-behaved correspondence between the two descriptions, the localization functions should sum to unity in every point in space:

$$\sum_i g_i(\mathbf{q}) = 1 \quad \forall \mathbf{q} \tag{3.56}$$

The concept of localization function will be the core of this thesis work and its analog in the quantum tunneling context will be introduced in chapter 4.

The second step in finding the relation existing between the two descriptions is to recognize how different processes can happen during the system dynamics. The first type of process is represented by the kinetic transfer of population between two different domains while the second one, hereafter called librational, is represented by motions within the same domain. A substantial time-scale separation exists between these two motions, with the former experiencing a slower relaxation than the latter. This time separation, greater in the case of higher potential energy barriers, translates into a gap in the eigenvalue spectrum of the FPS operator in which the lower set of eigenvalues are associated with the kinetic modes. This allows for a simplified description of the system in which only the lower eigenvalue band can be employed to the determination of the kinetic constants to be used in a Master-equation-like description. This projection action has a clear effect on the definition of the concept of the domain of attraction that should take into account the relaxation of the librational modes. This influences the definition of the localization function that, for this reason, should not have components along these fast relaxing modes.

Starting from this idea the projection operator $\hat{\mathcal{P}}$, capable of extracting from a given function its projection onto the kinetic subspace, can be defined according to:

$$\hat{\mathcal{P}} = \sum_{j,k} |g_j\rangle \left(\mathbf{S}^{-1}\right)_{j,k} \langle g_k | p_{\mathrm{eq}} \tag{3.57}$$

where $\mathbf{S}$ represents the overlap matrix $S_{i,j} = \langle g_i | p_{\mathrm{eq}} | g_j \rangle$ and $p_{\mathrm{eq}}(\mathbf{q})$ plays the role of integration factor. Adopting the ideas discussed above, one can express eq. 3.54 in terms of the FPS evolution:

$$\frac{dc_i(t)}{dt} = \int d\mathbf{q}\, g_i(\mathbf{q}) \frac{\partial p(\mathbf{q}, t)}{\partial t} = -\int d\mathbf{q}\, g_i(\mathbf{q}) \hat{\Gamma} p(\mathbf{q}, t) = -\int d\mathbf{q}\, p(\mathbf{q}, t) \hat{\Gamma}^\dagger g_i(\mathbf{q}) \tag{3.58}$$

As discussed by Moro [50], the term $\hat{\Gamma}^\dagger g_i(\mathbf{q})$ belongs to the kinetic subspace and, as such, must not be effected by the projection operator from eq. 3.57. This allows us to obtain:

$$\frac{dc_i(t)}{dt} = -\int d\mathbf{q}\, p(\mathbf{q}, t) \hat{\mathcal{P}} \hat{\Gamma}^\dagger g_i(\mathbf{q}) = -\sum_{j,k} \left(\mathbf{S}^{-1}\right)_{j,k} \langle g_k | p_{\mathrm{eq}} \hat{\Gamma}^\dagger | g_i \rangle \int d\mathbf{q}\, p(\mathbf{q}, t) g_j(\mathbf{q}) \tag{3.59}$$

Recalling eq. 3.55 and observing that $p_{\mathrm{eq}}(\mathbf{q}) \hat{\Gamma}^\dagger = \hat{\Gamma} p_{\mathrm{eq}}(\mathbf{q})$ one can easily verify how:

$$\frac{dc_i(t)}{dt} = -\sum_{j,k} c_j(t) \left(\mathbf{S}^{-1}\right)_{j,k} \Gamma_{k,i} \quad \text{with} \quad \Gamma_{k,i} = \langle g_k | \hat{\Gamma} p_{\mathrm{eq}} | g_i \rangle \tag{3.60}$$

From which, by direct comparison with eq. 3.54, the explicit expression for the kinetic constants $k_{j \to i}$ can be obtained according to:

$$k_{j \to i} = -\sum_k \left(\mathbf{S}^{-1}\right)_{j,k} \Gamma_{k,i} \tag{3.61}$$

This equality, representing a direct connection between the theoretical description of stochastic processes and the chemical kinetics, is capable of translating the distribution-based description, characteristic of the Fokker-Planck treatment, in easily accessible experimental data allowing for the interpretation of physically relevant phenomena.

3.2.2 Kramers theory

The theory described in the previous paragraph gives a general overview of the relation existing between the stochastic description of a diffusive system and the study of activated processes. Often however an even simpler formulation is required in order to easily connect the kinetic behavior of a system to some meaningful geometrical properties of the mean-field potential $U(\mathbf{q})$. For this reason in what follows we will discuss more in detail the problem of evaluating the escape rate of a stochastic particle from a site of a bi-stable potential evaluating, in this way, a simple approximation to its transition rate constant. In the present section, we will present, following the discussion proposed by Zwanzig [51], a simple discussion of the problem based on the concept of mean first passage time. Keep in mind that this is not the only possible way to discuss the problem and that similar results can be also obtained starting from the previously introduced localization function approach.

The concept of first passage time is quite intuitive and coincides with the time employed by a Brownian particle, moving in the phase space according to the Langevin equation, to leave the volume of space V associated with a given site. The dynamics of an ensemble of systems, characterized by different initial points $\mathbf{x}_0$, can be described by invoking the proper Fokker-Planck equation in which the volume V is surrounded by a surface ∂V characterized by absorbing boundary conditions. Starting at $t = 0$ with an initial distribution centered around $\mathbf{x}_0$, the following formal solution can be adopted for the probability distribution:

$$p(\mathbf{x}, t) = e^{-t\hat{\Gamma}}\delta(\mathbf{x} - \mathbf{x}_0) \tag{3.62}$$

Please notice how, due to the population loss induced by the absorbing boundary conditions, the probability of finding the particle in the volume V decays over time according to:

$$\mathcal{S}(t, \mathbf{x}_0) = \int_V p(\mathbf{x}, t)d\mathbf{x} \leq 1 \tag{3.63}$$

At any instant in time the variation of the $\mathcal{S}(t, \mathbf{x}_0)$ corresponds to the population loss experienced by the volume V or, in other terms, the derivative of the $\mathcal{S}(t, \mathbf{x}_0)$ function represents the probability distribution $\rho(t, \mathbf{x}_0)$ associated with the first passage time:

$$\rho(t, \mathbf{x}_0) = \frac{\partial \mathcal{S}(t, \mathbf{x}_0)}{\partial t} \tag{3.64}$$

The mean first passage time $\tau(\mathbf{x}_0)$ can now be computed as the average time:

$$\tau(\mathbf{x}_0) = \int_0^\infty t\rho(t, \mathbf{x}_0)dt \tag{3.65}$$

By recalling the relation in eq. 3.64, by applying the integration by parts and, finally, by applying the relations in eqs. 3.62 and 3.63; the following can be written:

$$\tau(\mathbf{x}_0) = \int_0^\infty dt\, \mathcal{S}(t, \mathbf{x}_0) = \int_0^\infty dt \int_V e^{-t\hat{\Gamma}}\delta(\mathbf{x} - \mathbf{x}_0)d\mathbf{x} = \int_0^\infty dt\, e^{-t\hat{\Gamma}^\dagger}1 \tag{3.66}$$

A simpler expression can now be obtained acting with $\hat{\Gamma}^\dagger$ on both sides of the equation:

$$\hat{\Gamma}^\dagger\tau(\mathbf{x}_0) = \int_0^\infty dt\, \hat{\Gamma}^\dagger e^{-t\hat{\Gamma}^\dagger}1 = \int_0^\infty dt\, \frac{\partial}{\partial t}e^{-t\hat{\Gamma}^\dagger}1 = -1 \tag{3.67}$$

If the case of a diffusive one-dimensional system, whose evolution is described by the Fokker-Planck-Smoluchowski operator from eq. 3.46, the solution can be easily found by multiple one-dimensional integration according to:

$$\tau(x_0) = D^{-1}\int_x^b dy\, e^{\frac{U(y)}{k_BT}}\int_a^y dz\, e^{\frac{-U(z)}{k_BT}} \tag{3.68}$$

where $b > x_0$ represents the position of the absorbing boundary while the point $a < x_0$ is here used to mark the starting point for the integration and it represents the position of a hypothetical reflection barrier used to redirect the system motion toward the b side.

Now that the expression of mean first passage time has been obtained, as a function of the potential $U(x)$, the simple case of a bi-stable potential can be considered. In such a case the integration limit a can be moved to $-\infty$ leaving us with the following expression for the mean first passage time:

$$\tau(x_0) = D^{-1} \int_x^b dy\, e^{\frac{U(y)}{k_B T}} \int_{-\infty}^y dz\, e^{\frac{-U(z)}{k_B T}} \tag{3.69}$$

By inspecting the integrand of the rightmost integral, it is easy to see how the maximum of the function must be encountered in correspondence to the minimum of the potential $U(x)$. Indicating such a point with $x_{\min}$ and adopting the symbol $\omega^2_{\min}$ to represent the curvature of the potential in that point, the following approximation, usually named the Laplace method, can be applied to the integral:

$$\int_{-\infty}^y dz\, e^{-\frac{U(z)}{k_B T}} \simeq e^{-\frac{U(x_{\min})}{k_B T}} \int_{-\infty}^{+\infty} dz\, e^{-\frac{\omega^2_{\min}}{2k_B T}(z-x_{\min})^2} = e^{-\frac{U(x_{\min})}{k_B T}} \sqrt{\frac{2\pi k_B T}{\omega^2_{\min}}} \tag{3.70}$$

At this point, the dependence of the remaining integral over the y variable upon the rightmost one is dropped and the Laplace approximation can be invoked for the second time. Indicating with $x_{\max}$ the maximum of the potential, this time correspondent to a minimum of the integral function, and adopting the symbol $\omega^2_{\max}$ to represent the curvature of the potential at that point, the following can be written:

$$\int_x^b dy\, e^{\frac{U(y)}{k_B T}} \simeq \frac{1}{2} e^{\frac{U(x_{\max})}{k_B T}} \int_{-\infty}^{+\infty} dz\, e^{-\frac{\omega^2_{\max}}{2k_B T}(y-x_{\max})^2} = \frac{1}{2} e^{\frac{U(x_{\max})}{k_B T}} \sqrt{\frac{2\pi k_B T}{\omega^2_{\max}}} \tag{3.71}$$

Adopting these approximated results in the mean first passage time definition it is easy to obtain:

$$\tau(x_0) = \frac{1}{D} \frac{\pi k_B T}{\omega_{\min}\omega_{\max}} e^{\frac{\Delta U}{k_B T}} \tag{3.72}$$

where $\Delta U = U_{\max} - U_{\min}$ represents the potential barrier height. Considering that a particle at the top of the potential barrier has an equal probability of either crossing it or falling back to the original minimum, one can easily conclude how the transition rate must be evaluated as half the arrival rate at the barrier top. Observing that this last quantity can be computed as the inverse of the mean first passage time, the following result can be obtained for the transition rate constant:

$$k = D \frac{\omega_{\min}\omega_{\max}}{2\pi k_B T} e^{-\frac{\Delta U}{k_B T}} \tag{3.73}$$

Please notice the similarity existing between this equation and the usual Arrhenius-like expression recovered from the transition state theory (TST) usually widely employed in the context of chemical kinetics.

3.3 Smoluchowski-Hamiltonian isomorphism

In this section we will make use of all the theoretical elements, so far described, in order to highlight the isomorphic relation existing between the quantum Hamiltonian description of the nuclear motion and the description, given according to the rules of stochastic dynamics, of a diffusive activated process. In order to do so, we will start by comparing the structures of the operators from eqs. 3.13 and 3.52 looking for a possible correspondence. This, however, must be done carefully recalling that different normalization rules have been employed across the two descriptions. While the wave-function in the quantum framework has been considered as invariant under coordinate transformation, as prescribed by eq. 3.6, the probability distribution has been considered as normalized by simple integration over the stochastic variable domain and hence its form must be modified, whenever a coordinate change is applied, by taking into account the absolute value of the Jacobian matrix determinant. In order to compare the two operators a new definition of probability density, invariant under a coordinate transformation, must be introduced in the Fokker-Planck-Smoluchowski description. This choice alters, depending on the coordinate system adopted, the structure of the FPS operator in eq. 3.52 that will preserve its current self-adjoint form only for a set of Cartesian coordinates.

In order to obtain the generalized formulation of the operator in eq. 3.52, let us start by rewriting its Cartesian expression in a more compact form. With this aim in mind let us introduce the primed variable

$\mathbf{x}'$ to highlight the Cartesian nature of the coordinate and let us make use of the Einstein summation notation. Under these assumptions the following form can be recovered:

$$\begin{aligned}\hat{\tilde{\Gamma}} &= -p_{\mathrm{eq}}(\mathbf{x}')^{-\frac{1}{2}}\partial_{i'}D(\mathbf{x}')^{i'j'}p_{\mathrm{eq}}(\mathbf{x}')\partial_{j'}p_{\mathrm{eq}}(\mathbf{x}')^{-\frac{1}{2}} = \\ &= p_{\mathrm{eq}}(\mathbf{x}')^{-\frac{1}{2}}\partial_{i'}^{\dagger}D(\mathbf{x}')^{i'j'}p_{\mathrm{eq}}(\mathbf{x}')\partial_{j'}p_{\mathrm{eq}}(\mathbf{x}')^{-\frac{1}{2}}\end{aligned} \tag{3.74}$$

If a new set of generalized configuration coordinates $\mathbf{x}$ is now introduced, one can express the Cartesian derivative operator on the new coordinate space according to $\partial_{i'} = \mathcal{J}_{i'}^{j}\partial_j$, where the symbol $\mathcal{J}_{i'}^{j}$ has been used to represent the Jacobian matrix element defined according to:

$$\frac{\partial x^{i'}}{\partial x^j} = \mathcal{J}_j^{i'} \quad \text{and} \quad \frac{\partial x^j}{\partial x^{i'}} = \mathcal{J}_{i'}^{j} \tag{3.75}$$

As anticipated above one can now introduce an invariant definition for the probability distribution by setting the following normalization rule over the new coordinate set:

$$\int_{\mathcal{D}'} p(\mathbf{x}',t)d\mathbf{x}' = \int_{\mathcal{D}} \sqrt{G}\, p(\mathbf{x}',t)|_{\mathbf{x}'=\mathbf{x}'(\mathbf{x})}\, d\mathbf{x} = 1 \tag{3.76}$$

where, in perfect analogy with the notation adopted in sec. 3.1.1, the symbol $\sqrt{G}$ has been used to represent the absolute value of the Jacobian matrix determinant. Under this formulation the probability distribution $p(\mathbf{x},t)$, in an arbitrary set of coordinate $\mathbf{x}$, can be computed by simply applying the proper variable substitution $p(\mathbf{x},t) \equiv p(\mathbf{x}',t)\big|_{\mathbf{x}'=\mathbf{x}'(\mathbf{x})}$.

At this point, the coordinate transformation rule for the operator can be easily implemented by enforcing the condition by which its spectral properties must not be influenced by a change in the coordinate set definition. This in turn can be easily obtained by both introducing the concept of scalar product between functions in the Hilbert space and imposing its invariance under a coordinate transformation. With this idea in mind the following relations chain can be obtained:

$$\begin{aligned}\langle\tilde{\rho}(t)|\hat{\tilde{\Gamma}}|\tilde{\rho}(t)\rangle &= \langle p_{\mathrm{eq}}^{-\frac{1}{2}}\tilde{\rho}(t)|\partial_{i'}^{\dagger}D^{i'j'}p_{\mathrm{eq}}\partial_{j'}|p_{\mathrm{eq}}^{-\frac{1}{2}}\tilde{\rho}(t)\rangle = \langle\partial_{i'}p_{\mathrm{eq}}^{-\frac{1}{2}}\tilde{\rho}(t)|D^{i'j'}p_{\mathrm{eq}}|\partial_{j'}p_{\mathrm{eq}}^{-\frac{1}{2}}\tilde{\rho}(t)\rangle = \\ &= \int_{\mathcal{D}'} d\mathbf{x}'\,\partial_{i'}\left[p_{\mathrm{eq}}(\mathbf{x}')^{-\frac{1}{2}}\tilde{\rho}(\mathbf{x}',t)\right]D^{i'j'}(\mathbf{x}')p_{\mathrm{eq}}(\mathbf{x}')\partial_{j'}p_{\mathrm{eq}}(\mathbf{x}')^{-\frac{1}{2}}\tilde{\rho}(\mathbf{x}',t) = \\ &= \int_{\mathcal{D}} d\mathbf{x}\sqrt{G}\,\mathcal{J}_{i'}^{a}\partial_a\left[p_{\mathrm{eq}}(\mathbf{x})^{-\frac{1}{2}}\tilde{\rho}(\mathbf{x},t)\right]D^{i'j'}(\mathbf{x}')\big|_{\mathbf{x}'=\mathbf{x}'(\mathbf{x})}p_{\mathrm{eq}}(\mathbf{x})\mathcal{J}_{j'}^{b}\partial_b p_{\mathrm{eq}}(\mathbf{x})^{-\frac{1}{2}}\tilde{\rho}(\mathbf{x},t) = \\ &= \int_{\mathcal{D}} d\mathbf{x}\sqrt{G}\,p_{\mathrm{eq}}(\mathbf{x})^{-\frac{1}{2}}\tilde{\rho}(\mathbf{x},t)\partial_a^{\dagger}D^{ab}(\mathbf{x})p_{\mathrm{eq}}(\mathbf{x})\partial_b p_{\mathrm{eq}}(\mathbf{x})^{-\frac{1}{2}}\tilde{\rho}(\mathbf{x},t)\end{aligned} \tag{3.77}$$

where the symbol $D^{ab}(\mathbf{x})$ has been introduced to represent the form of the diffusion tensor over the new coordinate set:

$$D^{ab}(\mathbf{x}) = \mathcal{J}_{i'}^{a}D^{i'j'}(\mathbf{x}')\big|_{\mathbf{x}'=\mathbf{x}'(\mathbf{x})}\mathcal{J}_{j'}^{b} \tag{3.78}$$

By recalling the definition of scalar product in generalized coordinates, that due to the selected normalization condition must correspond to the one introduced in eq. 3.7, the following form of the symmetrized FPS operator in generalized coordinates can be easily obtained:

$$\hat{\tilde{\Gamma}} = p_{\mathrm{eq}}(\mathbf{x})^{-\frac{1}{2}}\partial_a^{\dagger}D^{ab}(\mathbf{x})p_{\mathrm{eq}}(\mathbf{x})\partial_b p_{\mathrm{eq}}(\mathbf{x})^{-\frac{1}{2}} \tag{3.79}$$

Under the conditions posed, the relation existing between the derivative operator and its adjoint must be dictated by eq. 3.12. By simple substitution it is therefore easy to show how the previous operator can be rewritten in the form:

$$\hat{\tilde{\Gamma}} = -\frac{1}{\sqrt{G}}p_{\mathrm{eq}}(\mathbf{x})^{-\frac{1}{2}}\partial_a\sqrt{G}D^{ab}(\mathbf{x})p_{\mathrm{eq}}(\mathbf{x})\partial_b p_{\mathrm{eq}}(\mathbf{x})^{-\frac{1}{2}} \tag{3.80}$$

Now that the generalized form of the Fokker-Planck-Smoluchowski operator has been obtained under the proper normalization condition, we can move back our attention to the problem of understanding the relation existing between such an operator and the Born-Oppenheimer quantum Hamiltonian from eq. 3.13.

In order to do so, let us start our analysis by observing how the definition of the ground-state wave-function $\psi_0(\mathbf{x})$, according to the Hamiltonian eigenvalue problem:

$$\hat{H}\psi_0(\mathbf{x}) = -\frac{\hbar^2}{2\sqrt{G}}\partial_a\sqrt{G}\mu^{ab}\partial_b\psi_0(\mathbf{x}) + V(\mathbf{x})\psi_0(\mathbf{x}) = E_0\psi_0(\mathbf{x}) \tag{3.81}$$

establishes a bi-univocal connection between the quantum potential form $V(\mathbf{x})$ and the correspondent ground state wave-function. This relation has, as a matter of fact, bidirectional nature and can also be interpreted as a definition expressing, with an intrinsic unknown energy bias correspondent to the zero-point energy, the quantum potential profile associated with a hypothetically given ground-state wave-function $\psi_0(\mathbf{x})$. By inverting the above expression such a relation can be trivially rewritten according to:

$$\delta V(\mathbf{x}) := V(\mathbf{x}) - E_0 = \frac{\hbar^2}{2\sqrt{G}}\psi_0(\mathbf{x})^{-1}\partial_a\sqrt{G}\mu^{ab}\partial_b\psi_0(\mathbf{x}) \tag{3.82}$$

where the δ symbol has been here introduced, and used hereafter, to indicate relative energies measured taking the ground-state energy E_0 as a reference. Please notice how a "procedural asymmetry" characterizes the problem: the determination of the ground-state wave-function associated with a generic mean-field potential is a tough problem often requiring elaborated strategies for its solution; the other way around, on the other hand, is essentially effortless. This observation opens a new paradigm in quantum potential modeling changing the focus from the proper modeling of quantum mean-field potential to the definition of well-behaved ground-state distributions from which the target potential can be obtained by application of eq. 3.82. Adopting the ground-state energy as the zero of the energy scale a shifted Hamiltonian operator $\delta\hat{H} = \hat{H} - E_0$ can be introduced according to:

$$\delta\hat{H} = -\frac{\hbar^2}{2\sqrt{G}}\partial_a\sqrt{G}\mu^{ab}\partial_b + \delta V(\mathbf{x}) \tag{3.83}$$

With little elaboration the just obtained operator can be rewritten in the following form:

$$\delta\hat{H} = -\frac{\hbar^2}{2\sqrt{G}}\psi_0(\mathbf{x})^{-1}\partial_a\sqrt{G}\mu^{ab}\psi_0(\mathbf{x})^2\partial_b\psi_0(\mathbf{x})^{-1} \tag{3.84}$$

In order to demonstrate the equivalence between the expression in eqs. 3.83 and 3.84 let us start elaborating the latter to obtain the former according to:

$$\begin{aligned}
\delta\hat{H}f(\mathbf{x}) &= -\frac{\hbar^2}{2\sqrt{G}}\psi_0(\mathbf{x})^{-1}\partial_a\sqrt{G}\mu^{ab}\psi_0(\mathbf{x})^2\partial_b\psi_0(\mathbf{x})^{-1}f(\mathbf{x}) = \\
&= -\frac{\hbar^2}{2\sqrt{G}}\psi_0(\mathbf{x})^{-1}\partial_a\sqrt{G}\mu^{ab}\left\{\psi_0(\mathbf{x})\left[\partial_b f(\mathbf{x})\right] - f(\mathbf{x})\left[\partial_b\psi_0(\mathbf{x})\right]\right\} = \\
&= -\frac{\hbar^2}{2\sqrt{G}}\partial_a\sqrt{G}\mu^{ab}\left[\partial_b f(\mathbf{x})\right] - -\frac{\hbar^2}{2\sqrt{G}}\psi_0(\mathbf{x})^{-1}\left[\partial_a\psi_0(\mathbf{x})\right]\sqrt{G}\mu^{ab}\left[\partial_b f(\mathbf{x})\right] + \\
&\quad + \frac{\hbar^2}{2\sqrt{G}}\psi_0(\mathbf{x})^{-1}f(\mathbf{x})\partial_a\sqrt{G}\mu^{ab}\left[\partial_b\psi_0(\mathbf{x})\right] + \frac{\hbar^2}{2\sqrt{G}}\psi_0(\mathbf{x})^{-1}\left[\partial_a f(\mathbf{x})\right]\sqrt{G}\mu^{ab}\left[\partial_b\psi_0(\mathbf{x})\right] = \\
&= \left[-\frac{\hbar^2}{2\sqrt{G}}\partial_a\sqrt{G}\mu^{ab}\partial_b + \frac{\hbar^2}{2\sqrt{G}}\psi_0(\mathbf{x})^{-1}\partial_a\sqrt{G}\mu^{ab}\partial_b\psi_0(\mathbf{x})\right]f(\mathbf{x})
\end{aligned} \tag{3.85}$$

in which the symmetry property of the mass tensor $\mu^{ab} = \mu^{ba}$ has been used to simplify the expression.

Please notice how if the FPS equilibrium distribution $p_{\mathrm{eq}}(\mathbf{x})$ is interpreted as the squared, real-valued, ground-state wave-function $p_{\mathrm{eq}}(\mathbf{x}) = \psi_0(\mathbf{x})^2$, the operator in eq. 3.84 became isomorphic to the symmetrized FPS operator from eq. 3.80 according to:

$$\delta\hat{H} = \hbar\hat{\tilde{\Gamma}} \quad \text{with} \quad D^{ab} = \frac{\hbar}{2}\mu^{ab} \tag{3.86}$$

in which the $\hbar$ proportionality coefficient adjusts the unit of measurement by translating the transition frequency units, returned by the FPS operator, into the proper energy units characterizing the Hamiltonian operator. Following this similarity relation one can go one step forward; by taking inspiration

from the Boltzmann distribution from eq. 3.43, the concept of equilibrium potential $U(\mathbf{x})$ can also be introduced in the context of quantum mechanics according to the relations:

$$\psi_0(\mathbf{x}) := \mathcal{N} e^{-\frac{1}{2}U(\mathbf{x})} \quad \text{or} \quad U(x) := -2\ln\left[\mathcal{N}^{-1}\psi_0(x)\right] \tag{3.87}$$

where $\mathcal{N}$ has been used to indicate the proper normalization coefficient. This quantity, despite not having a direct physical correspondence in the quantum description, is usually very easy to manipulate and will be used extensively throughout this thesis with the aim of simplifying the theoretical treatment. Adopting this quantity in the expression of the shifted quantum potential from eq. 3.82 one can easily show how:

$$\delta V(\mathbf{x}) = -\frac{\hbar^2}{4\sqrt{G}}\partial_a\sqrt{G}\mu^{ab}\left[\partial_b U(\mathbf{x})\right] + \frac{\hbar^2}{8\sqrt{G}}\left[\partial_a U(\mathbf{x})\right]\sqrt{G}\mu^{ab}\left[\partial_b U(\mathbf{x})\right] \tag{3.88}$$

Before moving on, let us underline how this isomorphic relation represents a pure mathematical link between the two theoretical treatments that is limited to the analysis of the spectral properties of the two operators. From the phenomenological point of view, no relation exists between the time evolution characterizing the two problems that, as a matter of fact, display radically different behaviors: the dynamics of an isolated quantum system, described by the Schrödinger equation, is characterized by an oscillating coherent behavior while the stochastic one is instead dominated by an overall relaxation toward equilibrium.

This isomorphism relation opens a direct correspondence between the eigenvalue problems of the two operators allowing the direct application of theoretical tools, usually applied in the field of stochastic analysis, to the study of the eigenvalue spectrum of the Hamiltonian operator. The relevance of this similarity is particularly evident if the problem of tunneling splitting in the vibrational ground-state is examined. In such a situation the ground state tunneling splitting pattern finds direct correspondence in the eigenvalue structure of the low lying kinetic modes of the FPS operator and can be expressed directly in terms of the expectation value of the shifted Hamiltonian operator on a properly defined approximation of the first excited state. Following this inspiration, the localization function approach will be adapted in chapter 4 to the study of simple mono-dimensional tunneling problems. In the same chapter, the problem of vibrationally excited tunneling splitting will be also discussed and we will show how, despite being connected to the FPS librational eigenvalues, their evaluation can also take advantage of the theoretical structure here introduced. This similarity relation creates a powerful and suggestive connection between the tunneling splitting estimation and the computation of transition rates in the framework of the Smoluchowski description of activated processes that will be examined throughout the rest of this thesis.

Chapter 4

Tunneling splitting in one dimension

In chapter 3 the isomorphic relation existing between the Born-Oppenheimer nuclear Hamiltonian operator and the Fokker-Planck-Smoluchowski one has been presented and the relation existing between the evaluation of tunneling splitting and the study of activated processes has been outlined. The aim of this chapter is to discuss the application of those results in the simple case of a one-dimensional symmetric bi-stable system in which the mass of the system is considered as a constant. The simplicity of the system will allow us to obtain a clear description of the problem that will be used as the foundation of more advanced theoretical discussions. In section 4.1 the localization function method will be presented for the case of the ground state tunneling splitting and, starting from such a result, a general Kramers-like asymptotic approximation will be presented. The problem of defining a well-behaved ground state model will be discussed in section 4.2 and two simple double-Gaussian distribution models will be presented. In the same section, the accuracy of the localization function method will be tested in the case of both model systems. The chapter is closed by section 4.3 in which the problem of computing vibrationally excited tunneling splitting will be discussed in the framework of a generalized localization function method.

4.1 Ground-state localization function method

Let us start our discussion by considering a simple one-dimensional symmetric bi-stable potential $V(x)$ defined, according to eq. 3.82, upon a given ground-state wave-function $\psi_0(x)$. For sake of generality let us, for the time being, leave the definition of $\psi_0(x)$ unspecified. Let us set the maximum point of the potential barrier as the origin of the reference system, such that the symmetry condition can be easily enforced according to $\psi_0(x) = \psi_0(-x)$, and let us consider the mass m of the system as a constant. Under these hypotheses, a shifted Hamiltonian operator can be defined, as prescribed by eq. 3.84, according to:

$$\delta\hat{H} = \hat{H} - E_0 = -\frac{\hbar^2}{2m}\psi_0(x)^{-1}\frac{\partial}{\partial x}\psi_0(x)^2\frac{\partial}{\partial x}\psi_0(x)^{-1} \tag{4.1}$$

Starting from such a definition, the tunneling splitting δE_1 can be simply computed as the expectation value of the shifted Hamiltonian operator $\delta E_1 = E_1 - E_0 = \langle\psi_1|\delta\hat{H}|\psi_1\rangle$ in respect to the first excited state normalized wave-function $\psi_1(x)$.

The exact shape of the first excited-state wave-function is clearly not known *a-priori* but a reasonable approximation of it can be obtained, in the limit of high potential energy barriers, by taking inspiration from the description of activated processes commonly adopted in the framework of stochastic analysis. In order to do so, let us start by introducing the quantum-mechanical definition of localization function $g(x)$ as the ratio between the first excited wave-function $\psi_1(x)$ and the ground-state one $\psi_0(x)$:

$$g(x) := \frac{\psi_1(x)}{\psi_0(x)} \tag{4.2}$$

Making use of such a newly introduced function, the following form of the shifted-Hamiltonian eigenvalue problem, referred to the first excited-state, can be obtained:

$$\delta\hat{H}\psi_1(x) = -\frac{\hbar^2}{2m}\psi_0(x)^{-1}\frac{\partial}{\partial x}\psi_0(x)^2\frac{\partial}{\partial x}g(x) = \delta E_1\psi_1(x) \tag{4.3}$$

in which $g(x)$, being defined upon the exact first excited-state wave-function, still represents an unknown quantity. At this point, an approximated form of the localization function can be searched in the limit of high potential energy barriers ($\Delta V \to +\infty$) for which the tunneling splitting, being a measurement of the coupling between states, tend to vanish ($\delta E_1 \to 0$). Under these hypotheses, by applying a double one-dimensional integration, one can easily obtain the following relation:

$$g(x) = \int c_1 \psi_0(x)^{-2} dx + c_2 \tag{4.4}$$

where c_1 and c_2 represent two integration coefficients to be determined. Just by looking at eq. 4.4 one can easily see how the obtained relation presents, due to the vanishing nature of the wave-function for $x \to \pm\infty$, a diverging behavior that, as such, prevents its direct application to the definition of a well-behaved localization function. To circumvent this issue a patched definition of localization function must be introduced. No *a-priori* information is available about how this patching scheme must be defined but the variational argument can always be invoked to evaluate the validity of the choice. As a matter of fact, the symmetry of the system imposes a partition in the Hilbert space $\mathcal{H}$ in which the Hamiltonian operator, commuting with the proper symmetry operator, does not mix functions belonging to the even $\mathcal{H}_+$ and odd $\mathcal{H}_-$ sub-spaces. This imparts to the $\psi_1(x)$ wave-function the status of lower-state of the odd Hilbert subspace that, consequently, must obey to the variational theorem. In what follows we will adopt, without excluding that a better definition can be possibly found, the following piece-wise definition of the localization function:

$$g(x) := \begin{cases} -1 & x < -x_m \\ I^{-1} \int_0^x \psi_0(y)^{-2} dy & -x_m \leq x \leq x_m \\ 1 & x > x_m \end{cases} \tag{4.5}$$

where $\pm x_m$ indicate the locations of the minima of the mean field potential $U(x)$, corresponding to the maxima of $\psi_0(x)$, while the constant I denotes the integral:

$$I := \int_0^{x_m} \psi_0(y)^{-2} dy \tag{4.6}$$

Please notice how the definition from eq. 4.5 must be properly normalized in order to return, when applied to the ground-state model $\psi_0(x)$, an unitary-norm approximation, hereafter indicated with $\psi_1^g(x)$, of the first excited-state wave-function $\psi_1(x)$:

$$\psi_1^g(x) := N g(x) \psi_0(x) \quad \text{with} \quad N = \langle g|\psi_0^2|g\rangle^{-\frac{1}{2}} \tag{4.7}$$

By adopting this approximated form in the expression for the shifted-Hamiltonian expectation value, it is simple to obtain the following estimate for the tunneling splitting:

$$\delta E_1^g := \langle \psi_1^g | \delta \hat{H} | \psi_1^g \rangle = \frac{\hbar^2}{m I \langle g|\psi_0^2|g\rangle} \tag{4.8}$$

where the integration by parts has been employed to simplify the expression. As can be seen from the result just obtained, the localization function approach allows for a simple analytical approximation of the tunneling splitting whose evaluation requires the computation of only two one-dimensional integrals. Giving to the reader a universal estimate of the accuracy associated with the proposed approach is difficult since its overall performance strongly depends upon the ground state model adopted. Some general results will be discussed in section 4.2.2 where two simple well-behaved ground state models will be introduced and studied.

Before moving on with our discussion, let us focus briefly on the meaning of the quantum localization function and on the relation connecting it to its stochastic counterpart. First of all, just by looking at the definition from eq. 4.5, one can easily appreciate how the localization function $g(x)$ presents two flat regions connected by a sharp change in value confined, due to the fact that the ground state wave-function is localized about the potential minima, to a narrow domain centered at the location of the potential maximum [50, 52]. Starting from such a definition, the linear combinations $g^{\pm}(x) := [1 \pm g(x)]/2$ can be defined. These quantities, hereafter addressed with the name of site-localization functions, resemble unitary step functions ($0 \leq g(x) \leq 1$) capable of identifying the proper domain

of attraction associated with one of the two potential wells. These site-localization functions play a fundamental role in understanding the meaning of the asymptotic treatment and, as a matter of fact, are very much connected to the same idea of site states that has been used in sec. 2.3 to introduce the reader to the origin of tunneling splitting. In order to better explain such a point let us invoke the asymptotic limit of high barrier in which the proper set of site-states ($|R\rangle$ and $|L\rangle$) can be considered as orthogonal $\langle R|L\rangle = 0$. By simply expressing the localization function $g(x)$ in terms of site states, the following can be written:

$$g(x) = \frac{\varphi_R(x) - \varphi_L(x)}{\varphi_R(x) + \varphi_L(x)} \tag{4.9}$$

where $\varphi_R(x)$ and $\varphi_L(x)$ represents the wave-functions associated to each site. Starting from this definition it is trivial to observe how the proper spatial distribution associated to a given site can be obtained from the action of proper site-localization function on the ground-state wave-function:

$$\varphi_R(x) = g^-(x)\psi_0(x) \quad \text{while} \quad \varphi_L(x) = g^+(x)\psi_0(x) \tag{4.10}$$

This result has remarkable illustrative power and shows how, once again, a strong similarity exists between the quantum description based on the $g^{\pm}(x)$ functions and its stochastic counterpart presented in eq. 3.55.

4.1.1 Asymptotic limit approximation

In the previous paragraph, the concept of localization function has been introduced and a simple approximated integral expression for the ground-state tunneling splitting has been obtained. In the present section, starting from such a relation, reported in eq. 4.8, a simple asymptotic approximation will be formulated. In order to do so let us start by examining the I integral from eq. 4.6 that, recalling the definition of the mean-field potential $U(x)$ from eq. 3.87, could easily be rewritten in the form:

$$I = \frac{1}{2}\mathcal{N}^{-2}\int_{-x_m}^{x_m} e^{U(x)}dx \tag{4.11}$$

Given the bi-stable nature of the potential $U(x)$, one can easily conclude that, in the considered integration domain, the involved integrand must represent a function with a single maximum located at $x = 0$. Starting from this observation, one can invoke the Laplace method, discussed in appendix C, to approximate the I integral according to the expression:

$$I = \frac{1}{2}\mathcal{N}^{-2}e^{U(0)}\int_{-\infty}^{+\infty} e^{\frac{1}{2}U''(0)x^2}dx = \frac{1}{2}\mathcal{N}^{-2}e^{U(0)}\sqrt{\frac{2\pi}{|U''(0)|}} \tag{4.12}$$

If now we focus our attention to the normalization factor expression:

$$N = \int_{-\infty}^{+\infty} g(x)^2\psi_0(x)^2dx \tag{4.13}$$

we can easily see how, in the asymptotic case of high potential barriers, the localization function $g(x)$ must manifest a very steep change in value around $x = 0$, passing from a negative unitary value to a positive one. This step-like behavior allows us to neglect the localization function contribution in the normalization integral that, for this reason, can be approximated according to:

$$N = \int_{-\infty}^{+\infty} \psi_0(x)^2dx \tag{4.14}$$

The argument of this integral clearly represents a bi-modal distribution symmetric in respect to the origin. This observation allows us to rewrite the normalization integral in the form:

$$N = 2\int_{0}^{+\infty} \psi_0(x)^2dx = 2\mathcal{N}^2\int_{0}^{+\infty} e^{-U(x)}dx \tag{4.15}$$

Once again, recognizing that the argument of the integral must be a function with a maximum centered in $x = x_m$, the Laplace approximation can be invoked to obtain the expression:

$$N = 2\mathcal{N}^2e^{-U(x_m)}\int_{-\infty}^{+\infty} e^{-\frac{1}{2}U''(x_m)(x-x_m)^2}dx = 2\mathcal{N}^2e^{-U(x_m)}\sqrt{\frac{2\pi}{U''(x_m)}} \tag{4.16}$$

Substituting the results from eqs. 4.12 and 4.16 in eq. 4.8, it is possible to obtain the following asymptotic tunneling splitting estimate:

$$\delta E_1^{\text{asy}} = \frac{\hbar^2}{2m\pi}\sqrt{U''(x_m)\,|U''(0)|}e^{-\Delta U} \tag{4.17}$$

where $\Delta U = U(0) - U(x_m)$ represents the mean-field potential barrier height. Recalling that, due to the isomorphic relation existing between the FPS operator and the quantum Hamiltonian, the estimation of tunneling splitting corresponds exactly to the evaluation of the classical kinetic constants; one can easily conclude that the just obtained approximation must represent the quantum equivalent of the Kramers estimate from eq. 3.73. Please notice how these two relations share the same mathematical structure.

The relation just obtained clearly represents a general formulation derived under a double Laplace integration. The validity of such an approximation is not, however, guaranteed and must be verified on the basis of the selected ground-state model. In section 4.2.3 we will show how the previous result fails to reproduce, in the case of a double Gaussian distribution, the correct asymptotic behavior for the tunneling splitting and how the correct asymptotic approximation can be recovered.

4.2 Ground state distribution models

The starting point of the procedure described in section 4.1 is represented by the definition of a proper ground-state distribution capable of describing, through the relation imposed by eq. 3.82, a well-behaved and physically meaningful quantum potential model. The aim of the present section is to both give to the reader a general overview of the pitfalls encountered during such modeling effort and to demonstrate how a set of well-behaved ground-state models can be obtained starting from a simple two-Gaussian distribution (TGD).

In principle, the definition of a ground-state model can be achieved following different approaches. These ranges form of a direct definition of the ground state wave-function $\psi_0(x)$, either directly or through its correspondent probability distribution $\rho_0(x) = \psi_0(x)^2$, to the direct specification of a mean-field potential model $U(x)$. The selection of one of these functions is however not trivial and often seemingly reasonable ground-states models result in quantum potentials $V(x)$ showing a profile either non-physical or non-bi-stable. This is, for instance, what is often found when mean-field potential models, routinely adopted in the field of activated processes, are employed. In order to demonstrate the last statement, let us consider, as an example, a generic mean-field potential defined according to $U(x) = \Delta U s(x)$, where the term ΔU represents the barrier height while $s(x) = s(-x)$ represents a parameterized symmetric "shape-function", responding to the condition $s(0) - s(\pm x_m) = 1$, characterized by two minima at $x = \pm x_m$ and a maximum at the origin. By considering the large barrier limit of the quantum potential definition from eq. 3.88, it is simple to obtain the expression $\delta V(x) = \Delta U^2(\hbar^2/8m)s'(x)^2$ as the leading contribution in ΔU that, due to its dependence upon the square of the shape-function first derivative, must be characterized by minima in correspondence of the stationary points of $s(x)$. This not only implies the existence of a potential minimum at the point of minimum of $s(x)$ but also at its local maximum. In other words, by increasing the barrier height ΔU, for a fixed definition of shape function $s(x)$, one induces a change on the quantum potential profile moving from a standard bi-stable form to a completely different profile with three minima. A clear example of what just discussed can be seen by looking at figure 4.1 where a shape-function defined in the form of the quartic polynomial $s(x) = \left(1 - x^2/x_0^2\right)^2$, in which x_0 represents the length scale determined by the minimum location, has been considered for a variable value of the barrier height. In order to represent these data a new energy unit E_u has been introduced according to:

$$E_u := \frac{\hbar^2}{2mx_0^2} \tag{4.18}$$

A typical E_u value of 0.8kJ/mol in molar units or 67cm^{-1} wavenumbers is recovered for 1Å displacement of an hydrogen atom between the two minima at $\pm x_0$. This unit will be adopted throughout this chapter to report energy quantities in adimensional form.

The issue just discussed points out the intrinsic difficulty encountered when trying to define a proper, well-behaved, ground-state distribution starting from a model for the mean-field potential $U(x)$. For this reason, in what follows, our analysis will be oriented toward the adoption of, more easily tunable, wave-function-based definitions that, as will be demonstrated in the following sections, allows for the

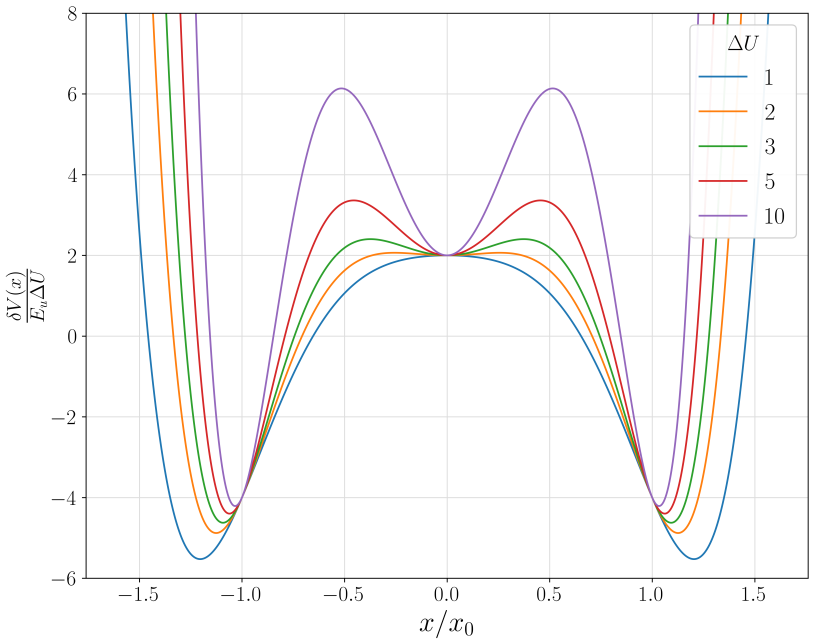

Figure 4.1: Quantum potential profiles $\delta V(x)$ obtained from the quartic mean-field potential $U(x) = \Delta U(1 - x^2/x_0^2)^2$ for different values of the barrier height ΔU. The quantum potential is evaluated in E_u units (see eq. 4.18) and is scaled by the barrier height ΔU in order to obtain roughly superimposable profiles.

obtainment of realistic potential profiles with the adaption of reasonably simple parametrizations. We have found that the direct modeling of the equilibrium distribution $\rho_0(x) = \psi_0(x)^2$ by means of Gaussian functions can provide an effective solution to the problem. This observation opens different possibilities in terms of parametrization that can range from the analytical definition of simple model potentials by means of two-Gaussian distributions, as will be discussed in sections 4.2.1 and 4.2.2, to the application of computationally-assisted fitting procedures capable of reproducing, within a certain extension in space, an arbitrary quantum potential profile.

4.2.1 Simple Two-Gaussian-Distribution model

The simplest formulation of a bi-modal ground-state probability distribution, associated with a bi-stable potential system, can be expressed as the combination of two Gaussian profiles symmetrically arranged about the origin. In such a simple model two independent parameters can be set: the width σ of the Gaussians and the center x_0 of the rightmost one:

$$\rho_0(x) := \frac{1}{\sqrt{8\pi\sigma^2}} \left[e^{-\frac{(x-x_0)^2}{2\sigma^2}} + e^{-\frac{(x+x_0)^2}{2\sigma^2}} \right] \tag{4.19}$$

Starting from such a simple definition, the corresponding mean-field potential can be specified, according to eq. 3.87, as:

$$U(x) = -\ln\left[\sqrt{8\pi\sigma^2}\rho_0(x)\right] = \frac{x_0^2 + x^2}{2\sigma^2} - \ln\left(e^{\frac{xx_0}{\sigma^2}} + e^{-\frac{xx_0}{\sigma^2}}\right) \tag{4.20}$$

where a suitable scale factor, correspondent to the $\mathcal{N}^{-2}$ coefficient from eq. 3.87, has been introduced in order to deal with an adimensional argument of the logarithm. At this point the result from eq. 4.20 can be applied into eq. 3.88 to obtain a simple formulation of the shifted quantum potential:

$$\delta V(x) = \frac{\hbar^2}{8m\sigma^4} \left\{ \left[x - x_0 \tanh\left(\frac{xx_0}{\sigma^2}\right) \right]^2 - 2\sigma^2 + 2x_0^2 \mathrm{sech}^2\left(\frac{xx_0}{\sigma^2}\right) \right\} \tag{4.21}$$

Looking at the structure of the system it is possible to observe how the maxima of $\rho_0(x)$, and consequently the minima of $U(x)$, are located near the centers of the Gaussian distributions, $x_m \simeq x_0$, with

displacements, in units of x_0, of the order of $\mathcal{S} := \exp\{-2x_0^2/\sigma^2\}$. The ratio σ/x_0, correspondent to the Gaussian width normalized by its displacement from the origin, plays the role of the control parameter of the model dictating the overlap between the two distributions. The parameter $\mathcal{S}$ can be adopted as a measurement of the superposition between the Gaussians, with the two limits of a vanishing superposition ($\mathcal{S} = 0$) for infinitely narrow Gaussians, and of a complete overlay ($\mathcal{S} = 1$) for a vanishing separation ($x_0/\sigma \to 0$). The objective of describing the tunneling splitting requires a clear definition of localized states at an energy lower than that of the barrier top which, in turn, translates to the situation of two well-separated local Gaussian contributions. This calls for a small enough superposition coefficient $\mathcal{S}$ and, for this reason, we will assume, from now on, that $\mathcal{S}$ is small enough to allow for the identification of the mean-field minima with the centers of the Gaussians, $x_m = x_0$.

Now that a general formulation, connecting the TGD model to the correspondent quantum potential, has been introduced, let us briefly discuss how the parameters selection impacts the structure of the model and, consequently, the main geometrical features of the potential. In order to do so, let us start by introducing the parabolic approximations around both the minima and the saddle-point, of the two-potentials forms reported in eqs. 4.20 and 4.21. Considering that a single Gaussian function can be adopted as a good approximation of the ground-state distribution near the minimum, the following parabolic expansions can be easily obtained:

$$U(x) = \frac{(x \mp x_0)^2}{2\sigma^2} \tag{4.22}$$

$$\delta V(x) = \frac{\hbar^2}{4m\sigma^2}\left[\frac{(x \mp x_0)^2}{2\sigma^2} - 1\right] \tag{4.23}$$

For the sake of comparison, the profiles produced by these results have been reported, together with their correspondent potential functions, in fig. 4.2. Notice how these parabolic expansions reproduce well the full potential in all the regions of x where the overlap of the two Gaussian functions vanishes.

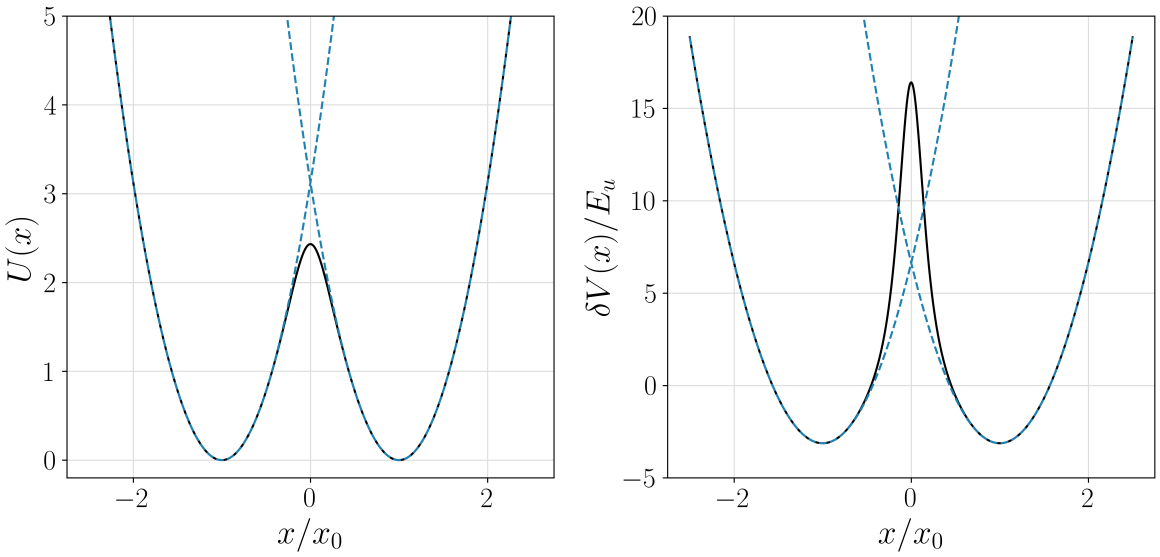

Figure 4.2: In the left panel the mean-field potential from eq. 4.20 (solid line) and its parabolic approximation from eq. 4.22 (dashed line) are reported for $\sigma/x_0 = 0.4$. The correspondent quantum potential from eq. 4.21 (solid line) is represented, together with its parabolic approximation from eq. 4.23, in the right panel.

Around the saddle point, where both Gaussian functions contribute to the definition of the potential, the second-order Taylor expansion can be invoked in order to obtain:

$$U(x) = \frac{x_0^2}{2\sigma^2} - \ln 2 - \left(\frac{x_0^2}{\sigma^2} - 1\right)\frac{x^2}{2\sigma^2} + \mathcal{O}(x^4) \tag{4.24}$$

$$\delta V(x) = \frac{\hbar^2}{4m\sigma^2}\left[\frac{x_0^2}{\sigma^2} - 1 - \left(\frac{x_0^4}{\sigma^4} + 2\frac{x_0^2}{\sigma^2} - 1\right)\frac{x^2}{2\sigma^2}\right] + \mathcal{O}(x^4) \tag{4.25}$$

Please notice how eq. 4.25 implies that, for values of the control parameter σ/x_0 less than $1+\sqrt{2}$, the quantum potential must always have its maximum at the origin. From these parabolic expansions the curvatures near the maximum and near the minima can be easily approximated according to:

$$U''(x_m) = \frac{1}{\sigma^2} \qquad U''(0) = -\frac{1}{\sigma^2}\left(\frac{x_0^2}{\sigma^2} - 1\right) \tag{4.26}$$

$$V''(x_m) = \frac{\hbar^2}{4m\sigma^4} \qquad V''(0) = -\frac{\hbar^2}{4m\sigma^4}\left(\frac{x_0^4}{\sigma^4} + 2\frac{x_0^2}{\sigma^2} - 1\right) \tag{4.27}$$

Starting from the just obtained parabolic approximations, the potential barrier heights for both the $U(x)$ and the $\delta V(x)$ potentials can be easily estimated according to the approximated relations:

$$\Delta U := U(0) - U(x_m) = \frac{x_0^2}{2\sigma^2} - \ln 2 \tag{4.28}$$

$$\Delta V := \delta V(0) - \delta V(x_m) = \frac{\hbar^2 x_0^2}{4m\sigma^4} \tag{4.29}$$

By comparing eqs. 4.28 and 4.29, the relation allowing for the direct conversion of the mean-field barrier ΔU into the corresponding quantum potential barrier ΔV can also be obtained:

$$\frac{\Delta V}{E_u} = (\Delta U + \ln 2)^2 \tag{4.30}$$

Please notice how, as prescribed by eq. 4.28, the barrier height ΔU shows an inverse squared dependence upon the control parameter σ/x_0. For instance decreasing the control parameter σ/x_0 from 1/2 to 1/5 increases the barrier from 1.3 to 11.8. This effect is even more substantial in the case of the quantum potential barrier ΔV that, as shown by eq. 4.30, is connected to ΔU by a quadratic relation.

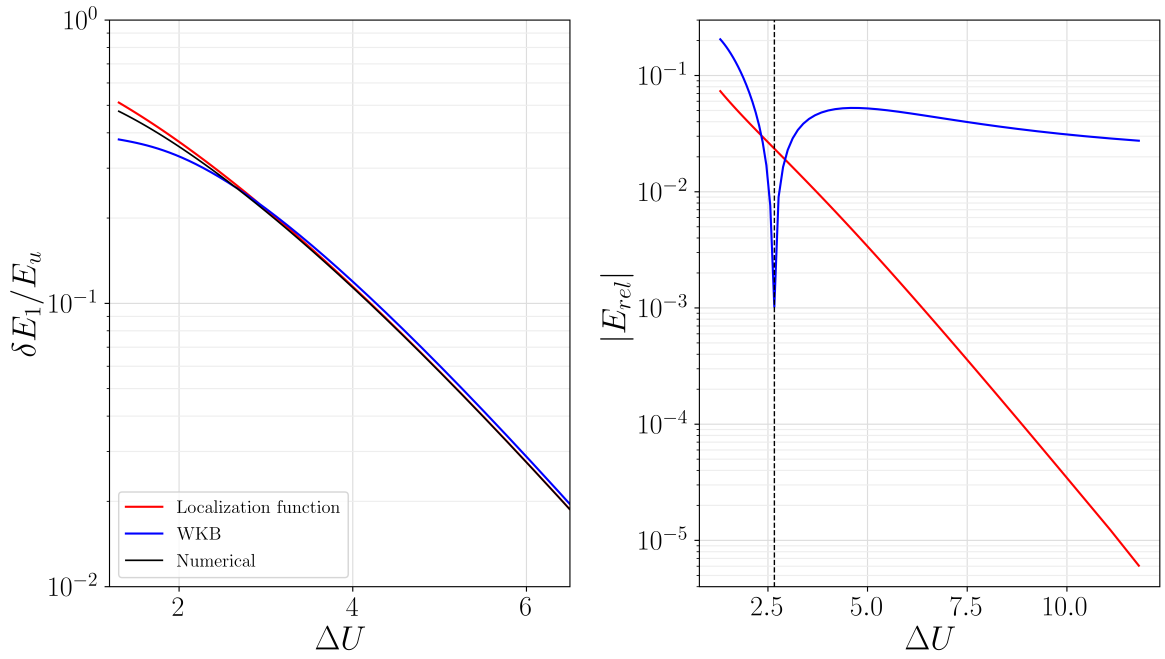

Figure 4.3: The left panel shows a comparison between the numerically exact tunneling splitting δE_1, the localization function integral estimate δE_1^g from eq. 4.8 and the WKB value from the Garg [7] formula. The right panel displays the relative errors of the approximations with respect to the numerical tunneling splitting. The vertical dashed line on the lower panel represent the point in which the WKB estimate exactly matches the numerical reference resulting in a vanishing error.

Now that a consistent definition of the potentials' key features has been presented, one can obtain, by properly adjusting the parameters of the TGD model from eq. 4.19, a potential profile suitable to

represent simple tunneling problems. Once this has been done, the tunneling splitting associated with such a system can be easily estimated by invoking the approximation δE_1^g from eq. 4.8. In order to verify the accuracy of the obtained predictions, various system parametrizations have been considered and the correspondent Hamiltonian eigenvalue problems have been solved numerically by expansion over a set of Hermite functions. In figure 4.3 we report, as a function of the mean-field potential barrier ΔU, the converged numerical values δE_1 (black line) and the correspondent δE_1^g estimates produced by the localization function method (red line). In the same figure, we also report, as a reference, the WKB estimate (blue line) obtained using the pre-exponential factor, obtained in sec. 2.4.2, proposed by Garg [7]. The integrals involved in the WKB estimation have been evaluated numerically adopting *ad hoc* procedures to counteract the diverging behavior of the integrands near the minima.

As expected from the asymptotic origin of the localization function method, deriving from the starting assumption of dealing with a vanishing tunneling splitting in the limit of high potential energy barriers, the accuracy of the estimation increases moving toward higher values of the mean-field potential barrier ΔU. For barriers ΔU of the order of unity the deviations of the approximated result from the reference numerical value are still less than 10% certifying the quality of the integral approximation δE_1^g from eq. 4.8. With barriers ΔU of few units the deviations of δE_1^g from the exact values are already so small that they cannot be perceived directly by looking at the tunneling splitting estimate displayed in the left panel of fig. 4.3. For this reason, in the right panel of such figure we have reported the relative error $(\delta E_1^g - \delta E_1)/\delta E_1$ of the estimate with respect to the exact numerical value δE_1. As it can see from such a figure an exponentially smaller relative error is observed for a linear increase of the mean-field potential barrier ΔU. This demonstrates how the localization function method allows for high-quality estimates of the tunneling splitting for intermediate to large barriers ΔU.

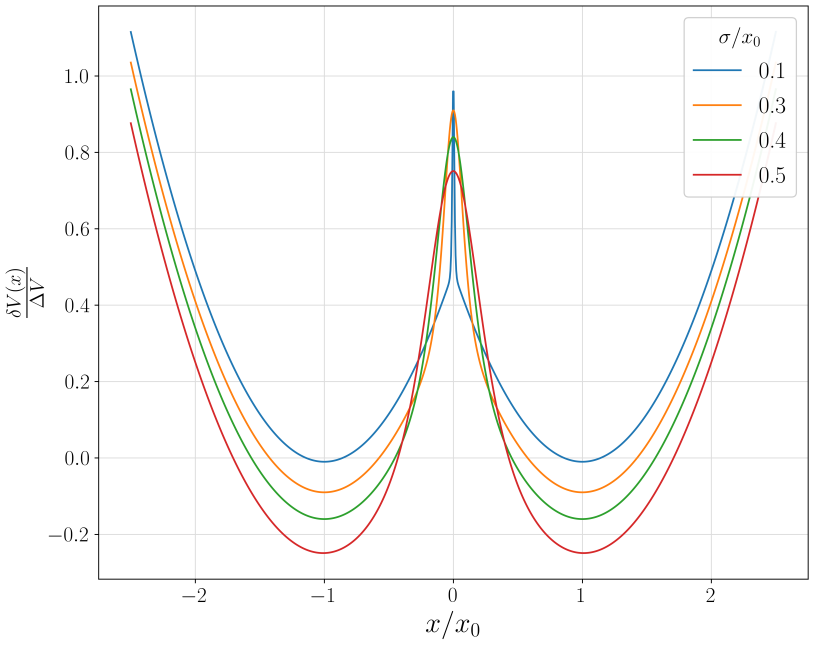

Figure 4.4: Effects of the control parameter σ/x_0 on the quantum potential shape represented as $\delta V(x)$ scaled by its barrier height ΔV. Each profile is labelled by the corresponding value of σ/x_0.

Our previous analysis showcases the simplicity associated with working with the two-Gaussian distribution model from eq. 4.19, and, at the same time, it demonstrates the high accuracy that can be achieved by adopting the localization function approach to the estimation of the tunneling splitting. However, one should not conceal the shortcomings of such a simple TGD model in relation to the corresponding quantum potential profile. This is quite evident by examining the shape of the quantum potential by means of the scaling with respect to the barrier height ΔV, as done in Figure 4.4. For decreasing values of the control parameter σ/x_0, the quantum potential develops a cusp-like component in correspondence of the maximum. Another shortcoming is that this model has only two independent parameters, x_0 and

σ, which determine the length scale of the tunneling and the mean-field barrier height ΔU according to eq. 4.28 or, equivalently, the quantum potential barrier according to eq. 4.29. This implies that once these features are fixed, there is no more room to choose another important property of the quantum potential: the width of the barrier. In the analysis of the tunneling splitting of specific molecular systems, one needs a parameterized model that is flexible enough to reproduce the most relevant features of the quantum potential. This calls for a three-parameter model in order to take into account, besides the length scale of tunneling and the barrier height, also the barrier width. This problem will be addressed in sec. 4.2.2 where a modulated double-Gaussian distribution will be presented and characterized.

4.2.2 Modulated Two-Gaussian-Distribution model

In the present section, a modulated two-Gaussian distribution model will be introduced. This model will preserve the methodological benefits of the simple two-Gaussian model form eq. 4.19 while fulfilling the requirement of a more flexible potential parametrization. This extended two-Gaussian model is specified according to three parameters: x_0, σ and α. The parameters x_0 and σ will set, as in eq. 4.19, the position and width (for $\alpha = 1$) of each Gaussian function; while the new parameter α represents a power factor both modulating the two-Gaussian combination and their amplitude. A possible formulation of such a model can be expressed according to:

$$\rho_0(x) := \frac{N}{\sqrt{8\pi\sigma^2}} \left[e^{-\frac{(x-x_0)^2}{2\alpha\sigma^2}} + e^{-\frac{(x+x_0)^2}{2\alpha\sigma^2}} \right]^{\alpha} \tag{4.31}$$

in which N is a nearly unitary constant assuring the normalization of the distribution. Please notice how the simpler TGD model from eq. 4.19 is recovered for $\alpha = 1$. The mean-field potential associated with such a distribution assumes the form:

$$U(x) := -\ln\left(\frac{\sqrt{8\pi\sigma^2}}{N}\rho_0(x)\right) = \frac{x_0^2 + x^2}{2\sigma^2} - \alpha \ln\left(e^{\frac{xx_0}{\alpha\sigma^2}} + e^{-\frac{xx_0}{\alpha\sigma^2}}\right) \tag{4.32}$$

while the corresponding quantum potential is defined, according to eq. 3.88, as:

$$\delta V(x) = \frac{\hbar^2}{8m\sigma^4}\left\{ \left[x - x_0 \tanh\left(\frac{xx_0}{\alpha\sigma^2}\right)\right]^2 - 2\sigma^2 + \frac{2x_0^2}{\alpha}\operatorname{sech}^2\left(\frac{xx_0}{\alpha\sigma^2}\right) \right\} \tag{4.33}$$

Now that a general definition of the model has been presented, let us focus our attention onto the description of its characteristic geometrical features. In order to do so, let us start by observing how, near the Gaussian centers ($x \simeq \pm x_0$), the distribution is well approximated, besides corrections of the order of the superposition coefficient $\mathcal{S} := \exp\{-2x_0^2/\alpha\sigma^2\}$, by a single Gaussian independent of the power parameter α:[1]

$$\rho_0(x) \simeq \frac{1}{\sqrt{8\pi\sigma^2}} e^{-\frac{(x\pm x_0)^2}{2\sigma^2}} \quad \text{for} \quad x \to \pm x_m \tag{4.34}$$

From this observation, one can easily conclude that the same parabolic expansions from eqs. 4.22 and 4.23 are recovered also for the modulated two-Gaussian model. Please notice how, similarly to what has been done in the context of the simple two-Gaussian model, the smallness of the superposition coefficient $\mathcal{S}$ can be invoked to justify the approximation $x_m = x_0$. Taking inspiration from what has already been done previously, one can obtain the parabolic approximation at the saddle point by performing a second-order Taylor expansion according to:

$$U(x) = \frac{x_0^2}{2\sigma^2} - \alpha \ln 2 - \left(\frac{x_0^2}{\alpha\sigma^2} - 1\right)\frac{x^2}{2\sigma^2} + \mathcal{O}(x^4) \tag{4.35}$$

$$\delta V(x) = \frac{\hbar^2}{4m\sigma^2}\left\{ \frac{x_0^2}{\alpha\sigma^2} - 1 - \left[\frac{x_0^4(2-\alpha)}{\alpha^3\sigma^4} + 2\frac{x_0^2}{\alpha\sigma^2} - 1\right]\frac{x^2}{2\sigma^2} \right\} + \mathcal{O}(x^4) \tag{4.36}$$

Starting from these approximated forms, one can evaluate the most important parameters characterizing the mean-field and the quantum potentials, such as the barrier heights and the curvatures at the saddle

[1] Please notice how eq. 4.34 represents a local approximation of a distribution near the minimum and hence it does not represent a normalized probability distribution.

point, according to:

$$\Delta U = \frac{x_0^2}{2\sigma^2} - \alpha \ln 2 \tag{4.37}$$

$$\Delta V = \frac{\hbar^2 x_0^2}{4m\alpha\sigma^4} \tag{4.38}$$

$$U''(0) = -\frac{1}{\sigma^2}\left(\frac{x_0^2}{\alpha\sigma^2} - 1\right) \tag{4.39}$$

$$V''(0) = -\frac{\hbar^2}{4m\sigma^4}\left[\frac{x_0^4(2-\alpha)}{\alpha^3\sigma^4} + 2\frac{x_0^2}{\alpha\sigma^2} - 1\right] \tag{4.40}$$

Please notice how, on the base of what observed before, the curvatures at the minima must be the same of those obtained in the case of the simple two-gaussian model.

By taking into account that the length unit is arbitrary, one concludes that the interplay between the two control parameters, σ/x_0 and α allows the independent control of the barrier height and of the width of the quantum potential as desired. The latter, hereafter indicated with w, is evaluated, in what follows, as the width of the $\delta V(x)$ quantum potential barriers at half its height ΔV. In order to characterize the quantum potential generated by the extended two-Gaussian model, let us consider, for a variable value of the parameter α, the case of a quantum potential whose barrier height has been fixed, by properly adjusting the value of σ/x_0, at $\Delta V/E_u = x_0^4/2\alpha\sigma^4 = 30$. A representative set of resulting profiles of the quantum potentials is drawn in Figure 4.5, while the corresponding values of the most significant parameters are reported in Table 4.1. These data demonstrate how, by increasing the power coefficient α from 1 to 3, a decrease of nearly two orders of magnitude is observed for the absolute value of the curvature $V''(0)$ at the saddle point that, for this reason, approaches the curvature $V''(\pm x_m)$ at the minima. The visible effect on the shape of the quantum potential is the elimination of the cusp-like behavior at the saddle point to attain a similar parabolic profile, besides the opposite sign of the curvature, at the saddle point and at the minima. This, in turn, corresponds to a significant increment of the barrier width. Notice that there is an upper limit on the parameter α ensuring the presence of two minima in the quantum potential. For example, for the potentials showed in fig. 4.5, increasing further α would generate positive values for the curvature $V''(0)$, that is the appearance of a further minimum of the quantum potential at $x = 0$.

The quantum potential resulting from the extended two-Gaussian distribution from eq. 4.33 is a flexible model which can be adapted to the study of specific tunneling conditions. In order to do so, one needs to specify the three main quantum potential features determining the tunneling effect magnitude: the distance between the two equivalent minima, the barrier height and the barrier width. From these data, the three independent parameters of the model: x_0, σ and α, can be easily computed. Once the desired model has been specified the tunneling splitting δE_1 can be estimated by adopting the localization-function-based approximation δE_1^g from eq. 4.8 that, also in this case, demonstrated a very good accuracy when compared to exact numerical solution.

Table 4.1: Parameters for the quantum potentials displayed in Fig. 4.5 at $\Delta V/E_u = 30$. Dimensionless units have been employed for the second derivatives $V''(x)$ of the quantum potential by scaling them according to E_u/x_0^2.

α	σ/x_0	ΔU	$V''(0)$	$V''(\pm x_m)$	w/x_0	$\mathcal{S}$
1.0	0.3593	3.18	-2235	30	0.33	$1.9 \cdot 10^{-7}$
1.5	0.3247	3.70	-1124	45	0.49	$3.2 \cdot 10^{-6}$
2.0	0.3021	4.09	-597	60	0.64	$1.7 \cdot 10^{-5}$
2.5	0.2857	4.39	-300	75	0.76	$5.6 \cdot 10^{-5}$
3.0	0.2730	4.63	-115	90	0.86	$1.3 \cdot 10^{-4}$

Among the benefits already discussed, this three-parameters model allows us to easily study the effect that, under the imposition of a fixed barrier height ΔV, the barrier width w/x_0 has on the tunneling splitting of the system. In what follows, we discuss the tunneling splitting obtained for barrier heights $\Delta V/E_u$ equals to 30 and 15. The comparison between exact numerical results (black lines) and the

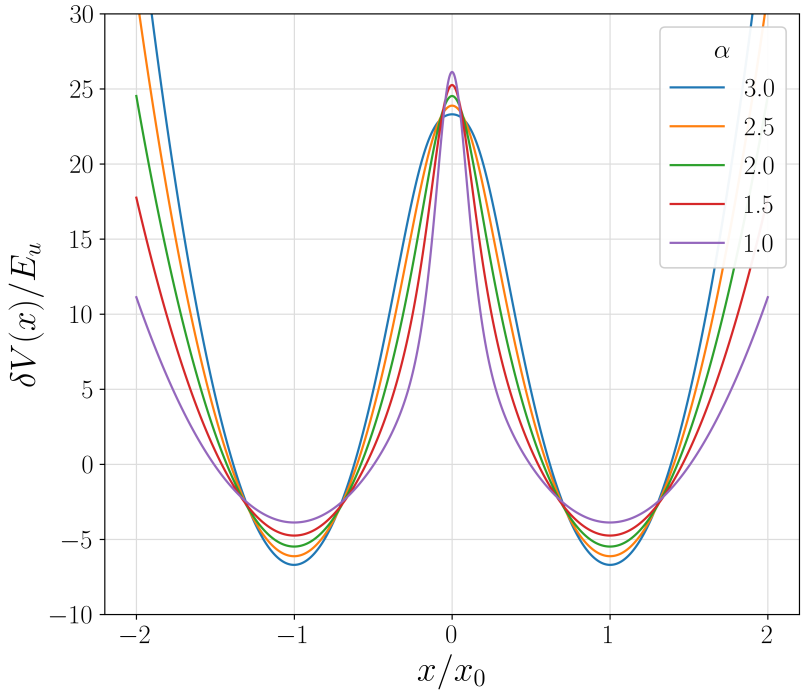

Figure 4.5: Quantum potentials deriving from the extended two-Gaussian model for the quantum barrier height $\Delta V/E_u = 30$. Each profile is labelled by the value of the power coefficient α. See Table 4.1 for the corresponding values of the most significant parameters.

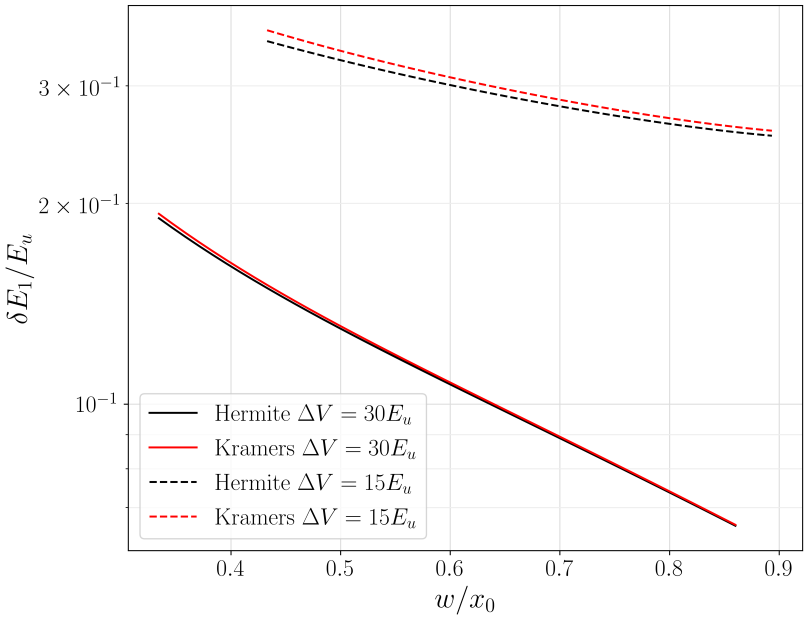

Figure 4.6: Comparison, for the case of the extended two-Gaussian model eq. 4.31, between the numerically exact tunneling splitting δE_1 (black lines) with the localization function approximation δE_1^g (red lines) as a function of the width w of the quantum barrier for fixed height (values reported in the legend).

approximation δE_1^g resulting from the localization function approach (red lines) is reported in fig. 4.6. As expected the increase of the barrier width, and correspondingly of the size of coordinate domain representing classically forbidden configurations, produces, for fixed barrier height, a significant decrease of the tunneling splitting. For the $\Delta V/E_u = 30$ barrier, the two kinds of results are nearly superimposed

and differences can be detected only in the low range of barrier width, that is for the power parameter α close to 1, which correspond to the lower values of the barrier height ΔU of the mean-field potential (see table 4.1). The differences between the exact and the approximated tunneling splitting are more significant for the quantum potential barrier $\Delta V/E_u = 15$, however, this is not surprising given that the mean-field barrier height is in the order of $\Delta U \simeq 2$. This range of barriers represents, for the stochastic problem, the lower limit for the range of barriers that legitimate any approximation relying on the gap between the kinetic eigenvalues of the FPS operator and the eigenvalues describing localized relaxation modes [50].

4.2.3 Estimates in the asymptotic limit

In section 4.1.1 a general procedure for the estimation of the tunneling splitting in the asymptotic limit of high barriers has been discussed. The core of the presented approach was a double Laplace integration capable of translating the integral expression from eq. 4.8 into the simpler formula reported in eq. 4.17. In this section such a result will be tested in the case of the TGD model from eq. 4.19 returning, as will be discussed, the wrong asymptotic behavior due to the Laplace approximation failure. In order to solve the issue, a new asymptotic procedure, inspired by the TGD structure, will be introduced.

In order to start our discussion, let us derive the specific form that the asymptotic approximation from eq. 4.17, assumes in the particular case of our TGD model. To do so, let us consider the relations from eqs. 4.26 and 4.28 that, by simple substitution into eq. 4.17, allow us to obtain:

$$\delta E_1^{\text{asy}} = \frac{\hbar^2 \sqrt{x_0^2 - \sigma^2}}{m\pi\sigma^3} e^{-\frac{x_0^2}{2\sigma^2}} \tag{4.41}$$

The tunneling splitting estimates δE_1^{asy} obtained with such a relation are reported (blue line) in fig. 4.7 together with the results δE_1^g (green) produced by the integral form from eq. 4.8. As can be seen by looking at such a figure, the asymptotic approximation shows a quite substantial relative error over all the range of considered ΔU barriers reaching, in the limit of high barrier, a somewhat stable error near the 26% mark.

This substantial degradation in the estimate accuracy can be attributed, as anticipated, to the Laplace approximation failing to reproduce a reasonably accurate integrand profile. This calls for a new asymptotic form inspired by the structure of the TGD model. In order to do so, let us start by analyzing the structure of the I integral from eq. 4.6 that, by recalling eq. 4.32, can be rewritten according to:

$$I = \int_0^{x_0} \rho_0^{-1}(x)dx = \sqrt{8\pi\sigma^2} \int_0^{x_0} e^{U(x)}dx = \sqrt{8\pi\sigma^2} e^{\frac{x_0^2}{2\sigma^2}} \int_0^{x_0} e^{\frac{x^2}{2\sigma^2} - \ln\left(e^{\frac{x x_0}{\sigma^2}} + e^{-\frac{x x_0}{\sigma^2}}\right)} dx \tag{4.42}$$

By applying the substitution $y = x_0 x/\sigma^2$ to the just obtained integral it is now possible to obtain:

$$I = \sqrt{8\pi}\frac{\sigma^3}{x_0} e^{\frac{x_0^2}{2\sigma^2}} \int_0^{x_0^2/\sigma^2} e^{\frac{y^2\sigma^2}{2x_0^2} - \ln\left(e^y + e^{-y}\right)} dy \tag{4.43}$$

That, in the asymptotic limit of $\sigma \to 0$, can be simplified in order to obtain:

$$I = \sqrt{8\pi}\frac{\sigma^3}{x_0} e^{\frac{x_0^2}{2\sigma^2}} \int_0^{+\infty} \frac{1}{e^y + e^{-y}} dy = \frac{\pi\sigma^3}{x_0}\sqrt{\frac{\pi}{2}} e^{\frac{x_0^2}{2\sigma^2}} \tag{4.44}$$

Once this result has been obtained, we can move our attention onto the normalization factor. Such an integral can easily be simplified recalling that, in the asymptotic case of high potential barriers, the localization function $g(x)$ must manifest a very steep change in value around $x = 0$. This step-like behavior allows us to neglect its contribution to the integral and, therefore, to obtain the following relation:

$$N = \int_{-\infty}^{+\infty} g(x)^2 \rho_0(x)dx = \int_{-\infty}^{+\infty} \rho_0(x)dx \tag{4.45}$$

Given the wave-function normalization, this terms integrates to the unit value. By substituting the obtained results in the integral form from eq. 4.8 it is simple to obtain the following asymptotic approximation:

$$\delta E_1^{\text{Asy}} = \frac{\hbar^2 x_0}{m\pi\sigma^3}\sqrt{\frac{2}{\pi}} e^{-\frac{x_0^2}{2\sigma^2}} \tag{4.46}$$

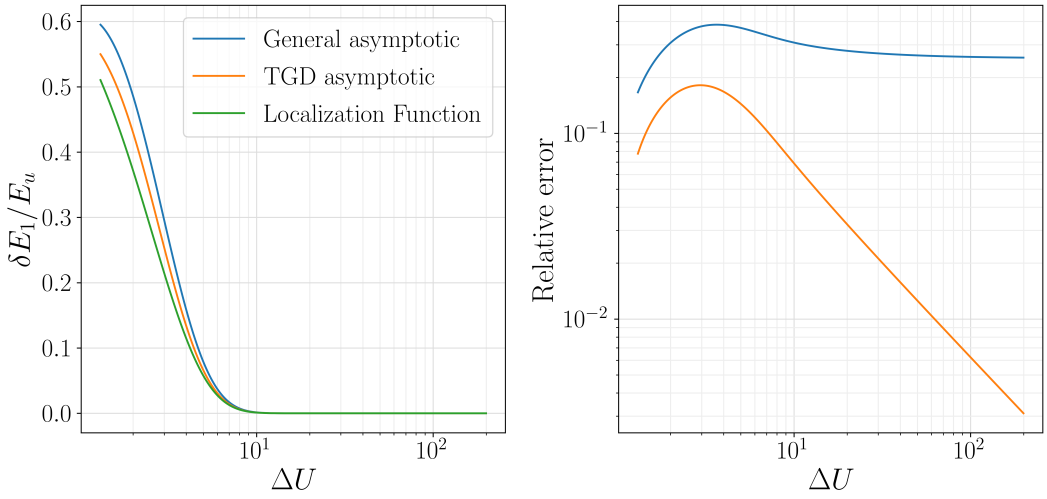

Figure 4.7: In the left panel we report the tunneling splitting estimates from: the general asymptotic approximation from eq. 4.17 (blue line), the revised asymptotic form from eq. 4.46 (orange line) and the integral estimation from eq. 4.8 (green line). In the right panel we report, with the same color scheme the relative error of the former two in respect to the latter.

As can be seen from fig. 4.7 the newly introduced asymptotic approximation (orange line) shows significantly better performances. The correct asymptotic behavior is captured and, in the limit of high potential barriers, the relative error shows a magnitude decreasing roughly as a negative power of the ΔU barrier.

4.3 Vibrational localization function method

Until now, the main focus of this chapter has been to outline a general procedure capable of returning accurate ground state tunneling splitting in the case of simple, one-dimensional, model systems. These quantities represent a first step in the interpretation of the microwave tunneling spectra of these systems, where transitions between states of the same doublet can usually be observed. In the present section, we will instead focus on the problem of computing tunneling splitting for vibrationally excited states. These play a primary role in the interpretation of vibrational spectra of tunneling systems where, as discussed in sec. 2.3, transitions between states of opposite parity belonging to different doublets can be observed. This will allow us to give to the reader a general overview of how these quantities can be derived in the context of the asymptotic analysis presented in this chapter and what kind of accuracy can be expected from the obtained approximations.

As discussed in sec. 3.3, if the ground state wave-function $\psi_0(x)$ for a molecular system is known, or can be properly modeled, an isomorphic relation between the mathematical structure of the symmetrized Fokker-Planck-Smoluhowski (FPS) operator and the Born-Oppenheimer Hamiltonian can be established. This, however, is not restrained to the sole ground-state and instead it represents a quite general property that can be applied to each eigenfunction of the system. In order to demonstrate this point let us consider, as did before, a one-dimensional quantum system characterized by a symmetrical quantum potential $V(x)$. Under these conditions, all the well-states of energy lower than the barrier top can mix resulting in an eigenvalue spectrum composed by doublets of states of opposite parity. Let us adopt the notation $\psi_{n\pm}(x)$ to indicate the state of the n-th doublet responding to the symmetry condition $\psi_{n\pm}(x) = \pm\psi_{n\pm}(-x)$. The eigenfunctions $\psi_{n\pm}(x)$ of the problem are defined by the time-independent Schrödigner equation:

$$-\frac{\hbar^2}{2m}\frac{\partial^2\psi_{n\pm}(x)}{\partial x^2} + V(x)\psi_{n\pm}(x) = E_{n\pm}\psi_{n\pm}(x) \tag{4.47}$$

which fixes a bi-univocal relation between $V(x)$ and the whole spectrum of $\psi_{n\pm}(x)$. If one of the system

eigenfunctions is known the quantum potential $V(x)$ can be computed directly inverting eq. 4.47:

$$V(x) = \frac{\hbar^2}{2m}\psi_{n\pm}(x)^{-1}\frac{\partial^2\psi_{n\pm}(x)}{\partial x^2} + E_{n\pm} \tag{4.48}$$

where the energy $E_{n\pm}$ is unknown and can be assumed as the new zero of the energy scale. Adopting this new energy reference, a generalized definition of the shifted Hamiltonian operator $\delta_{n\pm}\hat{H} := \hat{H} - E_{n\pm}$ can be introduced according to:

$$\delta_{n\pm}\hat{H} = \frac{\hbar^2}{2m}\left[\psi_{n\pm}(x)^{-1}\frac{\partial^2\psi_{n\pm}(x)}{\partial x^2} - \frac{\partial^2}{\partial x^2}\right] \tag{4.49}$$

where the $\delta_{n\pm}$ symbol has been introduced in order to denote how the operator is referred to the new shifted energy scale. Please notice how the δ symbol without any label will, according to what has been done in the first part of this chapter, still be used to indicate energy quantities referring to the ground state as the zero of the energy scale ($\delta \equiv \delta_{0+}$).

Starting from eq. 4.49 the symmetrized Fokker-Planck-Smoluchowski form of the Hamiltonian can be easily obtained according to:

$$\delta_{n\pm}\hat{H} = -\frac{\hbar^2}{2m}\psi_{n\pm}(x)^{-1}\frac{\partial}{\partial x}\psi_{n\pm}(x)^2\frac{\partial}{\partial x}\psi_{n\pm}(x)^{-1} \tag{4.50}$$

In perfect analogy with what observed before, the eigenfunctions $\psi_{m\pm}(x)$ for this new shifted operator are the same of those associated to the Born-Oppenheimer nuclear Hamiltonian while the corresponding eigenvalues are simply shifted by the energy $E_{n\pm}$ of the selected reference state $\psi_{n\pm}(x)$. If the lower state of the n-th doublet $\psi_{n+}(x)$ is selected as the reference state, the application of $\delta_{n+}\hat{H}$ to the upper state of the same doublet $\psi_{n-}(x)$ will return the correspondent tunneling splitting $\Delta E_n \equiv \delta_{n+}E_{n-} = E_{n-} - E_{n+}$:

$$\delta\hat{H}_{n+}\psi_{n-}(x) = \Delta E_n\psi_{n-}(x) \tag{4.51}$$

This opens the way to an asymptotic approach to the problem based on the fact that, in the limit of high potential barriers, the tunneling splitting must vanish due to the energy spectrum collapsing in a combination of two, symmetrically degenerate, isolated quantum systems energy spectra. Introducing the n-th doublet localization function $g_n(x)$ according to:

$$g_n(x) := \frac{\psi_{n-}(x)}{\psi_{n+}(x)} \tag{4.52}$$

one can find that, in the asymptotic limit, the following relation for $g_n(x)$ is obtained:

$$\frac{\partial}{\partial x}\psi_{n+}(x)^2\frac{\partial}{\partial x}g_n(x) = 0 \tag{4.53}$$

The direct integration of the obtained equation, similarly to what observed in the case of eq. 4.4, cannot lead to a well-behaved solution with a finite norm and must therefore be patched in order to return a proper localization function model. Also in this case, the patching operation represents a delicate operation with little to no *a-priori* indication about the optimal procedure. This is particularly true in the context of excited states where the variational justification cannot be adopted for approximated definitions of the reference state. In what follows we will adopt the same constant patching approximation from eq. 4.5 without excluding that better patching solutions can possibly be developed. Notice how this choice presents a local character focusing the description of the tunneling splitting onto the function behavior in the region near the barrier and neglecting every contribution possibly coming from longer-range effects. Within this approximation the localization function can be written in the form:

$$g_n(x) := \begin{cases} -1 & x < -x_p \\ I_n^{-1}\int_0^x \frac{1}{\psi_{n+}(y)^2}dy & -x_p \leq x \leq x_p \\ 1 & x > x_p \end{cases} \tag{4.54}$$

where x_p represent the extension of the patching region. This quantity must be selected carefully in order to amend the diverging behavior of the integrand near the zeros of the reference function. Similarly to what done in eq. 4.6, the constant factor I_n can be defined according to the integral:

$$I_n := \int_0^{x_p}\frac{1}{\psi_{n+}^2(y)}dy \tag{4.55}$$

Please notice how the proper normalization factor N_n should be applied to the localization function from eq. 4.54 to obtain a normalized approximation $\psi^g_{n-}(x)$ of the upper odd function $\psi_{n-}(x)$ of the doublet:

$$\psi^g_{n-}(x) = N_n g_n(x)\psi_{n+}(x) \quad \text{with} \quad N_n = \langle g_n|\psi^2_{n+}|g_n\rangle^{-\frac{1}{2}} \tag{4.56}$$

By considering the expression for the expectation value of the shifted Hamiltonian operator $\delta_{n+}\hat{H}$ in respect to the $\psi^g_{n-}(x)$ wave-function, one can easily recover the following approximated expression for n-th doublet tunneling splitting ΔE_n:

$$\Delta E^g_n := \langle\psi^g_{n-}|\delta_{n+}\hat{H}|\psi^g_{n-}\rangle = \frac{\hbar^2}{mI_nN_n} \tag{4.57}$$

where integration by parts has been invoked to simplify the expression.

Now that the asymptotic procedure has been extended to the problem of a generic doublet of states, the problem of computing excited states tunneling splitting ΔE_n has been translated to the issue of generating good approximations of the lower state of the doublet $\psi_{n+}(x)$. Once a ground state distribution $\psi_{0+}(x)$ is employed to define the system potential shape, no more freedom is left to the definition of the other system eigenfunctions. As a consequence, the excited reference state $\psi_{n+}(x)$ is fixed and must be recovered from the $\psi_{0+}(x)$ definition by means of a proper approximation. This is a crucial task and shows how this way of operating involves a two-stage approximation that, in order to ensure a reasonable prediction accuracy, should be carried out with care introducing ad-hoc approximation based on the ground state definition. In what follows the two-Gaussian distribution models from sections 4.2.1 and 4.2.2 will be considered ad approximated procedures will be defined in order to approximate their second excited state $\psi_{1+}(x)$.

In order to clarify how this can be done let us start our analysis by introducing a new type of localization function $\varphi_{n\pm}(x)$, hereafter addressed as "fixed-reference" localization function, capable of extracting a general reference function $\psi_{n\pm}(x)$ form the ground state wave-function $\psi_{0+}(x)$:

$$\varphi_{n\pm}(x) = \frac{\psi_{n\pm}(x)}{\psi_{0+}(x)} \tag{4.58}$$

In figure 4.8 the fixed-reference localization functions associated with the first three, numerically computed, excited states have been reported for the case of a modulated two-Gaussian distribution model.

Starting from such a definition one can easily verify how, considering the application of $\delta\hat{H}$ to the reference function $\psi_{1+}(x)$, the following equality can be obtained:

$$\rho_{0+}(x)^{-1}\frac{\partial}{\partial x}\rho_{0+}(x)\varphi'_{1+}(x) = -\frac{2m\delta E_{1+}}{\hbar^2}\varphi_{1+}(x) \tag{4.59}$$

If the asymptotic limit of high barriers ($\sigma \to 0$) is now invoked, one can estimate the limit value for the second excited state energy δE_{1+} in terms of the characteristic parameters of the problem. As a matter of fact, in these conditions, the system behaves like a couple of isolated harmonic wells whose ground state distribution is represented by a single Gaussian. Applying the $\delta\hat{H}$ operator to the reference state, considering that in this limit $\varphi'_{1+}(x)$ assumes constant value, it can be easily verified how:

$$\frac{2m\delta E_{1+}}{\hbar^2} \simeq \frac{1}{\sigma^2} \tag{4.60}$$

Adopting this limit value in eq. 4.59 and taking the derivative on both sides allow us to obtain the following approximated equation for $\Phi(x) := \varphi'_{1+}(x)$:

$$\Phi(x) = -\sigma^2\frac{\partial}{\partial x}\rho_{0+}(x)^{-1}\frac{\partial}{\partial x}\rho_{0+}(x)\Phi(x) \tag{4.61}$$

Starting from this result, a "direct" formulation of the fixed reference localization function will be presented in section 4.3.1 for the general case of a modulated two-Gaussian distribution model. Furthermore, a simplified "heuristic" approach to the problem will be explored in sec. 4.3.2 for the case of the simple two-Gaussian distribution model.

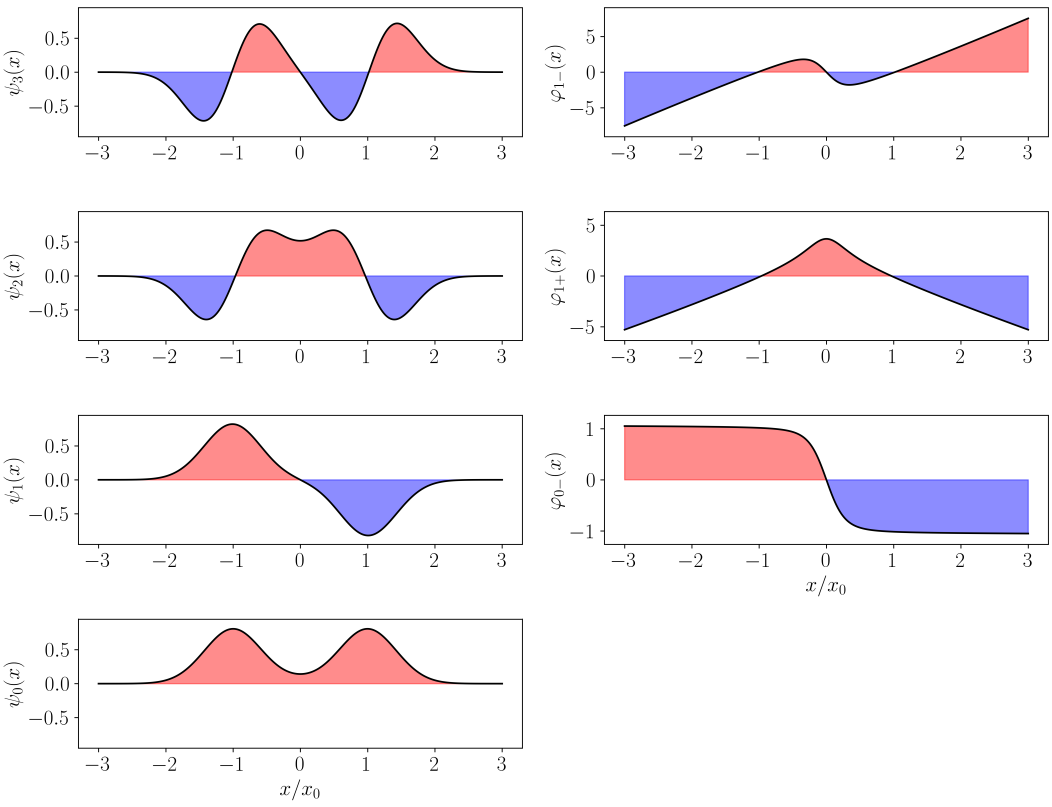

Figure 4.8: On the left side the first four eigenfunctions $\psi_{n\pm}(x)$ of the modulated TGD model from eq. 4.31 ($\sigma/x_0 = 0.3$, $\alpha = 3.0$) have been reported. On the right side the correspondent fixed-reference localization functions $\varphi_{n\pm}(x)$ are shown.

4.3.1 Direct approximation of the reference state

In the present section a "direct" approach to the evaluation of $\varphi_{1+}(x)$ will be obtained by leveraging the particular structure of the two-Gaussian model from eq. 4.31. The starting point of this approach is represented by the introduction of a new scaled coordinate, hereafter indicated with z, defined according to:

$$z := \frac{x_0 x}{\alpha\sigma^2} \tag{4.62}$$

Adopting this new variable definition in eq. 4.61 allows us to obtain the following relation:

$$\Phi(z) = -\frac{x_0^2}{\alpha^2\sigma^2}\frac{\partial}{\partial z}\tilde{\rho}_{0+}(z)\frac{\partial}{\partial z}\tilde{\rho}_{0+}(z)\Phi(z) \tag{4.63}$$

where $\Phi(z)$ and $\tilde{\rho}_{0+}(z)$ are intended as the functions obtained from $\Phi(x)$ and $\rho_{0+}(x)$ by simple variable substitution. By applying the same variable transformation to the ground state distribution from eq. 4.31, the following form can be obtained:

$$\tilde{\rho}_{0+}(z) = \frac{N}{\sqrt{8\pi\sigma^2}} e^{-\frac{z^2\alpha^2\sigma^2}{2x_0^2} - \frac{x_0^2}{2\sigma^2}} \left[e^z + e^{-z}\right]^\alpha \tag{4.64}$$

In the asymptotic limit of $\sigma \to 0$ the left side of eq. 4.63 can be neglected and the following expression for the ground state distribution can be adopted:

$$\tilde{\rho}_{0+}(z) = \frac{N2^\alpha}{\sqrt{8\pi\sigma^2}} e^{-\frac{x_0^2}{2\sigma^2}} \cosh^\alpha(z) \tag{4.65}$$

Under these conditions the following equation for $\Phi(z)$ can be recovered:

$$\frac{\partial}{\partial z}\cosh^{-\alpha}(z)\frac{\partial}{\partial z}\cosh^\alpha(z)\Phi(z) = 0 \tag{4.66}$$

The solution of this equality can be obtained by simple integration. Recalling that, due to the parity of the reference state, $\Phi(0) = 0$ and reverting the expression back to the x variable allows us to obtain:

$$\Phi(x) = \frac{1}{B}\cosh^{-\alpha}\left(\frac{x_0 x}{\alpha\sigma^2}\right)\int_0^{\frac{x_0 x}{\alpha\sigma^2}}\cosh^{\alpha}(z')dz' \tag{4.67}$$

From which the fixed-reference localization function $\varphi_{1+}(x)$ can be obtained by integration:

$$\varphi_{1+}(x) = \frac{\alpha\sigma^2}{x_0 B}\int_0^{\frac{x_0 x}{\alpha\sigma^2}} dz \int_0^{z}\frac{\cosh^{\alpha}(z')}{\cosh^{\alpha}(z)}dz' + \frac{A}{B} \tag{4.68}$$

where B can be computed by imposing the normalization of the reference state and A by ensuring its orthogonality with the ground state. Please notice how the symmetry parted Hilbert space together with the orthogonalization action performed by the A term impart to the obtained reference state estimation a variational character. If the value $\alpha = 1$ is considered, eq. 4.31 becomes the simpler two-Gaussian model from eq. 4.19. In this context the expression from eq. 4.67 becomes:

$$\Phi(x) = \frac{1}{B}\tanh\left(\frac{x_0 x}{\sigma^2}\right) \tag{4.69}$$

and the double integral in eq. 4.68 can be solved analytically according to:

$$\int_0^{\frac{x_0 x}{\sigma^2}} dz \int_0^{z}\frac{\cosh(z')}{\cosh(z)}dz' = \ln\left[\cosh\left(\frac{x_0 x}{\sigma^2}\right)\right] \tag{4.70}$$

From this result the following form of the fixed reference localization function can be obtained:

$$\varphi_{1+}(x) = \frac{\sigma^2}{x_0 B}\ln\left[\cosh\left(\frac{x_0 x}{\sigma^2}\right)\right] + \frac{A}{B} \tag{4.71}$$

The accuracy of both the presented approximation and that of the correspondent tunneling splitting estimation will be discussed in section 4.3.3.

4.3.2 Heuristic approximation of the reference state

The result obtained in the previous section surely represents the most direct approach to the problem allowing the obtainment of an analytical approximation of the fixed-reference localization function $\varphi_{1+}(x)$ without the need of invoking *a-priori* modeling assumptions. The discussed strategy however does not represent the only possibility and a more heuristic approach, starting from some form of *a-priori* model for the fixed-reference localization function, is clearly possible. In order to outline a possible procedure let us consider, for sake of simplicity, the simple two-Gaussian distribution model from eq. 4.19. The shape of the fixed reference localization function emerging from such a model, together with that of its first derivative, are reported in figure 4.9 for a variable value of σ/x_0.

Just by looking at fig. 4.9 one can appreciate how the fixed reference localization function $\varphi_{1+}(x)$ is characterized by two nearly constant slope regions connected by a smooth, non-rectilinear, section of having a constant curvature sign. This imparts to its first derivative $\Phi(x)$ a step-like behavior in which two constant regions are smoothly connected near the maximum of the barrier. This observation clearly does not give definitive information about the functional form of the solution but it allows us to formulate an educated guess about the possible functional form that can be employed for the purpose of its fitting. In what follows, the error-function profile:

$$\Phi(x) \propto \mathrm{erf}(\gamma x) \tag{4.72}$$

will be considered. In order to evaluate the optimal value of the γ parameter, let us start by recalling the condition imposed by eq. 4.61. Starting from such a relation and considering that $\rho_{0+}(x) \propto \exp\{-U(x)\}$, the following can easily be obtained:

$$\Phi(x) = -\sigma^2\frac{\partial}{\partial x}\left[\Phi'(x) - U'(x)\Phi(x)\right] \tag{4.73}$$

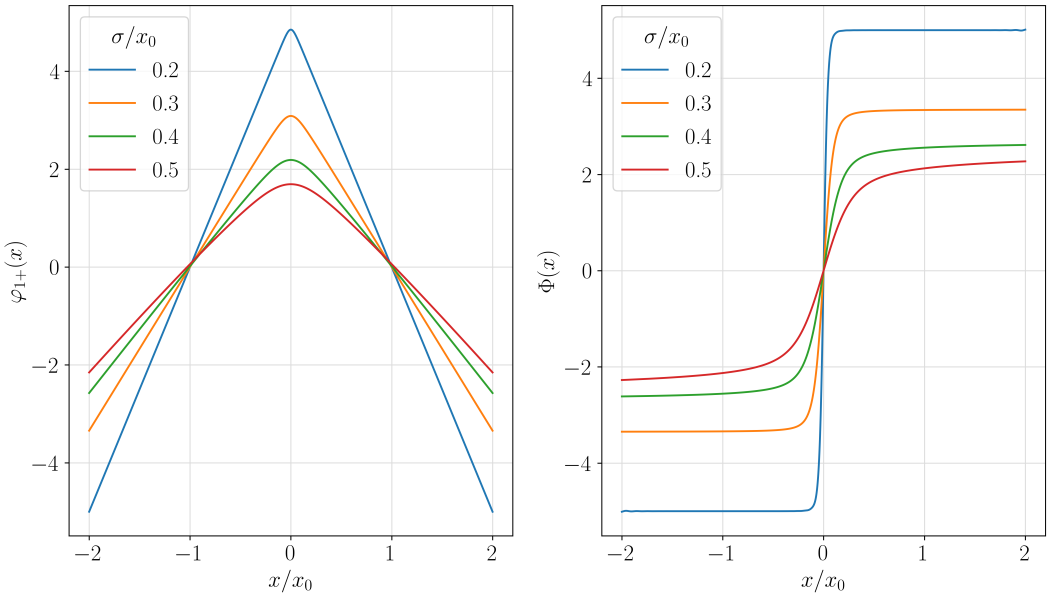

Figure 4.9: Numerically computed fixed reference localization functions $\varphi_{1+}(x)$ (left) and their first derivative $\Phi(x)$ (right) for the case of a simple two-Gaussian distribution model characterized by a variable σ/x_0 value.

If now the Maclaurin expansions of the involved functions are invoked, the following approximations can be obtained:

$$\Phi(x) = \sum_{n=0}^{+\infty} a_{2n+1} x^{2n+1} \qquad \text{and} \qquad U'(x) = \sum_{n=0}^{+\infty} b_{2n+1} x^{2n+1} \tag{4.74}$$

Starting from these results it is simple to obtain, by simple derivation, the following results:

$$\Phi'(x) = \sum_{n=0}^{+\infty} a_{2n+1}(2n+1)x^{2n} = a_1 + \sum_{n=0}^{+\infty} a_{2n+3}(2n+3)x^{2n+2} \tag{4.75}$$

$$U'(x)\varphi'_{1+}(x) = \sum_{n=0}^{+\infty} b_{2n+1} x^{2n+1} \sum_{m=0}^{+\infty} a_{2m+1} x^{2m+1} = \sum_{n=0}^{\infty} x^{2n+2} \sum_{m=0}^{n} a_{2m+1} b_{2(n-m)+1} \tag{4.76}$$

Substituting the just obtained expressions into eq. 4.73 one can obtain the following relation:

$$-a_{2n+1} = \sigma^2(2n+2)\left[a_{2n+3}(2n+3) - \sum_{n=0}^{m} a_{2m+1} b_{2(n-m)+1}\right] \tag{4.77}$$

that, in the particular case of $n = 0$, results in the equality:

$$\frac{a_3}{a_1} = \frac{1}{3} b_1 - \frac{1}{6\sigma^2} \tag{4.78}$$

This equality fixes a direct relation between the a_n coefficients, defined on the base of the $\Phi(x)$ model used for the fitting, and the b_n coefficients characterizing the system to be fitted. Starting from this result we can now express the γ coefficient as a function of the characteristic parameters of the TGD model. Observing that $b_1 = U''(0)$ and recalling the expression from eq. 4.20, it is possible to verify how:

$$U'(x) = \frac{x}{\sigma^2} - \frac{x_0}{\sigma^2} \tanh\left(\frac{x_0 x}{\sigma^2}\right) \tag{4.79}$$

$$U''(x) = \frac{1}{\sigma^2} - \frac{x_0^2}{\sigma^4} \operatorname{sech}^2\left(\frac{x_0 x}{\sigma^2}\right) \tag{4.80}$$

From which, evaluating the second derivative for $x = 0$, it is simple to conclude that:

$$b_1 = \frac{1}{\sigma^2}\left(1 - \frac{x_0^2}{\sigma^2}\right) \quad \Rightarrow \quad \frac{a_3}{a_1} = -\frac{1}{3\sigma^2}\left(\frac{x_0^2}{\sigma^2} - \frac{1}{2}\right) \tag{4.81}$$

Once the coefficient ratio from the two-Gaussian distribution model has been obtained we can compare it with the Maclaurin expansion of the error-function model from eq. 4.72:

$$\mathrm{erf}(\gamma x) = \frac{2}{\sqrt{\pi}}\left[\gamma x - \frac{1}{3}\gamma^3 x^3 + \mathcal{O}(x^5)\right] \tag{4.82}$$

From this, the following expression in terms of γ can be obtained:

$$\frac{a_3}{a_1} = -\frac{1}{3}\gamma^2 \quad \Rightarrow \quad \gamma = \sqrt{\frac{1}{\sigma^2}\left(\frac{x_0^2}{\sigma^2} - \frac{1}{2}\right)} \tag{4.83}$$

Now that the derivative of $\varphi_{1+}(x)$ has been defined, the fixed reference localization function itself can be recovered by simple integration:

$$\varphi_{1+}(x) - \varphi_{1+}(0) = \int_0^x \mathrm{erf}(\gamma y)dy = \frac{2}{\sqrt{\pi}}\int_0^x dy \int_0^{\gamma y} dz\, e^{-z^2} = x\mathrm{erf}(\gamma x) + \frac{1}{\gamma\sqrt{\pi}}\left[e^{-\gamma^2 x^2} - 1\right] \tag{4.84}$$

The offset $\varphi_{1+}(0)$ can be computed by imposing the orthogonality of the second excited state $\psi_{1+}(x) \propto \varphi_{1+}(x)\psi_{0+}(x)$ with the ground state $\psi_{0+}(x)$ while its normalization can be imposed by simple integration.

In section 4.3.3 the results obtained from this heuristic approach will be discussed and compared with those returned by the "direct" approach described in sec. 4.3.1.

4.3.3 Results

Now that both the "direct" and "heuristic" approaches to the estimation of the $\psi_{1+}(x)$ reference state have been introduced, let us evaluate how they perform in terms of accuracy when applied to the simple two-Gaussian model from eq. 4.19. In order to do so, the shifted Hamiltonian expectation value $\delta E_{1+} = \langle\psi_{1+}|\delta\hat{H}|\psi_{1+}\rangle$, computed with respect to the approximated definition of the $\psi_{1+}(x)$ reference states, has been evaluated by numerical integration. The obtained results, together with the reference value obtained by solving the Hamiltonian eigenvalue problem by expansion on a non-orthogonal basis-set of Hermite functions, are reported in figure 4.10.

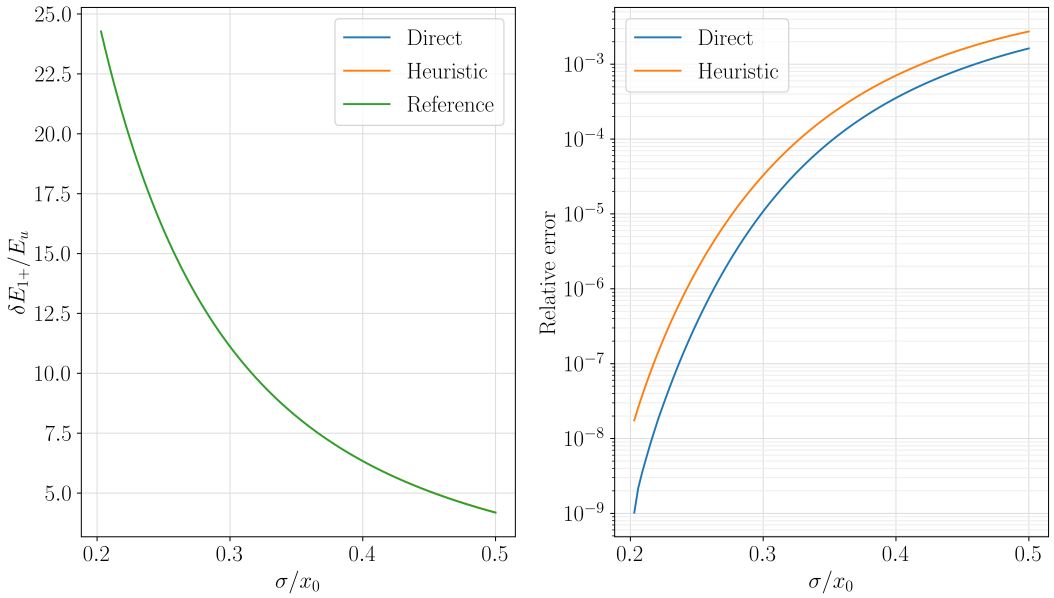

Figure 4.10: In the left panel we report, for a simple two-Gaussian distribution model with variable σ/x_0 value, the energy computed for the $\psi_{1+}(x)$ state adopting the direct method (blue line), the heuristic approach (orange line) and a numerical diagonalization of the Hamiltonian (green line). The error of the former estimates with respect to the latter are reported in the right panel.

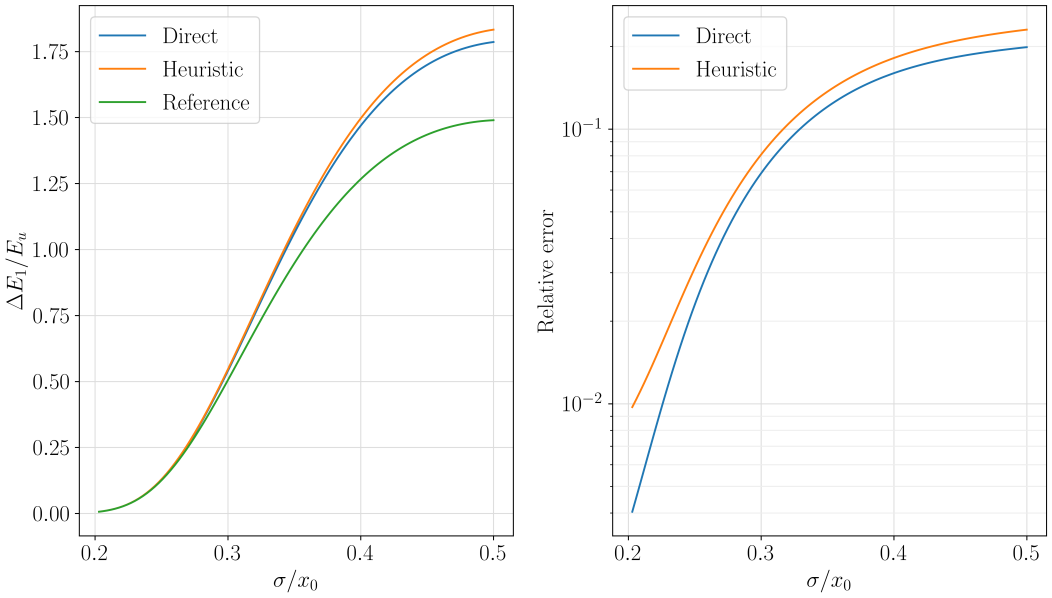

Figure 4.11: In the left panel we report, for a simple two-Gaussian distribution model with variable σ/x_0 value, the first excited-state tunneling splitting computed adopting the $\psi_{1+}(x)$ estimates returned by the direct method (blue line) and the heuristic approach (orange line). For sake of comparison, the numerical reference value (green line) has also been reported. The errors of the former estimates with respect to the latter are reported in the right panel.

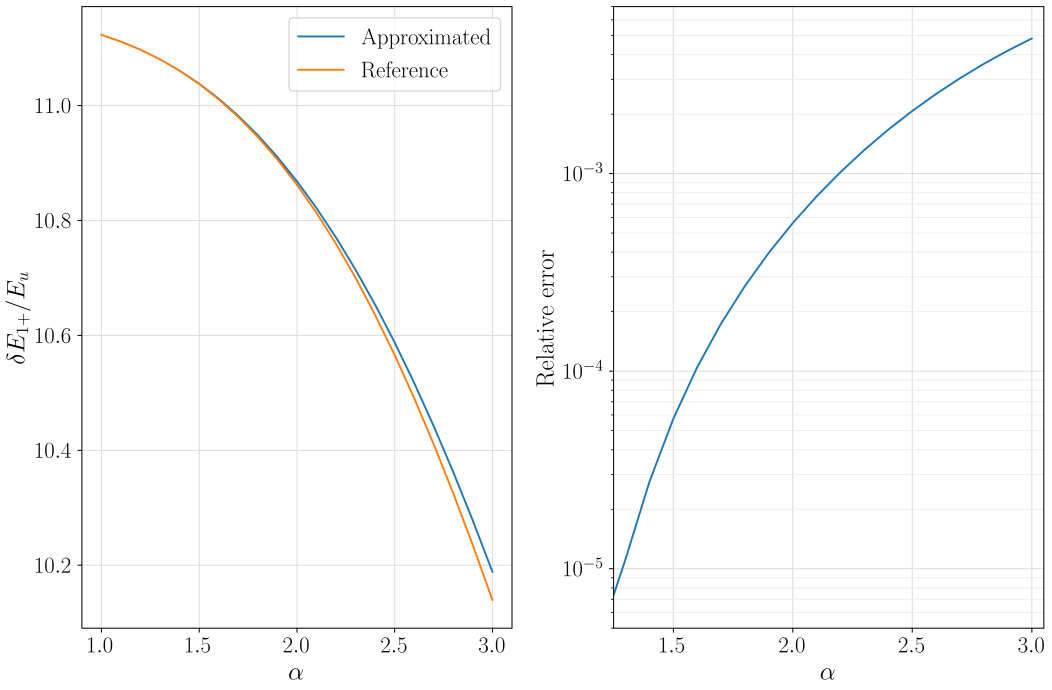

Figure 4.12: In the left panel we report, for a modulated two-Gaussian distribution model characterized by $\sigma/x_0 = 0.3$ and by a variable α value, the energy computed for the $\psi_{1+}(x)$ state by adopting the direct method (blue line) and the numerical diagonalization of the Hamiltonian (orange line). The error of the former estimates with respect to the latter are reported in the right panel.

As can be grasped by looking at such a figure both the "direct" and the "heuristic" methods shown reasonably good accuracy over the whole range of σ/x_0 values considered with a better performance

encountered, due to the asymptotic nature of the approximation, for lower values of σ/x_0. The "direct" method consistently shows a better accuracy with a relative error lower than that obtained from the "heuristic" approach. This different accuracy impacts also the quality of the first excited-state tunneling splitting that, as can be seen by looking at fig. 4.11, shows better accuracy in the case of estimates based on the reference state generated by the "direct" method. As can be seen from such a figure the accuracy of the tunneling splitting estimate shows far lower performances if compared with the ground-state counterpart. This however is not surprising given both the approximated nature of the reference state and the remarkably simple localization function approximation invoked in eq. 4.54. Besides these technical aspects, one should also take into account that, due to the higher energy of the reference state, the validity of the asymptotic approximation of high barriers is less justified in the case of excited-state tunneling splittings and therefore less accurate estimations must be expected. In general, however, the asymptotic profile is conserved with a better accuracy observed in the limit of high barriers.

If the modulated two-Gaussian distribution model from eq. 4.31 is now considered, one can invoke the direct method to obtain, adopting the numerical integration to solve the double integral from eq. 4.68, the required reference state $\psi_{1+}(x)$. In order to evaluate the accuracy of such a procedure the case of a modulated two-Gaussian distribution characterized by $\sigma/x_0 = 0.3$ and a variable α parameter has been considered. The obtained energy estimates for the lower state of the first excited doublet are reported in fig. 4.12 together with their relative error in respect to the numerical reference. Just by looking a such a plot one can see how a degree of accuracy similar to the one observed in the case of a simple TGD model is recovered also in this case.

Chapter 5

Multidimensional tunneling splitting

In chapter 4 the problem of describing the tunneling splitting in simple one-dimensional model systems has been discussed and the possibility of obtaining high accuracy estimations through the use of an asymptotic theory has been demonstrated. In the present chapter, our attention will be moved to the problem of computing approximated ground-state tunneling splitting estimates in the case of multidimensional systems. The chapter is open by section 5.1 where a simple Kramers-like asymptotic approximation, obtained by adopting a second-order Taylor expansion around the mean-field potential saddle-point, will be recovered. The key assumption adopted in formulating such an asymptotic approximation is represented, as usual, by the *a-priori* knowledge of a proper ground-state model capable of representing the potential system under study. This issue, already not trivial in one dimension, is even more complex in the case of multidimensional systems. In sec. 5.2, starting from the discussion presented in sec. 4.2, a simple multidimensional two-Gaussian distribution model will be formulated and characterized. Such a model is far from perfect and, besides being cursed by the same shortcomings already encountered during our one-dimensional analysis, it is also affected by the issue of generating additional high-energy local potential minima whenever an improper selection of parameters is considered. Despite these problems, the simple mathematical structure associated with such a two-Gaussian distribution model makes it a natural choice for the analysis of the asymptotic problem and, for this reason, such a model will be the central subject of the discussion presented in this chapter. In sec. 5.3.1, making use of the two-Gaussian model presented in sec. 5.2, the Kramers-like asymptotic model from sec. 5.1 will be characterized from the accuracy standpoint. As will be discussed, the Kramers-like approximation poorly performs under these circumstances with an overall accuracy nearly not-influenced, within the set of considered parameters, by the mean-field potential barrier height. This, however, is not surprising given that, as already seen in sec. 4.2.3, local approximation of the mean-field potential are usually not fitted to well reproduce the tunneling splitting associated with a two-Gaussian distribution model. This issue will be addressed in section 5.4 where an asymptotic approximation, specifically designed upon the two-Gaussian distribution structure, will be obtained and characterized. As it will be discussed, this new approximation captures the correct asymptotic behavior resulting in a better accuracy when the high barrier limit is considered.

5.1 Multidimensional Kramers' theory

In the present section, a simple asymptotic approximation of the ground-state tunneling splitting will be developed for the case of a multidimensional bi-stable system. The starting point of this analysis is represented by the application of the multidimensional molecular Hamiltonian, defined by eq. 3.84, to the first excited state wave-function of the system under study. In doing so, the following equality can be obtained:

$$\frac{\hbar^2}{2}\psi_0(\mathbf{x})^{-1}\partial_a^\dagger\mu^{ab}\psi_0(\mathbf{x})^2\partial_b g(\mathbf{x}) = \delta E_1\psi_1(\mathbf{x}) \tag{5.1}$$

in which δE_1 indicates, as usual, the ground-state tunneling splitting while $g(\mathbf{x})$ represents the multi-dimensional localization function defined, in perfect analogy with its one-dimensional counterpart from eq. 4.2, as the ratio between the first excited-state wave-function and the ground-state one:

$$g(\mathbf{x}) = \frac{\psi_1(\mathbf{x})}{\psi_0(\mathbf{x})} \tag{5.2}$$

If the asymptotic limit of high barriers is once again invoked, the tunneling splitting must vanish ($\delta E_1 \to 0$) and, as such, the relation from eq. 5.1 can be rewritten in the form:

$$\partial_a^\dagger \mu^{ab} \psi_0(\mathbf{x})^2 \partial_b g(\mathbf{x}) = 0 \tag{5.3}$$

The solution of the just obtained equation is not trivial due to its complex dependence upon the configurational coordinate. In order to obtain a simple solution to the problem, a threefold local approximation can be invoked by considering the mean-field saddle point $\mathbf{x}_s$ as the reference point. Firstly, we will approximate the mass-tensor $\mu^{ab}(\mathbf{x})$, over all the configuration space, with its constant value $\mu_s^{ab} := \mu^{ab}(\mathbf{x}_s)$. Secondly, we will consider the $G(\mathbf{x})$ factor as being the constant $G = G(\mathbf{x}_s)$.[1] Finally, the following quadratic approximation will be adopted to represent the mean-field potential:

$$U(\mathbf{x}) = U(\mathbf{x}_s) + \frac{1}{2}\delta\mathbf{x}^T \mathbf{U}_s^{(2)} \delta\mathbf{x} \tag{5.4}$$

where $\delta\mathbf{x} = \mathbf{x} - \mathbf{x}_s$ represents the displacement of the point $\mathbf{x}$ from the mean-field potential saddle-point $\mathbf{x}_s$ while $\mathbf{U}_s^{(2)}$ represents the mean-field potential Hessian matrix computed in that point. Under these approximations the relation from eq. 5.3 can be easily simplified to the form:

$$\partial_a \mu_s^{ab} e^{-\frac{1}{2}\delta\mathbf{x}^T \mathbf{U}_s^{(2)} \delta\mathbf{x}} \partial_b g(\mathbf{x}) = 0 \tag{5.5}$$

that, due to the definition of the $\delta\mathbf{x}$ variable, can immediately be rewritten according to:

$$\frac{\partial}{\partial \delta\mathbf{x}}^T \boldsymbol{\mu}_s e^{-\frac{1}{2}\delta\mathbf{x}^T \mathbf{U}_s^{(2)} \delta\mathbf{x}} \frac{\partial}{\partial \delta\mathbf{x}} g(\mathbf{x}) = 0 \tag{5.6}$$

At this point, the main difficulty in solving the just obtained equation is represented by the non-diagonal nature of the exponent that, as such, induces coupling between different components of the displacement vector $\delta\mathbf{x}$. By considering the proper variable substitution, this issue can be easily solved and the equation can be rewritten as the sum of independent terms. In order to show how this can be done, let us consider the following eigenvalue problem:

$$\boldsymbol{\Upsilon}\mathbf{S} = \mathbf{S}\boldsymbol{\Lambda} \qquad \text{with} \qquad \boldsymbol{\Upsilon} = \boldsymbol{\mu}_s^{\frac{1}{2}} \mathbf{U}_s^{(2)} \boldsymbol{\mu}_s^{\frac{1}{2}} \tag{5.7}$$

where $\mathbf{S}$ represent the orthogonal matrix ($\mathbf{S}^T = \mathbf{S}^{-1}$), containing the eigenvectors of the $\boldsymbol{\Upsilon}$ mass-weighted Hessian matrix, while $\boldsymbol{\Lambda}$ represent the correspondent diagonal eigenvalue matrix defined according to $\Lambda_{i,j} = \delta_{i,j}\lambda_i$. Please notice how due to both the positive definite nature of the mass tensor $\boldsymbol{\mu}_s$ and the fact that a single negative curvature direction can be found at a first order saddle-point, a single negative eigenvalue $\lambda_1 < 0 < \lambda_2 < ... < \lambda_N$ is encountered in the $\boldsymbol{\Upsilon}$ matrix eigenvalue spectrum. Such a negative eigenvalue plays a fundamental role in the model since it is associated to the reactive motion at the mean-field potential saddle point.

Starting from these considerations, one can easily appreciate how the variable $\mathbf{z} := \mathbf{S}^T \boldsymbol{\mu}_s^{-1/2} \delta\mathbf{x}$ can be conveniently introduced in eq. 5.6 in order to simplify its structure. Considering that $\delta\mathbf{x} = \boldsymbol{\mu}_s^{1/2}\mathbf{S}\mathbf{z}$, the following transformations can easily be obtained:[2]

$$\frac{\partial}{\partial \delta\mathbf{x}} = \frac{\partial \mathbf{z}}{\partial \delta\mathbf{x}} \frac{\partial}{\partial \mathbf{z}} = \boldsymbol{\mu}_s^{-\frac{1}{2}} \mathbf{S} \frac{\partial}{\partial \mathbf{z}} \tag{5.8}$$

$$\delta\mathbf{x}^T \mathbf{U}_s^{(2)} \delta\mathbf{x} = \mathbf{z}^T \mathbf{S}^T \boldsymbol{\mu}_s^{\frac{1}{2}} \mathbf{U}_s^{(2)} \boldsymbol{\mu}_s^{\frac{1}{2}} \mathbf{S}\mathbf{z} = \mathbf{z}^T \mathbf{S}^T \boldsymbol{\Upsilon} \mathbf{S}\mathbf{z} = \mathbf{z}^T \boldsymbol{\Lambda} \mathbf{z} = \sum_i \lambda_i z_i^2 \tag{5.9}$$

Taking into account these results, it is simple to conclude that the relation form eq. 5.6 can, by simple substitution, be rewritten according to the following form:

$$\frac{\partial}{\partial \mathbf{z}}^T e^{-\frac{1}{2}\mathbf{z}^T \boldsymbol{\Lambda} \mathbf{z}} \frac{\partial}{\partial \mathbf{z}} g(\mathbf{z}) = 0 \tag{5.10}$$

[1] Please notice how a constant G-factor translates, thanks to the definition in eq. 3.12, into the equivalence: $\partial_a^\dagger = -\partial_a$.

[2] In general terms, if the coordinate transformation $\mathbf{y} = \mathbf{M}\mathbf{x}$ is considered, the following can be obtained:

$$\frac{\partial}{\partial x_i} = \sum_j \frac{\partial y_j}{\partial x_i} \frac{\partial}{\partial y_j} = \sum_{jk} M_{jk} \frac{\partial x_k}{\partial x_i} \frac{\partial}{\partial y_j} = \sum_{jk} M_{jk} \delta_{ki} \frac{\partial}{\partial y_j} = \sum_j M_{ji} \frac{\partial}{\partial y_j} = \sum_j (M^T)_{ij} \frac{\partial}{\partial y_j} = \left[\mathbf{M}^T \frac{\partial}{\partial \mathbf{y}} \right]_i$$

If, at this point, the left side of the previous equation is multiplied by the reciprocal of the exponential factor, the following factored form can be easily obtained:

$$\sum_i e^{\frac{1}{2}\lambda_i z_i^2}\frac{\partial}{\partial z_i}e^{-\frac{1}{2}\lambda_i z_i^2}\frac{\partial}{\partial z_i}g(\mathbf{z}) = 0 \tag{5.11}$$

This result represents a crucial element of our theoretical analysis that shows how all the coordinate contributions are, in fact, factored along the directions defined by the $\mathbf{z}$ coordinate space. Interestingly, the just obtained equation is compatible with an error-function-like localization function expression dependent only upon the coordinate z_1 associated to the single negative eigenvalue λ_1. As a matter of fact, if a single variable dependence $g(\mathbf{z}) := g(z_1)$ is invoked for the solution, the following condition can be obtained:

$$e^{\frac{1}{2}\lambda_1 z_1^2}\frac{\partial}{\partial z_1}e^{-\frac{1}{2}\lambda_1 z_1^2}\frac{\partial}{\partial z_1}g(z_1) = 0 \tag{5.12}$$

the solution of which can be written according to:

$$g(z_1) = \mathrm{erf}\left(\sqrt{\frac{|\lambda_1|}{2}}z_1\right) \tag{5.13}$$

Please notice how the asymptotic limit condition $\lim_{z_1\to\pm\infty} g(z_1) = \pm 1$ has been imposed to the result. At this point, in perfect analogy with our one-dimensional analysis, the tunneling splitting can be approximated according to the relation:

$$\delta E_1^g := \langle\psi_0 g|\delta\hat{H}|\psi_0 g\rangle = \frac{\hbar^2}{2}\langle\partial_i g|\mu^{ij}\psi_0^2|\partial_j g\rangle \tag{5.14}$$

where the integration by parts has been invoked to simplify the expression. At this point, starting from the result in eq. 5.13, it is simple to observe how:

$$\partial_1 g \equiv \frac{\partial g(z_1)}{\partial x_i} = \frac{\partial z_1}{\partial x_i}\frac{\partial g(z_1)}{\partial z_1} = u_i\sqrt{\frac{2\,|\lambda_1|}{\pi}}e^{-\frac{1}{2}|\lambda_1|z_1^2} \equiv u_i\sqrt{\frac{2\,|\lambda_1|}{\pi}}e^{-\frac{1}{2}|\lambda_1|(\mathbf{u}^T\delta\mathbf{x})^2} \tag{5.15}$$

where the $\mathbf{u}$ vector has been introduced according to $u_i = [\boldsymbol{\mu}_s^{-1/2}\mathbf{S}]_{i,1}$ and z_1 has been written according to $z_1 = \mathbf{u}^T\delta\mathbf{x}$. From such a result, the following expression can be easily obtained:

$$\delta E_1^g = \frac{|\lambda_1|\,\hbar^2}{\pi}\langle u_i\mu^{ij}(\mathbf{x})u_j\psi_0(\mathbf{x})^2 e^{-|\lambda_1|(\mathbf{u}^T\delta\mathbf{x})^2}\rangle \tag{5.16}$$

Please notice how the coordinate dependence of the mass-tensor and that of the G-factor are included in the final integration. At the moment it is impossible to be more specific about the nature of the multidimensional integral involved in eq. 5.16 since its structure strongly depends upon the adopted ground-state model. In sec. 5.3 the case of a two-Gaussian distribution, characterized by constant mass-tensor and G-factor, will be considered and we will show how such an integral can be computed analytically and which kind of accuracy figures can be expected from the presented asymptotic approach.

5.2 Multidimensional Two-Gaussian-Distribution model

In the present section, starting from the experience gained from the one-dimensional analysis presented in section 4.2, a simple two-Gaussian ground-state distribution model will be introduced and characterized. This model represents one of the simplest formulations capable of representing a symmetric multidimensional potential showing a reasonably well-behaved profile. In order to fulfill such a task, let us introduce, with the purpose of parameterizing the configuration space, a set $\mathbf{x} = \{x_1, x_2, ..., x_N\}$ of N internal coordinates describing the tunneling dynamic of the system. Let us indicate with $\hat{R}$ the operator encoding the symmetry of the system such that the ground-state probability distribution $\rho_0(\mathbf{x})$ must be invariant under its action: $\hat{R}\rho_0(\mathbf{x}) = \rho_0(\mathbf{x})$. As highlighted before, the symmetry of the system plays a fundamental role in the description of the tunneling process: considering the closure relation $\hat{R}^2 = \hat{I}$, one can easily see how the symmetry operator $\hat{R}$, together with the identity one $\hat{I}$, must form a group and, as such, the coordinate set $\mathbf{x}$ can be chosen as composed by components that are a basis for the irreducible representations of the group itself. Under these conditions, the coordinate set $\mathbf{x} = (\mathbf{x}^+, \mathbf{x}^-)$ can be parted

into symmetric $\mathbf{x}^+$ and anti-symmetric coordinates $\mathbf{x}^-$ such that the action of the symmetry operator $\hat{R}$, whose representation onto the coordinate basis set is represented by the matrix $\mathbf{R} = \mathbf{R}^T$, has the only effect of changing the sign of the anti-symmetric ones: $\hat{R}\mathbf{x} \equiv \mathbf{R}(\mathbf{x}^+, \mathbf{x}^-) = (\mathbf{x}^+, -\mathbf{x}^-)$. Starting from these preliminary pieces of information and considering that a single normalized multi-dimensional anisotropic Gaussian function $G_{\mathbf{\Sigma}}(\mathbf{x} - \mathbf{x}_0)$ can be defined according to:

$$G_{\mathbf{\Sigma}}(\mathbf{x} - \mathbf{x}_0) := \frac{1}{\sqrt{(2\pi)^N \det(\mathbf{\Sigma})}} e^{-\frac{1}{2}(\mathbf{x}-\mathbf{x}_0)^T \mathbf{\Sigma}^{-1}(\mathbf{x}-\mathbf{x}_0)} \tag{5.17}$$

where $\mathbf{x}_0$ represents the center of the distribution while $\mathbf{\Sigma} = \mathbf{\Sigma}^T$ its variance matrix, the following expression can be adopted to define the desired two-Gaussian distribution model:

$$\rho_0(\mathbf{x}) := \frac{1}{2} G_{\mathbf{\Sigma}}(\mathbf{x} - \mathbf{x}_0) + \frac{1}{2} G_{\mathbf{\Sigma}_R}(\mathbf{x} - \mathbf{x}_0^R) \tag{5.18}$$

in which $\mathbf{\Sigma}_R = \mathbf{R}\mathbf{\Sigma}\mathbf{R}$ while $\mathbf{x}_0^R = \mathbf{R}\mathbf{x}_0$. Different ground-state distributions can be defined by properly adjusting the model parameters; in figure 5.1 a simple bi-dimensional system composed by an anti-symmetric coordinate and a symmetric one is reported as an illustrative example.

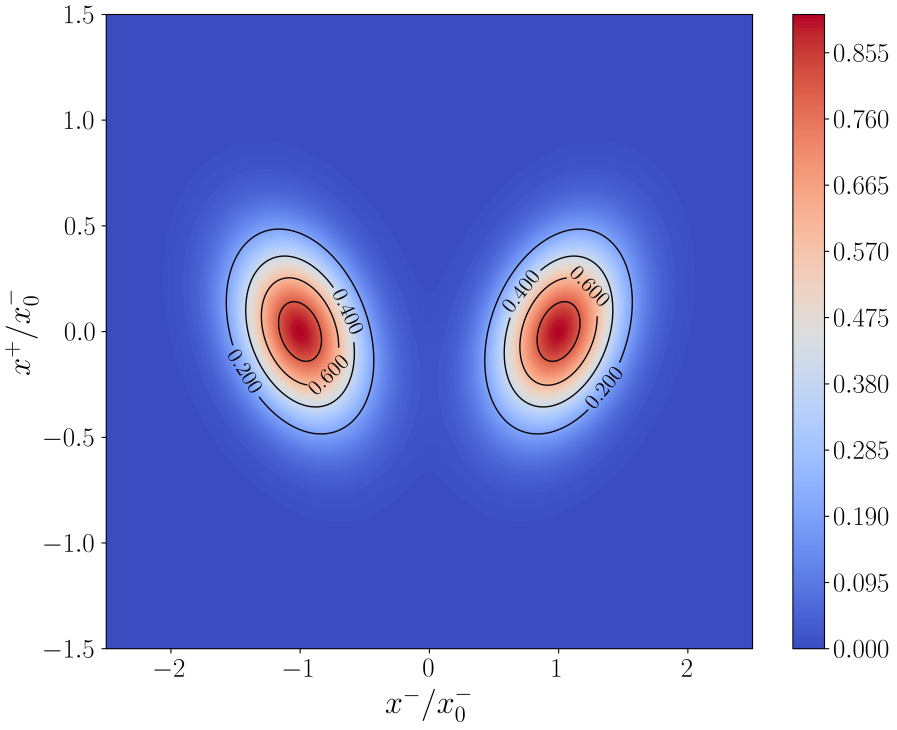

Figure 5.1: Bi-dimensional ground state distribution having one anti-symmetrical coordinate x^- coupled to a symmetrical one x^+. The $\mathbf{x}_0$ parameter, fixing the center of the Gaussian functions, is set to $\mathbf{x}_0 = (0, x_0^-)$ while the variance matrix $\mathbf{\Sigma} = \mathbf{\Theta}^T \mathbf{\Lambda}_\sigma^2 \mathbf{\Theta}$ has been obtained applying the matrix $\mathbf{\Theta}$, encoding a rotation of $\pi/6$, to a diagonal matrix $\mathbf{\Lambda}_\sigma$ having as its principal variance values $\mathbf{\Lambda}_\sigma^{--} = 0.35/x_0^-$ and $\mathbf{\Lambda}_\sigma^{++} = 0.25/x_0^-$.

By adopting the proper scale factor to ensure an adimensional logarithm argument, the following definition for the mean-field potential $U(\mathbf{x})$ can be obtained:

$$U(\mathbf{x}) := -\ln\left[2\sqrt{(2\pi)^N \det(\mathbf{\Sigma})}\rho_0(\mathbf{x})\right] = -\ln\left[e^{-\frac{1}{2}(\mathbf{x}-\mathbf{x}_0)^T\mathbf{\Sigma}^{-1}(\mathbf{x}-\mathbf{x}_0)} + e^{-\frac{1}{2}(\mathbf{x}-\mathbf{x}_0^R)^T\mathbf{\Sigma}_R^{-1}(\mathbf{x}-\mathbf{x}_0^R)}\right] \tag{5.19}$$

Considering that $\mathbf{x}_0 = (\mathbf{x}_0^+, \mathbf{x}_0^-)$ one can easily verify how $\mathbf{x}_0^R = \mathbf{R}\mathbf{x}_0 = (\mathbf{x}_0^+, -\mathbf{x}_0^-)$ or, in simpler term, how the matrix representation $\mathbf{R}$ of the symmetry operator $\hat{R}$ must assume, on the symmetric set of

coordinates, the form:

$$\mathbf{R} = \begin{pmatrix} \mathbf{I} & 0 \\ 0 & -\mathbf{I} \end{pmatrix} \tag{5.20}$$

Starting from this observation, it is simple to verify how:

$$\mathbf{A} := \mathbf{\Sigma}^{-1} = \begin{pmatrix} \mathbf{A}^{++} & \mathbf{A}^{+-} \\ \mathbf{A}^{-+} & \mathbf{A}^{--} \end{pmatrix} \quad \text{and} \quad \mathbf{\Sigma}_R^{-1} = \begin{pmatrix} \mathbf{A}^{++} & -\mathbf{A}^{+-} \\ -\mathbf{A}^{-+} & \mathbf{A}^{--} \end{pmatrix} \tag{5.21}$$

where the blocks of the $\mathbf{A}$ matrix can be easily computed according to the rules, derived in appendix E, for the inversion of a block matrix:

$$\mathbf{A}^{++} = \left[\mathbf{\Sigma}^{++} - \mathbf{\Sigma}^{+-}(\mathbf{\Sigma}^{--})^{-1}\mathbf{\Sigma}^{-+}\right]^{-1} \tag{5.22}$$

$$\mathbf{A}^{+-} = -(\mathbf{\Sigma}^{++})^{-1}\mathbf{\Sigma}^{+-}\left[\mathbf{\Sigma}^{--} - \mathbf{\Sigma}^{-+}(\mathbf{\Sigma}^{++})^{-1}\mathbf{\Sigma}^{+-}\right]^{-1} \tag{5.23}$$

$$\mathbf{A}^{-+} = -(\mathbf{\Sigma}^{--})^{-1}\mathbf{\Sigma}^{-+}\left[\mathbf{\Sigma}^{++} - \mathbf{\Sigma}^{+-}(\mathbf{\Sigma}^{--})^{-1}\mathbf{\Sigma}^{-+}\right]^{-1} \tag{5.24}$$

$$\mathbf{A}^{--} = \left[\mathbf{\Sigma}^{--} - \mathbf{\Sigma}^{-+}(\mathbf{\Sigma}^{++})^{-1}\mathbf{\Sigma}^{+-}\right]^{-1} \tag{5.25}$$

Please notice how, given the symmetric nature of the variance matrix $\mathbf{\Sigma} = \mathbf{\Sigma}^T$, its inverse must be symmetric as well. Consequently, the diagonal blocks of such a matrix must be symmetrical $\mathbf{A}^{\pm\pm} = (\mathbf{A}^{\pm\pm})^T$, while the out diagonal ones must respond to the relation: $(\mathbf{A}^{\pm\mp})^T = \mathbf{A}^{\mp\pm}$. Starting from these observations it is simple to show how, with a little elaboration of the exponential terms, the expression from eq. 5.19 can be rewritten according to:

$$U(\mathbf{x}) = U_+(\mathbf{x}) - \ln\left\{2\cosh\left[U_-(\mathbf{x})\right]\right\} \tag{5.26}$$

where each mean-field potential component $U_\pm(x)$, characterized by the symmetry property $U_\pm(x) = \pm U_\pm(\hat{R}x)$, can be defined according to:

$$\begin{aligned} U_+(x) := \frac{1}{2}(\mathbf{x}^+ - \mathbf{x}_0^+)^T\mathbf{A}^{++}(\mathbf{x}^+ - \mathbf{x}_0^+) + \frac{1}{2}(\mathbf{x}^-)^T\mathbf{A}^{--}\mathbf{x}^- + \\ + \frac{1}{2}(\mathbf{x}_0^-)^T\mathbf{A}^{--}\mathbf{x}_0^- - (\mathbf{x}^+ - \mathbf{x}_0^+)^T\mathbf{A}^{+-}\mathbf{x}_0^- \end{aligned} \tag{5.27}$$

$$U_-(x) := (\mathbf{x}^+ - \mathbf{x}_0^+)^T\mathbf{A}^{+-}\mathbf{x}^- - (\mathbf{x}^-)^T\mathbf{A}^{--}\mathbf{x}_0^- \tag{5.28}$$

Now that the overall system definition has been presented, we can move our attention to the characterization of its key geometrical features such as the position $\mathbf{x}_s$ of the saddle point connecting the two potential wells and the correspondent barrier height $\Delta U = U(\mathbf{x}_s) - U(\mathbf{x}_0)$. In order to do so, one can consider that, given the bi-stable symmetric nature of the system, the saddle point position cannot have components along the set of anti-symmetric coordinates: $\mathbf{x}_s = (\mathbf{x}_s^+, \mathbf{0})$. As such, its position can be easily computed imposing the condition:

$$\left.\frac{\partial U(\mathbf{x})}{\partial \mathbf{x}^+}\right|_{\mathbf{x}^-=\mathbf{0}} = \mathbf{A}^{++}(\mathbf{x}^+ - \mathbf{x}_0^+) - \mathbf{A}^{+-}\mathbf{x}_0^- = \mathbf{0} \tag{5.29}$$

from which the symmetric component $\mathbf{x}_s^+$ of the saddle point position can be obtained in the form:

$$\mathbf{x}_s^+ = \mathbf{x}_0^+ + (\mathbf{A}^{++})^{-1}\mathbf{A}^{+-}\mathbf{x}_0^- \tag{5.30}$$

For illustrative purposes the mean-field potential correspondent to the ground state distribution represented in figure 5.1 has been reported in figure 5.2 together with the saddle-point position computed from eq. 5.30.

Now that the position of the saddle point has been identified one can easily approximate the barrier height ΔU according to:

$$\Delta U = U(\mathbf{x}_s) - U(\mathbf{x}_0) \simeq U(\mathbf{x}_s) = \frac{1}{2}(\mathbf{x}_0^-)^T\left[\mathbf{A}^{--} - \mathbf{A}^{-+}(\mathbf{A}^{++})^{-1}\mathbf{A}^{+-}\right]\mathbf{x}_0^- - \ln(2) \tag{5.31}$$

where the limit of low overlap between Gaussian functions has been invoked in order to neglect, near either one of the two minima, the effect induced by the Gaussian term localized in the other potential

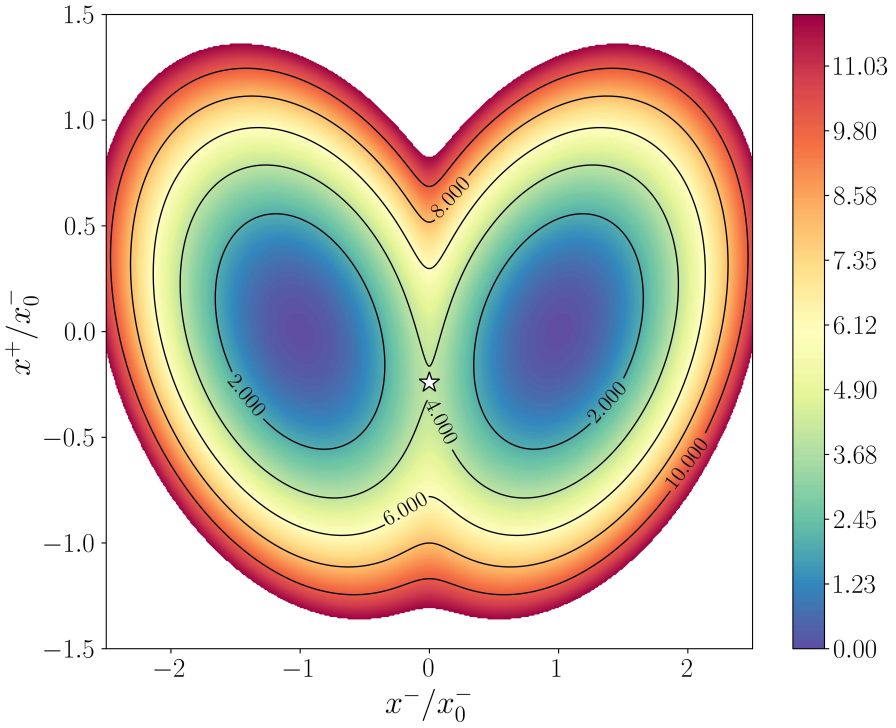

Figure 5.2: Mean filed potential $U(\mathbf{x})$ correspondent to the ground-state distribution from fig. 5.1. The white star represents the saddle point position computed according to eq. 5.30

site. Invoking once again the results obtained in appendix E about the inverse of a block matrix, the previous relation can be readily simplified according to:

$$\Delta U = \frac{1}{2}(\mathbf{x}_0^-)^T(\boldsymbol{\Sigma}^{--})^{-1}\mathbf{x}_0^- - \ln(2) \tag{5.32}$$

Starting from eq. 5.26 the component of the gradient vector and those of the Hessian matrix can be easily computed according to:

$$\frac{\partial U(\mathbf{x})}{\partial x_j} = \frac{\partial U_+(\mathbf{x})}{\partial x_j} - \tanh\left[U_-(\mathbf{x})\right]\frac{\partial U_-(\mathbf{x})}{\partial x_j} \tag{5.33}$$

$$\frac{\partial^2 U(\mathbf{x})}{\partial x_i \partial x_j} = \frac{\partial^2 U_+(\mathbf{x})}{\partial x_i \partial x_j} - \tanh\left[U_-(\mathbf{x})\right]\frac{\partial^2 U_-(\mathbf{x})}{\partial x_i \partial x_j} - \operatorname{sech}^2\left[U_-(\mathbf{x})\right]\frac{\partial U_-(\mathbf{x})}{\partial x_i}\frac{\partial U_-(\mathbf{x})}{\partial x_j} \tag{5.34}$$

Considering the definitions from eqs. 5.27 and 5.28, the first derivative terms can be easily computed according to:

$$\begin{aligned} \frac{\partial U_+(\mathbf{x})}{\partial \mathbf{x}^+} &= \mathbf{A}^{++}(\mathbf{x}^+ - \mathbf{x}_0^+) - \mathbf{A}^{-+}\mathbf{x}_0^- \qquad \frac{\partial U_+(\mathbf{x})}{\partial \mathbf{x}^-} = \mathbf{A}^{--}\mathbf{x}^- \\ \frac{\partial U_-(\mathbf{x})}{\partial \mathbf{x}^+} &= \mathbf{A}^{+-}\mathbf{x}^- \qquad \frac{\partial U_-(\mathbf{x})}{\partial \mathbf{x}^-} = \mathbf{A}^{-+}(\mathbf{x}^+ - \mathbf{x}_0^+) - \mathbf{A}^{--}\mathbf{x}_0^- \end{aligned} \tag{5.35}$$

from which, the following expressions can be obtained for the second derivative terms:

$$\begin{aligned} \frac{\partial^2 U_+(\mathbf{x})}{\partial \mathbf{x}^+ \partial \mathbf{x}^+} &= \mathbf{A}^{++} \qquad \frac{\partial^2 U_+(\mathbf{x})}{\partial \mathbf{x}^- \partial \mathbf{x}^-} = \mathbf{A}^{--} \qquad \frac{\partial^2 U_+(\mathbf{x})}{\partial \mathbf{x}^+ \partial \mathbf{x}^-} = \left(\frac{\partial^2 U_+(\mathbf{x})}{\partial \mathbf{x}^- \partial \mathbf{x}^+}\right)^T = \mathbf{0} \\ \frac{\partial^2 U_-(\mathbf{x})}{\partial \mathbf{x}^+ \partial \mathbf{x}^+} &= \mathbf{0} \qquad \frac{\partial^2 U_-(\mathbf{x})}{\partial \mathbf{x}^- \partial \mathbf{x}^-} = \mathbf{0} \qquad \frac{\partial^2 U_-(\mathbf{x})}{\partial \mathbf{x}^+ \partial \mathbf{x}^-} = \left(\frac{\partial^2 U_-(\mathbf{x})}{\partial \mathbf{x}^- \partial \mathbf{x}^+}\right)^T = \mathbf{A}^{-+} \end{aligned} \tag{5.36}$$

Starting from these results, the curvatures of the mean-field potential at the saddle point can be easily computed. Recalling that at the saddle point $\mathbf{x}^- = \mathbf{0}$ it is easy to observe how, according to eq. 5.28, the

$U_-(\mathbf{x})$ mean-field component must vanish. This leaves us with the following expression for the Hessian matrix elements:

$$\left.\frac{\partial^2 U(\mathbf{x})}{\partial x_i \partial x_j}\right|_{\mathbf{x}^-=\mathbf{0}} = \left.\frac{\partial^2 U_+(\mathbf{x})}{\partial x_i \partial x_j}\right|_{\mathbf{x}^-=\mathbf{0}} - \left.\frac{\partial U_-(\mathbf{x})}{\partial x_i}\right|_{\mathbf{x}^-=\mathbf{0}} \left.\frac{\partial U_-(\mathbf{x})}{\partial x_j}\right|_{\mathbf{x}^-=\mathbf{0}} \tag{5.37}$$

By simply substituting the results from eqs. 5.35 and 5.36 into the expression just derived, one can easily verify how the following expressions can be obtained:

$$\left.\frac{\partial^2 U(\mathbf{x})}{\partial \mathbf{x}^+ \partial \mathbf{x}^+}\right|_{\mathbf{x}=\mathbf{x}_s} = \mathbf{A}^{++} \tag{5.38}$$

$$\left.\frac{\partial^2 U(\mathbf{x})}{\partial \mathbf{x}^+ \partial \mathbf{x}^-}\right|_{\mathbf{x}=\mathbf{x}_s} = \left.\frac{\partial^2 U(\mathbf{x})}{\partial \mathbf{x}^+ \partial \mathbf{x}^-}\right|_{\mathbf{x}=\mathbf{x}_s} = \mathbf{0} \tag{5.39}$$

$$\left.\frac{\partial^2 U(\mathbf{x})}{\partial \mathbf{x}^- \partial \mathbf{x}^-}\right|_{\mathbf{x}=\mathbf{x}_s} = \mathbf{A}^{--} - \left[\left(\boldsymbol{\Sigma}^{--}\right)^{-1}\mathbf{x}_0^-\right] \otimes \left[\left(\boldsymbol{\Sigma}^{--}\right)^{-1}\mathbf{x}_0^-\right] \tag{5.40}$$

Now that the key geometrical features of the mean-field potential have been discussed, we can move our attention to the characterization of the quantum potential profile associated to our simple two-Gaussian distribution model. This task is however not trivially done in general terms given that, according to the definition given in eq. 3.88, the quantum potential definition depends, due to the structure of the Jacobian matrix, upon the coordinate-dependent mass tensor $\boldsymbol{\mu}$, its spatial derivatives and the metric-tensor determinant $G(\mathbf{x})$. The simplest case that can possibly be considered is represented by a system in which these quantities are assumed, either by definition or by approximation, as constants. This assumption clearly represents a strong simplification of a real molecular system, in which the coordinate dependence of the effective mass can play a relevant role. Despite these limitations, this simple assumption will be extensively applied in what follows; in section 5.2.1, this simplified model will allow us to give a general overview of the features and pitfalls associated to a multidimensional two Gaussian distribution model while, in sections 5.3.1 and 5.4.1, it will be used to test some early multidimensional asymptotic theory formulations.

5.2.1 Coordinate independent mass tensor approximation

If the coordinate dependence of the $\boldsymbol{\mu}$-tensor and that of the G-factor is dropped, the quantum potential definition from eq. 3.88 can be rewritten in simple form according to:

$$\delta V(\mathbf{x}) = \frac{\hbar^2}{2}\sum_{i,j}\left[\frac{1}{4}\mu_{ij}\frac{\partial U(\mathbf{x})}{\partial x_i}\frac{\partial U(\mathbf{x})}{\partial x_j} - \frac{1}{2}\mu_{ij}\frac{\partial^2 U(\mathbf{x})}{\partial x_i \partial x_j}\right] \tag{5.41}$$

Please notice how the mass-tensor $\boldsymbol{\mu}$, playing the role of coupling term between different derivative components, is strongly influenced by the symmetry of the system and, in fact, its action cannot mix coordinate components characterized by different parity. In order to verify this statement, it is sufficient to consider that the energetics of the system must be invariant under the action of the symmetry operator, or, in more formal terms, that the Hamiltonian operator must commute with the symmetry one: $[\hat{H}, \hat{R}] = 0$. Starting from this assumption, it is simple to show how the following relation must be verified:[3]

$$\mathbf{R}\boldsymbol{\mu}\mathbf{R} = \boldsymbol{\mu} \tag{5.42}$$

This allows us to conclude that the mass tensor must be composed by two non-zero diagonal blocks mixing only coordinates characterized the same parity:

$$\boldsymbol{\mu} = \begin{pmatrix} \boldsymbol{\mu}^{++} & \mathbf{0} \\ \mathbf{0} & \boldsymbol{\mu}^{--} \end{pmatrix} \tag{5.43}$$

[3] Please notice how, considering the symmetry of the coordinate components, the following relations must be verified:

$$\hat{R}\frac{\partial}{\partial \mathbf{x}} f(\mathbf{x}) = \mathbf{R}\frac{\partial}{\partial \mathbf{x}}\hat{R} f(\mathbf{x}) \qquad \text{and} \qquad \hat{R}\frac{\partial}{\partial \mathbf{x}}^T f(\mathbf{x}) = \frac{\partial}{\partial \mathbf{x}}^T \mathbf{R}\hat{R} f(\mathbf{x})$$

Recalling the symmetry invariance of the ground state distribution, the following can be easily obtained:

$$\hat{R}\hat{H} = -\frac{\hbar^2}{2}\rho_0(\mathbf{x})^{-\frac{1}{2}}\frac{\partial}{\partial \mathbf{x}}^T \mathbf{R}\boldsymbol{\mu}\mathbf{R}\rho_0(\mathbf{x})\frac{\partial}{\partial \mathbf{x}}\rho_0(\mathbf{x})^{-\frac{1}{2}}\hat{R}$$

Taking into account the commutation relation $\hat{R}\hat{H} = \hat{H}\hat{R}$, it is trivial to obtain the expression in eq. 5.42

Starting from these early definitions, the location of the quantum potential saddle-point can be easily identified by simply recalling that, due to the symmetry of the system, its coordinates cannot have components onto the anti-symmetric coordinate subspace. From these considerations, the following condition can be imposed:

$$\left.\frac{\partial \delta V(\mathbf{x})}{\partial \mathbf{x}^+}\right|_{\mathbf{x}^-=\mathbf{0}} = \mathbf{0} \tag{5.44}$$

In order to solve this equation, let us start by considering the gradient of the first term of $\delta V(\mathbf{x})$ in respect to the set $\mathbf{x}^+$ of symmetric coordinates. Each component of such a vector can be rewritten, thanks to the symmetry of the mass-tensor $\boldsymbol{\mu} = \boldsymbol{\mu}^T$, into the following form:

$$\left.\frac{\partial}{\partial x_k^+}\sum_{i,j}\mu_{ij}\frac{\partial U(\mathbf{x})}{\partial x_i}\frac{\partial U(\mathbf{x})}{\partial x_j}\right|_{\mathbf{x}^-=\mathbf{0}} = 2\sum_{i,j}\mu_{ij}\frac{\partial^2 U(\mathbf{x})}{\partial x_k^+ x_i}\frac{\partial U(\mathbf{x})}{\partial x_j} \tag{5.45}$$

Observing that for $\mathbf{x}^- = \mathbf{0}$ the term $U_-(\mathbf{x})$ vanishes and recalling the relations obtained in eqs. 5.35 and 5.36, the following result can be easily obtained:

$$\left.\frac{\partial}{\partial \mathbf{x}_k}\sum_{i,j}\mu_{ij}\frac{\partial U(\mathbf{x})}{\partial x_i}\frac{\partial U(\mathbf{x})}{\partial x_j}\right|_{\mathbf{x}^-=\mathbf{0}} = 2\mathbf{A}^{++}\boldsymbol{\mu}^{++}\left[\mathbf{A}^{++}(\mathbf{x}^+ - \mathbf{x}_0^+) - \mathbf{A}^{-+}\mathbf{x}_0^-\right] \tag{5.46}$$

where, according to eq. 5.43, the matrix $\boldsymbol{\mu}^{++}$ represents the block of the mass-tensor connecting symmetric coordinates. A similar operation can be done considering the second term in the $\delta V(\mathbf{x})$ expression for which the following result can be obtained:

$$\left.\frac{\partial}{\partial \mathbf{x}^+}\sum_{i,j}\mu_{ij}\frac{\partial^2 U(\mathbf{x})}{\partial x_i \partial x_j}\right|_{\mathbf{x}^-=\mathbf{0}} = -2\mathbf{A}^{-+}\boldsymbol{\mu}^{--}\left[\mathbf{A}^{-+}(\mathbf{x}^+ - \mathbf{x}_0^+) - \mathbf{A}^{--}\mathbf{x}_0^-\right] \tag{5.47}$$

where, in perfect analogy with the notation adopted before, $\boldsymbol{\mu}^{--}$ indicates the block of the mass-tensor connecting the anti-symmetric components. Substituting the results from eqs. 5.46 and 5.47 into the condition dictated by eq. 5.44 the following expression can be easily recovered for the symmetric component $\mathbf{x}_s^+$ of the saddle-point position:

$$\mathbf{x}_s^+ = \mathbf{x}_0^+ \left[\frac{1}{2}\mathbf{A}^{++}\boldsymbol{\mu}^{++}\mathbf{A}^{++} + \mathbf{A}^{-+}\boldsymbol{\mu}^{--}\mathbf{A}^{-+}\right]^{-1}\left[\frac{1}{2}\mathbf{A}^{++}\boldsymbol{\mu}^{++}\mathbf{A}^{-+} + \mathbf{A}^{-+}\boldsymbol{\mu}^{--}\mathbf{A}^{--}\right]\mathbf{x}_0^- \tag{5.48}$$

In figure 5.3 the quantum potential profile correspondent to the bi-dimensional equilibrium distribution represented in figure 5.1 is reported for the case of a diagonal mass-tensor proportional to the identity matrix. In the same figure, the position of the saddle point predicted using eq. 5.48 is marked by a white cross.

Please notice how, from now on, in order to deal with adimensional quantities, all the lengths will be expressed in units of a given reference length $\tilde{L}$, all the masses will be reported in units of a given reference mass $\tilde{m}$ while all the energies will be reported in terms of the unit E_u defined according to:

$$E_u := \frac{\hbar^2}{2\tilde{m}\tilde{L}^2} \tag{5.49}$$

the precise definition of these quantities will depend upon the considered problem and will be specified ad-hoc for each problem.

Just by looking at the potential function shown in figure 5.3 one can clearly see how the barrier shape shows, along the symmetry element, a somewhat sharp profile compatible with the cusp-like behavior observed for the simple one-dimensional two-Gaussian counterpart form eq. 4.19. This problem cannot be readily solved with a simple two-Gaussian formulation and calls, similarly to what did in our one-dimensional analysis, for more advanced multidimensional models. Furthermore, the multidimensional nature of the system opens new challenges in the ground state modeling that, sometimes, results, as can be seen from figure 5.4, in the formation of additional local high-energy minima. These shortcomings still represent an open issue whose discussion will not be presented in this thesis work.

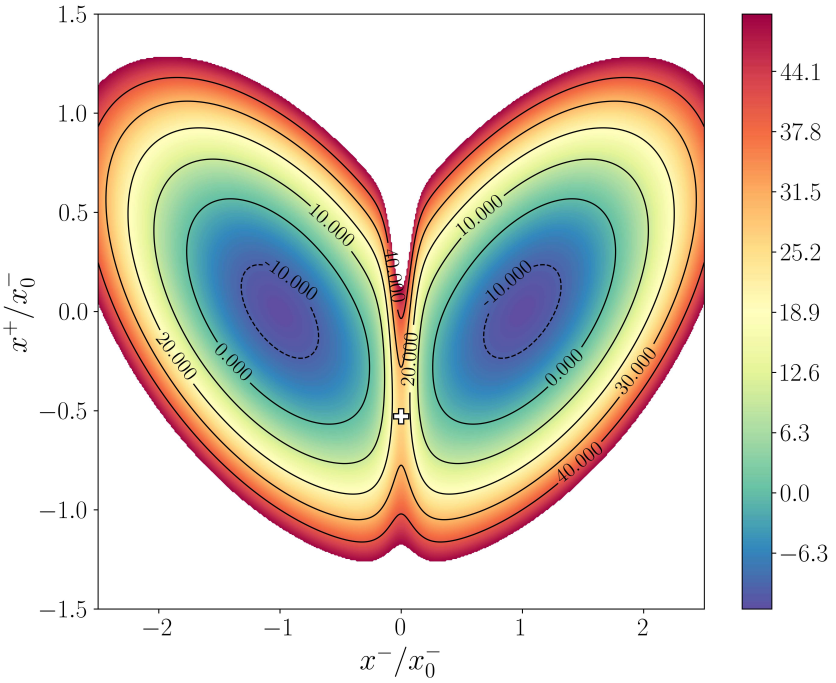

Figure 5.3: Quantum potential $\delta V(\mathbf{x})$ correspondent to the ground-state distribution from fig. 5.1. The mass tensor has been set to the identity matrix while the length scale has been fixed in unit of x_0^-. The white cross represents the saddle point position computed according to eq. 5.48

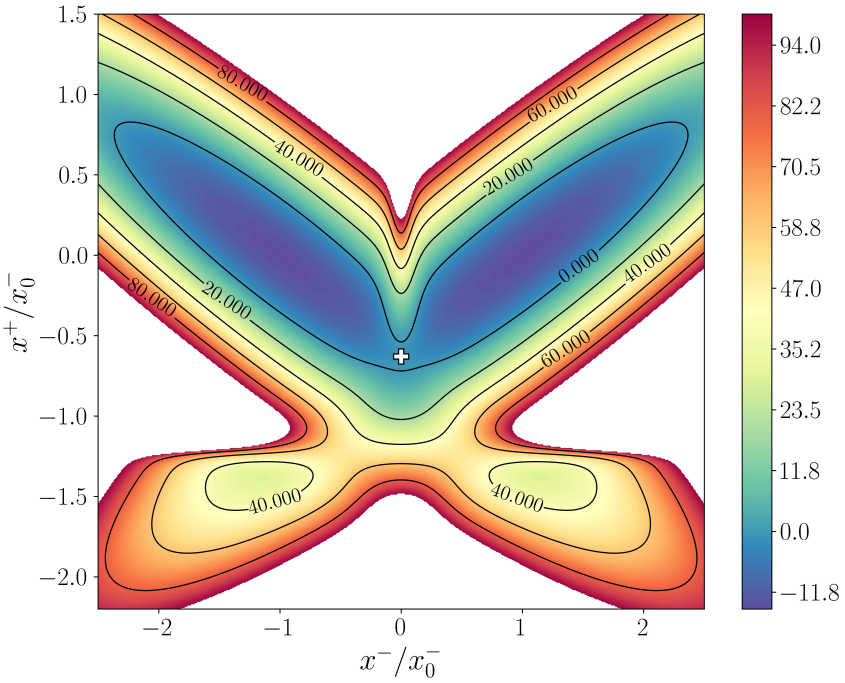

Figure 5.4: Quantum potential associated to a bi-dimensional ground-state distribution having one anti-symmetrical coordinate x^- coupled to a symmetrical one x^+. The $\mathbf{x}_0$ parameter, fixing the center of the Gaussian functions, is set to $\mathbf{x}_0 = (0, x_0^-)$ while the variance matrix $\mathbf{\Sigma} = \mathbf{\Theta}^T \mathbf{\Lambda}_\sigma^2 \mathbf{\Theta}$ has been obtained applying the matrix $\mathbf{\Theta}$, encoding a rotation of $\pi/6$, to a diagonal matrix $\mathbf{\Lambda}_\sigma$ having as its principal variance values $\mathbf{\Lambda}_\sigma^- = 0.45/x_0^-$ and $\mathbf{\Lambda}_\sigma^{++} = 0.2/x_0^-$.

5.2.2 The parametrization of the variance matrix

Now that the two-Gaussian distribution model has been introduced and characterized, let us take a moment to discuss how the $\mathbf{\Sigma}$ variance matrix, a key ingredient in the parametrization of the model, can be defined. In order to do so, let us start our discussion by observing how a generic multidimensional anisotropic Gaussian, parametrized by a center point $\mathbf{x}_0$ and a variance matrix $\mathbf{\Sigma}$, can be generated by applying a rotation $\hat{\Theta}$ to a non-rotated Gaussian function centered in the same $\mathbf{x}_0$ point. Please notice how this non-rotated function, characterized by a set of principal axis parallel to the reference system, needs to be parametrized by a diagonal $\mathbf{\Lambda}_\sigma$ variance matrix in which the diagonal elements represent the variance values describing the Gaussian profiles associated to each dimension. From these considerations it is easy to verify how the following expression can be recovered for the $\mathbf{\Sigma}$ variance matrix:

$$\mathbf{\Sigma} = \mathbf{\Theta}\mathbf{\Lambda}_\sigma\mathbf{\Theta}^T \tag{5.50}$$

where $\mathbf{\Theta}$ represent the rotation matrix associated to the rotation operator $\hat{\Theta}$. In two-dimension such a rotation matrix can be easily parametrized according to:

$$\mathbf{\Theta} = \begin{pmatrix} \cos\theta & -\sin\theta \\ \sin\theta & \cos\theta \end{pmatrix} \tag{5.51}$$

in which the θ angle represents the counterclockwise rotation applied to the non-rotated Gaussian distribution.[4] In three dimensions the rotation matrix can be expressed in terms of 3 Euler's angles while in the general N-dimensional case a set of $N(N-1)/2$ angular parameters must be invoked into the matrix parametrization. Giving a general analytical formulation for the multidimensional rotation matrix is not simple and will not be discussed in the present thesis work.[5]

5.3 Kramers' approximation for a two-Gaussian system

Now that the multidimensional two-Gaussian model has been introduced and characterized, let us employ it to evaluate the accuracy of the Kramers-like asymptotic approximation presented in sec. 5.1. In order to do so let us consider the simplest case possible: a system characterized by a constant mass-tensor $\mu^{ij}(\mathbf{x}) = \mu^{ij}(\mathbf{x}_s) = \mu_s^{ij}$ and a constant G-factor $G(\mathbf{x}) = G(\mathbf{x}_s) = G_s$. Under these assumptions the expression for the tunneling splitting form eq. 5.16 assumes the form:

$$\delta E_1^g = \frac{|\lambda_1|\,\hbar^2}{\pi} u_i \mu_s^{ij} u_j \frac{a + a_R}{2} \tag{5.52}$$

where a and a_R represent the integrals depending upon the single Gaussian distributions defining the two-Gaussian distribution model:

$$a = \int d\mathbf{x}\, e^{-|\lambda_1|(\mathbf{u}^T\delta\mathbf{x})^2} G_{\mathbf{\Sigma}}(\mathbf{x} - \mathbf{x}_0) \tag{5.53}$$

$$a_R = \int d\mathbf{x}\, e^{-|\lambda_1|(\mathbf{u}^T\delta\mathbf{x})^2} G_{\mathbf{\Sigma_R}}(\mathbf{x} - \mathbf{x}_0^R) \tag{5.54}$$

The evaluation of these integrals is simple and can be carried on analytically. In order to show how this can be done, let us consider, as an example, the a integral whose extended expression can be written according to:

$$a = \frac{1}{\sqrt{(2\pi)^N \det(\mathbf{\Sigma})}} \int d\mathbf{x}\, e^{-\frac{1}{2}(\mathbf{x}-\mathbf{x}_0)^T\mathbf{\Sigma}^{-1}(\mathbf{x}-\mathbf{x}_0) - |\lambda_1|(\mathbf{u}^T\delta\mathbf{x})^2} \tag{5.55}$$

[4] Please notice how in the bi-dimensional case the $\mathbf{\Theta}^T$ matrix, appearing on the right side of eq. 5.50, represents, in fact, a clockwise rotation of an angle θ applied to the coordinate vector. This clockwise rotation of the coordinate system corresponds, in the rotated reference system, to a counterclockwise rotation of the Gaussian function.

[5] If an explicit analytical formulation is not required, a possible parametrization of the rotation matrix can be generated numerically. Recalling that a generic rotation matrix $\mathbf{\Theta}$ is defined as an orthogonal matrix $\mathbf{\Theta}^{-1} = \mathbf{\Theta}^T$ having unitary determinant $\det\{\mathbf{\Theta}\} = 1$, the following practical implementation can be considered:

$$\mathbf{\Theta} = e^{\mathbf{\Omega}} \qquad \text{with} \qquad \mathbf{\Omega}^T = -\mathbf{\Omega}$$

where the skew-symmetric nature of $\mathbf{\Omega}$ impart to the $\mathbf{\Theta}$ matrix orthogonal character:

$$\mathbf{\Theta}^{-1} = e^{-\mathbf{\Omega}} = e^{\mathbf{\Omega}^T} = \mathbf{\Theta}^T$$

Please notice how the diagonal elements of a skew-symmetric matrix are zero and, therefore, so does its trace. As such $\det\{\mathbf{\Theta}\} = \exp\{\mathrm{Tr}[\mathbf{\Omega}]\} = 1$ as expected. Under this hypothesis, the parametrization of $\mathbf{\Theta}$ reduces to the definition of the desired skew-symmetric matrix $\mathbf{\Omega}$.

In order to deal with a more clear structure, let us group all the terms based on their dependence upon the coordinate. This can be done easily and, in doing so, the following expression can be recovered:

$$a = \frac{1}{\sqrt{(2\pi)^N \det(\mathbf{\Sigma})}} \int d\mathbf{x}\, e^{-\frac{1}{2}\left[\mathbf{x}^T\mathbf{B}\mathbf{x} - 2\mathbf{x}^T\mathbf{b} + c\right]} \tag{5.56}$$

where the following definitions have been introduced:

$$\mathbf{B} := \mathbf{\Sigma}^{-1} + 2\,|\lambda_1|\,\mathbf{u}\otimes\mathbf{u} \tag{5.57}$$

$$\mathbf{b} := \mathbf{\Sigma}^{-1}\mathbf{x}_0 + 2\,|\lambda_1|\,(\mathbf{x}_s\cdot\mathbf{u})\mathbf{u} \tag{5.58}$$

$$c := \mathbf{x}_0^T\mathbf{\Sigma}^{-1}\mathbf{x}_0 + 2\,|\lambda_1|\,(\mathbf{x}_s\cdot\mathbf{u})^2 \tag{5.59}$$

Observing that $\mathbf{B} = \mathbf{B}^T$,[6] the relation from eq. 5.55 can, with little elaboration, be rewritten in terms of a non-normalized Gaussian integral according to:

$$a = \frac{1}{\sqrt{(2\pi)^N \det(\mathbf{\Sigma})}} e^{\frac{1}{2}\left[\mathbf{b}^T\mathbf{B}^{-1}\mathbf{b} - c\right]} \int d\mathbf{x}\, e^{-\frac{1}{2}\left(\mathbf{x}-\mathbf{B}^{-1}\mathbf{b}\right)^T\mathbf{B}\left(\mathbf{x}-\mathbf{B}^{-1}\mathbf{b}\right)} \tag{5.60}$$

Recalling the definition of the normalized Gaussian from eq. 5.17 the following result can be easily obtained:

$$a = \sqrt{\frac{\det(\mathbf{B}^{-1})}{\det(\mathbf{\Sigma})}} e^{\frac{1}{2}\left[\mathbf{b}^T\mathbf{B}^{-1}\mathbf{b} - c\right]} = \frac{e^{\frac{1}{2}\left[\mathbf{b}^T\mathbf{B}^{-1}\mathbf{b} - c\right]}}{\sqrt{\det[\mathbf{I} + 2\,|\lambda_1|\,\mathbf{\Sigma}(\mathbf{u}\otimes\mathbf{u})]}} \tag{5.61}$$

where the property $\det(\mathbf{\Sigma})/\det\left(\mathbf{B}^{-1}\right) = \det(\mathbf{\Sigma}\mathbf{B})$ has been invoked. The same procedure can also be applied, after replacing $\mathbf{\Sigma}$ with $\mathbf{\Sigma}_R$ and $\mathbf{x}_0$ with $\mathbf{x}_0^R$, to the computation of the a_R integral. Now that an analytic expression for the involved a and a_R integrals has been obtained, the tunneling splitting approximation from eq. 5.52, can be easily evaluated by computing the $\mathbf{u}$ vector components. This, in turn, requires the diagonalization of the mass-weighted Hessian matrix whose elements can be analytically obtained starting from the relations presented in eqs. 5.38, 5.39 and 5.40.

5.3.1 Results in two-dimensions

Now that the theoretical framework has been clarified the accuracy of the Kramers-like asymptotic approximation from eq. 5.52 can be assessed by directly comparing it with reference numerical calculations. In order to do so, a bi-dimensional two-Gaussian model, characterized by a constant mass-tensor $\boldsymbol{\mu} = m^{-1}\mathbf{I}$, has been considered. In table 5.1 the approximated results, obtained for various variance principal values $\{\sigma_x^2, \sigma_y^2\}$ and tilt angles θ, are compared with the correspondent reference numerical results. The numerical method adopted to compute the reference values will be presented in detail in chapter 6.

Table 5.1: Comparison, for the case of a bi-dimensional two-Gaussian distribution model, between the tunneling splitting E_1^{asy} computed with the Kramers-like asymptotic approximation from eq. 5.52 and the reference value δE_1^{ref} obtained from the direct diagonalization of the shifted Hamiltonian. All the energy quantities have been reported in E_u units according to eq. 5.49 where $\tilde{L} = x_0^-$ and $\tilde{m} = m$. The relative error betweem the estimate is reported in the column marked with ε_{rel}. The square root of the principal variance values are marked with the label σ_x and σ_y while the tilt angle is marked with the label θ. The ΔU column report the mean-field potential barrier height.

σ_x	σ_y	θ	ΔU	$\delta E_1^{\text{asy}}/E_u$	$\delta E_1^{\text{ref}}/E_u$	ε_{rel}
0.4	0.3	0	2.43	0.3552	0.2886	0.23
0.4	0.3	$\pi/6$	2.82	0.2908	0.2305	0.26
0.4	0.3	$\pi/4$	3.31	0.2194	0.1719	0.28
0.3	0.2	0	4.86	0.0780	0.0631	0.23
0.3	0.2	$\pi/6$	5.76	0.0401	0.0324	0.24

As can be seen from such a table a generally poor accuracy characterizes the adopted Kramers-like approximation with a relative error always exceeding the 20% mark. This lack of accuracy, however, is

[6] Please notice how $(\mathbf{v}\otimes\mathbf{w})_{ij} = v_i w_j$ and, as such, the following can be obtained: $(\mathbf{u}\otimes\mathbf{u})_{ij} = u_i u_j = (\mathbf{u}\otimes\mathbf{u})_{ji}$.

not surprising given that the mean-field quadratic expansion, previously adopted in the one-dimensional asymptotic approximation presented in sec. 4.2.3, has already demonstrated its scarce compatibility with two-Gaussian distribution models resulting, usually, in a wrong pre-exponential factor. This interpretation is compatible with the collected data in which a quasi-constant relative error has been observed in the limit of high barriers. This calls for a new asymptotic approach capable of capturing the essence of the two-Gaussian system. This new asymptotic model will be presented and characterized in sec. 5.4.

5.4 An asymptotic approximation for the two-Gaussian model

In order to easily examine how an asymptotic approximation can be obtained for the particular case of a two-Gaussian distribution model, let us introduce a control parameter σ capable of single-handedly control the asymptotic behavior of the system. This can be easily done considering the following alternative parametrization of the multidimensional Gaussian definition from eq. 5.17:

$$G_{\mathbf{\Sigma}}(\mathbf{x}-\mathbf{x}_0) := \frac{1}{\sqrt{(2\pi\sigma^2)^N \det(\mathbf{\Sigma})}} e^{-\frac{1}{2\sigma^2}(\mathbf{x}-\mathbf{x}_0)^T \mathbf{\Sigma}^{-1}(\mathbf{x}-\mathbf{x}_0)} \tag{5.62}$$

that, when adopted into the two-Gaussian-distribution definition from eq. 5.18, allows for the achievement of the asymptotic limit of high barriers by simply adopting small values ($\sigma \to 0$) for the control parameter. Once this novel parametrization of the ground-state model has been set, the correspondent mean-field potential can be obtained, similarly to what presented in eq. 5.19, according to:

$$U(\mathbf{x}) := -\ln\left[\mathcal{Z}\rho_0(\mathbf{x})\right] = -\ln\left[e^{-\frac{1}{2\sigma^2}(\mathbf{x}-\mathbf{x}_0)^T \mathbf{\Sigma}^{-1}(\mathbf{x}-\mathbf{x}_0)} + e^{-\frac{1}{2\sigma^2}(\mathbf{x}-\mathbf{x}_0^R)^T \mathbf{\Sigma}_R^{-1}(\mathbf{x}-\mathbf{x}_0^R)}\right] \tag{5.63}$$

where $\mathcal{Z} = 2\sqrt{(2\pi\sigma^2)^N \det(\mathbf{\Sigma})}$ ensures an adimensional logarithm argument. At this point, let us observe how the origin of the $\mathbf{x}^+$ coordinate system is arbitrary and, as such, can be conveniently set to coincide with the correspondent Gaussian center components $\mathbf{x}_0^+$. Under these circumstances a lighter notation can be adopted where $\mathbf{x}_0^+ = \mathbf{0}$ and, as such, $\mathbf{x}_0 = \mathbf{0}^+ \oplus \mathbf{x}_0^-$.

Starting from these considerations, one can easily verify how the mean-field potential can be expressed according to the relation:

$$U(\mathbf{x}) = U_+(\mathbf{x}) - \ln\left\{\cosh\left[U_-(\mathbf{x})\right]\right\} \tag{5.64}$$

where the $U_\pm(\mathbf{x})$ terms explicitly depends upon the newly introduced control parameter σ and are defined according to:

$$U_+(\mathbf{x}) = U(\mathbf{0}) + \frac{1}{2\sigma^2}(\mathbf{x}^+)^T \mathbf{A}^{++}\mathbf{x}^+ + \frac{1}{2\sigma^2}(\mathbf{x}^-)^T \mathbf{A}^{--}\mathbf{x}^- - \frac{1}{\sigma^2}(\mathbf{x}^+)^T \mathbf{A}^{+-}\mathbf{x}_0^- \tag{5.65}$$

$$U_-(x) = \frac{1}{\sigma^2}(\mathbf{x}^-)^T \mathbf{A}^{--}\mathbf{x}_0^- - \frac{1}{\sigma^2}(\mathbf{x}^+)^T \mathbf{A}^{+-}\mathbf{x}^- \tag{5.66}$$

in which $U(\mathbf{0}) := (\mathbf{x}_0^-)^T \mathbf{A}^{--}\mathbf{x}_0^-/2\sigma^2 - \ln(2)$ represents the mean-field potential value at the origin. Starting from this definition, the mean-field saddle point position $\mathbf{x}_s = (\mathbf{x}_s^+, \mathbf{0})$ can be, once again, computed according to eq. 5.30 and, as such, if a set of coordinates $\delta\mathbf{x} = \mathbf{x} - \mathbf{x}_s$, defining the distance of a given point $\mathbf{x}$ from the mean-field potential saddle-point $\mathbf{x}_s$, is introduced, the following can be observed: $\delta\mathbf{x}^+ = \mathbf{x}^+ - \mathbf{x}_s^+$ while $\delta\mathbf{x}^- = \mathbf{x}^-$. From these results, the following forms for the $U_\pm(\delta\mathbf{x})$ mean-field potential terms can be obtained:

$$U_+(\delta\mathbf{x}) = U(\mathbf{x}_s) + \frac{1}{2\sigma^2}(\delta\mathbf{x}^+)^T \mathbf{A}^{++}\delta\mathbf{x}^+ + \frac{1}{2\sigma^2}(\delta\mathbf{x}^-)^T \mathbf{A}^{--}\delta\mathbf{x}^- \tag{5.67}$$

$$U_-(\delta\mathbf{x}) = \frac{1}{\sigma^2}(\delta\mathbf{x}^-)^T (\mathbf{\Sigma}^{--})^{-1}\mathbf{x}_0^- - \frac{1}{\sigma^2}(\delta\mathbf{x}^+)^T \mathbf{A}^{+-}\delta\mathbf{x}^- \tag{5.68}$$

where $U(\mathbf{x}_s) := (\mathbf{x}_0^-)^T (\mathbf{\Sigma}^{--})^{-1}\mathbf{x}_0^-/2\sigma^2 - \ln(2)$ represents, in perfect analogy with the result presented in eq. 5.31, the mean-field potential value at its saddle-point.

Now that the mean-field potential definition has been rewritten as a function of the displacements $\delta\mathbf{x}$ from the saddle point $\mathbf{x}_s$, the concept of reactive direction $\mathbf{v}^{\mathrm{rc}}$ can be introduced. This quantity represents the direction describing, at the mean-field potential saddle point, the reactive motion of the system and, as such, it must have an anti-symmetric character. To specify the $\mathbf{v}^{\mathrm{rc}}$ reactive coordinate

vector the proper combination of $\delta\mathbf{x}^-$ coordinates needs to be considered. This can be easily done taking inspiration from the linear term in $\delta\mathbf{x}^-$ appearing in eq. 5.68, from which the following reactive direction definition can be adopted:

$$\mathbf{v}^{\mathrm{rc}} := \frac{1}{a}(\boldsymbol{\Sigma}^{--})^{-1}\mathbf{x}_0^- \qquad \text{with} \qquad a := \left|(\boldsymbol{\Sigma}^{--})^{-1}\mathbf{x}_0^-\right| = \sqrt{(\mathbf{x}_0^-)^T(\boldsymbol{\Sigma}^{--})^{-2}\mathbf{x}_0^-} \tag{5.69}$$

where the a term plays the role of normalization factor ensuring that $(\mathbf{v}^{\mathrm{rc}})^T\mathbf{v}^{\mathrm{rc}} = 1$. Once the reactive direction $\mathbf{v}^{\mathrm{rc}} = \mathbf{v}_1$ has been fixed, a correspondent set of non reactive directions $\{\mathbf{v}_2, ..., \mathbf{v}_{N^-}\}$ can also be introduced. Please notice how the symbol N^- has been introduced to indicate the number of ant-symmetric coordinates. This set of vector can be easily defined by invoking the condition of forming, together with the reactive direction, a set $\{\mathbf{v}_i\}$ of orthonormal $\mathbf{v}_i^T\mathbf{v}_j = \delta_{ij}$ basis-vectors for the $\delta\mathbf{x}^-$ coordinate subspace. The newly defined vector set $\{\mathbf{v}_i\}$ represents the most convenient frame in which the asymptotic model can be derived and the corresponding coordinate components $\mathbf{y} = (y_1, y_2, ..., y_{N^-})$, with $y_1 = y_{\mathrm{rc}}$ and $\mathbf{y}^{\mathrm{nr}} = (y_2, ..., y_{N^-})$, can be computed according to $y_i = \mathbf{v}_i^T\delta\mathbf{x}^-$. By adopting this new coordinate set into eqs. 5.67 and 5.68 the following relations can be obtained:

$$\begin{aligned} U_+(\mathbf{y}, \delta\mathbf{x}^+) = U(\mathbf{x}_s) + \frac{1}{2\sigma^2}(\delta\mathbf{x}^+)^T\mathbf{A}^{++}\delta\mathbf{x}^+ + \frac{1}{2\sigma^2}y_{\mathrm{rc}}^2(\mathbf{v}^{\mathrm{rc}})^T\mathbf{A}^{--}\mathbf{v}^{\mathrm{rc}} + \\ + \frac{1}{2\sigma^2}y_{\mathrm{rc}}(\mathbf{v}^{\mathrm{rc}})^T\mathbf{A}^{-\mathrm{nr}}\mathbf{y}^{\mathrm{nr}} + \frac{1}{2\sigma^2}(\mathbf{y}^{\mathrm{nr}})^T\mathbf{A}^{\mathrm{nrnr}}\mathbf{y}^{\mathrm{nr}} \end{aligned} \tag{5.70}$$

$$U_-(\mathbf{y}, \delta\mathbf{x}^+) = \frac{a}{\sigma^2}y_{\mathrm{rc}} - \frac{1}{\sigma^2}y_{\mathrm{rc}}(\mathbf{v}^{\mathrm{rc}})^T\mathbf{A}^{-+}\delta\mathbf{x}^+ - \frac{1}{\sigma^2}(\mathbf{y}^{\mathrm{nr}})^T\mathbf{A}^{\mathrm{nr}+}\delta\mathbf{x}^+ \tag{5.71}$$

where the newly introduced matrices have been defined according to:

$$\mathbf{A}^{\mathrm{nr}+} = \mathbf{B}^{\mathrm{nr}-}\mathbf{A}^{-+} \tag{5.72}$$

$$\mathbf{A}^{-\mathrm{nr}} = \mathbf{A}^{--}\mathbf{B}^{-\mathrm{nr}} = \left(\mathbf{A}^{\mathrm{nr}-}\right)^T \tag{5.73}$$

$$\mathbf{A}^{\mathrm{nrnr}} = \mathbf{B}^{\mathrm{nr}-}\mathbf{A}^{--}\mathbf{B}^{-\mathrm{nr}} \tag{5.74}$$

and the rectangular transformation matrix $\mathbf{B}^{\mathrm{nr}-} = (\mathbf{B}^{-\mathrm{nr}})^T$ has been defined as the matrix having as rows the $\mathbf{v}_i$ vector associated to the non-reactive directions:

$$\mathbf{B}^{\mathrm{nr},-} = \begin{pmatrix} \mathbf{v}_2^T \\ \mathbf{v}_3^T \\ \vdots \\ \mathbf{v}_{N^-}^T \end{pmatrix} \tag{5.75}$$

Starting from the obtained results, it is now possible to examine the asymptotic behavior of the potential and, to fulfill this purpose, a new set of scaled asymptotic coordinates can be conveniently defined according to:

$$y_\infty^{\mathrm{rc}} := \frac{y_{\mathrm{rc}}}{\sigma^2} \qquad \mathbf{y}_\infty^{\mathrm{nr}} := \frac{\mathbf{y}^{\mathrm{rc}}}{\sigma} \qquad \delta\mathbf{x}_\infty^+ := \frac{\delta\mathbf{x}+}{\sigma} \tag{5.76}$$

Taking into account the obtained results and considering the asymptotic limit of $\sigma \to 0$, all the vanishing terms from eqs. 5.70 and 5.71 can be neglected allowing us to write the following expressions:

$$U_+^\infty = U_+(\mathbf{y}_\infty, \delta\mathbf{x}_\infty^+) = U(\mathbf{x}_s) + \frac{1}{2}(\delta\mathbf{x}_\infty^+)^T\mathbf{A}^{++}\delta\mathbf{x}_\infty^+ + \frac{1}{2}(\mathbf{y}_\infty^{\mathrm{nr}})^T\mathbf{A}^{\mathrm{nrnr}}\mathbf{y}_\infty^{\mathrm{nr}} \tag{5.77}$$

$$U_-^\infty = U_-(\mathbf{y}_\infty, \delta\mathbf{x}_\infty^+) = ay_\infty^{\mathrm{rc}} - (\mathbf{y}_\infty^{\mathrm{nr}})^T\mathbf{A}^{\mathrm{nr}+}\delta\mathbf{x}_\infty^+ \tag{5.78}$$

The result just obtained represent the key point of our asymptotic analysis that, differently from the Kramers-like one presented in sec. 5.1, directly derives from the structure of the two-Gaussian model itself. At this point the proper localization function approximation $g^\infty(\mathbf{x})$ can be recovered by solving, in the limit of $\sigma \to 0$, the following equation:

$$\partial_a^\dagger\mu^{ab}e^{-U_+^\infty(\mathbf{x})}\cosh\left[U_-^\infty(\mathbf{x})\right]\partial_b g^\infty(\mathbf{x}) = 0 \tag{5.79}$$

Please notice how this expression represents the equivalent of eq. 5.3 in which the $\psi_0^2(\mathbf{x}) \propto \exp[-U(\mathbf{x})]$ term has been adjusted considering the asymptotic form of eq. 5.64. At this point, considering the definition introduced in eq. 5.76, one can easily obtain the following relations between derivatives components:

$$\frac{\partial}{\partial\mathbf{x}^+} = \frac{1}{\sigma}\frac{\partial}{\partial\delta\mathbf{x}_\infty^+} \qquad \frac{\partial}{\partial x^-} = \frac{1}{\sigma^2}\mathbf{v}^{\mathrm{rc}}\frac{\partial}{\partial y_\infty^{\mathrm{rc}}} + \frac{1}{\sigma}\mathbf{B}^{-\mathrm{nr}}\frac{\partial}{\partial\mathbf{y}_\infty^{\mathrm{nr}}} \tag{5.80}$$

where, in the limit for $\sigma \to 0$, the derivative taken with respect to the reactive coordinate y^{rc} emerges as the leading term and, as such, eq. 5.79 can be simplified according to:

$$\frac{\partial}{\partial y^{\mathrm{rc}}_{\infty}} e^{-U^{\infty}_{+}(\mathbf{y}^{\mathrm{nr}}_{\infty}, \delta\mathbf{x}^{+}_{\infty})} \cosh\left[U^{\infty}_{-}(y^{\mathrm{rc}}_{\infty}, \mathbf{y}^{\mathrm{nr}}_{\infty}, \delta\mathbf{x}^{+}_{\infty})\right] \frac{\partial}{\partial y^{\mathrm{rc}}_{\infty}} g^{\infty}(y^{\mathrm{rc}}_{\infty}, \mathbf{y}^{\mathrm{nr}}_{\infty}, \delta\mathbf{x}^{+}_{\infty}) = 0 \tag{5.81}$$

Observing that, $U^{\infty}_{+}(\mathbf{y}^{\mathrm{nr}}_{\infty}, \delta\mathbf{x}^{+}_{\infty})$ does not depends upon the y^{rc}_{∞} coordinate, the following condition can be easily obtained:

$$\frac{\partial}{\partial y^{\mathrm{rc}}_{\infty}} \cosh\left[U^{\infty}_{-}(y^{\mathrm{rc}}_{\infty}, \mathbf{y}^{\mathrm{nr}}_{\infty}, \delta\mathbf{x}^{+}_{\infty})\right] \frac{\partial}{\partial y^{\mathrm{rc}}_{\infty}} g^{\infty}(y^{\mathrm{rc}}_{\infty}, \mathbf{y}^{\mathrm{nr}}_{\infty}, \delta\mathbf{x}^{+}_{\infty}) = 0 \tag{5.82}$$

that, after applying a simple integration, translates to the form:

$$\frac{\partial}{\partial y^{\mathrm{rc}}_{\infty}} g^{\infty}(y^{\mathrm{rc}}_{\infty}, \mathbf{y}^{\mathrm{nr}}_{\infty}, \delta\mathbf{x}^{+}_{\infty}) \propto \cosh\left[U^{\infty}_{-}(y^{\mathrm{rc}}_{\infty}, \mathbf{y}^{\mathrm{nr}}_{\infty}, \delta\mathbf{x}^{+}_{\infty})\right]^{-1} \tag{5.83}$$

Considering the substitution $y^{\mathrm{rc}}_{\infty} \to z$ where $z := U^{\infty}_{-}(y^{\mathrm{rc}}_{\infty}, \mathbf{y}^{\mathrm{nr}}_{\infty}, \delta\mathbf{x}^{+}_{\infty})$ the previous relation can be rewritten according to:

$$\frac{\partial}{\partial z} g^{\infty}(z) \propto \cosh(z)^{-1} \tag{5.84}$$

that, by simple integration, leads to the wanted localization function approximation:

$$g^{\infty}(z) = \frac{2}{\pi} \int_{0}^{a y^{\mathrm{rc}}_{\infty} - (\mathbf{y}^{\mathrm{nr}}_{\infty})^{T} \mathbf{A}^{\mathrm{nr}+} \delta\mathbf{x}^{+}_{\infty}} \cosh(z)^{-1} dz \tag{5.85}$$

where the proportionality factor has been set to ensure the condition $g(\pm\infty) \to 1$ while the integration limits have been set in order to impart to the localization function the correct inversion symmetry $\hat{R} g(\mathbf{x}^{+}, \mathbf{x}^{-}) = g(\mathbf{x}^{+}, -\mathbf{x}^{-}) = -g(\mathbf{x}^{+}, \mathbf{x}^{-})$. Please notice how, despite the one-dimensional integration applied to obtain eq. 5.85, the localization function still conserves the parametric dependence upon all the coordinate components.

Now that the proper asymptotic approximation of the localization function has been obtained the correspondent ground-state tunneling splitting estimate can easily be obtained according to:

$$\delta E^{\infty}_{1} = \frac{\langle g^{\infty}\psi_0 | \delta\hat{H} | g^{\infty}\psi_0 \rangle}{\langle g^{\infty}\psi_0 | g^{\infty}\psi_0 \rangle} \tag{5.86}$$

where, for sake of simplicity, we will assume to deal with a system well approximated by a coordinate independent mass tensor $\boldsymbol{\mu}$ and a constant G-factor. Invoking the asymptotic limit of low σ values one can neglect the normalization factor that, in the limit of well-localized distributions, assumes unitary value. By adopting the mean-field potential asymptotic approximation $U^{\infty}(\mathbf{x})$ in the definition of the ground state wave function, according to $\psi_0(\mathbf{x})^2 = e^{-U^{\infty}(\mathbf{x})}/\mathcal{Z}$, the following can be easily obtained:[7]

$$\delta E^{\infty}_{1} = \frac{\hbar^2}{2\mathcal{Z}} \left\langle \frac{\partial g^{\infty}}{\partial \mathbf{x}} \boldsymbol{\mu} e^{-U^{\infty}(\mathbf{x})} \frac{\partial g^{\infty}}{\partial \mathbf{x}} \right\rangle = \frac{2\hbar^2}{\pi^2 \mathcal{Z}} \int d\mathbf{x} \frac{\partial U^{\infty}_{-}(\mathbf{x})}{\partial \mathbf{x}} \boldsymbol{\mu} \frac{\partial U^{\infty}_{-}(\mathbf{x})}{\partial \mathbf{x}} \frac{e^{-U^{\infty}_{+}(\mathbf{x})}}{\cosh\left[U^{\infty}_{-}(\mathbf{x})\right]} \tag{5.87}$$

where $\mathcal{Z}$ represents the scale factor introduced in eq. 5.63. At this point, the integration variable can be changed in terms of the proper asymptotic variables $\mathbf{x} \to \{y^{\mathrm{rc}}_{\infty}, \mathbf{y}^{\mathrm{nr}}_{\infty}, \delta\mathbf{x}^{+}_{\infty}\}$ and the following integral expression can be obtained:

$$\delta E^{\infty}_{1} = \frac{2\hbar^2}{\pi^2 \mathcal{Z}} \sigma^{N-3} \int d\delta\mathbf{x}^{+}_{\infty} \int d\mathbf{y}^{\mathrm{nr}}_{\infty} \int dy^{\mathrm{rc}}_{\infty} \frac{e^{-U^{\infty}_{+}(\mathbf{x})}}{\cosh\left[U^{\infty}_{-}(\mathbf{x})\right]} \left[\sigma^4 \frac{\partial U^{\infty}_{-}(\mathbf{x})}{\partial \mathbf{x}} \boldsymbol{\mu} \frac{\partial U^{\infty}_{-}(\mathbf{x})}{\partial \mathbf{x}}\right] \tag{5.88}$$

[7] Please notice how, recalling the definition from eq. 5.85, the following can be obtained:

$$\frac{\partial g^{\infty}(\mathbf{x})}{\partial \mathbf{x}} = \frac{\partial z}{\partial \mathbf{x}} \frac{\partial g^{\infty}(z)}{\partial z} = \frac{2}{\pi} \frac{\partial U^{\infty}_{-}(\mathbf{x})}{\partial \mathbf{x}} \cosh\left[U^{\infty}_{-}(\mathbf{x})\right]$$

Starting from this result, the expression in eq. 5.87 can be easily obtained simply observing how, according to eq. 5.64, the following relation must be verified:

$$e^{-U^{\infty}(\mathbf{x})} = \cosh\left[U^{\infty}_{-}(\mathbf{x})\right] e^{-U^{\infty}_{+}(\mathbf{x})}$$

where the σ^{N+1} factor represents the determinant of the Jacobian matrix associated to the variable transformation. By invoking the asymptotic limit of $\sigma \to 0$ and recalling the relation, presented in eq. 5.80, existing between derivatives components, the following can easily be verified:

$$\lim_{\sigma\to 0}\left[\sigma^4 \frac{\partial U_-^{\infty}(\mathbf{x})}{\partial \mathbf{x}} \boldsymbol{\mu} \frac{\partial U_-^{\infty}(\mathbf{x})}{\partial \mathbf{x}}\right] = a^2 \mu_{\mathrm{rc}} \qquad \text{with} \qquad \mu_{\mathrm{rc}} = (\mathbf{v}^{\mathrm{rc}})^T \boldsymbol{\mu}^{--} \mathbf{v}^{\mathrm{rc}} \tag{5.89}$$

where the newly introduced μ_{rc} terms represents the diffusion coefficient along the reactive coordinate. Taking into account the result from eq. 5.89 into the tunneling splitting estimate from eq. 5.88, the following expression can be recovered:

$$\delta E_1^{\infty} = \frac{2a^2\hbar^2}{\pi^2 \mathcal{Z}} \sigma^{N-3} \mu_{\mathrm{rc}} \int d\delta \mathbf{x}_{\infty}^{+} \int d\mathbf{y}_{\infty}^{\mathrm{nr}}\, e^{-U_+^{\infty}(\mathbf{x})} \int dy_{\infty}^{\mathrm{rc}}\, \frac{1}{\cosh\left[U_-^{\infty}(\mathbf{x})\right]} \tag{5.90}$$

The relation just obtained represents a fundamental result for our asymptotic analysis since, as will be shown in what follows, an analytic solution can be easily obtained. In order to show how this can be done let us consider the last integral that, by simple variable substitution, can be solved according to:

$$\int_{-\infty}^{+\infty} \frac{dy_{\infty}^{\mathrm{rc}}}{\cosh\left[U_-^{\infty}(\mathbf{x})\right]} = \int_{-\infty}^{+\infty} \frac{dy_{\infty}^{\mathrm{rc}}}{\cosh\left[a y_{\infty}^{\mathrm{rc}} - (\mathbf{y}_{\infty}^{\mathrm{nr}})^T \mathbf{A}^{\mathrm{nr+}} \delta \mathbf{x}_{\infty}^{+}\right]} = \frac{1}{a} \int_{-\infty}^{+\infty} \frac{dz}{\cosh(z)} = \frac{\pi}{a} \tag{5.91}$$

Adopting this result in eq. 5.90 and recalling the definition of $U_+^{\infty}(\mathbf{x})$ from eq. 5.77, the following expression can be obtained:

$$\delta E_1^{\infty} = \frac{2a\hbar^2}{\pi \mathcal{Z}} \sigma^{N-3} \mu_{\mathrm{rc}} e^{-U(\mathbf{x}_s)} \int d\delta \mathbf{x}_{\infty}^{+} e^{-\frac{1}{2}(\delta \mathbf{x}_{\infty}^{+})^T \mathbf{A}^{++} \delta \mathbf{x}_{\infty}^{+}} \int d\mathbf{y}_{\infty}^{\mathrm{nr}}\, e^{-\frac{1}{2}(\mathbf{y}_{\infty}^{\mathrm{nr}})^T \mathbf{A}^{\mathrm{nrnr}} \mathbf{y}_{\infty}^{\mathrm{nr}}} \tag{5.92}$$

The integrals appearing in the previous expression can now be solved by simply invoking the definition of normalized Gaussian given in eq. 5.17, from which, the following can be easily obtained:

$$\delta E_1^{\infty} = \frac{2a\hbar^2}{\pi \mathcal{Z}} \mu_{\mathrm{rc}} \sqrt{\frac{(2\pi)^{N-1}}{\det[\mathbf{A}^{++}] \det[\mathbf{A}^{\mathrm{nrnr}}]}} \sigma^{N-3} e^{-U(\mathbf{x}_s)} \tag{5.93}$$

Finally, recalling the definition given for the $\mathcal{Z}$ factor, the following expression can be obtained for the asymptotic tunneling splitting estimate:

$$\delta E_1^{\infty} = \frac{a\hbar^2}{\pi\sigma^3} \mu_{\mathrm{rc}} \sqrt{\frac{\det[\mathbf{A}]}{2\pi \det[\mathbf{A}^{++}] \det[\mathbf{A}^{\mathrm{nrnr}}]}} e^{-U(\mathbf{x}_s)} \equiv \frac{a\hbar^2}{\pi\sigma^3} \mu_{\mathrm{rc}} \sqrt{\frac{\det[\mathbf{A}]}{2\pi \det[\mathbf{A}^{++}] \det[\mathbf{A}^{\mathrm{nrnr}}]}} e^{-\Delta U} \tag{5.94}$$

where the condition $\Delta U = U(\mathbf{x}_s)$ has been invoked to express the tunneling splitting estimate as a function of the barrier height.

The result just obtained demonstrates once again the nice mathematical behavior associated with Gaussian-based ground-state models that, even for multidimensional problems, allow for analytic asymptotic expressions. In the next section, the accuracy of the expression presented in eq. 5.94 will be tested in the case of a simple bi-dimensional double-Gaussian model and its accuracy will be assessed by direct comparison with a numerical reference method.

5.4.1 Results in two-dimensions

In the present section the accuracy associated with the asymptotic result from eq. 5.94 will be verified using, as the test subject, a bi-dimensional two-Gaussian model characterized by a constant mass-tensor $\boldsymbol{\mu} = m^{-1}\mathbf{I}$. A variable set of variance principal values $\{\sigma_x^2, \sigma_y^2\}$ and tilt angles θ have been considered in the model parameterization and the obtained results, together with the numerically computed reference values, are reported in table 5.2. For sake of comparison, all the parameters have been selected to match those adopted in table 5.1 to test the Kramers-like asymptotic model. Once again, the numerical method adopted to compute the reference values will be discussed in detail in chapter 6.

Just by comparing the results shown in such a table with the one obtained from the Kramers-like asymptotic model, one can easily appreciate how, adopting the estimate from eq. 5.94, a more accurate prediction is recovered in the case of small variance principal values. This improved accuracy behavior,

Table 5.2: Comparison between the tunneling splitting E_1^{asy} computed with the asymptotic approximation from eq. 5.94 and the reference value δE_1^{ref} obtained from the direct diagonalization of the shifted Hamiltonian. All the energy quantities have been reported in E_u units according to eq. 5.49 where $\tilde{L} = x_0^-$ and $\tilde{m} = m$. The relative error between the estimate is reported in the column marked with ε_{rel}. The square root of the principal variance values are marked with the label σ_x and σ_y while the tilt angle is marked with the label θ. The ΔU column report the mean-field potential barrier height.

σ_x	σ_y	θ	ΔU	$\delta E_1^{\text{asy}}/E_u$	$\delta E_1^{\text{ref}}/E_u$	ε_{rel}
0.4	0.3	0	2.43	0.3487	0.2886	0.21
0.4	0.3	$\pi/6$	2.82	0.2827	0.2305	0.23
0.4	0.3	$\pi/4$	3.31	0.2105	0.1719	0.22
0.3	0.2	0	4.86	0.0727	0.0631	0.15
0.3	0.2	$\pi/6$	5.76	0.0372	0.0324	0.15

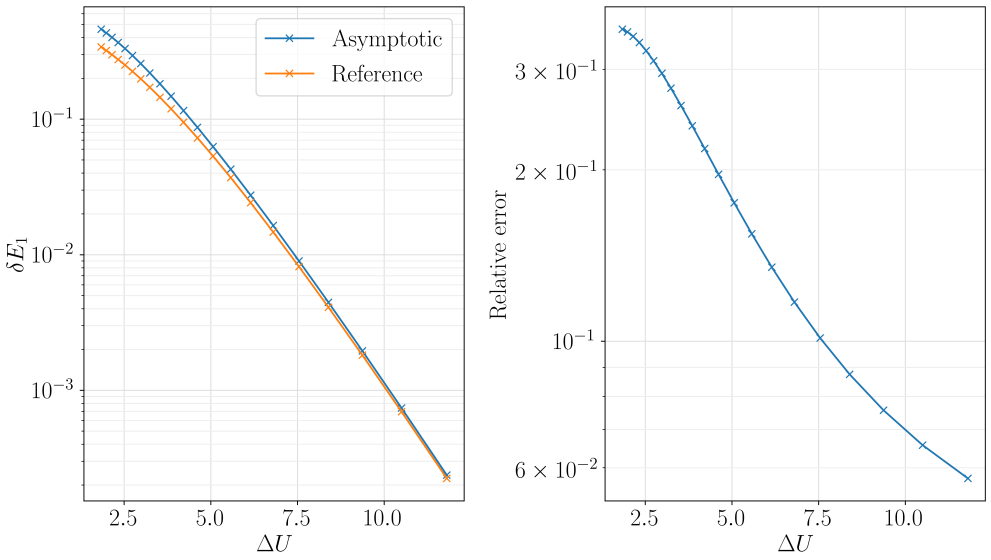

Figure 5.5: Left panel: Comparison between the tunneling splitting estimates obtained from the asymptotic model from eq. 5.94 and the correspondent numerical results, for the case a bi-dimensional two-Gaussian system parametrized by a variable σ_x^2 principal variance value. The results are reported as a function of the mean-field potential barrier height ΔU obtained for the range $\sigma_x/x_0^- = 0.2 - 0.5$. The other parameters have been kept fixed according to $\sigma_y/x_0^- = 0.2$ and $\theta = \pi/6$. Right panel: relative error computed for the asymptotic estimate in respect to the numerical reference.

however, must be discussed with care given that a non-trivial relation seems to exist between the asymptotic limit of low $\boldsymbol{\Sigma}$ principal values and the connected high limit of mean-field potential barriers ΔU. As a matter of fact, one can easily appreciate how changing the barrier height acting only on the tilt angle adopted in the parametrization of the model has a somewhat less pronounced effect on the accuracy than directly acting upon the variance principal-values.

Nevertheless, the data presented in table 5.2 suggest that the newly introduced asymptotic approach presents an overall better asymptotic behavior that, differently from the one presented in eq. 5.52, seems to be capable of recovering the correct pre-exponential factor. In order to further examine this statement, the case of a bi-dimensional two-Gaussian model characterized by a variable σ_x^2 principal value and fixed σ_y^2 and θ parameters has been considered. The asymptotic results obtained for the range $\sigma_x/x_0^- = 0.2-0.5$ with $\sigma_y/x_0^- = 0.2$ and $\theta = \pi/6$ are reported, together with their numerical reference, in figure 5.5. As can be seen from such a figure a monotonic decrease in relative error is observed in the limit of high barriers with an overall error approaching the 5% mark for $\sigma_x = 0.2x_0^-$. Showing how, despite the relatively low accuracy and the slow convergence, the obtained asymptotic model captures the essence of the system behavior in the high barrier limit.

Chapter 6

Numerical solution of the eigenvalue problem

In the previous chapters, the isomorphic relation existing between the Fokker-Planck-Smoluchowski operator and the quantum Hamiltonian has been invoked in order to obtain analytical asymptotic forms capable of approximating, with reasonable accuracy, the tunneling splitting in simple model systems. In this chapter, the problem of developing efficient numerical approaches, in the form of basis-set expansions, to study such problems will be presented. During our analysis we will show how, taking into consideration the results obtained from the asymptotic theory, efficient basis-sets, capable of returning high accuracy estimates, can easily be obtained. The present chapter will be entirely devoted to the explicit study of two-Gaussian distribution models that, due to their mathematical structure, allows for a simple discussion of the problem; nevertheless, most of the presented concepts can be easily adapted in order to study more complex model systems. The chapter is opened by section 6.1 in which the problem of obtaining high efficiency one-dimensional basis-set will be presented. In such a section the advantages deriving from the adoption of a modulated ground-state wave-function as a basis-set template will be discussed and a simple, yet efficient, asymptotically inspired definition will be presented. The chapter is closed by section 6.2 in which the numerical solution of a simple multidimensional problem, in which a single anti-symmetric coordinate is coupled with one or more symmetric ones, will be presented and characterized. As will be discussed, the obtained approach has the potential of producing multidimensional results of high accuracy requiring the sole employment of one-dimensional numerical integration in order to compute the involved matrix elements.

6.1 One-dimensional modulated ground-state basis sets

Whenever the solution of the Hamiltonian eigenvalue problem by expansion over a basis-set is considered, different choices can be made both in terms of the basis-set selection and in terms of the computation technique adopted to evaluate the integral forms involved in the matrix elements definition. In general terms, finding the best procedure for efficiently and accurately solve the problem associated with a given quantum potential is not trivial and little to no *a-priori* indications are usually available for the optimal basis-set selection. If, however, a ground-state model is adopted as the starting point in the definition of the potential profile, one can argue that a clear indication on the most convenient basis-set formulation can be easily obtained just by looking at the Fokker-Planck-Smoluchowski form of the shifted Hamiltonian operator. The expression of such an operator has been defined, for the simple case of a one-dimensional system characterized by a constant mass, in eq. 4.1. Starting from such a definition one can easily appreciate how the basis-set $\{\phi_n\}$, defined according to:

$$\phi_n(x) := \chi_n(x)\psi_0(x) \tag{6.1}$$

results in a simple form for the Hamiltonian matrix element in which the derivative operations can be applied directly to the modulation functions $\chi_n(x)$:

$$\langle\phi_i|\delta\hat{H}|\phi_j\rangle = \frac{\hbar^2}{2m}\int dx\, \frac{\partial\chi_i(x)}{\partial x}\frac{\partial\chi_j(x)}{\partial x}\psi_0(x)^2 \tag{6.2}$$

where the integration by parts has been invoked in order to simplify the integral expression. The corresponding overlap matrix element can, on the other hand, be computed according to:

$$\langle \phi_i | \phi_j \rangle = \int dx\, \chi_i(x)\chi_j(x)\psi_0(x)^2 \tag{6.3}$$

The basis-set definition form eq. 6.1 not only represents a convenient formulation capable of returning a simple form for the matrix elements but it also has the evocative power of connecting the basis-set definition to the concept of fixed-reference localization function $\varphi_{n\pm}(x)$ introduced in eq. 4.58. As a matter of fact, one can easily see how, under the hypothesis of dealing with a set of modulation functions $\{\chi_n\}$ capable of generating a complete set of basis-functions $\{\phi_n\}$, the following expression for the k-th system eigenfunction can be written:

$$\psi_k(x) = \sum_n C_{kn}\phi_n(x) = \psi_0(x)\sum_n C_{kn}\chi_n(x) \equiv \varphi_k(x)\psi_0(x) \tag{6.4}$$

where the symmetry label has been dropped and the notation $\varphi_k(x)$ has been adopted to indicate the fixed-reference localization function associated to the k-th eigenfunction. The obtained result clearly shows how finding the proper expansion coefficients C_{kn} capable of representing the eigenfunction $\psi_k(x)$ on the basis set $\{\phi_n\}$ is equivalent to find the proper combination of modulation functions $\{\chi_n\}$ to represent the corresponding fixed-reference localization function $\varphi_k(x)$. This observation is a powerful element suggesting a way to conveniently define good basis-set parametrizations. Different approaches can be adopted in the definition of an efficient basis-set; these ranges from defining an arbitrary set of model functions capable of mimic the desired behavior, to the modification, driven by the need of obtaining a basis-set capable of capturing local variation ad different distances from the barrier top, of existing localization function models. In the next section, starting from the asymptotic results presented in chapter 4, the latter approach will be presented.

6.1.1 Asymptotically inspired basis set

In the present section, taking inspiration from the mathematical structures of the asymptotic approximations presented in chapter 4, a new, asymptotically justified, basis-set will be presented for the study of a generic two-Gaussian model. This new set of functions will be capable of avoiding some of the shortcomings originated from the asymptotic approximation resulting in more accurate predictions of the system energy spectrum. As it will be discussed, this new basis-set shows good overall performances, resulting in a calculation setup both optimized, due to his origin, to efficiently reproduce the first two excited states ($\psi_1(x) \equiv \psi_{0-}(x)$ and $\psi_2(x) \equiv \psi_{1+}(x)$), and sufficiently flexible to reasonably reproduce excited states of higher order.

Let us start our discussion by recalling the obvious: due to the symmetry of the system, the Hilbert space $\mathcal{H}$ is parted in two sub-spaces $\mathcal{H} = \mathcal{H}_- \oplus \mathcal{H}_+$ containing functions of opposite symmetry that cannot mix under the action of the Hamiltonian operator. This means that two sets of basis functions, one for the odd sub-space $\mathcal{H}_-$ and one for the even one $\mathcal{H}_+$, need to be introduced. In what follows the odd set of functions $\{\chi_n^{\text{odd}}\}$ will be generated starting from the approximated form of the localization function $\varphi_1(x) \equiv \varphi_{0-}(x) \equiv g(x)$ defined in eq. 4.5, while the even set $\{\chi_n^{\text{even}}\}$ will be created adapting the heuristic model for the function $\varphi_2(x) \equiv \varphi_{1+}(x)$ presented in eq. 4.84.

Let us begin our analysis by focusing on the odd subspace that, on the basis of what was just discussed, can be constructed by taking inspiration from the localization function defined in eq. 4.5. Directly adapting such an equation to define a well-behaved basis-set can, however, be quite cumbersome given its piece-wise definition. In order both conserve the spirit of such an approximation and to avoid a complex definition, the following continuous formulation can be introduced:

$$\chi_n^{\text{odd}}(x) := \int_0^x f_n(y)\tilde{\rho}_0(y)^{-1}dy \tag{6.5}$$

where $f_n(x)$ represent a function modulating the integrand behavior while the $\tilde{\rho}_0(x)$ function represent a patched ground-state distribution defined according to:

$$\tilde{\rho}_0(x) := \begin{cases} \rho_0(x) & |x| \leq x_0 \\ \rho_0(x_m) & |x| > x_0 \end{cases} \tag{6.6}$$

Please notice how this last element needs to be introduced, in strong analogy with the analysis proposed in sec. 4.1, in order to ensure that far away from the barrier top the exponential vanishing of the probability distribution $\rho_0(x)$ does not cause the divergence of the integrand in eq. 6.5. Once accepted such a definition for the odd basis set, the choice of $\{f_n\}$ reduces to an action of "function engineering" in which, once granted the completeness of the basis set, one can modulate the definition in order to achieve the fastest convergence of the computed eigenvalues.

In order to discuss a possible approach to the definition of the $\{f_n\}$ function set, let us assume, for illustrative purposes, that the exact solution $\psi_1(x)$ for the first excited state wave-function is known *a-priori*. Under this assumption, the task of reconstructing such a known profile translates to the need of constructing a proper linear combination of functions $\{f_n\}$ capable of reproducing the target function $F(x)$ defined, by simple inversion of the relation 6.5, according to:

$$F(x) = \tilde{\rho}_0(x)\frac{\partial\varphi_1(x)}{\partial x} \tag{6.7}$$

where $\varphi_1(x)$ represent, in this case, the exact fixed-reference localization function profile recovered from the, hypothetically known, first exited state wave-function $\psi_1(x)$. Under these considerations, one can easily see how the $F(x)$ function represents the deviation of the system from his analytical asymptotic approximation and, as such, can have, depending upon the system at hand, significant contributions both near and far from the barrier top. For this reason, a good definition for the set $\{f_n\}$ cannot have a local character and must be able to reproduce the excited states behavior also in regions far away from the origin while avoiding, as much as possible, facing the problem of numerical linear dependence of the set. A well-behaved definition for the $\{f_n\}$ functions set turns out to be the Fourier basis:

$$f_n(x) = \cos(\omega_n x) \quad \text{where} \quad \omega_n = \frac{2\pi n}{\xi x_0} \tag{6.8}$$

in which the parameter ω_n sets the periodicity of the basis set to a length ξ times that of the distance x_0 of the minimum from the origin. The choice of a periodic basis set in order to describe a non-periodic problem can seem quite odd and one can argue that, since the r.h.s. of the relation 6.7 represent a non-periodic function, the discrete Fourier basis set from eq. 6.8 cannot be complete for representing the problem. Undeniably this is formally true but in the evaluation one must take into account that the localizing effect of the patched probability distribution magnifies the $f_n(x)$ function contribution near the origin of the system. This fact, together with the overall exponential decay of the ground state distribution pre-multiplying the definition 6.1, has, when a reasonably large value for ξ is selected, a strong suppressing effect on the spurious replicas generated by the Fourier series expansion of $F(x)$. This allows for an efficient mapping of the $F(x)$ function even when a limited number of basis functions is employed. An example of this is represented in figure 6.1 where a profile of the function $F(x)$, computed numerically by solving the Hamiltonian eigenvalue problem over a set of non-orthogonal Hermite functions, is well reproduced by the combination of a few Fourier basis-functions.

Now that the odd sub-space basis-set has been introduced, let us consider how a basis-set $\{\chi_n^{\text{even}}\}$ for the even sub-space can be defined. In order to do so, let us take inspiration from the heuristic approximation of the $\varphi_2(x) \equiv \varphi_{1+}(x)$ fixed-reference localization function obtained in eq. 4.84. By examining such an expression two contributions can be easily identified: the first one, imparting to the localization function its global profile, is represented by a modulated error-function, while the other one, having the character of local contribution centered at the barrier top, is instead defined as a shifted Gaussian profile. This bipartite structure of the localization function calls for the definition of an equally bipartite basis-set capable of reproducing the aforementioned functional behavior. Focusing our attention onto the error-function portion of the expression, a "primary" set of basis-function, shaping the overall solution profile, can be naturally introduced by extending the error-function term with a power pre-factor:

$$\chi_n^{\text{even},(a)} := x^{2n+1}\text{erf}(\gamma x) \tag{6.9}$$

This choice imparts to the global term in the $\varphi_2(x)$ function the nature of independent contribution to the basis-set definition and, consequently, it has direct effects on the computation of the optimal γ value to be used in the basis-set parametrization. The latter can be naturally obtained neglecting, for the purpose of computing γ, the local term in the fixed-reference localization function definition that, for this reason, reduces to $\varphi_2(x) \propto x\,\text{erf}(\gamma x)$. By considering the Taylor expansion of the correspondent

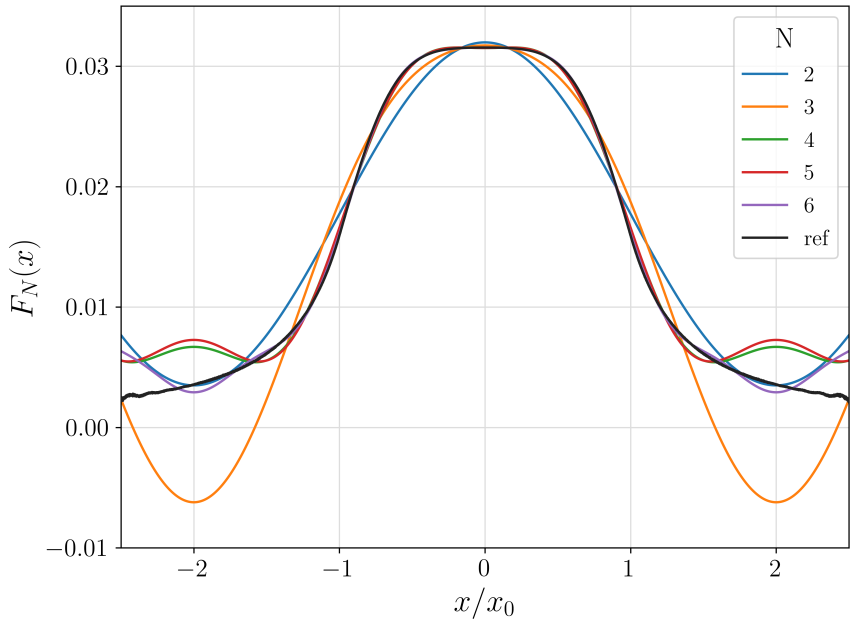

Figure 6.1: Comparison between the numerically computed $F(x)$ function (ref) and its approximated counterparts $F_N(x)$ obtained combining a different number N of Fourier functions for the case of a system defined from a simple two-Gaussian ground-state equilibrium distribution ($\sigma = 0.3x_0$). The periodicity has been set to $\xi = 4$.

$\Phi(x) = \varphi_2'(x)$ function, the following definition of the γ coefficient can be easily obtained:

$$\gamma = \sqrt{\frac{1}{2\sigma^2}\left(\frac{x_0^2}{\sigma^2} - \frac{1}{2}\right)} \tag{6.10}$$

Please notice how the just obtained result differs from the one presented in eq. 4.83 by a factor of $1/\sqrt{2}$. Now that the definition of the "primary" set of basis functions has been presented one can introduce a second "auxiliary" set of functions taking into account the local contribution deriving from the action of the Gaussian term located at the origin. A simple definition of this second set of functions can be obtained by, once again, extending the validity of the Gaussian term with a power modulating factor according to:

$$\chi_n^{\text{even},(b)} := \frac{x^{2n}}{\alpha\sqrt{\pi}}\left[e^{-\alpha^2 x^2} - 1\right] \tag{6.11}$$

Please notice the importance of this "auxiliary" basis-set in capturing local variations of the localization function behavior at the barrier top which has, as suggested by the asymptotic analysis, fundamental importance in determining the tunneling splitting magnitude. Before moving on, one should highlight how these functions constitute a good basis set only if some sort of adjustable offset is included. This problem, obviously connected to the omission of the arbitrary constant derived from taking the origin as the reference point during the integration procedure in eq. 4.84, can be easily fixed including the ground state distribution into the basis set. This operation corresponds indeed to include in the $\{\chi_i\}$ set a constant unitary value that encodes both the exact definition of the ground state and all the necessary offset to be added to the even functions space.

The numerical results obtained from the presented set of asymptotically inspired basis functions will be discussed in detail in section 6.1.3 and compared with reference numerical results obtained from expanding the eigenvalue problem over a set of non-orthogonal Hermite functions. Before doing so, however, some technical aspects concerning the numerical stability of the algorithm must be addressed. These problems, which can be traced back to the existence of numerical linear dependencies between functions of a given basis-set, are omnipresent when dealing with non-orthogonal basis-set and, as such, are an attribute also of the just-introduced asymptotically inspired function sets. This issue will be discussed in section 6.1.2 where the standard procedure of canonical orthogonalization will be introduced.

6.1.2 Managing numerical instability

As demonstrated in appendix B, whenever a non-orthogonal basis-set is employed in the expansion of a generic quantum Hamiltonian $\hat{H}$, the following generalized eigenvalue problem needs to be solved:

$$\mathbf{HC} = \mathbf{SC\Lambda} \tag{6.12}$$

where the symbol $\mathbf{C}$ has been used to represent the coefficient matrix, obtained ordering by columns the eigenvectors of the systems, $\mathbf{\Lambda}$ represents the diagonal matrix having as diagonal elements the ordered set of eigenvalues, while $\mathbf{H}$ and $\mathbf{S}$ represent the Hamiltonian and overlap matrices whose elements are defined according to:

$$H_{ij} = \langle \phi_i | \hat{H} | \phi_j \rangle \qquad S_{ij} = \langle \phi_i | \phi_j \rangle \tag{6.13}$$

Many strategies can be adopted to solve the problem in eq. 6.12 whose aim is, in essence, that of removing the dependence of the problem upon the overlap matrix $\mathbf{S}$; converting eq. 6.12 into a regular eigenvalue problem.

Despite the formal simplicity of such a mathematical transformation, different issues appear when the problem is considered from a numerical standpoint resulting often in numerically unstable algorithms. This instability issues stem from the fact that, whenever a number is represented on a digital computer, a finite binary representation of it needs to be adopted in order to map the number itself onto the computational hardware. This limits the precision with which the number can be represented and, in simple approximated terms, gives to the user a limited number of available digits. Often this representation error has a negligible impact on the outcome of a calculation but in some situations, it can play a substantial role. In order to make an example of this, let us consider the case in which the difference between two very similar numbers, sharing most of their digits, is considered. Whenever this operation is performed most of the available digits cancel out leaving, as the calculating outcome, a representation of the result with an highly reduced intrinsic precision. This kind of error, together with the truncation applied to the representation of the matrix elements, reduces the ability of many numerical algorithms in generating orthogonal basis-vector from a set of closely related non-orthogonal basis-functions inducing, as a consequence, the problem of numerical linear-dependence of the basis set.

Different techniques can be applied to the mitigation of such a numerical problem; these ranges from the brute-force approach of working with a Gram-Schmidt process implemented using an arbitrary precision numerical library, to more refined numerical algorithm as the canonical orthogonalization procedure [53] or the pivoted Cholesky decomposition approach [54]. In what follows the canonical orthogonalization procedure, widely use in the context of quantum chemistry calculation, will be described. Such a procedure has been successfully employed throughout this thesis, whenever a non-orthogonal basis set has been used, returning well-behaved sets of eigevalues.

In order to discuss how the canonical orthogonalization procedure works, let us start by observing how the overlap matrix $\mathbf{S}$ is Hermitian and, as such, can be diagonalized by a unitary matrix $\mathbf{U}$. Indicating with $\mathbf{\Lambda}_s$ the diagonal matrix containing the overlap matrix eigenvalues, the following can be written:

$$\mathbf{U}^\dagger \mathbf{S} \mathbf{U} = \mathbf{\Lambda}_s \tag{6.14}$$

Starting from these considerations, a new transformation matrix $\mathbf{Q}$ can be introduced according to:

$$\mathbf{Q} = \mathbf{U} \mathbf{\Lambda}_s^{-1/2} \tag{6.15}$$

The columns of this newly defined matrix are represented by the eigenvectors of the $\mathbf{S}$ matrix divided by the square root of the correspondent eigenvalues. Please notice how such a matrix responds to the relation:

$$\mathbf{Q}^\dagger \mathbf{S} \mathbf{Q} = \mathbf{\Lambda}_s^{-1/2} \mathbf{U}^\dagger \mathbf{S} \mathbf{U} \mathbf{\Lambda}_s^{-1/2} = \mathbf{\Lambda}_s^{-1/2} \mathbf{\Lambda}_s \mathbf{\Lambda}_s^{-1/2} = \mathbf{I} \tag{6.16}$$

where the property $\mathbf{\Lambda}_s^\dagger = \mathbf{\Lambda}_s$ has been invoked. Now that the $\mathbf{Q}$ matrix has been introduced, one can speculate on how the numerical precision may impact its components. In order to discuss such a question, one may observe how the eigenvalues of the overlap matrix $\mathbf{S}$ may fall in a wide rage of values in which the smaller ones have, due to their role of fraction denominator, the strongest impact on the matrix elements of $\mathbf{Q}$. These small values, more likely originated from the subtraction of similar numbers during the numerical procedure used to diagonalize the overlap matrix, can, on the base of their magnitude, be

selectively neglected in order to ensure numerical stability. In practical terms, a new reduced rectangular matrix $\tilde{\mathbf{Q}}$ can be defined by neglecting the columns of $\mathbf{Q}$ correspondent to eigenvalue smaller than a given threshold [53]. Once this has been done, a new reduced coefficient matrix $\tilde{\mathbf{C}}$ can be indirectly introduced according to:

$$\mathbf{C} = \tilde{\mathbf{Q}}\tilde{\mathbf{C}} \tag{6.17}$$

Substituting the just obtained definition in eq. 6.12 the following can be obtained:

$$\mathbf{H}\tilde{\mathbf{Q}}\tilde{\mathbf{C}} = \mathbf{S}\tilde{\mathbf{Q}}\tilde{\mathbf{C}}\mathbf{\Lambda} \tag{6.18}$$

Multiplying both sides of the previous equation by $\tilde{\mathbf{Q}}^\dagger$ it is simple to obtain:

$$\tilde{\mathbf{Q}}^\dagger\mathbf{H}\tilde{\mathbf{Q}}\tilde{\mathbf{C}} = \tilde{\mathbf{Q}}^\dagger\mathbf{S}\tilde{\mathbf{Q}}\tilde{\mathbf{C}}\mathbf{\Lambda} \tag{6.19}$$

At this point, by observing how the property from eq. 6.16 holds also in the case of the reduced matrix $\tilde{\mathbf{Q}}$, one can easily see how the contribution of the overlap matrix $\mathbf{S}$ vanishes and, consequently, how the following relation, representing the eigenvalue problem associated to the $\tilde{\mathbf{H}} = \tilde{\mathbf{Q}}^\dagger\mathbf{H}\tilde{\mathbf{Q}}$ matrix, can be easily obtained:

$$\tilde{\mathbf{H}}\tilde{\mathbf{C}} = \tilde{\mathbf{C}}\mathbf{\Lambda} \tag{6.20}$$

As anticipated before, the canonical orthogonalization allowed us to convert the generalized eigenvalue problem, expressed by the $\mathbf{H}$ and $\mathbf{S}$ matrices, into a regular eigenvalue problem based on the newly defined $\tilde{\mathbf{H}}$ matrix. By diagonalizing the latter the eigenvalues matrix $\mathbf{\Lambda}$ of the original problem can be directly computed while the correspondent eigenvectors matrix $\mathbf{C}$ can be obtained from the $\tilde{\mathbf{C}}$ by simply invoking eq. 6.17.

6.1.3 One-dimensional results

In order to evaluate the accuracy of the asymptotically inspired basis-set presented in sec. 6.1.1 a two-Gaussian distribution model, defined according to eq. 4.19, has been considered in the case of a variable σ/x_0 value. Reference values for the energy levels of the system have been computed numerically by solving the Hamiltonian eigenvalue problem by expansion over a set of non-orthogonal, numerically optimized, Hermite functions centered both at the maximum and at the minimum of the potential. In order to check for convergence of the reference method, up to 100 function at the origin and 100 couples of functions on the minima have been considered. The converged numerical results for the first two excited states of the odd subspace are compared in table 6.1 with the result obtained from the asymptotically inspired basis set. The same comparison for the even subspace is presented instead in table 6.2. In order to perform both the reference calculations and the ones based on the asymptotically inspired basis set, the canonical orthogonalization procedure, described in sec. 6.1.2, has been followed and all vectors corresponding to overlap eigenvalues smaller than 10^{-10} have been discarded.

Table 6.1: Numerical estimates for the energy of the first two excited states of the odd subspace in the case of a two-Gaussian distribution model with a variable σ/x_0 parameter. N indicates the number of asymptotically inspired basis functions and ξ their periodicity. The ε_{rel} column contains the relative errors of the asymptotically inspired estimates (Asy.) in respect to the reference ones (Ref.). All the energy quantities are represented in E_u units according to eq. 4.18.

σ/x_0	N	ξ	$\delta E_1/E_u$			$\delta E_3/E_u$		
			Asy.	Ref.	ε_{rel}	Asy.	Ref.	ε_{rel}
0.2	20	4	$2.23812 \cdot 10^{-4}$	$2.23814 \cdot 10^{-4}$	$-5.4 \cdot 10^{-6}$	$2.50050 \cdot 10^{1}$	$2.50049 \cdot 10^{1}$	$3.0 \cdot 10^{-6}$
0.3	20	6	$6.3144790 \cdot 10^{-2}$	$6.3144789 \cdot 10^{-2}$	$1.9 \cdot 10^{-8}$	$1.16278 \cdot 10^{1}$	$1.16277 \cdot 10^{1}$	$2.6 \cdot 10^{-6}$
0.4	20	6	$2.8861843 \cdot 10^{-1}$	$2.8861842 \cdot 10^{-1}$	$4.0 \cdot 10^{-8}$	4.600853	7.600849	$5.5 \cdot 10^{-7}$
0.5	20	6	$4.7625860 \cdot 10^{-1}$	$4.7625858 \cdot 10^{-1}$	$4.7 \cdot 10^{-8}$	5.671373	5.671370	$6.4 \cdot 10^{-7}$

Looking at the data reported in tabs. 6.1 and 6.2 one can clearly appreciate the high accuracy characterizing the estimates obtained from the asymptotically inspired basis-set even when a small number of basis-functions is considered. As can be seen from examining the results obtained, the asymptotic nature of the basis-set is clearly visible and directly translates to a better accuracy when higher potential energy barriers ($\sigma \to 0$) are involved. This observation becomes even more interesting if the estimate for the first excited state energy is considered. As can be seen by looking at tab. 6.1, for $\sigma = 0.2x_0$

Table 6.2: Numerical estimates for the energy of the first two excited states of the even subspace in the case of a two-Gaussian distribution model with a variable σ/x_0 parameter. The N columns contains the composition of the basis set in the form $N_a : N_b : 1$ where N_a represent the maximum order of the functions from eq. 6.9, N_b the maximum order of the functions form eq. 6.11 and 1 recalls that the ground state wave-function is also included in the basis-set. The ε_{rel} column contains the relative errors of the asymptotically inspired estimates (Asy.) in respect to the reference ones (Ref.). All the energy quantities are represented in E_u units according to eq. 4.18.

σ/x_0	N	$\delta E_2/E_u$			$\delta E_4/E_u$		
		Asy.	Ref.	ε_{rel}	Asy.	Ref.	ε_{rel}
0.2	3:3:1	$2.500002021 \cdot 10^1$	$2.500002018 \cdot 10^1$	$1.2 \cdot 10^{-9}$	$5.0000898 \cdot 10^1$	$5.0000896 \cdot 10^1$	$4.8 \cdot 10^{-8}$
0.3	5:4:1	$1.11230 \cdot 10^1$	$1.11229 \cdot 10^1$	$2.6 \cdot 10^{-6}$	$2.2421 \cdot 10^1$	$2.2420 \cdot 10^1$	$4.6 \cdot 10^{-6}$
0.4	5:5:1	6.334541	6.334535	$8.3 \cdot 10^{-7}$	$1.32424 \cdot 10^1$	$1.32423 \cdot 10^1$	$2.6 \cdot 10^{-6}$
0.5	5:5:1	4.181673	4.181668	$1.3 \cdot 10^{-6}$	9.09179	9.09176	$3.4 \cdot 10^{-6}$

the asymptotically inspired basis-set returns, for such a state, an energy estimate lower than the one computed by the reference method. Considering that the first excited state represents the ground-state of the odd subspace and, as such, it must be subject to the variational theorem, one can easily conclude how the value produced by the asymptotically inspired basis-set emerges as the more accurate. This evidence points to the asymptotic basis-set as the natural reference for calculation performed in the limit of high barriers.

As can be expected the accuracy of the energy estimation and the subsequent basis-set dimension depends upon the energy of the state considered. In general terms, the higher the order of the target state considered the lower intrinsic accuracy must be expected and, as such, a larger basis set must be employed to obtain good convergence. This, however, depending upon the system configuration, can have effects on the numerical stability of the algorithm with the general behavior being that higher-order basis-function are often more prone to induce numerical linear dependence issues. Looking at the number of functions discarded during the canonical orthogonalization procedure can be a good meter to judge the numerical stability of the protocol. By looking at such an element more in detail one can verify how the even space seems to encounter the limit of numerical linear dependence faster than the odd one. This, however, impacts the accuracy only marginally given that, on the basis of what has been observed in table 6.2, a few basis functions are enough to reach a quite accurate result for the first two states of such a sub-space. Before moving on, another practical aspect needs to be stressed: the choice of the periodicity parameter ξ is critical and has a strong impact on the basis-set completeness. There is no exact recipe to chose such a value however a sensible choice, joined with the variational character of the first eigenvalue, is usually sufficient, as far as we had verified, to obtain fast convergence to the correct value.

Now that we demonstrated how both sets of functions are capable of reproducing the proper eigenvalues with high accuracy, let us move our attention on the characterization of the convergence performances of the newly introduced sets of functions. In the case of the odd basis-set, such information can be easily grasped by looking at the plot reported in figure 6.2. In such a graph the final energy value for the first excited state δE_1, computed employing the largest basis set of 20 functions, is used as a reference to evaluate the relative error associated with the estimates obtained from each examined basis-set dimension. Please notice how this way of looking at the data expresses only a relative information based on the underlying assumption that the last value must represent, since referred to the largest basis set, the best approximation of the true value in the succession of data. Looking at such a plot it can be clearly seen how the convergence of the method improves with the increasing of the potential energy barrier as one can expect from its asymptotic origin. The reader will surely note how this is exactly opposite to what is usually expected when expanding the Hamiltonian eigenvalue problem on a typical basis set, e.g. Hermite functions, where a higher potential energy barrier usually imply a fast varying solution that needs a larger basis set to be properly reproduced.

The study of the convergence in the case of the even set of functions is a little more complex given the fact that having a bipartite set of functions requires the discussion of the overall convergence in terms of the number of functions considered for each sub-set. For sake of simplicity let us adopt a simplified representation of the data in which only the best function combination for each overall basis-set dimen-

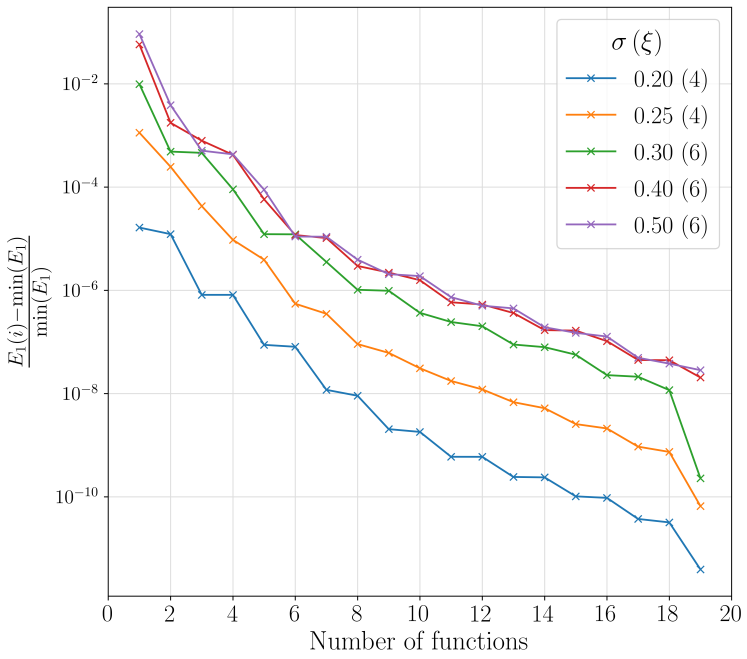

Figure 6.2: Relative error on the first excited state eigenvalue computed by a set of variable dimension in respect to the value produced by a set of 20 basis functions. The value of the σ/x_0 parameter, together with the periodicity ξ, are reported in the legend.

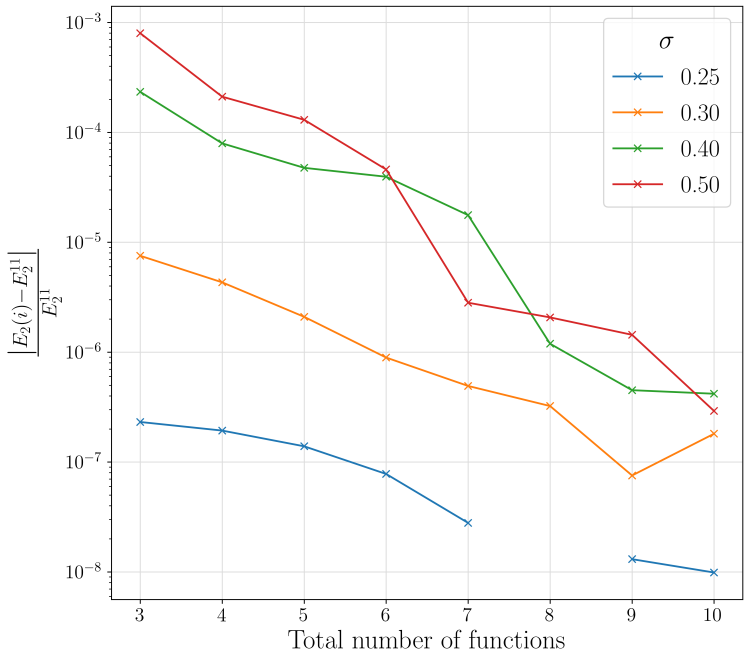

Figure 6.3: Minimum absolute relative error for the second excited state eigenvalue $E_2(n)$ computed using a composite functions-set of variable dimension n in respect to the limit converged result E_2^{11} produced by a set of 11 basis functions. The value of the σ/x_0 parameter is reported in the legend. The missing points in the graph represent values having relative errors smaller than 10^{-10}.

sion will be considered. In such a calculation a maximum of 5 functions defined according to eq. 6.9 and 5 functions defined according to eq. 6.11, have been used to compose, together with the ground-state wave-function, a basis-set of variable dimension. All the functions, up to the defined order, have been

included and the best eigenvalue estimation for each basis-set dimension has been reported in figure 6.3. As can be easily seen, the same considerations already discussed for the odd subspace are valid also for the even one, with the latter being generally more precise in the limit of small-basis sets and showing an overall slower convergence.

Now that the accuracy and convergence characteristics of the newly introduced basis-set have been discussed such a function-set can be applied to the solution of more complex problems. In the next section, the problem of a multidimensional two-Gaussian system in which a single anti-symmetrical coordinate is coupled to one or more symmetrical ones will be considered and we will show how good accuracy estimates can be easily obtained starting from the one-dimensional results presented in this section.

6.2 Numerical approach to simple multidimensional systems

The numerical analysis of multidimensional systems through the use of the expansion onto a basis-set is a challenging task requiring many conditions to be satisfied in order to obtain a scalable protocol capable of returning accurate results. Two main issues hinder the application of this technique: the first one is represented by the basis-set definition, which must be carefully chosen in order to both ensure fast convergence, with the employment of a manageable basis-set size, and impart numerical stability to the algorithm itself. The second one, not independent from the first one, is represented by the computation of the matrix elements which should, when possible, avoid the calculation of computationally expensive multidimensional integrals.

In this section, working under the simple assumption of dealing with a system characterized by a single anti-symmetrical coordinate x coupled to a set $\mathbf{y}$ of one or more symmetric coordinates, a simple numerical protocol will be developed in order to solve the eigenvalue problem associated to the multidimensional two-Gaussian distribution model defined in eq. 5.18. Starting from this assumption we will demonstrate how, under the only hypothesis of dealing with a constant mass tensor $\boldsymbol{\mu}$ and G factor, the mathematical structure of the two-Gaussian model can be exploited in order to obtain simple overlap and Hamiltonian matrix elements expressions, involving only the numerical evaluation of one-dimensional integrals. A simple composite basis-set will be introduced to this purpose with the asymptotically inspired basis sets, discussed in sec. 6.1.1, playing the role of function-set for the reactive coordinate. In section 6.2.1 this approach will be tested in the case of a simple bi-dimensional system allowing us to give to the reader a better insight into the origin of the numerical reference values presented in chapter 5 to discuss the development of multidimensional asymptotic theories.

In order to show how the anticipated results can be obtained, let us start our discussion by observing how, under the conditions described in the previous paragraph, the shifted quantum Hamiltonian can be written according to the form:

$$\delta\hat{H} = -\frac{\hbar^2}{2}\rho_0(\mathbf{q})^{-\frac{1}{2}}\frac{\partial}{\partial\mathbf{q}}^T\boldsymbol{\mu}\rho_0(\mathbf{q})\frac{\partial}{\partial\mathbf{q}}\rho_0(\mathbf{q})^{-\frac{1}{2}} \tag{6.21}$$

where the coordinate vector $\mathbf{q} = (x, \mathbf{y})$ has been introduced to describe the configuration of the system. Similarly to what done in chapter 5, let us indicate with $\mathbf{R}$ the matrix representation of the symmetry operator, such that: $\mathbf{Rq} = \mathbf{R}(x, \mathbf{y}) = (-x, \mathbf{y})$. At this point, given the translational invariance of the problem, the center of the two Gaussian functions can be assumed as the zero of the symmetric set of coordinates and, as such, once the center $\mathbf{q}_0 = (x_0, \mathbf{0})$ of one of the two functions has been defined, the position of the other can be easily obtained according to $\mathbf{Rq}_0 = -\mathbf{q}_0$. Under these assumptions, the definition from eq. 5.18 can be written in compact form according to:

$$\rho_0(\mathbf{q}) = \frac{1}{2\sqrt{(2\pi)^N \det\{(\boldsymbol{\Sigma})\}}}\sum_{s=\pm1} e^{-\frac{1}{2}\delta\mathbf{q}_s^T\boldsymbol{\Sigma}_s^{-1}\delta\mathbf{q}_s} \tag{6.22}$$

in which the subscript s discriminates between the left and right Gaussian functions according to: $\boldsymbol{\Sigma}_1 = \boldsymbol{\Sigma}_R$, $\boldsymbol{\Sigma}_{-1} = \boldsymbol{\Sigma}$ and $\delta\mathbf{q}_s = \mathbf{q} + s\mathbf{q}^0$. If now, similarly to what already done in eq. 5.21, the matrices $\mathbf{A}_s := \boldsymbol{\Sigma}_s^{-1}$ are introduced; their partition into blocks, acting on different types of coordinates, can be defined as follows:

$$\mathbf{A}_s = \begin{pmatrix} A_{0,0} & \mathbf{a}_s^T \\ \mathbf{a}_s & \mathbf{A}^{(1,1)} \end{pmatrix} \tag{6.23}$$

By invoking the definition of the inverse of a block matrix, presented in appendix E, it is simple to obtain:

$$\delta\mathbf{q}_s^T\boldsymbol{\Sigma}_s^{-1}\delta\mathbf{q}_s = \delta\mathbf{y}_s^T\mathbf{A}^{(1,1)}\delta\mathbf{y}_s + \frac{\delta x_s^2}{\sigma_r^2} \tag{6.24}$$

in which the following definitions have been introduced:

$$\delta x_s := x + sx^0 \tag{6.25a}$$

$$\delta\mathbf{y}_s := \mathbf{y} + \delta x_s \left(\mathbf{A}^{(1,1)}\right)^{-1}\mathbf{a}_s \tag{6.25b}$$

$$\sigma_r^2 := (\boldsymbol{\Sigma}_{0,0})^{-1} = \left[\mathbf{A}_{0,0} - \mathbf{a}_s^T\left(\mathbf{A}^{(1,1)}\right)^{-1}\mathbf{a}_s\right]^{-1} \tag{6.25c}$$

Please notice how, given the diagonal nature of the reflection matrix and the fact that the only reflected coordinate is represented by the reactive one, only the block $\mathbf{a}_s$ and its transpose $\mathbf{a}_s^T$ are affected by the index s. Please notice how the result in equation 6.24 has the fundamental effect of splitting the probability distribution into two parts: one depending upon the newly introduced "reactive coordinate" δx_s and one defined on the basis of the newly defined "coupled" ones $\delta\mathbf{y}_s$. This feature will be the key for obtaining matrix elements for the multidimensional problem whose calculation, as anticipated, will require only one-dimensional numerical integration.

At this point, in order to fully use the advantages deriving form the mathematical structure of the two-Gaussian distribution model and from the form of the shifted Hamiltonian, the composite basis set $\{\varphi_{\mathbf{k}}\}$ can be considered:

$$\varphi_{\mathbf{k}}(x,\mathbf{y}) = \rho_0(x,\mathbf{y})^{\frac{1}{2}}\chi_{k_0}(x)\prod_{i=1}^{N-1} y_{i-1}^{k_i} \tag{6.26}$$

in which $\mathbf{k} = (k_0, k_1, ..., k_{N-1})$ represent the labels vector uniquely individuating each basis-function while $\{\chi_i\}$ represents a set of modulating functions for the reactive coordinate. In what follows the asymptotically inspired sets of modulation functions, defined in sec. 6.1.1, will be adopted to fulfill such a role. The set of functions defined in equation 6.26 is clearly not-orthogonal and therefore, in order to compute the energy spectrum of the system, a generalized eigenvalue problem must be solved. In order to do so, the elements of the the overlap matrix $S_{\mathbf{k},\mathbf{k}'}$ and those of the Hamiltonian matrix $\delta H_{\mathbf{k},\mathbf{k}'}$ need to be computed. Starting from the structure of shifted Hamiltonian presented in equation 6.21, the latter can be written as:

$$\delta H_{\mathbf{k},\mathbf{k}'} = -\frac{\hbar^2}{2}\int dx \int d\mathbf{y}\,\chi_{k_0}(x)\prod_{i=1}^{N-1} y_{i-1}^{k_i}\frac{\partial}{\partial\mathbf{q}}^T\boldsymbol{\mu}\rho_0(x,\mathbf{y})\frac{\partial}{\partial\mathbf{q}}\left[\chi_{k_0'}(x)\prod_{i=1}^{N-1} y_{i-1}^{k_i'}\right] \tag{6.27}$$

Integrating by parts and recalling the properties of the mass-matrix it is easy to rewrite the matrix element expression in the following form:

$$\begin{aligned}\delta H_{\mathbf{k},\mathbf{k}'} = \frac{\hbar^2}{2}\mu_{0,0}\int dx\,\frac{\partial\chi_{k_0}(x)}{\partial x}\frac{\partial\chi_{k_0'}(x)}{\partial x}\int d\mathbf{y}\,\rho_0(x,\mathbf{y})\prod_{i=1}^{N-1} y_{i-1}^{k_i+k_i'} + \\ + \frac{\hbar^2}{2}\sum_{n=1}^{N-1}\sum_{m=1}^{N-1} k_n k_m'\mu_{n,m}\int dx\,\chi_{k_0}(x)\chi_{k_0'}(x)\int d\mathbf{y}\,\rho_0(x,\mathbf{y})\prod_{i=1}^{N-1} y_{i-1}^{k_i+k_i'-\delta_{i,n}-\delta_{i,m}}\end{aligned} \tag{6.28}$$

Now that this expression has been obtained, let us stop for a moment to examine the structure of the overlap matrix element:

$$S_{\mathbf{k},\mathbf{k}'} = \int dx\,\chi_{k_0}(x)\chi_{k_0'}(x)\int d\mathbf{y}\,\rho_0(x,\mathbf{y})\prod_{i=1}^{N-1} y_{i-1}^{k_i+k_i'} \tag{6.29}$$

As can be easily seen, the expressions in equation 6.28 and 6.29 have in common the same structure for the integral on the $\mathbf{y}$ coordinates. This fact represents the key advantage of this calculation procedure since, as will be demonstrated in the following paragraph, this integral can be computed analytically leaving only the integral over the reactive coordinate x to be computed numerically.

In order to show how the analytical integration can be carried out, let us consider the general integral form:

$$I(\mathbf{m}) = \int d\mathbf{y}\, \rho_0(x, \mathbf{y}) \prod_{i=0}^{N-2} y_i^{m_i} \tag{6.30}$$

where the symbol $\mathbf{m} = (m_0, m_1, ..., m_{N-2})$ has been introduced to indicate the vector whose elements represent the exponent to which each y_i coordinate needs to be elevated to. Recalling, at this point, the TGD definition given in equation 6.22 it is possible, by simple substitution, to obtain the following expression:

$$I(\mathbf{m}) = \frac{1}{2\sqrt{(2\pi)^N \det\{\mathbf{\Sigma}\}}} \sum_{s=\pm 1} e^{-\frac{\delta x_s^2}{2\sigma_r^2}} I_s(\mathbf{m}) \qquad \text{with} \qquad I_s(\mathbf{m}) = \int d\mathbf{y}\, e^{-\frac{1}{2}\delta\mathbf{y}_s^T \mathbf{A}^{(1,1)} \mathbf{y}_s} \prod_{i=0}^{N-2} y_i^{m_i} \tag{6.31}$$

By considering the matrix $\mathbf{V}$, representing the orthogonal transformation matrix that diagonalizes the $\mathbf{A}^{(1,1)}$ into the matrix $\mathbf{\Lambda} = \mathbf{V}^T \mathbf{A}^{(1,1)} \mathbf{V}$, a new integration variable $\mathbf{z} = \mathbf{V}^T \delta\mathbf{y}_s$ can be introduced. By adopting such a substitution, the dependence of the integral upon the label s can be written in explicit form and, as such, the subscript s can be dropped from the integration variable, allowing us to write:

$$I_s(\mathbf{m}) = \det\{\mathbf{V}\} \int d\mathbf{z}\, e^{-\frac{1}{2}\mathbf{z}^T \mathbf{\Lambda} \mathbf{z}} \prod_{i=0}^{N-2} \left\{ \sum_{j=0}^{N-2} V_{i,j} z_j - \delta x_s \left[\left(\mathbf{A}^{(1,1)} \right)^{-1} \mathbf{a}_s \right]_i \right\}^{m_i} \tag{6.32}$$

The intricate mathematical structure obtained should not hide the fact that, with the applied transformations, we have generated a diagonal exponent. This means that, with a little algorithmic exercise, it is possible to convert the product of sums exponentiation in the sum of products of coordinates elevated to the proper exponents:

$$\prod_{i=0}^{N-2} \left\{ \sum_{j=0}^{N-2} V_{i,j} z_j - \delta x_s \left[\left(\mathbf{A}^{(1,1)} \right)^{-1} \mathbf{a}_s \right]_i \right\}^{m_i} = \sum_{\mathbf{p} \in \mathbb{P}} \eta_s(\mathbf{p}) \delta x_s^{p_0} \prod_{k=1}^{N-1} (\mathbf{z}_s)_{k-1}^{p_k} \tag{6.33}$$

these exponents are hereafter organized in the $\mathbf{p} = (p_0, p_1, ..., p_{N-1})$ vectors belonging to the space $\mathbb{P}$ of "valid" exponents that, in turn, is set by the order vector $\mathbf{m}$. The coefficient of each term is generated by the function $\eta_s(\mathbf{p})$ whose values are produced by the previously mentioned algorithmic procedure. Applying the relation 6.33 to the definition 6.32 it is possible to obtain:

$$I_s(\mathbf{m}) = \det\{\mathbf{V}\} \sum_{\mathbf{p}} \eta_s(\mathbf{p}) \delta x_s^{p_0} \prod_{k=0}^{N-2} \int dz_k\, z_k^{p_{k+1}} e^{-\frac{1}{2}\lambda_k z_k^2} \tag{6.34}$$

in which we introduced the notation $\lambda_k = \mathbf{\Lambda}_{k,k}$. The obtained equation can be further simplified considering that whenever a odd number is present in the exponent vector $\mathbf{p}$ the correspondent integral in the product must vanish due to parity. Consequently the summation can be limited to the subset of vector $\mathbf{p} \in \mathbb{P}_{\text{even}} \subset \mathbb{P} \iff \forall p_i \in \mathbf{p} : p_i \bmod 2 = 0$ having only even components. Considering the general relation:

$$\int_{-\infty}^{+\infty} dz\, z^p e^{-\frac{1}{2}\lambda z^2} = \sqrt{\frac{2\pi}{\lambda^{p+1}}} (p-1)!! \tag{6.35}$$

It is possible to conclude that:

$$I_s(\mathbf{m}) = \sqrt{(2\pi)^{N-1}} \det\{\mathbf{V}\} \sum_{\mathbf{p}} \eta_s(\mathbf{p}) \delta x_s^{p_0} \prod_{k=0}^{N-2} \frac{(p_{k+1}-1)!!}{\sqrt{\lambda_k^{p_{k+1}+1}}} \tag{6.36}$$

The substitution of this result in equation 6.31 allows one to obtain an explicit form for the integral $I(\mathbf{m})$ and subsequently a way of analytically compute the the integrals, over the coupled coordinates, encountered in the evaluation of the overlap and Hamiltonian matrix elements.

6.2.1 Results for the bi-dimensional case

In the present section, the just discussed multidimensional basis-set expansion method will be tested on the simple case of a bi-dimensional potential system defined according to a two-Gaussian ground-state distribution model. During all the presented evaluations, the G factor has been considered as a constant and the mass-tensor $\boldsymbol{\mu}$ has been considered as proportional to the identity matrix $\mathbf{I}$. For this reason, the energy unit E_u, defined in eq. 4.18, will be adopted to represent all the energy quantities. Please notice how, due to the definition of the $\boldsymbol{\mu}$-tensor, the mass m appearing in eq. 4.18 must represents, in this case, the hypothetical effective mass responding to the relation $\boldsymbol{\mu} = m^{-1}\mathbf{I}$.

As anticipated before, the asymptotically inspired set of modulation functions, presented in sec. 6.1.1, will be adopted to model the reactive coordinate behavior. For this reason, in order to give a short representation of the basis-set employed during the numerical calculations, the following notation will be adopted: [O, E:L:1, C] where O represents the number of odd modulation functions, E and L represent respectively the number of even function of error-function and Gaussian types, while C represent the number of modulation power employed in the coupled coordinates modeling. The additional 1, reported in the even basis block, reminds to the reader that the ground state is always included in the basis-set.

In order to start our discussion, let us examine the simple case of a two-Gaussian model characterized by a diagonal variance matrix $\boldsymbol{\Sigma}$. This represents the simplest possible case in which the reactive coordinate is uncoupled from the non-reactive one and, as such, the Hamiltonian operator can be factored in the product of two terms acting independently upon each coordinate component. Under these assumptions the distribution along the non-reactive coordinate appears as Gaussian and, as such, it imparts to the non-reactive coordinate a purely harmonic profile. The distribution along the reactive coordinate presents, on the other hand, a simple one-dimensional two-Gaussian probability distribution profile that can be easily studied using simple one-dimensional numerical techniques. This simple situation allows us to evaluate the correctness of the protocol implementation without invoking more advanced calculation approaches. In order to do so a value of $\sigma_x = 0.3x_0$ has been selected for the reactive coordinate while a value of $\sigma_y = 0.2x_0$ has been selected for the non-reactive one. Under these circumstances, the separation, in E_u energy units, existing between energy levels along the harmonic component can be computed as $\Delta E^y = E^y_{n+1} - E^y_n = 1/\sigma^2$. The results obtained comparing the multidimensional basis-set expansion protocol from sec. 6.2 with the results obtained from the combination of one-dimensional analysis are presented in table 6.3. As can be grasped by looking at such a table a reasonably good accuracy is recovered for the majority of energy eigenvalues. A constant performance degradation is observed when moving toward higher degrees of excitation for which the asymptotic justification is less applicable. This, however, is a general problem of all the basis-set expansion approaches in which a big number of high-order basis functions is required in order to well approximate the high-energy eigenfunctions. Despite this observation, even with the small basis set employed the error propagation can be considered as well under control.

Now that the validity of the implementation has been verified and the base accuracy that can be expected for the uncoupled case has been assessed, we can now move our attention to the validation of the protocol in presence of coupling. This has been done considering as a model system a two-Gaussian ground-state distribution in which the Gaussian functions, tilted by $\pi/6$ in respect to the anti-symmetric coordinate, have been defined setting $\sigma_x = 0.3x_0$ and $\sigma_y = 0.2x_0$ as their principal variance values. The accuracy evaluation is, however, not a simple task given that, as discussed before, defining accurate protocols to estimate multidimensional tunneling splitting is a complicated problem. In what follows we will compare the results obtained from the asymptotically inspired basis-set with the eigenvalues computed by expanding the Hamiltonian eigenvalue problem on a set of, numerically optimized, orthogonal Hermite functions centered on the origin. This last method is far from ideal and has insufficient accuracy to fully evaluate the performance of the more advanced protocol presented in this chapter. However, despite these limitations, just by looking at the results reported in table 6.4, one can easily appreciate how the two series of results are compatible within an error of less than 1%. Examining the sign of the relative error one can easily see how our protocol consistently produces lower estimates than the reference one indicating how, considering the variational character of the first excited state, it should represent the more accurate method.

Now that the accuracy of the method has been discussed, one can get a more in-depth insight into the stability and efficiency of the protocol by looking at the convergence profiles obtained when a variable number of functions are included in the basis set. In order to do so, the same two-Gaussian model

Table 6.3: Comparison between the numerical results obtained for an uncoupled two-Gaussian distribution model ($\sigma_x = 0.3x_0$, $\sigma_y = 0.2x_0$, $\theta = 0$). The n column represent the index of the eigenfunction while n_x and n_y represents the corresponding quantum numbers describing the excitation of, respectively, the reactive and non reactive coordinates. The column $\delta E_n^{\text{app}}/E_u$ contains the results produced by our asymptotically inspired procedure while the $\delta E_n^{\text{ref}}/E_u$ column represent the energy computed starting from one-dimensional results. The ε_{rel} contains the relative error of the former in respect to the latter. A [10, 4:4:1, 6] basis-set has been employed in the multidimensional calculation while a threshold of $1 \cdot 10^{-8}$ has been adopted in the canonical orthogonalization procedure.

n	n_x	n_y	$\delta E_n^{\text{app}}/E_u$	$\delta E_n^{\text{ref}}/E_u$	ε_{rel}
1	1	0	$6.314481 \cdot 10^{-2}$	$6.314479 \cdot 10^{-2}$	$3.9 \cdot 10^{-7}$
2	2	0	$1.112299 \cdot 10^{1}$	$1.112295 \cdot 10^{1}$	$3.6 \cdot 10^{-6}$
3	3	0	$1.162853 \cdot 10^{1}$	$1.162774 \cdot 10^{1}$	$6.8 \cdot 10^{-5}$
4	4	0	$2.242142 \cdot 10^{1}$	$2.242040 \cdot 10^{1}$	$4.5 \cdot 10^{-5}$
5	5	0	$2.406696 \cdot 10^{1}$	$2.406364 \cdot 10^{1}$	$1.4 \cdot 10^{-4}$
6	0	1	$2.500000 \cdot 10^{1}$	$2.500000 \cdot 10^{1}$	$8.0 \cdot 10^{-11}$
7	1	1	$2.506314 \cdot 10^{1}$	$2.506314 \cdot 10^{1}$	$1.2 \cdot 10^{-9}$
8	6	0	$3.440560 \cdot 10^{1}$	$3.437069 \cdot 10^{1}$	$1.0 \cdot 10^{-3}$
9	2	1	$3.612299 \cdot 10^{1}$	$3.612295 \cdot 10^{1}$	$1.1 \cdot 10^{-6}$
10	3	1	$3.662861 \cdot 10^{1}$	$3.662774 \cdot 10^{1}$	$2.4 \cdot 10^{-5}$

Table 6.4: Comparison between the numerical results obtained for the first 6 eigenfuntions of a two-Gaussian distribution model ($\sigma_x = 0.3x_0$, $\sigma_y = 0.2x_0$, $\theta = \pi/6$). The values obtained with the protocol presented in this chapter (basis set: [16, 6:6:1, 10], threshold: $1 \cdot 10^{-8}$) are reported in the row marked by $\delta E_n^{\text{app}}/E_u$ while the reference values are reported in the row marked by $\delta E_n^{\text{ref}}/E_u$. The reference values have been computed adopting 40 Hermite functions for the reactive coordinate and 30 for the coupled one. Both set of Hermite functions have been numerically optimized in order to facilitate convergence. The ε_{rel} row report the correspondent relative errors.

n	1	2	3	4	5	6
$\delta E_n^{\text{app}}/E_u$	$3.2365 \cdot 10^{-2}$	$1.1115 \cdot 10^{1}$	$1.1392 \cdot 10^{1}$	$2.2290 \cdot 10^{1}$	$2.3273 \cdot 10^{1}$	$2.5002 \cdot 10^{1}$
$\delta E_n^{\text{ref}}/E_u$	$3.2631 \cdot 10^{-2}$	$1.1120 \cdot 10^{1}$	$1.1393 \cdot 10^{1}$	$2.2310 \cdot 10^{1}$	$2.3278 \cdot 10^{1}$	$2.5004 \cdot 10^{1}$
ε_{rel}	$-8.1 \cdot 10^{-3}$	$-4.4 \cdot 10^{-4}$	$-1.3 \cdot 10^{-4}$	$-9.1 \cdot 10^{-4}$	$-2.0 \cdot 10^{-4}$	$-5.8 \cdot 10^{-5}$

presented in the previous paragraph ($\sigma_x = 0.3x_0$, $\sigma_y = 0.2x_0$, $\theta = \pi/6$), has been adopted as the test subject and the canonical orthogonalization threshold has been set to 10^{-8} in order to ensure numerical stability.

In order to evaluate how the number of functions adopted to study the reactive coordinate impacts the algorithm convergence, the number of functions associated with both the odd and even sub-spaces has been individually varied while keeping all the parameters fixed. For the case of the odd subspace, a basis-set of the type [O, 4:4:1, 10] with $O \in [2, 30]$ has been considered while a basis set [5, X:Y:1, 10] with $X, Y \in [2, 8]$ has been adopted to evaluate the convergence of the even subspace. The results obtained from those analyses are presented in figure 6.4 where the relative error of a given basis-set dimension is computed taking as a reference the result obtained from the largest basis-set considered. As did before we decided, for sake of simplicity, to report the even subspace data in therm of the total number $X + Y$ of basis function employed. As can be seen from such a figure, a reasonably fast convergence is observed in the case of the first 6 eigenvalues with the even ones being characterized by a more precise prediction in the case of smaller basis sets. In general terms, a quasi-monotonic decrease in relative error is observed for all the eigenvalues with the exception of the 4-th excited state whose convergence seems characterized by a somewhat more complicated behavior resulting in a nearly fixed number of stable digits.

Now that the convergence behavior of the algorithm as a function of the reactive-coordinate basis-set dimension has been discussed, we can move our attention to the evaluation of the convergence profile associated with a variable basis-set dimension for the non-reactive coordinate. In order to examine such behavior, the basis sets [25, 4:4:1, Z] have been considered for the range $[2, 15]$ of Z values. The re-

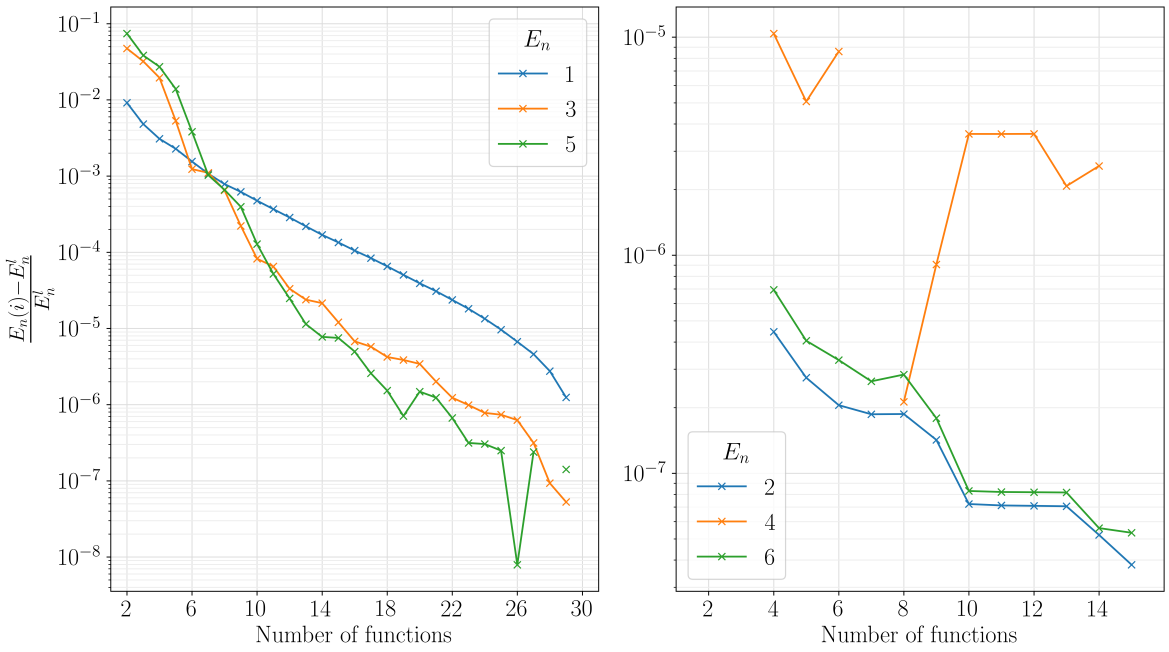

Figure 6.4: On the left panel the convergence behavior observed for the odd basis-set [O, 4:4:1, 10] is reported for $O \in [2, 30]$. On the right panel the convergence behavior observed for the even basis-set [5, X:Y:1, 10] is reported in terms of the total number $X + Y$ of basis functions. The examined range for the even space has been set to $X, Y \in [2, 8]$.

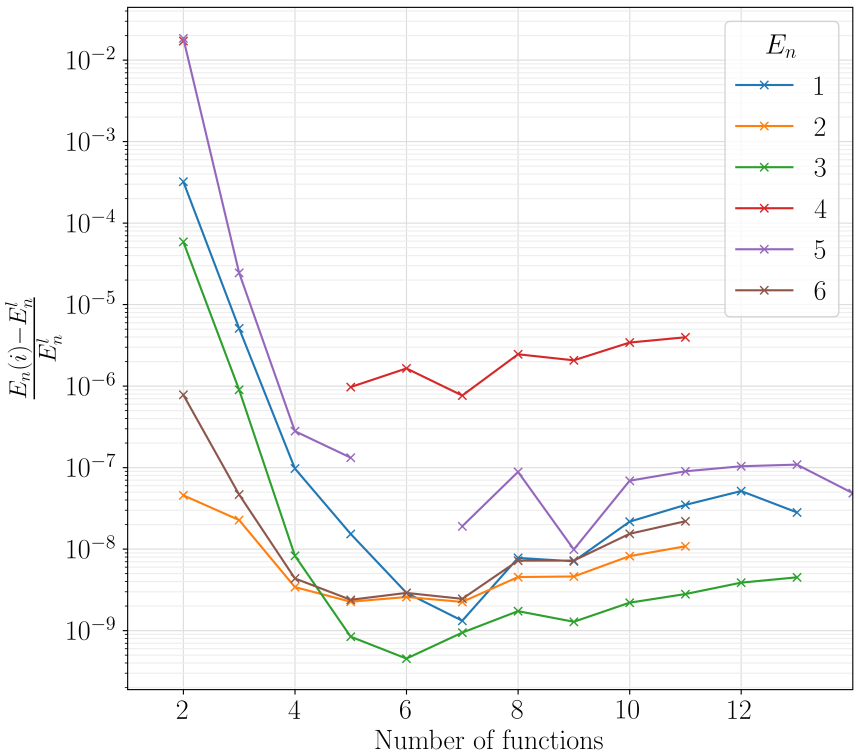

Figure 6.5: Convergence behavior observed for the non-reactive coordinate basis-set [25, 4:4:1, Z] is reported for $Z \in [2, 15]$.

sults obtained from these calculations are reported in fig. 6.5. As can be grasped by looking a such a plot, a good degree of convergence is obtained for all the considered eigenvalues that, for large basis set dimensions, reach some sort of convergence plateau. This is a clear signal of the achievement of some sort of basis-set limit condition in which the convergence profile shows no significant dependence upon the information carried by higher basis-set dimensions. Also in this case the behavior of the 4-th excited state appears different from the one observed for the other eigenvalues showing a convergence trend nearly unaffected by the basis set dimension.

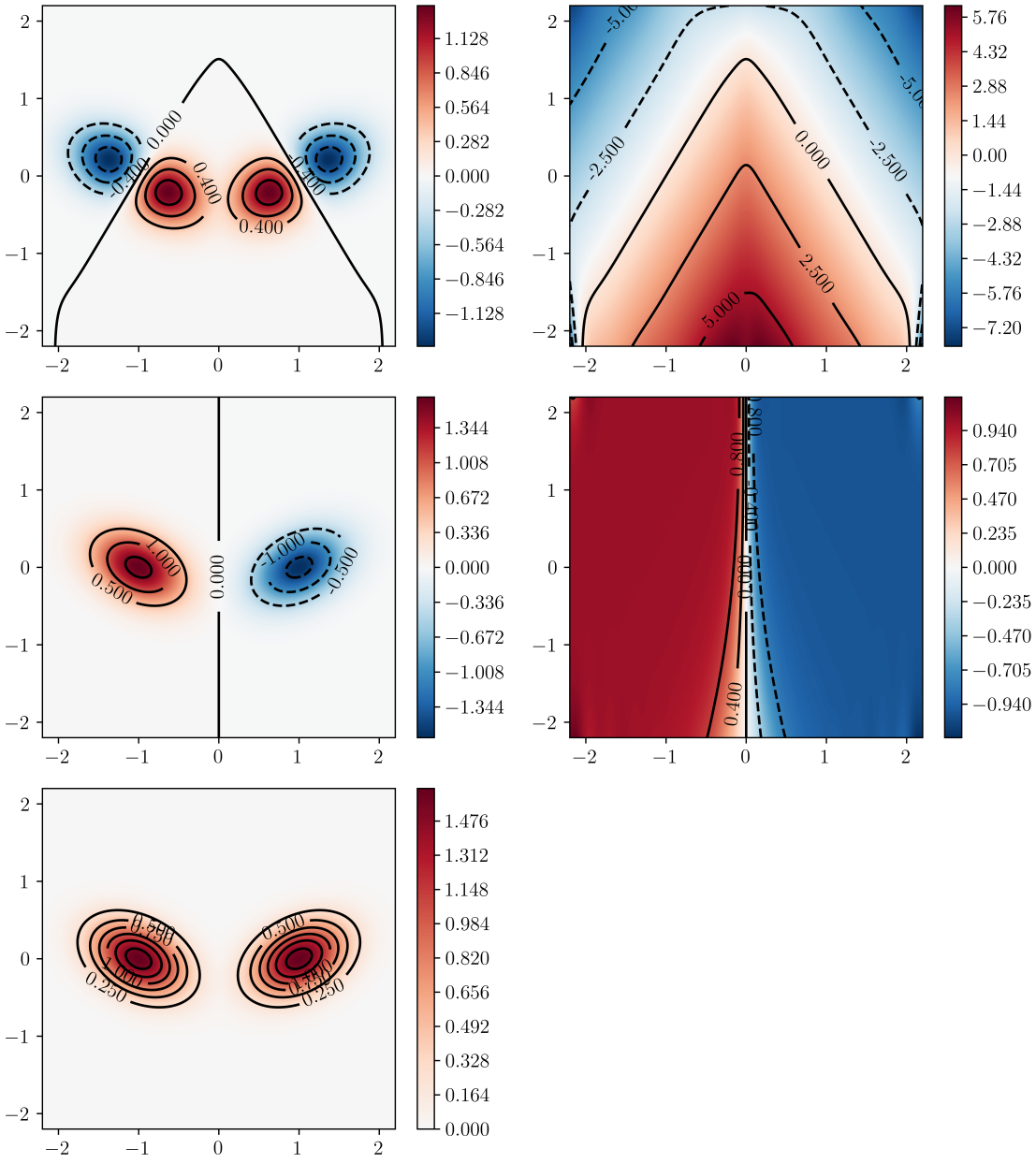

Figure 6.6: On the left side: Profile of the first three eigenfunctions of a two-Gaussian system defined according to the parameters $\sigma_x = 0.3x_0$, $\sigma_y = 0.2x_0$ and $\theta = \pi/6$. On the right side: Profile of the correspondent fixed-reference localization functions. The calculation has been performed adopting a [25, 6:6:1, 6] basis-set considering a canonical orthogonalization threshold of 10^{-8}.

Now that the numerical behavior of the algorithm has been discussed, we can now look at the shape of the eigenfunctions that can be obtained using the presented numerical protocol. This not only will allow us to inspect the produced profile to verify possible non-physical features but will also give an

overall picture of the structure assumed by the corresponding fixed reference localization function. The eigenfunctions associated with the two-Gaussian model previously presented are reported, together with the correspondent localization functions, in figure 6.6. As can be seen from such a representation, the eigenfunctions are reproduced without any noticeable distortion and the correspondent localization functions present a good behavior in the region between the two-Gaussian functions. Local spurious effects are encountered only in high-energy regions in which the vanishing of the wave-function induces numerical oscillations in the result.

Chapter 7

Conclusions and perspectives

The tunneling splitting represents an important quantum mechanical observable that can be experimentally detected in a multitude of molecular systems and, as such, its prediction represents a fundamental tool both in the interpretation of the experimental data and in the understanding of the system dynamics. In the present thesis work, a new approach to the estimation of tunneling splitting has been presented based on the isomorphic relation, discussed in detail in chapter 3, existing between the Born-Oppenheimer quantum Hamiltonian and the symmetrized Fokker-Planck-Smoluchowski operator, commonly adopted in the stochastic description of diffusive processes in the configuration space. This new approach allowed us to formulate a direct correspondence between the tunneling splitting estimation and the problem of evaluating the kinetic constants of an activated process from the continuous description given by the Smoluchowski equation. This parallelism between the Kramers problem and the estimation of tunneling splitting, allowed the application of the localization function concept to the quantum mechanical problem opening, as such, the way to a new computational paradigm having the potential to allow for high accuracy tunneling splitting predictions in the asymptotic limit of high potential energy barriers.

The starting point of our computational protocol is represented by the definition of an effective potential surface through the direct parametrization of a ground-state model specified either in terms of the ground-state wave-function or in terms of the correspondent probability distribution. This assumption represents a particularly critical element of the protocol given the inherently complicated nature of constructing ground-state models corresponding to physically meaningful potential profiles. In the present thesis, the simple case of two-Gaussian distribution models has been considered both for the case of one-dimensional problems, for which the correspondent potential models have been characterized in secs. 4.2.1 and 4.2.2, and for the case of multi-dimensional systems whose features have been discussed in sec. 5.2. This approach represents the simplest one among the possible solution to the problem and, thanks to its practical analytical structure, it has been used throughout this thesis as a test-bench for our asymptotic theory. Many other approaches to the issue are, in fact, possible and should be tested in the future; among these the numerical optimization of a ground-state model, expressed as the linear combination of localized Gaussian functions, seems to represent the most practical solution to the problem, conjugating the theoretical foundation of what discussed in this thesis with the flexibility of a numerical procedure. This has already partially been tested in the case of one-dimensional potential systems in which a ground-state wave-function, defined as a linear combination of a symmetrized set of Gaussian functions, has been fitted to reproduce, in a reasonable range of energies, the behavior of the quartic potential function returning good results. In the generic case of multidimensional problems, similar approaches can possibly be applied through the adoption of both adequate sampling techniques and sufficiently powerful fitting algorithms in the form of either deterministic protocols, heuristic procedures, or even machine learning schemes.

The core of our approach is represented, as anticipated, by the quantum localization function that has been introduced, for the first time, in chapter 4 as the ratio between the first excited state wave-function and the ground state one. This quantity represents a direct connection between the eigenstates of the system and the site-states localized in the potential wells and, as such, it allows for a direct evaluation of the tunneling splitting starting from the ground-state wave-function definition. A general procedure to define an analytic approximation of the localization function has been obtained, in the case of one-dimensional systems, in sec. 4.1 allowing us to derive a simple tunneling splitting expression involving

the computation of simple one-dimensional integrals. The obtained expression showcased the intrinsic accuracy of the protocol returning exponentially better results with a linear increase of the barrier height. Starting from this analytic expression for the localization function, an asymptotic approximation in the limit of high barriers has been obtained in sec. 4.2.3 by exploiting the characteristic structure of the two-Gaussian model. This result represents an interesting element of our analysis showing how the usual procedure, based upon the Laplace approximation of the stochastic mean-field potential, fails to recover the correct asymptotic behavior. This result inspired our approach to the study of two-Gaussian multi-dimensional systems examined in chapter 5 allowing us to define a multidimensional asymptotic model capable of recovering the proper asymptotic behavior in the limit of high barriers. The latter represents our first attempt to tackle the analytic treatment of a multidimensional tunneling problem for which a truly general analytical approximation to the localization function is still lacking. This point represents the biggest open challenge in this new research field and as such represents the most interesting perspective of this work having the potential to outline a completely general and system-independent protocol to study tunneling systems. In the past, some analytical attempt has been made to formulate a generic localization function expression based upon the probability current lines and their orthogonality to the symmetry element, however, a definitive result has still to be obtained.

Another point to be discussed is represented by the possibility of applying what discussed in this thesis to the study of real molecular systems in full or properly reduced dimensionality. This implicitly requires the definition of a set of internal coordinates subject to the symmetry constraints discussed in chapter 5. A general procedure in the definition of this coordinate set for an arbitrary molecular system is, at the moment, not available but we observe how, for simple molecular systems, an acceptable definition can be obtained by considering a proper set of coordinates generated by a linear combination of bond lengths, angles and dihedral angles. This set of symmetry coordinates can be parted into a defined number of symmetric and anti-symmetric coordinates in which the number of each coordinate type must be defined by the structure of the system itself. A general symmetry theory, based upon the permutation symmetry induced by the reactive process and capable, as such, of describing the set of coordinates and their symmetry, has still to be formulated but we suggest that, in practical terms, the number of symmetric and anti-symmetric coordinates can possibly be obtained studying the point group symmetry of the symmetric transition state. Please notice how also this point must be considered with care given that the symmetry prediction made considering the normal mode analysis on the transition state is not formally connected with the non-linear definition of the internal coordinate set. In this sense, further investigation is needed. Once the proper set of internal symmetry coordinates has been defined the proper definition of the mass tensor must be evaluated either analytically or numerically. Given the early stage of this work, in which a general formal definition of a set of symmetry coordinate is still lacking, we adopted an automatic differentiation protocol obtaining good accuracy results. The last issue hindering the application of the protocol to real molecular systems is represented by the definition of a general procedure capable of fitting the two-Gaussian distribution model onto a given potential profile. This point represents a still unexplored problem that, however, can possibly be tackled by a procedure based upon the fitting of a defend set of potential properties such as the barrier height, the position and the curvature of both the minima and the transition state. We hope to solve these few last problems in the near future in order to achieve the first molecular implementation and, as such, the first real performance comparison between our approximated and numerical approaches, discussed respectively in chapters 5 and 6, with the state of the art computational techniques commonly adopted in the literature.

This thesis only covers a small portion of the topics that can be tackled by adopting the quantum localization function approach and we think that further developments are possible in the near term. Among these, we observe how the localization function approach can be easily generalized to the case of a multiple site system possibly returning estimates of accuracy comparable with the one discussed in this thesis for the bi-stable case. We, in fact, already explored this possibility in the past and obtained, for the case of a one-dimensional potential system defined by a multiple Gaussian ground-state model, the same exponential accuracy improvement discussed in section 4.2.1 for the double-well potential. Furthermore, we observe how the localization function method can possibly be introduced also in the study of those systems characterized by asymmetrical potential wells and, in combination with a multi-site theory, represent a useful tool in the study of the Anderson problem in real potential systems.

We think that what presented in this thesis represents an interesting methodological approach to the problem of tunneling splitting that, by creating an interesting parallelism between otherwise unrelated

phenomena, allowed us to shine new light on a classical problem of quantum mechanics.

Appendices

Appendix A

Hilbert space, position and momentum representations

In formal terms, a Hilbert space represents a vector space in which an inner product operation is defined. In quantum mechanics such a space is usually intended as an infinite-dimensional function space in which a generic quantum state $|\psi\rangle$ can be treated according to the rules of linear algebra and its projection onto another state $|\phi\rangle$ can be computed according to the inner product $\langle\psi|\phi\rangle$. Each vector in the Hilbert space can be represented by expansion over a complete orthonormal basis-set and can, as such, be expressed as a complex-valued vector of coefficients. In such a context the inner product between the states directly translates to the inner product between two complex vectors.

Often in quantum mechanics we are used to discuss the state of a given particle in terms of the value assumed by its wave-function is space. In order to better understand how this can be formalized let us consider the space of states $|x\rangle$ spanned by the position operator $\hat{x}$ according to:

$$\hat{x}|x\rangle = x|x\rangle \tag{A.1}$$

that, according to their positional meaning, must respond to the orthogonality condition:

$$\langle x|x'\rangle = \delta(x - x') \tag{A.2}$$

These states represent a complete basis-set to describe the position of a given particle and as such the identity operator $\hat{I}$ assumes, in such a space, the following definition:

$$\hat{I} = \int dx\, |x\rangle\langle x| \tag{A.3}$$

The amplitude $\psi(x,t)$ of a given state $|\psi\rangle$ in the point x in space can be computed as the projection of the state onto the position eigenstate $|x\rangle$ according to:

$$\psi(x,t) = \langle x|\psi(t)\rangle \tag{A.4}$$

Starting from this definition one can easily see how the usual position space definition of the scalar product between two states can be justified:

$$\langle\psi_a(t)|\psi_b(t)\rangle = \int dx\, \langle\psi_a(t)|x\rangle\langle x|\psi_b(t)\rangle = \int dx\, \psi_a^*(x,t)\psi_b(x,t) \tag{A.5}$$

Similarly to what discussed in the case of the position representation, an equivalent momentum space can also be introduced adopting as a basis-set the eigenstates $|p\rangle$ of the linear-momentum operator $\hat{p}$ defined according to:

$$\hat{p}|p\rangle = p|p\rangle \tag{A.6}$$

Similarly to what discussed before the $|p\rangle$ states are orthonormal and represents a complete basis set to map the Hilbert space:

$$\langle p|p'\rangle = \delta(p - p') \qquad \text{and} \qquad \hat{I} = \int dp\, |p\rangle\langle p| \tag{A.7}$$

At this point, given the independent nature of the position of a particle from its momentum, one can easily see how the following equation must be verified:

$$\hat{p}\langle x|p\rangle = \langle x|\hat{p}|p\rangle = p\langle x|p\rangle \tag{A.8}$$

from which, starting from the definition of $\hat{p} = -i\hbar\partial/\partial x$, the following relation can easily be obtained for the continuous function $\langle x|p\rangle$:

$$\langle x|p\rangle = \frac{1}{\sqrt{2\pi\hbar}} e^{\frac{i}{\hbar}px} \tag{A.9}$$

please notice how the coefficient ensures the orthonormality of the momentum states according to:

$$\langle p|p'\rangle = \int dx\, \langle p|x\rangle\langle x|p'\rangle = \frac{1}{2\pi\hbar}\int dx\, e^{\frac{i}{\hbar}(p'-p)x} \tag{A.10}$$

that represents the definition of the Dirac delta function $\delta(p-p') = \delta(p'-p)$:

$$\delta(p-p') = \frac{1}{2\pi\hbar}\int dx\, e^{\frac{i}{\hbar}(p-p')x} \tag{A.11}$$

Appendix B

The generalized eigenvalue problem

The energy structure of a quantum system is encoded into the definition of the correspondent Hamiltonian operator $\hat{H}$. The eigenstates $|\psi_n\rangle$ and eigenvalues E_n of such an operator, defining the energy spectrum of the system, can be computed by solving the time-independent Schrödinger equation:

$$\hat{H}|\psi_n\rangle = E_n|\psi_n\rangle \tag{B.1}$$

where, due to the self-adjoint nature of the Hamiltonian operator, the eigenvalues are reals and the eigenfunctions corresponding to non-degenerate eigenvalues are orthogonal $\langle\psi_n|\psi_m\rangle = \delta_{nm}$.

In order to solve eq. B.1, a basis-set of $\{|i\rangle\}$ states can be invoked to represent the set of eigenfunctions $|\psi_n\rangle$ according to the expansion:

$$|\psi_n\rangle = \sum_j C_{jn}|j\rangle \tag{B.2}$$

where the coefficient matrix $\mathbf{C}$ has been introduced as the matrix having as its n-th column the vector containing the expansion coefficients of the n-th eigenstate over the basis of $\{|i\rangle\}$ sates. Substituting such a definition in eq. B.1 and taking the scalar product of both sides of the equation with respect to the generic $|i\rangle$ state, allows us to obtain:

$$\sum_j C_{jn}H_{ij} = E_n \sum_j C_{jn}S_{ij} \tag{B.3}$$

where the matrix elements of the Hamiltonian matrix $\mathbf{H}$ and those of the overlap matrix $\mathbf{S}$ have been introduced according to:

$$H_{ij} := \langle i|\hat{H}|j\rangle \qquad S_{ij} := \langle i|j\rangle \tag{B.4}$$

Recalling the definition of the product of two matrices eq. B.3 can be rewritten in the form:

$$(\mathbf{HC})_{nj} = E_n(\mathbf{SC})_{nj} \tag{B.5}$$

Introducing the eigenvalues matrix $\mathbf{\Lambda}$, whose matrix element are define according to $\Lambda_{ij} = \delta_{ij}E_i$, it is simple to show ho the following relation can be obtained:

$$\mathbf{HC} = \mathbf{SC\Lambda} \tag{B.6}$$

The obtained equation is usually known as generalized eigenvalue problem.

Appendix C

The Laplace method

Let us consider the integral I of a function $f(x) \geq 0$ characterized by a maximum located at $x = x_0$ and defined according to:

$$I := \int_a^b f(x)dx \tag{C.1}$$

Let us introduce a function $u(x)$ defined according to $u(x) = -\ln[f(x)]$ and let us consider its quadratic expansion around x_0 such that:

$$u(x) \simeq U(x_0) + \frac{1}{2}u''(x_0)(x - x_0)^2 \tag{C.2}$$

By simple substitution into the integral definition, the following result can easily be obtained:

$$I = \int_{-\infty}^{+\infty} e^{-u(x)}dx = e^{-u(x_0)} \int_{-\infty}^{+\infty} e^{-\frac{1}{2}u''(x_0)(x-x_0)^2}dx \tag{C.3}$$

where the integration range has been extended to infinity committing, thanks to the vanishing nature of the local function approximation, a negligible error. Recalling the definition of a normalized Gaussian function, the following result can be easily obtained:

$$I = \sqrt{\frac{2\pi}{u''(x_0)}}e^{-u(x_0)} = \sqrt{\frac{2\pi}{u''(x_0)}}f(x_0) \tag{C.4}$$

Please notice how, in general terms, such an approximation is usually progressively more accurate for large value of the curvature $u''(x_0) \to +\infty$.

Appendix D

The Fokker-Planck equation

In the present appendix, starting from the Chapman-Kolmogorov relation obtained in eq. 3.37, the Fokker-Planck equation will be obtained for the simple case of a one-dimensional Markov process. In order to start our discussion let us consider a twice differentiable function $g(x)$ responding to the following conditions:

$$g(x_{\min}) = g(x_{\max}) = 0 \qquad \frac{dg(x)}{dx}\Big|_{x=x_{\min}} = \frac{dg(x)}{dx}\Big|_{x=x_{\max}} = 0 \tag{D.1}$$

where $x_{\min}$ and $x_{\max}$ represent the boundaries of the system. Let us compute at this point, the average value $G(t)$ of such a function over the probability distribution $p(x,t)$, according to:

$$G(t) = \int dx\, g(x)p(x,t) \tag{D.2}$$

If the time derivative of such a quantity is computed, the following result can be easily obtained:

$$\frac{dG(t)}{dt} = \int dx\, g(x)\frac{\partial p(x,t)}{\partial t} \tag{D.3}$$

where the time derivative of the probability can be approximated in terms of infinitesimal differences:

$$\frac{\partial p(x,t)}{\partial t} = \lim_{\Delta t\to 0}\frac{p(x,t+\Delta t) - p(x,t)}{\Delta t} \tag{D.4}$$

If the Chapman-Kolmogorov equation from eq. 3.37 is now invoked, the following condition can be easily recovered:

$$\frac{\partial p(x,t)}{\partial t} = \lim_{\Delta t\to 0}\frac{1}{\Delta t}\left[-p(x,t) + \int dx'\ \rho(x,t+\Delta t|x',t)p(x',t)\right] \tag{D.5}$$

from which, the relation from eq. D.3 can be rewritten according to:

$$\frac{dG(t)}{dt} = \lim_{\Delta t\to 0}\frac{1}{\Delta t}\left[\int dx\int dx'\ g(x)\rho(x,t+\Delta t|x',t)p(x',t) - \int dx\, g(x)p(x,t)\right] \tag{D.6}$$

Observing how the integral result must be independent from the integration label, the following equality can be obtained:

$$\int dx\int dx'\ g(x)\rho(x,t+\Delta t|x',t)p(x',t) = \int dx\int dx'\ g(x')\rho(x',t+\Delta t|x,t)p(x,t) \tag{D.7}$$

At this point, one may notice how for short time intervals $\Delta t \to 0$ the conditional probability $\rho(x,t+\Delta t|x',t)$ must rapidly approach zero for high values of the distance $|x-x'|$. This tells us that a local approximation of $g(x')$, around the x value, is sufficient to evaluate the inner integral in eq. D.7. In order to do so, let us consider the following quadratic expansion:

$$g(x') = g(x) + g'(x)(x'-x) + \frac{1}{2}g''(x)(x'-x)^2 \tag{D.8}$$

If this result is substituted, taking into account the equality from eq. D.7, into eq. D.6 the following result can be obtained with little elaboration:

$$\frac{dG(t)}{dt} = \int dx\, g'(x)A(x,t)p(x,t) + \frac{1}{2}\int dx\, g''(x)B(x,t)p(x,t) \tag{D.9}$$

where the terms $A(x,t)$ and $B(x,t)$ representing the drift and generalized diffusion coefficient have been defined according to:

$$A(x,t) := \lim_{\Delta t \to 0} \frac{1}{\Delta t} \int dx'(x'-x)\rho(x', t+\Delta t|x,t) \tag{D.10}$$

$$B(x,t) := \lim_{\Delta t \to 0} \frac{1}{\Delta t} \int dx'(x'-x)^2\rho(x', t+\Delta t|x,t) \tag{D.11}$$

At this point by properly applying the integration by parts to eq. D.9 the following relation can be obtained:

$$\frac{dG(t)}{dt} = \int dx\, g(x) \left\{ -\frac{\partial \left[A(x,t)p(x,t)\right]}{\partial x} + \frac{1}{2}\frac{\partial^2 \left[B(x,t)p(x,t)\right]}{\partial x^2} \right\} \tag{D.12}$$

Comparing the result just obtained with the definition from eq. D.3 the following equation can be obtained:

$$\frac{\partial p(x,t)}{\partial t} = -\frac{\partial \left[A(x,t)p(x,t)\right]}{\partial x} + \frac{1}{2}\frac{\partial^2 \left[B(x,t)p(x,t)\right]}{\partial x^2} \tag{D.13}$$

that represents the Fokker-Planck equation for a one-dimensional non-stationary Markov process. The procedure presented in this appendix can easily be generalized in order to obtain the multi-dimensional Fokker-Planck equation presented in eq. 3.38.

Appendix E

The inverse of a block matrix

Let us consider an invertible squared block matrix $\mathbf{A}$ of dimension n and its inverse $\mathbf{B} = \mathbf{A}^{-1}$ as the matrices defined according to:

$$\mathbf{A} = \begin{pmatrix} \mathbf{A}_{1,1} & \mathbf{A}_{1,2} \\ \mathbf{A}_{2,1} & \mathbf{A}_{2,2} \end{pmatrix} \qquad \text{and} \qquad \mathbf{B} = \begin{pmatrix} \mathbf{B}_{1,1} & \mathbf{B}_{1,2} \\ \mathbf{B}_{2,1} & \mathbf{B}_{2,2} \end{pmatrix} \tag{E.1}$$

Starting from the condition $\mathbf{AB} = \mathbf{I}$, where $\mathbf{I}$ represents the identity matrix, the components of the $\mathbf{B}$ matrix can easily be defined in terms of the ones appearing in the $\mathbf{A}$ matrix definition. This can be easily written in explicit form according to:

$$\mathbf{AB} = \begin{pmatrix} \mathbf{A}_{1,1}\mathbf{B}_{1,1} + \mathbf{A}_{1,2}\mathbf{B}_{2,1} & \mathbf{A}_{1,1}\mathbf{B}_{1,2} + \mathbf{A}_{1,2}\mathbf{B}_{2,2} \\ \mathbf{A}_{2,1}\mathbf{B}_{1,1} + \mathbf{A}_{2,2}\mathbf{B}_{2,1} & \mathbf{A}_{2,1}\mathbf{B}_{1,2} + \mathbf{A}_{2,2}\mathbf{B}_{2,2} \end{pmatrix} = \begin{pmatrix} \mathbf{I}_k & \mathbf{0}_{k,n-k} \\ \mathbf{0}_{n-k,k} & \mathbf{I}_{n-k} \end{pmatrix} = \mathbf{I} \tag{E.2}$$

where k represents the dimension of the $\mathbf{A}_{1,1}$ square block. That in unrolled form can be rewritten according to the following system of equations:

$$\begin{cases} \mathbf{A}_{1,1}\mathbf{B}_{1,1} + \mathbf{A}_{1,2}\mathbf{B}_{2,1} = \mathbf{I}_k \\ \mathbf{A}_{1,1}\mathbf{B}_{1,2} + \mathbf{A}_{1,2}\mathbf{B}_{2,2} = \mathbf{0}_{k,n-k} \\ \mathbf{A}_{2,1}\mathbf{B}_{1,1} + \mathbf{A}_{2,2}\mathbf{B}_{2,1} = \mathbf{0}_{n-k,k} \\ \mathbf{A}_{2,1}\mathbf{B}_{1,2} + \mathbf{A}_{2,2}\mathbf{B}_{2,2} = \mathbf{I}_{n-k} \end{cases} \tag{E.3}$$

Considering the second and third relations of the previous system of equations, the following conditions can be obtained:

$$\mathbf{B}_{1,2} = -\mathbf{A}_{1,1}^{-1}\mathbf{A}_{1,2}\mathbf{B}_{2,2} \tag{E.4}$$

$$\mathbf{B}_{2,1} = -\mathbf{A}_{2,2}^{-1}\mathbf{A}_{2,1}\mathbf{B}_{1,1} \tag{E.5}$$

from which, considering the first and fourth relations form eq. E.3, the following can be written:

$$\left[\mathbf{A}_{1,1} - \mathbf{A}_{1,2}\mathbf{A}_{2,2}^{-1}\mathbf{A}_{2,1}\right]\mathbf{B}_{1,1} = \mathbf{I}_k \tag{E.6}$$

$$\left[\mathbf{A}_{2,2} - \mathbf{A}_{2,1}\mathbf{A}_{1,1}^{-1}\mathbf{A}_{1,2}\right]\mathbf{B}_{2,2} = \mathbf{I}_{n-k} \tag{E.7}$$

By simple inversion the following can easily be obtained:

$$\mathbf{B}_{1,1} = \left[\mathbf{A}_{1,1} - \mathbf{A}_{1,2}\mathbf{A}_{2,2}^{-1}\mathbf{A}_{2,1}\right]^{-1} \tag{E.8}$$

$$\mathbf{B}_{2,2} = \left[\mathbf{A}_{2,2} - \mathbf{A}_{2,1}\mathbf{A}_{1,1}^{-1}\mathbf{A}_{1,2}\right]^{-1} \tag{E.9}$$

From which, by simple substitution into eqs. E.4 and E.5 the following can easily be obtained:

$$\mathbf{B}_{1,2} = -\mathbf{A}_{1,1}^{-1}\mathbf{A}_{1,2}\left[\mathbf{A}_{2,2} - \mathbf{A}_{2,1}\mathbf{A}_{1,1}^{-1}\mathbf{A}_{1,2}\right]^{-1} \tag{E.10}$$

$$\mathbf{B}_{2,1} = -\mathbf{A}_{2,2}^{-1}\mathbf{A}_{2,1}\left[\mathbf{A}_{1,1} - \mathbf{A}_{1,2}\mathbf{A}_{2,2}^{-1}\mathbf{A}_{2,1}\right]^{-1} \tag{E.11}$$

Bibliography

1. Landau, L. D. & Lifšits, E. M. *Quantum mechanics : non-relativistic theory* ISBN: 978-0750635394 (Butterworth Heinemann, Amsterdam, 1977).
2. Bell, R. P. *The tunnel effect in chemistry* ISBN: 978-1-4899-2891-7 (Chapman and Hall, London New York, 1980).
3. Hänggi, P., Talkner, P. & Borkovec, M. Reaction-rate theory: fifty years after Kramers. *Reviews of Modern Physics* **62,** 251. https://journals.aps.org/rmp/abstract/10.1103/RevModPhys.62.251 (Apr. 1990).
4. Messiah, A. *Quantum Mechanics* ISBN: 9780486784557 (Dover Publications, City, 2014).
5. Schlosshauer, M. Decoherence, the measurement problem, and interpretations of quantum mechanics. *Rev. Mod. Phys.* **76,** 1267–1305. https://link.aps.org/doi/10.1103/RevModPhys.76.1267 (4 Feb. 2005).
6. Griffiths, D. *Introduction to quantum mechanics* ISBN: 978-0131118928 (Pearson Prentice Hall, Upper Saddle River, NJ, 2005).
7. Garg, A. Tunnel splittings for one-dimensional potential wells revisited. *American Journal of Physics* **68,** 430. https://doi.org/10.1119/1.19458 (2000).
8. Mátyus, E., Wales, D. J. & Althorpe, S. C. Quantum tunneling splittings from path-integral molecular dynamics. *The Journal of Chemical Physics* **144,** 114108. https://doi.org/10.1063/1.4943867 (2016).
9. Vaillant, C. L., Wales, D. J. & Althorpe, S. C. Tunneling splittings from path-integral molecular dynamics using a Langevin thermostat. *The Journal of Chemical Physics* **148,** 234102. ISSN: 0021-9606. https://aip.scitation.org/doi/abs/10.1063/1.5029258 (June 2018).
10. Vaillant, C. L., Wales, D. J. & Althorpe, S. C. Tunneling Splittings in Water Clusters from Path Integral Molecular Dynamics. *The Journal of Physical Chemistry Letters* **10,** 7300–7304. https://pubs.acs.org/doi/full/10.1021/acs.jpclett.9b02951 (Nov. 2019).
11. Quack, M. & Suhm, M. A. Accurate quantum Monte Carlo calculations of the tunneling splitting in $(HF)_2$ on a six-dimensional potential hypersurface. *Chemical Physics Letters* **234,** 71–76. ISSN: 0009-2614 (Mar. 1995).
12. Gregory, J. K. & Clary, D. C. Calculations of the tunneling splittings in water dimer and trimer using diffusion Monte Carlo. *The Journal of Chemical Physics* **102,** 7817. ISSN: 0021-9606. https://aip.scitation.org/doi/abs/10.1063/1.468982 (June 1998).
13. Webb, S. P., Iordanov, T. & Hammes-Schiffer, S. Multiconfigurational nuclear-electronic orbital approach: Incorporation of nuclear quantum effects in electronic structure calculations. *Nuclear-electronic orbital Ehrenfest dynamics The Journal of Chemical Physics* **117,** 4106. https://doi.org/10.1063/1.1494980 (2002).
14. Coutinho-Neto, M. D., Viel, A. & Manthe, U. The ground state tunneling splitting of malonaldehyde: Accurate full dimensional quantum dynamics calculations. *The Journal of Chemical Physics* **121,** 9207–9210. https://doi.org/10.1063/1.1814356 (2004).
15. Hazra, A., Skone, J. H. & Hammes-Schiffer, S. Combining the nuclear-electronic orbital approach with vibronic coupling theory: Calculation of the tunneling splitting for malonaldehyde. *The Journal of Chemical Physics* **130,** 054108. https://doi.org/10.1063/1.3068526 (2009).
16. Wu, F., Ren, Y. & Bian, W. The hydrogen tunneling splitting in malonaldehyde: A full-dimensional time-independent quantum mechanical method. *The Journal of Chemical Physics* **145,** 74309. https://doi.org/10.1063/1.4960789 (2016).

17. Chen, H., Liu, S. & Light, J. C. Six-dimensional quantum calculation of the intermolecular bound states for water dimer. *The Journal of Chemical Physics* **110,** 168. ISSN: 0021-9606. https://aip.scitation.org/doi/abs/10.1063/1.478092 (Dec. 1998).

18. Leforestier, C., Braly, L. B., Liu, K., Elrod, M. J. & Saykally, R. J. Fully coupled six-dimensional calculations of the water dimer vibration-rotation-tunneling states with a split Wigner pseudo spectral approach. *The Journal of Chemical Physics* **106,** 8527. ISSN: 0021-9606. https://aip.scitation.org/doi/abs/10.1063/1.473908 (Aug. 1998).

19. Takada, S. & Nakamura, H. Wentzel–Kramers–Brillouin theory of multidimensional tunneling: General theory for energy splitting. *The Journal of Chemical Physics* **100,** 98. ISSN: 0021-9606. https://aip.scitation.org/doi/abs/10.1063/1.466899 (Aug. 1998).

20. Eraković, M., Vaillant, C. L. & Cvitaš, M. T. Instanton theory of ground-state tunneling splittings with general paths. *J. Chem. Phys* **152,** 84111. https://doi.org/10.1063/1.5145278 (2020).

21. Richardson, J. O. & Althorpe, S. C. Ring-polymer instanton method for calculating tunneling splittings. *The Journal of Chemical Physics* **134,** 054109. ISSN: 0021-9606. https://aip.scitation.org/doi/abs/10.1063/1.3530589 (Feb. 2011).

22. Poirier, B. & Light, J. C. Efficient distributed Gaussian basis for rovibrational spectroscopy calculations. *Journal of Chemical Physics* **113,** 211–217. ISSN: 00219606. https://aip.scitation.org/doi/abs/10.1063/1.481787 (July 2000).

23. Hamilton, I. P. & Light, J. C. On distributed Gaussian bases for simple model multidimensional vibrational problems. *The Journal of Chemical Physics* **84,** 306–317. ISSN: 00219606. https://aip.scitation.org/doi/abs/10.1063/1.450139 (Jan. 1985).

24. Bowman, J. M., Carrington, T. & Meyer, H. D. Variational quantum approaches for computing vibrational energies of polyatomic molecules. *Molecular Physics* **106,** 2145–2182. ISSN: 13623028. https://www.tandfonline.com/doi/abs/10.1080/00268970802258609 (2008).

25. Feynman, R. *Quantum mechanics and path integrals* ISBN: 978-0486477220 (Dover Publications, Mineola, N.Y, 2010).

26. Tuckerman, M. *Statistical mechanics : theory and molecular simulation* ISBN: 978-0198525264 (Oxford University Press, Oxford, 2010).

27. Craig, I. R. & Manolopoulos, D. E. Quantum statistics and classical mechanics: Real time correlation functions from ring polymer molecular dynamics. *The Journal of Chemical Physics* **121,** 3368. ISSN: 0021-9606. https://aip.scitation.org/doi/abs/10.1063/1.1777575 (Aug. 2004).

28. Habershon, S., Manolopoulos, D. E., Markland, T. E. & Miller III, T. F. Ring-Polymer Molecular Dynamics: Quantum Effects in Chemical Dynamics from Classical Trajectories in an Extended Phase Space. *Annual Review of Physical Chemistry* **64,** 387. www.annualreviews.org (2013).

29. Parrinello, M. & Rahman, A. Study of an F center in molten KCl. *The Journal of Chemical Physics* **80,** 860. ISSN: 0021-9606. https://aip.scitation.org/doi/abs/10.1063/1.446740 (June 1998).

30. Tuckerman, M. E., Berne, B. J., Martyna, G. J. & Klein, M. L. Efficient molecular dynamics and hybrid Monte Carlo algorithms for path integrals. *The Journal of Chemical Physics* **99,** 2796. ISSN: 0021-9606. https://aip.scitation.org/doi/abs/10.1063/1.465188 (June 1998).

31. Cao, J. & Voth, G. A. The formulation of quantum statistical mechanics based on the Feynman path centroid density. IV. Algorithms for centroid molecular dynamics. *The Journal of Chemical Physics* **101,** 6168. ISSN: 0021-9606. https://aip.scitation.org/doi/abs/10.1063/1.468399 (Aug. 1998).

32. Haynes, W. *CRC handbook of chemistry and physics : a ready-reference book of chemical and physical data* ISBN: 978-1-4822-0868-9 (CRC Press, Boca Raton, Florida, 2014).

33. Wright, N. & Randall, H. M. The Far Infrared Absorption Spectra of Ammonia and Phosphine Gases under High Resolving Power. *Physical Review* **44,** 391 (1933).

34. Cleeton, C. E. & Williams, N. H. Electromagnetic Waves of 1.1 cm Wave-Length and the Absorption Spectrum of Ammonia. *Physical Review* **45,** 234 (1934).

35. Barker, E. F. The molecular spectrum of ammonia II. The double band at 10μ. *Physical Review* **33,** 684 (1929).

36. Dennison, D. M. & Hardy, J. D. The parallel type absorption bands of ammonia. *Physical Review* **39,** 938 (1932).

37. Sitnitsky, A. E. Exactly solvable double-well potential in Schrödinger equation for inversion mode of phosphine molecule. *Computational and Theoretical Chemistry* **1200,** 113220. https://doi.org/10.1016/j.comptc.2021.113220 (June 2021).

38. Sousa-Silva, C., Tennyson, J. & Yurchenko, S. N. Communication: Tunnelling splitting in the phosphine molecule. *J. Chem. Phys* **145,** 91102. http://dx.doi.org/10.1063/1.4962259 (2016).

39. Baba, T., Tanaka, T., Morino, I., Yamada, K. M. T. & Tanaka, K. Detection of the tunneling-rotation transitions of malonaldehyde in the submillimeter-wave region. *The Journal of Chemical Physics* **110,** 4131. ISSN: 0021-9606. https://aip.scitation.org/doi/abs/10.1063/1.478296 (Feb. 1999).

40. Wassermann, T. N., Luckhaus, D., Coussan, S. & Suhm, M. A. Proton tunneling estimates for malonaldehyde vibrations from supersonic jet and matrix quenching experiments. *Physical Chemistry Chemical Physics* **8,** 2344–2348. ISSN: 1463-9084. https://pubs.rsc.org/en/content/articlehtml/2006/cp/b602319n (May 2006).

41. Mizukami, W., Habershon, S. & Tew, D. P. A compact and accurate semi-global potential energy surface for malonaldehyde from constrained least squares regression. *The Journal of Chemical Physics* **141,** 144310. ISSN: 0021-9606. https://aip.scitation.org/doi/abs/10.1063/1.4897486 (Oct. 2014).

42. Tanaka, K. *et al.* Determination of the proton tunneling splitting of tropolone in the ground state by microwave spectroscopy. *The Journal of Chemical Physics* **110,** 1969. ISSN: 0021-9606. https://aip.scitation.org/doi/abs/10.1063/1.477863 (Jan. 1999).

43. Paz, J. J., Moreno, M. & Lluch, J. M. Bidimensional tunneling splitting in the $\tilde{A}^1B_2$ and $\tilde{X}^1A_1$ states of tropolone. *The Journal of Chemical Physics* **103,** 353. ISSN: 0021-9606. https://aip.scitation.org/doi/abs/10.1063/1.469647 (June 1998).

44. Tautermann, C. S., Voegele, A. F. & Liedl, K. R. The ground-state tunneling splitting of various carboxylic acid dimers. *J. Chem. Phys* **120,** 631. https://doi.org/10.1063/1.1630565 (2004).

45. McCarthy, M. C., Thorwirth, S., Gottlieb, C. A. & Thaddeus, P. Tetrasulfur, S_4: Rotational spectrum, interchange tunneling, and geometrical structure. *The Journal of Chemical Physics* **121,** 632. ISSN: 0021-9606. https://aip.scitation.org/doi/abs/10.1063/1.1769372 (June 2004).

46. Keutsch, F. N. & Saykally, R. J. Water clusters: Untangling the mysteries of the liquid, one molecule at a time. *Proceedings of the National Academy of Sciences of the United States of America* **98,** 10533–10540. ISSN: 00278424 (Sept. 2001).

47. Richardson, J. O. *et al.* Concerted hydrogen-bond breaking by quantum tunneling in the water hexamer prism. *Science* **351,** 1310–1313 (Mar. 2016).

48. Lin, C. C. & Swalen, J. D. Internal Rotation and Microwave Spectroscopy. *Reviews of Modern Physics* **31,** 841. https://journals.aps.org/rmp/abstract/10.1103/RevModPhys.31.841 (Oct. 1959).

49. Islampour, R. Generalized coordinates molecular Hamiltonian. *Molecular Physics* **101,** 2489–2496. https://doi.org/10.1080/0026897032000112883 (2003).

50. Moro, G. J. Kinetic equations for site populations from the Fokker–Planck equation. *The Journal of Chemical Physics* **103,** 7514–7531. https://doi.org/10.1063/1.470320 (1995).

51. Zwanzig, R. *Nonequilibrium statistical mechanics* ISBN: 0195140184 (Oxford University Press, Oxford New York, 2001).

52. Moro, G. & Nordio, P. L. Diffusive and jump description of hindered motions. *Molecular Physics* **56,** 255–269. https://doi.org/10.1080/00268978500102301 (1985).

53. Szabo, A. & Ostlund, N. S. *Modern Quantum Chemistry: Introduction to Advanced Electronic Structure Theory* First (Dover Publications, Inc., Mineola, 1996).

54. Lehtola, S. Curing basis set overcompleteness with pivoted Cholesky decompositions. *Journal of Chemical Physics* **151,** 241102. ISSN: 00219606 (2019).